UNIVERSIDADE FEDERAL DE GOIÁS (UFG)
INSTITUTO DE QUÍMICA (IQ)
PROGRAMA DE PÓS GRADUAÇÃO EM QUÍMICA

Ricardo Alves Bernardo

Oral squamous cell carcinoma lipid differentiation in gingiva tissue by mass spectrometry

Diferenças de lipídios do carcinoma oral de células escamosas em amostras de gengiva empregando espectrometria de massas

GOIÂNIA
2022

UFG

UNIVERSIDADE FEDERAL DE GOIÁS
INSTITUTO DE QUÍMICA

TERMO DE CIÊNCIA E DE AUTORIZAÇÃO (TECA) PARA DISPONIBILIZAR VERSÕES ELETRÔNICAS DE TESES

E DISSERTAÇÕES NA BIBLIOTECA DIGITAL DA UFG

Na qualidade de titular dos direitos de autor, autorizo a Universidade Federal de Goiás (UFG) a disponibilizar, gratuitamente, por meio da Biblioteca Digital de Teses e Dissertações (BDTD/UFG), regulamentada pela Resolução CEPEC nº 832/2007, sem ressarcimento dos direitos autorais, de acordo com a Lei 9.610/98, o documento conforme permissões assinaladas abaixo, para fins de leitura, impressão e/ou download, a título de divulgação da produção científica brasileira, a partir desta data.

O conteúdo das Teses e Dissertações disponibilizado na BDTD/UFG é de responsabilidade exclusiva do autor. Ao encaminhar o produto final, o autor(a) e o(a) orientador(a) firmam o compromisso de que o trabalho não contém nenhuma violação de quaisquer direitos autorais ou outro direito de terceiros.

1. Identificação do material bibliográfico

[ ] Dissertação [X] Tese [ ] Outro*:_____

*No caso de mestrado/doutorado profissional, indique o formato do Trabalho de Conclusão de Curso, permitido no documento de área, correspondente ao programa de pós-graduação, orientado pela legislação vigente da CAPES.

Exemplos: Estudo de caso ou Revisão sistemática ou outros formatos.

2. Nome completo do autor

Ricardo Alves Bernardo

3. Título do trabalho

Oral squamous cell carcinoma lipid differentiation in gingiva tissue by mass spectrometry

4. Informações de acesso ao documento (este campo deve ser preenchido pelo orientador)

Concorda com a liberação total do documento [X] SIM [ ] NÃO[1]

[1] Neste caso o documento será embargado por até um ano a partir da data de defesa. Após esse período, a possível disponibilização ocorrerá apenas mediante:
a) consulta ao(à) autor(a) e ao(à) orientador(a);
b) novo Termo de Ciência e de Autorização (TECA) assinado e inserido no arquivo da tese ou dissertação.
O documento não será disponibilizado durante o período de embargo.
Casos de embargo:
- Solicitação de registro de patente;
- Submissão de artigo em revista científica;
- Publicação como capítulo de livro;
- Publicação da dissertação/tese em livro.

Obs. Este termo deverá ser assinado no SEI pelo orientador e pelo autor.

Documento assinado eletronicamente por **Andrea Rodrigues Chaves**, **Professor do Magistério Superior**, em 18/11/2022, às 16:20, conforme horário oficial de Brasília, com fundamento no § 3º do

art. 4º do Decreto nº 10.543, de 13 de novembro de 2020.

Documento assinado eletronicamente por **RICARDO ALVES BERNARDO**, **Discente**, em 18/11/2022, às 16:56, conforme horário oficial de Brasília, com fundamento no § 3º do art. 4º do Decreto nº 10.543, de 13 de novembro de 2020.

A autenticidade deste documento pode ser conferida no site https://sei.ufg.br/sei/controlador_externo.php?acao=documento_conferir&id_orgao_acesso_externo=0, informando o código verificador **3345839** e o código CRC **C3345FBD**.

Referência: Processo nº 23070.044595/2022-09 SEI nº 3345839

Ricardo Alves Bernardo

Oral squamous cell carcinoma lipid differentiation in gingiva tissue by mass spectrometry

Diferenças de lipídios do carcinoma oral de células escamosas em amostras de gengiva empregando espectrometria de massas

A thesis presented to the Programa de Pós-Graduação em Química, of the Instituto de Química of Universidade Federal de Goiás as a requirement for obtaining the title of Doctor in Chemistry.
Área de concentração: Química
Linha de pesquisa: Química Analítica

Supervisor: Profa. Dra. Andréa Rodrigues Chaves

GOIÂNIA

2022

Ficha de identificação da obra elaborada pelo autor, através do
Programa de Geração Automática do Sistema de Bibliotecas da UFG.

Bernardo, Ricardo Alves
Oral squamous cell carcinoma lipid differentiation in gingiva tissue by mass spectrometry [manuscrito] / Ricardo Alves Bernardo. - 2022.
225 f.: il.

Orientador: Profa. Dra. Andréa Rodrigues Chaves.
Tese (Doutorado) - Universidade Federal de Goiás, Instituto de Química (IQ), Programa de Pós-Graduação em Química, Goiânia, 2022.
Bibliografia. Anexos.
Inclui siglas, abreviaturas, gráfico, tabelas, lista de figuras, lista de tabelas.

1. Oral squamous cell carcinoma. 2. Lipids. 3. LLME. 4. MALDI. 5. Mass spectrometry imaging. I. Chaves, Andréa Rodrigues, orient. II. Título.

CDU 543

UFG

UNIVERSIDADE FEDERAL DE GOIÁS

INSTITUTO DE QUÍMICA

ATA DE DEFESA DE TESE

Ata nº **152** da sessão da Defesa de Doutorado de **Ricardo Alves Bernardo**, que confere o título de **Doutor em Química**, na área de concentração em **Química**.

Aos **23 (vinte e três) dias do mês de setembro de 2022 (dois mil e vinte e dois)**, a partir das **09h00, via videoconferência**, realizou-se a sessão pública da Defesa de Doutorado intitulada **"Oral squamous cell carcinoma lipid differentiation in gingiva tissue by mass spectrometry"**. Os trabalhos foram instalados pela Orientadora, **Profª. Drª. Andréa Rodrigues Chaves (UFG)**, com a participação dos demais membros da Banca Examinadora: **Prof. Dr. Wendell Karlos Tomazelli Coltro (UFG), Profª. Drª. Andréia de Melo Porcari (Universidade São Francisco) , Prof. Dr. Christian Janfelt (University of Copenhagen) e Profª. Drª. Eliana Martins Lima (UFG)**. Durante a arguição os membros da banca não fizeram sugestão de alteração do título do trabalho.A banca sugeriu modificações no documento de tese que o candidato deverá efetuar em até 60 dias, sob supervisão da orientadora. A Banca Examinadora reuniu-se em sessão secreta a fim de concluir o julgamento da Defesa de Doutorado, tendo sido o candidato **aprovado** pelos seus membros. Proclamados os resultados pela Profª. Drª. Andrea Rodrigues Chaves, Presidente da Banca Examinadora, foram encerrados os trabalhos e, para constar, lavrou-se a presente ata que é assinada pelos Membros da Banca Examinadora, aos 23 (vinte e três) dias do mês de setembro de 2022 (dois mil e vinte e dois).

TÍTULO SUGERIDO PELA BANCA

Documento assinado eletronicamente por **Andrea Rodrigues Chaves**, **Professor do Magistério Superior**, em 23/09/2022, às 12:45, conforme horário oficial de Brasília, com fundamento no § 3º do art. 4º do Decreto nº 10.543, de 13 de novembro de 2020.

Documento assinado eletronicamente por **Wendell Karlos Tomazelli Coltro**, **Professor do Magistério Superior**, em 23/09/2022, às 12:45, conforme horário oficial de Brasília, com fundamento no § 3º do art. 4º do Decreto nº 10.543, de 13 de novembro de 2020.

Documento assinado eletronicamente por **Andréia de Melo Porcari**, **Usuário Externo**, em 23/09/2022, às 13:45, conforme horário oficial de Brasília, com fundamento no § 3º do art. 4º do Decreto nº 10.543, de 13 de novembro de 2020.

Documento assinado eletronicamente por **Eliana Martins Lima**, **Professora do Magistério Superior**, em 18/11/2022, às 13:42, conforme horário oficial de Brasília, com fundamento no § 3º do art. 4º do Decreto nº 10.543, de 13 de novembro de 2020.

A autenticidade deste documento pode ser conferida no site https://sei.ufg.br/sei/controlador_externo.php?acao=documento_conferir&id_orgao_acesso_externo=0, informando o código verificador **3212712** e o código CRC **6A9BE21D**.

Referência: Processo nº 23070.044595/2022-09 SEI nº 3212712

UFG

UNIVERSIDADE FEDERAL DE GOIÁS
INSTITUTO DE QUÍMICA

DESPACHO

Atesto, na condição de presidente da banca examinadora, conforme o item 04 da instrução normativa da PRPG nº 001, de 27 de março de 2020, que o **Prof. Dr. Christian Janfelt (University of Copenhagen)** participou como membro avaliador da banca examinadora de defesa de doutorado intitulada **"Oral squamous cell carcinoma lipid differentiation in gingiva tissue by mass spectrometry"** do discente Ricardo Alves Bernardo, ocorrida aos 23 (vinte e três) dias do mês de setembro de 2022 (dois mil e vinte dois). Essa declaração se fez necessária em virtude da indisponibilidade da assinatura do professor supracitado no Sistema Eletrônico de Informações (SEI) da UFG.

Profª. Drª. Andréa Rodrigues Chaves (UFG)

Presidente da Banca Examinadora

Documento assinado eletronicamente por **Andrea Rodrigues Chaves**, **Professor do Magistério Superior**, em 08/11/2022, às 10:37, conforme horário oficial de Brasília, com fundamento no § 3º do art. 4º do Decreto nº 10.543, de 13 de novembro de 2020.

A autenticidade deste documento pode ser conferida no site https://sei.ufg.br/sei/controlador_externo.php?acao=documento_conferir&id_orgao_acesso_externo=0, informando o código verificador **3318255** e o código CRC **D91D8F87**.

Referência: Processo nº 23070.044595/2022-09 SEI nº 3318255

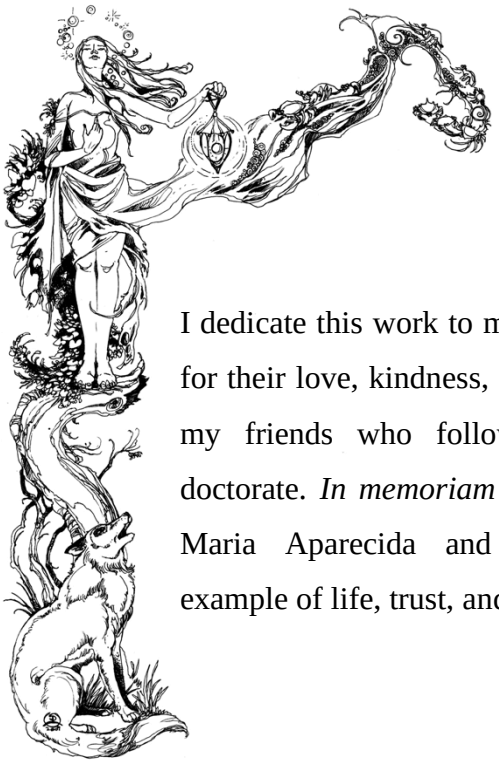

I dedicate this work to my parents and brother for their love, kindness, and support and to all my friends who followed me during my doctorate. *In memoriam* of my grandmothers, Maria Aparecida and Antônia, for their example of life, trust, and encouragement.

ACKNOWLEDGEMENTS

To my Family for all support, love, kindness, and encouragement dedicated to me. Thank you for your patience and understanding in the tough times and the joy in the good times. Thank you so much for the trust, effort, and time dedicated to my growth.

To my supervisor, Profa. Dra. Andréa Rodrigues Chaves, I appreciate all the commitment and trust during my postgraduate period. There have been long and fruitful years of tireless work for me to have a unique academic and personal formation. Thank you very much.

To the professors, Dr. Boniek Gontijo Vaz, Dr. Carlos Arterio Sorgi, Dra. Patrícia Verardi Abdelnur e Dra. Eliana Martins Lima, for all the help and knowledge shared in this project elaboration.

To the professor Dr. Christian Janfelt, for welcoming me with open arms and sparing no effort so that I could have a unique training and learning experience in his research group.

To the professor, Dra. Nádia do Lago Costa, Dr. Virgílio Moreira Roriz and MSc. Germano Angarani, for providing the samples and helping to interpret the histological images. This work would not have gotten so far without their support.

A special thanks to Lanaia Ítala Louzeiro Maciel, who helped me get started with MALDI in our lab and spared no effort to ensure everything went right.

To Raul Izidoro Ribeiro and Daniel Graziani for helping me in the cryosectioning, staining process, and histological image analysis. Thank you very much.

Jussara Valente Roque, thank you very much for helping me with the chemometrics analysis. You were essential for this outcome, and I am profoundly grateful.

To my friends who laughed and cried with me about the sweets and bitters of graduate school life.

To my lab mates, for all those hours of talking, laughing, and sharing knowledge during the coffee break.

To all the patients who accepted to be part of this study and kindly donated the samples.

To anyone who directly or indirectly contributed to my training and this work.

CAPES and FAPEG for the funding provided in this research and exchange period.

“Where there is desire, there is gonna be a flame
Where there is a flame, someone’s bound to get burned
But just because it burns doesn’t mean you’re gonna die
You gotta get up and try… try… try…”

P!nk – Try

RESUMO

O carcinoma oral de células escamosas (OSCC) é o câncer da cavidade oral mais comum, responsável por cerca de 90% dos casos de câncer na região da cabeça-pescoço, com exceção do câncer de pele não-melanoma. Um diagnóstico rápido, preciso e barato é necessário para detectar a presença do OSCC em estágios recentes, aumentando assim, a chance de sucesso no tratamento. Em geral, os diagnósticos são feitos com base em análises proteômicas e histológicas, porém os lipídios desempenham importantes papeis no metabolismo celular. Portanto, entender a diferença lipídica entre tecidos saudáveis e com câncer é importante na predição de candidatos a biomarcadores na tentativa de antecipar o diagnóstico. Com isso, uma nova metodologia para extração simultânea de RNA e lipídios usando solução TRIzol® foi desenvolvida, e o perfil lipídico nos dois grupos de amostras foi estudado. As amostras armazenadas em TRIzol® foram homogeneizadas e submetidas a microextração líquido-líquido (LLME), utilizando clorofórmio como solvente extrator. Em seguida, a fase orgânica foi coletada e submetida à extração Bligh & Dyer. A extração simultânea de RNA e lipídios teve sua performance analítica avaliada de acordo com os parâmetros descritos pela Agência Nacional de Vigilância Sanitária. Para tanto, duas curvas analíticas foram construídas, sendo a primeira preparada utilizando tecido em metanol, e a segunda, tecido em solução TRIzol®. As amostras foram então dopadas com concentrações variáveis de solução padrão de PC 17:0/17:0, e cafeína-(trimetil-^{13}C) utilizada como padrão interno, e introduzidas no sistema de espectrometria de massas por infusão direta no modo positivo de ionização. Ensaios de precisão e exatidão intra e inter-dias, recuperação absoluta e efeito matriz foram avaliados em três níveis de concentração em replicata (n=5). Os limites de detecção e quantificação foram estimados na ordem de ng mL^{-1} com linearidade (r^2> 0,99), precisão e exatidão (< 15%), enquanto os valores de recuperação absoluta variaram de 90 a 110%. Os espectros de massas foram então submetidos à plataforma *Global Natural Product Social Molecular Networking* (GNPS) para anotação de picos. Análise discriminante por quadrados mínimos parciais (PLS-DA) foi realizada para a classificação dos grupos de amostras controle e com câncer. A PLS-DA revelou 15 lipídios responsáveis por descrever o grupo controle e 8 lipídios responsáveis por descrever o grupo com câncer, no modo positivo. Já para o modo negativo, 10 lipídios descreveram o grupo controle e 10 descreveram o grupo com câncer. Para validar a correlação entre os lipídios e as células tumorais, fatias de tecido gengival (controle e com câncer) de 10 µm de espessura foram analisadas por dessorção/ionização a laser assistida por matriz seguido de imageamento por espectrometria de massas (MALDI-MSI). As análises de MALDI-MSI demonstraram que os lipídios avaliados no extrato e responsáveis pela classificação do grupo OSCC estão mais abundantes ao longo do tecido tumoral comparado com o tecido saudável. O método de extração descrito neste estudo, bem como as confirmações realizadas por MALDI-MSI são adequadas para classificação de amostras de OSCC com relação ao seu conteúdo lipídico.

Palavras-chave: Carcinoma oral de células escamosas; Lipídios; LLME; MALDI; Imageamento químico por espectrometria de massas.

ABSTRACT

Oral squamous cell carcinoma (OSCC) is the most common oral cavity cancer, responsible for 90% of all cancers in the head-neck region, except for non-melanoma skin cancer. A fast, accurate, and cheap diagnosis is required to detect the presence of OSCC in the preliminary stages providing better chances of success in cancer treatment. In general, the diagnosis is performed using proteomics and histological data. However, lipids play a key role in cellular metabolism. Therefore, understanding the lipid differentiation between healthy and cancer tissues could be important to predict biomarkers candidates and improve the diagnosis system. Furthermore, a new methodology for simultaneous RNA and lipid extraction using TRIzol® solution was developed, and the lipid profile in both sample groups was studied. The samples stored in TRIzol® solution were homogenized and submitted to liquid-liquid microextraction (LLME) using chloroform as an extractive solvent. Therefore, the organic phase was collected and submitted to the Bligh & Dyer extraction. The simultaneous RNA and lipid extraction was validated according to the parameters described by the Brazilian Nation Health Surveillance Agency. An analytical curve of tissue in methanol and another one of tissue in TRIzol® solution were performed for method evaluation. The sample solutions were spiked with different concentrations of PC 17:0/17:0 standard solution, and caffeine-(trimethyl-^{13}C) was used as the internal standard and directly infused into the mass spectrometer on positive ion mode. Intra-day and inter-day precision, accuracy, absolute recovery, and matrix effect were evaluated in three concentration levels in replicate (n=5). Limits of detection and quantification were estimated in the order of ng mL^{-1} with good linearity ($r^2 > 0.99$), precision and accuracy (< 15%), and absolute recovery values ranging from 90 to 110%. The mass spectra were submitted to the Global Natural Product Social Network (GNPS) platform for peak annotation. The partial least-square discriminant analysis (PLS-DA) was performed in all samples clustering the healthy samples and separating them from the cancer ones. The PLS-DA revealed that 15 lipids were responsible for describing the healthy group in the positive ion mode, while 8 lipids described the cancer one. In the negative ion mode, 10 lipids described the healthy group, while 10 lipids described the cancer one. Furthermore, cryosections of gingiva tissue (healthy and cancer ones) with 10 µm thickness were analyzed by matrix-assisted laser desorption/ionization mass spectrometry imaging (MALDI-MSI) to investigate which lipids pointed by the PLS-DA delimit the cancer region. The MALDI-MSI analyses showed that the lipids responsible for OSCC group classification are more abundant in the cancer tissue compared to the healthy one. The extraction methodology reported here, and the MALDI-MSI as confirmation technique are adequate for classification of OSCC samples regarding lipid content.

Keywords: Oral squamous cell carcinoma; Lipids; LLME; MALDI; Mass spectrometry imaging.

LIST OF FIGURES

Figure 1. Estimated numbers of all HNCs new cases (solid lines) and deaths (dashed lines) from 2020 to 2040 in females aging from 0 to 85+ years old in the Brazilian population 14
Figure 2. Estimated numbers of all HNCs new cases (solid lines) and deaths (dashed lines) from 2020 to 2040 in males aging from 0 to 85+ years old in the Brazilian population 15
Figure 3. Schematic representation of MALDI ion source.....21
Figure 4. Workflow for the total extraction of lipids in samples homogenized in TRIzol® solution 29
Figure 5. In-house matrix application system with electronic speed control 33
Figure 6. MS spectra for extraction performed in TRIzol® (full scan (a) and zooming (b)). The internal standard (800 ng mL^{-1}) is the blue mark, and the PC (17:0/17:0) (2000 ng mL^{-1}) is the green mark in the full scan spectrum.....36
Figure 7. MS spectra for extraction performed in methanol (full scan (a) and zooming (b)). The internal standard (800 ng mL^{-1}) is the blue mark, and the PC (17:0/17:0) (2000 ng mL^{-1}) is a green mark in the full scan spectrum.....37
Figure 8. Full scan mass spectra for positive (a) and negative (b) ion mode of lipid extracts in OSCC and healthy gingiva tissue stored in TRIzol® solution.....42
Figure 9. OSCC and healthy group classification for negative (a) and positive ion mode (b) 44
Figure 10. Importance of selected variables by OPSDA for negative (a) and positive ion mode (b) 45
Figure 11. Positive ion mode MALDI-MSI for ions m/z 760.58500 and 524.37100, colocalization (m/z 760.58500 in red, and 524.37100 in green), and hematoxylin/eosin staining for OSCC sample defrosted during the shippment to Denmark.....48
Figure 12. Negative ion mode MALDI-MSI and DAPI imaging of OSCC and healthy slices for the most important variables selected by the OPSDA model.....49
Figure 13. Positive ion mode MALDI-MSI and DAPI imaging of OSCC and healthy slices for the most important variables selected by the OPSDA model.....50

LIST OF TABLES

Table 1. Biomarkers for the OSCC with their respective matrix, classification, and analytical instrumentation 16
Table 2. Typical MALDI matrices for different polarities and applications 21
Table 3. MALDI source parameters for both positive and negative ion mode for gingiva samples imaging 34
Table 4. Linear regression, determination coefficient (R^2), LOD and LOQ, and their respective p-value in the ANOVA test for lipid extractions performed in TRIzol® and methanol 39
Table 5. Intra and inter-day precision, accuracy, and absolute recovery of the lipid extraction performed in quintuplicate assays using TRIzol® reagent 40
Table 6. Classification parameters for PLS-DA with OPSDA model for negative and positive ion mode 43
Table 7. Peak annotation for the most important variables in OPSDA for OSCC classification 46

LIST OF ABBREVIATIONS

9AA – 9-aminoacridine

A% – accuracy

Ace – average experimental concentration

Acer – 1-0-acyl ceramide

CAPES – Higher Education Personnel Improvement Coordination, from Portuguese: *Coordenação de Aperfeiçoamento de Pessoal de Nível Superior*

CD44 – cluster of differentiation 44

CE – cholesterol ester

Cer – ceramide

CGDB-FO-UFG – Mouth Disease Center in Goiás in Dentistry Faculty of Federal University of Goiás, from Portuguese: *Centro Goiano de Doenças de Boca da Faculdade de Odontologia da Universidade Federal de Goiás*

CHCA – α-cyano-4-hydroxycinnamic acid

CL – cholesterol

DAN – 1.5-diaminonaphthalene

DAPI – 4',6-diamidino-2-phenylindole

DART – direct analysis in real-time

DESI – desorption electrospray ionization

DGTA – diacylglyceryl hydroxymethyltrimethyl-β-alanine

DHB – 2,5-dihydroxybenzoic acid

EIC – extracted ion chromatogram

ELISA – enzyme-linked immunosorbent assay

FA – fatty acid

FN – false negative

FP – false positive

FT-ICR-MS – Fourier-transform ion cyclotron resonance mass spectrometry

GC/FID – gas chromatography with flame ionization detector

GlcCer – glucosylceramide

GNPS – Global Natural Product Social Network

HCC-1 – hemofiltrate CC chemokine 1

HIV – human immunodeficiency virus

HexCer – hexosyl ceramide

HNCs – head-neck region cancers

HPV – human papillomavirus

HSP90 – heat shock protein 90

IL-6 – interleukine-6

IL-8 – interleukine-8

IS – internal standard

ITO – indium tin oxide

LAESI – laser ablation electrospray ionization

LC-MS/MS – liquid chromatography coupled to tandem mass spectrometry

LLME – liquid-liquid microextraction

LOD – limit of detection

LOQ – limit of quantification

LPA – lysophosphatidic acid

LysoPC – lyso-glycerophosphocholine

MALDI – matrix-assisted laser desorption/ionization

MCP-1 – monocyte chemoattractant protein

ME% - matrix effect

mRNA – micro-ribonucleic acid

MS – mass spectrometry

MSI – mass spectrometry imaging

n/v – number of latent variables

NAS – net analyte signal

NSSC – non-spiked sample concentration

nvars – number of selected variables

OCT – tissue-tek optimal cutting temperature compound

OSCC – oral squamous cell carcinoma

P% - precision

PBS – phosphate buffer solution

PC – glycerophosphocholine or phosphocholine

PE – glycerophosphoethanolamine or phosphoethanolamine

PF-4 – platelet factor 4

PG – glycerophosphoglycerol or phosphoglycerol

PGAM1 – phosphoglycerate mutase 1

PI – glycerophosphoinositol or phosphoinositol

PLS-DA – partial least-square discriminant analysis

qRT-PCR – quantitative reverse transcription polymerase chain reaction

R% - absolute recovery

RAC – response in the analytical curve

RCC – response in the calibration curve

REG – regression coefficient

RNA – ribonucleic acid

S100A7 – psoriasin

S100P – S100 Ca-binding protein located on 4p16

SC – sample concentration

SCARA5 – scavenger receptor class A member 5

SM – sphingomyelin

SSC – spiked sample concentration

STD – standard deviation

TC – theoretical concentration

TCNQ – 7,7,8,8-tetracyanoquinodimethane

TG – tri(acyl/alkyl)glycerol

TIC – total ion current

TN – true negative

TNF-α – tumor necrosis factor-α

TOF – time-of-flight mass analyzer

TP – true positive

UPLC-MS – ultra-performance liquid chromatography coupled to mass spectrometry

SUMMARY

1 INTRODUCTION 11

1.1 Oral squamous cell carcinoma 12

1.2 Biomarkers for OSCC 16

1.3 Lipid analysis 17

1.4 Mass Spectrometry Imaging 20

2 OBJECTIVES 26

2.1 General Objective 26

2.2 Specific Objectives 26

3 MATERIALS AND METHODS 27

3.1 Materials 27

3.2 OSCC and healthy gingiva sampling 27

3.3 TRIzol® lipid extraction in pig's tongue 28

3.4 Mass spectrometry analysis for lipid extracts in pig's tongue 29

3.5 Analytical performance evaluation 30

3.6 Mass spectrometry analysis for lipid extracts in gingiva samples 31

3.7 Data processing 31

3.8 MALDI-MSI 32

3.9 Histological staining 34

4 RESULTS AND DISCUSSION 36

4.1 Mass spectrometry analysis of TRIzol® lipid extractions from pig's tongue 36

4.2 Analytical performance 39

4.3 Mass spectrometry in lipid extracts of gingiva samples and data analysis 41

4.4 MALDI-MSI 47

5 CONCLUSION 54

REFERENCES 55

ATTACHMENT 66

1 INTRODUCTION

Cancer is one of the main causes of death and an important barrier to increasing life expectancy worldwide (SUNG; FERLAY; SIEGEL; LAVERSANNE *et al.*, 2021). The cancer metabolism research relies on the principle that metabolic activities are dysregulated in cancer cells compared to normal cells to support malignant properties. Alongside with the advances in cancer research, the mass spectrometry approaches for cancer metabolism studies has enabled a more in-depth comprehensive understanding of cancer progression (MA; FERNÁNDEZ, 2022).

Metabolomics is applied to investigate changes in metabolic pathways, in which disturbed biological systems are compared to undisturbed reference systems. Changes in lipid metabolism and/or RNA transcription can provide information about differential gene and transcript expression patterns in healthy and disease cells/tissues, such as in cancer (VALDES-MORA; HANDLER; LAW; SALOMON *et al.*, 2018; WANG; WANG; LI; HOU *et al.*, 2017), neurodegenerative diseases (FERNANDES; PATIKAS; FOSKOLOU; FIELD *et al.*, 2020; MACÍAS-GARCÍA; PERIÑÁN; MUÑOZ-DELGADO; JIMENEZ-JARABA *et al.*, 2021; OOI; VACY; BOON, 2021), cardiovascular disease (KANEKO; ITOH; KIRIYAMA; KAMON *et al.*, 2021; WIRKA; PJANIC; QUERTERMOUS, 2018), and diabetes (JENKINSON; GÖRING; ARYA; BLANGERO *et al.*, 2016; OJO; OJO; ZAND; WANG, 2021).

Regarding cancer research, many efforts have been made to enhance diagnosis and prognosis since cancer diseases are one of the most health problems worldwide (BRAY; FERLAY; SOERJOMATARAM; SIEGEL *et al.*, 2018). In the literature, plenty of studies investigated biomarkers candidates such as lipids (ISLAM; MANNA, 2019; PARK; COFFEY; LIMOGES; LE, 2018), proteins (FERRARI; PEZZI; CASSI; PERTINHEZ *et al.*, 2021; LEE; WONG; HSIAO; WANG *et al.*, 2018), and mRNA (SUN; CAO; WANG; SONG *et al.*, 2018).

Broadfield and co-workers, 2021 (BROADFIELD; PANE; TALEBI; SWINNEN *et al.*, 2021) reported that multiple mechanisms, proteins, and pathways are involved in the cancer disease to support aberrant cellular replication, dissemination, immune evasion, and secondary tumor establishment. The lipid metabolism is changed in tumor cells to provide energy and plasma membrane synthesis. These changes often lead to dysregulation of fatty acid metabolism, influencing the lipid membrane composition, tolerance to reactive oxygen species, and cancer cell survival. One of the metabolic alterations in cancer is the upregulation of fatty

acid synthesis, which provides phospholipids for cellular membranes to sustain proliferation (RÖHRIG; SCHULZE, 2016).

1.1 Oral squamous cell carcinoma

Oral squamous cell carcinoma (OSCC) is the most common oral cavity cancer, being responsible for 90% of all types of malignancy in the head-neck region cancers (HNCs) except for non-melanoma skin cancer (ALI, 2022; ALVES; DIEL; LAMERS, 2018). The Global Cancer Observatory reported 377,713 new cases and 177,757 deaths related to the OSCC in 2020 (SUNG; FERLAY; SIEGEL; LAVERSANNE *et al.*, 2021).The incidence and mortality trends related to the OSCC in Brazil follow the same pattern reported by the Global Cancer Observatory in 2020 (SUNG; FERLAY; SIEGEL; LAVERSANNE *et al.*, 2021). Figures 1 and 2 show the incidence and mortality of OSCC in Brazil for the next 20 years.

The major risk factors for OSCC include tobacco use in any form (traditional cigarettes, electronic cigarettes, hookah, cigar, pipe tobacco, wet snuff, dry snuff, and chewing tobacco) (ZHANG; HE; HE; HUANG *et al.*, 2019), alcohol use (ABATI; BRAMATI; BONDI; LISSONI *et al.*, 2020), and infection by human papillomavirus (HPV) (RAJ; PATIL; GUPTA; RAJKUMAR *et al.*, 2019). In addition, other risks are considered as additional factors, such as betel quid consumption (YANG; WANG; HUANG; YU *et al.*, 2021), infections by other microorganisms (*Candida*, *Neisseria*, and streptococci) (WANG; GANLY, 2014), dietary factors and nutrients deficiencies (BRAVI; BOSETTI; FILOMENO; LEVI *et al.*, 2013), immunosuppressed conditions (HIV-positive, organ transplant recipients) (ENGELS, 2019), environmental pollutants (CHU; KAO; TANTOH; KO *et al.*, 2019), occupational exposures (AWAN; HEGDE; CHEEVER; CARROLL *et al.*, 2018), and heritable conditions (CHI; DAY; NEVILLE, 2015).

The 5-year survival rate is around 80% when the OSCC is diagnosed in stage 1 and below 40% in stages 3 and 4 (GUALTERO; SUAREZ CASTILLO, 2016), which requires an early diagnosis and treatment to optimize long-term cure and survival. A dentist often makes the OSCC diagnosis during routine appointments. The diagnosis techniques consist of vital staining, tissue fluorescence imaging, chemiluminescence, histological techniques (incisional and excisional biopsy), cytological techniques (oral brush biopsy, liquid-based cytology), molecular analyses (gene alterations, epigenic alterations, viral genome studies, immunohistochemical identification), and imaging techniques (optical coherence tomography) (CARRERAS-TORRAS; GAY-ESCODA, 2015). However, the diagnosis is visual-dependent,

and the diagnosis techniques are applied when the cancer is already developed. Therefore, many studies have been reported aiming at discovering new biomarkers for early-stage diagnosis.

Figure 1. Estimated numbers of all HNCs new cases (solid lines) and deaths (dashed lines) from 2020 to 2040 in females aging from 0 to 85+ years old in the Brazilian population

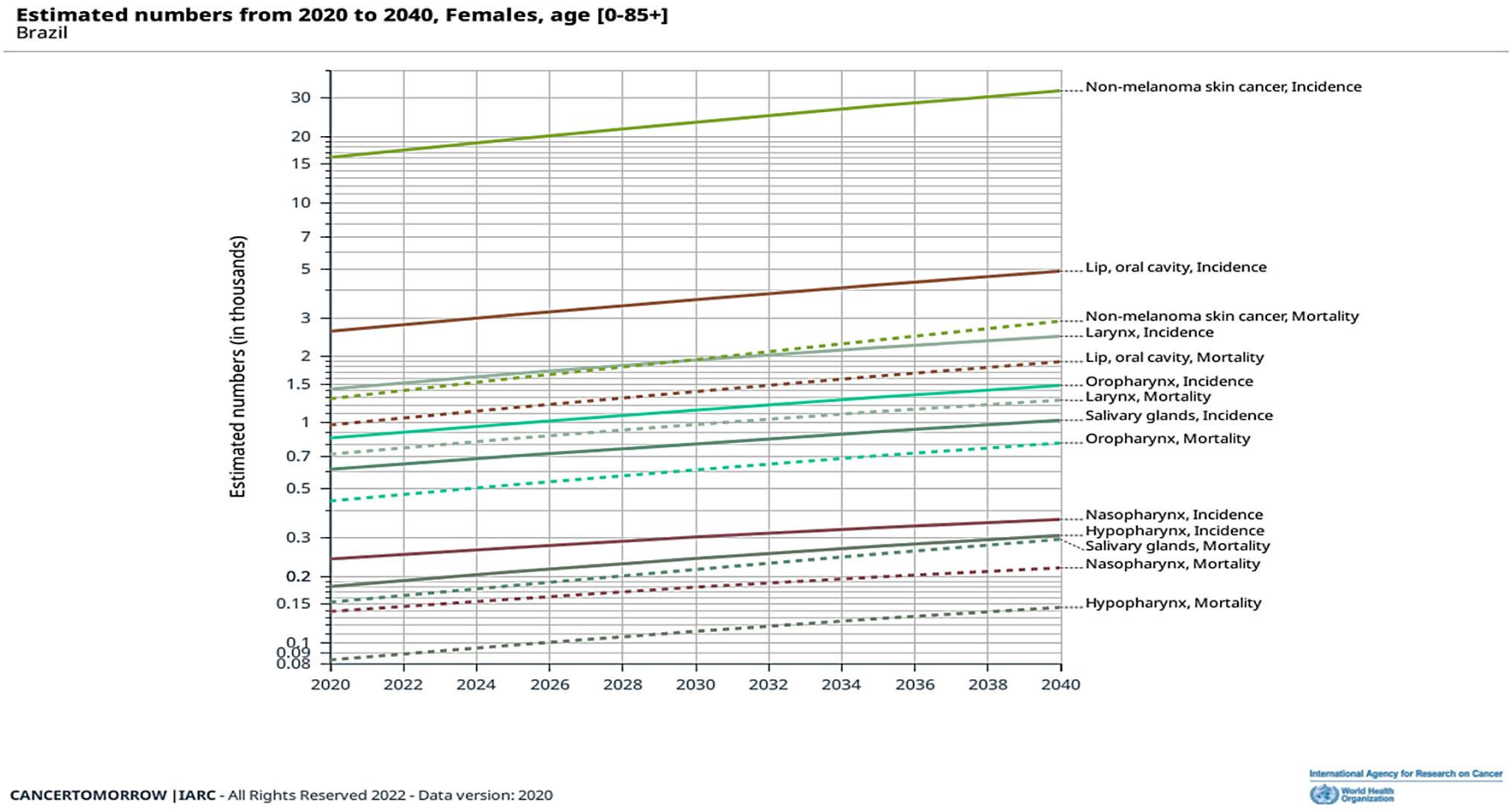

Source: Global Cancer Observatory, accessed July 5th, 2022.

Figure 2. Estimated numbers of all HNCs new cases (solid lines) and deaths (dashed lines) from 2020 to 2040 in males aging from 0 to 85+ years old in the Brazilian population

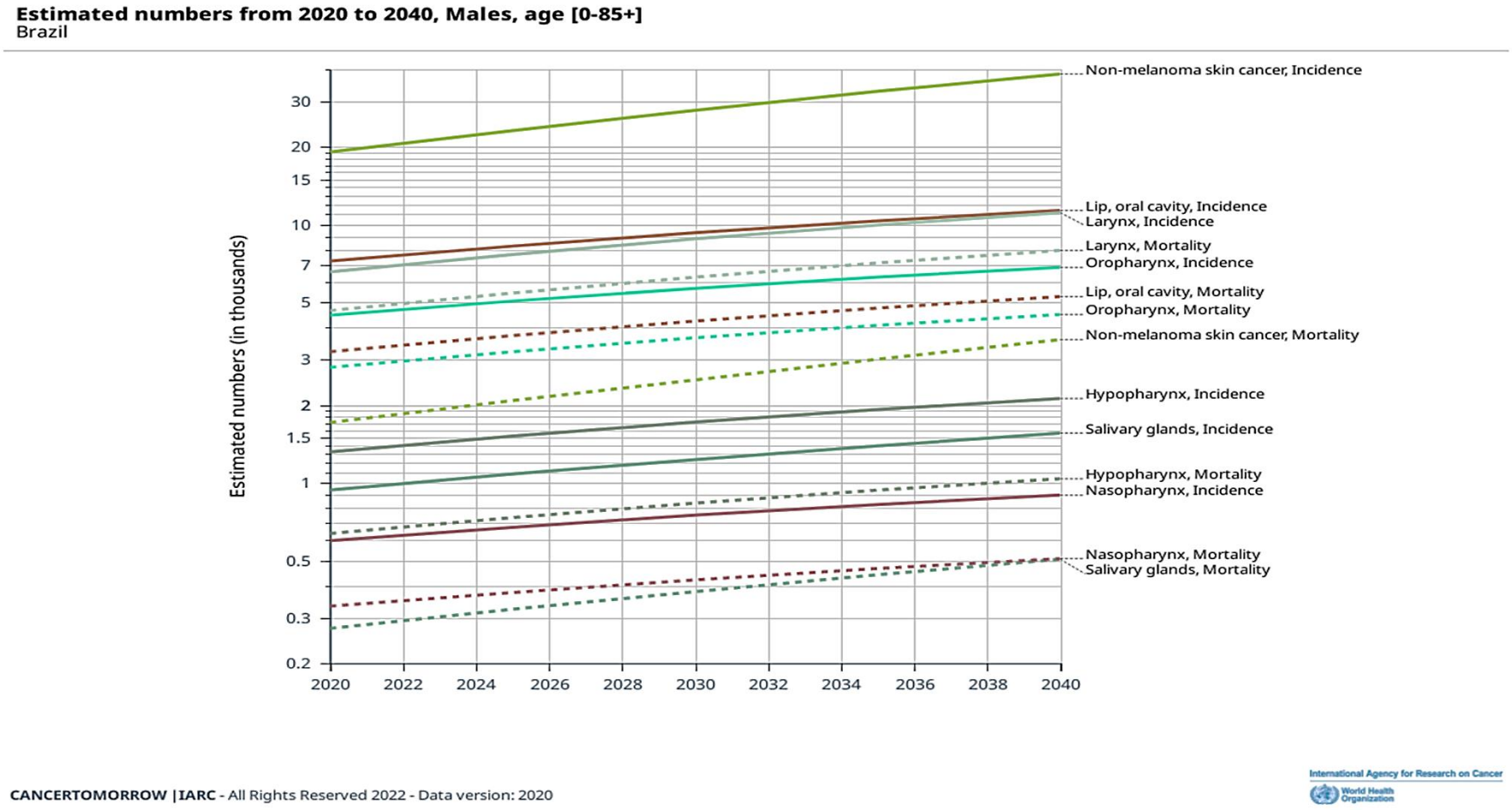

Source: Global Cancer Observatory, accessed July 5th, 2022.

1.2 Biomarkers for OSCC

Biomarkers in cancer research are defined as molecules secreted by tumor cells or a specific body response to the presence of cancer (HUSS, 2015). Table 1 presents few publications from 2017 to 2022 in the oncology, analytical chemistry, pathology, and medicine fields correlating biological matrix, biomarkers, classification, and analytical techniques.

Table 1. Biomarkers for the OSCC with their respective matrix, classification, and analytical instrumentation

Matrix	Biomarker	Classification	Analytical Instrumentation	Reference
Plasma	miR-200b-3p	miRNA	qRT-PCR	(SUN; CAO; WANG; SONG *et al.*, 2018)
Serum	SCARA5	Protein	MALDI-TOF-MS	(LIU; TAN; SUN; JU *et al.*, 2018)
Oral cavity, nasopharynx, laryngopharynx, oropharynx tissues	Vimentin Keratin type II Hsp90 Prelamin-A/C PGAM1	Protein	MALDI-MSI LC-MS/MS Immunohistochemistry	(HOFFMANN; UMBREIT; KRÜGER; PELZEL *et al.*, 2019)
Saliva	CD44 S100A7 S100P	Protein	ELISA	(SIVADASAN; GUPTA; SATHE; SUGHEENDRA *et al.*, 2020)
Plasma	MCP-1 HCC-1 PF-4	Protein	Multiplex Immunoassay	(DIKOVA; JANTUS-LEWINTRE; BAGAN, 2021)
Plasma	9 PC 4 PE 2 Cer 1 GlcCer 1 SM Trihexosylceramide 1 LysoPC 1 PG	Lipid	UPLC-MS	(WANG; WANG; LI; HOU *et al.*, 2017)

miRNA: micro-ribonucleic acid; qRT-PCR: quantitative reverse transcription polymerase chain reaction; SCARA5: scavenger receptor class A member 5; MALDI-TOF-MS: matrix-assisted laser desorption/ionization time-of-flight mass spectrometry; Hsp90: heat shock protein 90; PGAM1: phosphoglycerate mutase 1; CD44: cluster of differentiation 44; S100A7: psoriasin; S100P: S100 Ca-binding protein located on 4p16; ELISA: enzyme-linked immunosorbent assay; MSI: mass spectrometry imaging; LC-MS/MS: liquid chromatography coupled to tandem mass spectrometry; MCP-1: monocyte chemoattractant protein; HCC-1: hemofiltrate CC chemokine 1; PF-4: platelet factor 4; PC: glycerophosphocholine; PE: glycerophosphoethanolamine; Cer: ceramide; GlcCer: glucosylceramide; SM: sphingomyelin; LysoPC: lyso-glycerophosphocholine; PG: glycerophosphoglycerol; UPLC-MS: ultra-performance liquid chromatography coupled to mass spectrometry.

As presented in Table 1, many analytical techniques are used for biomarkers determination in patients diagnosed with OSCC. Most biomarkers reported in the literature are related to gene and protein expression. Lipids also correlate to inflammatory and immune responses, but they play a minor role in this research field. Moreover, the workflow for sample preparation in transcriptomics/proteomics is quite different from lipidomics, and other samples are required for both purposes (PODECHARD; DUCHEIX; POLIZZI; LASSERRE *et al.*, 2018).

Sridharan and co-workers, 2019 applied metabolomics to investigate differences between oral leukoplakia and OSCC by LC-MS. Leukoplakia is one of the major forms of potentially malignant disorder, and it is easily confused with OSCC, and differentiating both diseases is still a challenge. The authors report that dysregulations in metabolic pathways for sphingolipids, carbohydrates, aminoacids, and nucleotide biosynthesis. Moreover, up-regulated levels of salivary metabolites such as galactosyl sphingosine, sphinganine-1-phosphate, pseudouridine, inositol 1,3,4-triphosphate, 4-nitroquinoline-1-oxide, estrone-3-glucuronide, ubiquinone, and amino acid metabolites are involved in oral leukoplakia and OSCC. The authors suggest the LC-MS proposed method as a promising tool in identification of tumor specific biomarkers in early diagnosis.

1.3 Lipid analysis

Lipid analysis can be performed by extracting lipids from a biological matrix (e.g., serum, plasma, whole blood, saliva, tissue) using a total or single lipid extraction or directly analyzed in the sample surface by many mass spectrometry ion sources, such as desorption electrospray ionization (DESI) (UNSIHUAY; SU; HU; QIU *et al.*, 2021), MALDI (LIU; WANG; LIN; LIN *et al.*, 2021), laser ablation electrospray ionization (LAESI) (SHRESTHA; SRIPADI; RESCHKE; HENDERSON *et al.*, 2014), direct analysis in real time (DART) (CODY; MCALPIN; COX; JENSEN *et al.*, 2015).

Regarding the lipid extraction techniques, the most used ones are the Bligh & Dyer method, based on chloroform, methanol, and water liquid-liquid extraction (LLE) (BLIGH; DYER, 1959), Folch method (FOLCH; LEES; STANLEY, 1957), based on chloroform, and methanol LLE, and Matyash method (MATYASH; LIEBISCH; KURZCHALIA; SHEVCHENKO *et al.*, 2008), based on methyl *tert*-butyl ether (MTBE), methanol and water LLE. Those methods are employed to total lipid extraction since they are not specific to any lipid class. However, in the literature, some methods are reported for specific lipid classes, such

as the extraction of sphingolipids (XU; LI; HAN; WANG *et al.*, 2022) and eicosanoids (YAMADA; KITA; KOHIRA; YOSHIDA *et al.*, 2015).

Podechard and co-workers, 2018, developed a methodology for dual extraction of RNA and lipids from the same sample using TRIzol® solution and Bligh & Dyer extraction (BLIGH; DYER, 1959) for the extraction and analysis of triglycerides (TG), cholesterol (CL), cholesterol esters (CE), and fatty acids (FA) by gas-liquid chromatography technique. However, no data about precision, accuracy, and recovery is presented. The authors evaluated the RNA portion by real-time quantitative polymerase chain reaction (qPCR), and the paper's discussion focuses on RNA expression. TRIzol® solution is a commercially available reagent for RNA extraction, and the authors evaluated the lipids extracted during the RNA extraction with TRIzol®.

The lipid extracts used to be often analyzed by gas chromatography with a flame ionization detector (GC/FID), liquid chromatography coupled to tandem mass spectrometry (LC-MS/MS), and direct infusion into the mass spectrometer equipment. FAs exhibit low volatility and strong polarity and require methyl ester derivatization prior to GC/FID analyses (WU; ZHANG; LI; PU *et al.*, 2017). LC-MS/MS has been reported as a sensitive and selective method for arachidonic acid and its metabolites and eicosanoids analyses in various biological matrices (CHHONKER; KANVINDE; AHMAD; SINGH *et al.*, 2021; DU; HU; AN; LI *et al.*, 2020).

The direct infusion of lipid extracts into the mass spectrometer (known as shotgun lipidomics) has been widely used for targeted and untargeted lipidomics (HSU, 2018). Compared to GC/FID and LC-MS/MS, the advantages of shotgun lipidomics are high throughput analysis in a shorter time since it does not require chromatographic separation and the possibility to detect individual species of any targeted lipid classes at the level of instrumentation sensitivity direct from lipid extracts of biological samples (HU; DUAN; HAN, 2020). This strategy improves the analytical throughput in routine analyses, in which a substantial number of samples can be analyzed in a shorter period. Once no separation is performed, no analyte or sample volume are lost during this step. However, it is susceptible to ion suppression, loss of sensitivity, and resolving isobaric/isomeric masses issues once endogenous matrix compounds can be not fully removed during the sample preparation step and remaining during MS analysis, inferring onto MS method results.

Matthiesen and co-workers, 2021 (MATTHIESEN; LAUBER; SAMPAIO; DOMINGUES *et al.*, 2021) applied shotgun lipidomics for lipid profile evaluation in plasma samples from inflammatory diseases patients, such as cardiovascular and ischemic stroke and systemic lupus erythematosus. The authors claimed that the time invested per sample is a barrier

to large-scale clinical validation when chromatographic separations are used prior to mass spectrometry. According to them, a lipid extraction based on a mixture of plasma, water, MTBE, ethanol, and ammonium bicarbonate was performed, and 623 lipids spanning 15 lipid classes were identified and quantified, and 596 of these lipids were used for cardiovascular and ischemic stroke, and systemic lupus erythematosus classification.

Zeissig's group reported a lipid profile evaluation in colorectal cancer tissue using shotgun lipidomics mass spectrometry. In their study, the frozen cancer tissue was homogenized in isopropanol, and the lipid extraction was performed using MTBE, methanol, and water. Even though the authors observed a modest increase in phosphoethanolamine (PE), lyso-phosphatidylinositol (LPI), and ceramide (Cer) abundance, and a decrease in lyso-phosphocholine (LPC) and lyso-phosphoethanolamine (LPE), the lipid profile between normal and cancer tissue did not change, but the tri(acyl/alkyl)glycerol (TG) content strongly varied between samples (WANG; HINZ; UCKERMANN; HÖNSCHEID *et al.*, 2020).

Many advances in shotgun lipidomics have been made regarding extraction techniques, derivative methods (if necessary), and bioinformatics developments, as well advances in commercially available mass spectrometers improved shotgun lipidomics strategies (WANG; WANG; HAN; HAN, 2016). A lipid class which is ion-suppressed by other abundant lipid class(es) can still be identified and quantified if the ion suppression process occurs in a constant concentration, but the lipid class/specie to be identified and quantified must be sensitively ionized or produce specific fragments ions. Derivatization steps are also used to add a polar group enhancing the ionization of individual molecular species, improving the analytical signal and quantification assays (WANG; WANG; HAN; HAN, 2016).

As reported by Wang and Han, 2019 (WANG; HAN, 2019), the goal of lipidomic analysis is to achieve full and precise coverage of structural analysis, accurate quantification, and comprehensive understanding of lipid dynamics at all levels. Surma and co-workers, 2015 (SURMA; HERZOG; VASILJ; KLOSE *et al.*, 2015) reported an automated shotgun lipidomics platform for quantitative analysis of blood plasma intact lipids. The authors normalized the de-isotoped intensity of the monoisotopic peak of endogenous species (lipids) to the de-isotoped intensity of the monoisotopic peak of the internal standard of the same lipid class. The authors state that the analysis is fully automated, and high throughput shotgun-lipidomic methods for screening of plasma samples was reported.

There are two analytical challenges for shotgun lipidomics: precise determination of structural information, and accurate quantification of low-to-modest abundance lipids. LIPID MAPS reports that the concentration range of lipids in a biological sample can vary from amol

to nmol/mg of protein. Moreover, due to the ion suppression by high abundant species during ionization, the accurate quantification is limited. However, specific lipid classes extractions, selective ionization methods, pre-separation techniques, and derivatization strategies enhances the analytical signal for low abundant lipids, improving the accuracy for quantification (WANG; HAN, 2019)

Another lipid analysis approach that has emerged as a versatile technique for lipidomic studies, providing valuable information about the spatial localization of lipids in anatomical structures and abundance of lipid species is the mass spectrometry imaging (ABBAS; NOUN; TOUBOUL; SAHALI *et al.*, 2019).

1.4 Mass Spectrometry Imaging

Mass spectrometry imaging (MSI) emerged as a powerful technique for the morphological characterization of biological structures, providing information about the spatial localization of lipids, proteins, amino acids, and hormones. Among the MSI ion sources, DESI and MALDI are the most used for this purpose.

DESI, as introduced by Cooks and co-workers in 2004 (TAKÁTS; WISEMAN; GOLOGAN; COOKS, 2004), consists of a charged spray directed to the sample, which is placed on an insulating surface. In the DESI procedure, the formation of a primary spray occurs with charged solvent droplets and high-pressure gas (usually N_2) ablating the sample surface. Therefore, the analytes are desorbed by the spray impact onto the sample. Then, a secondary spray if formed containing the sample's analyte that were desorbed by the primary spray. The desorbed ions are guided to the mass spectrometer by a high voltage applied between the sprayer and the mass spectrometer inlet. Regarding imaging assays, the image resolution is directly related to the droplet size formed by the primary spray, charge, solvent composition, and focus of the electrospray (GREEN; SALTER; GILMORE; STOKES *et al.*, 2010).

Regarding MALDI, the ionization process occurs in two steps (Figure 3): the analyte is first dissolved in an organic matrix with high absorption in the laser wavelength. The mixture is dried, and any liquid solvent used in the solution (matrix+analyte) is removed. The second step involves ablating bulk portions of this solid solution by intense laser pulses over a short duration (DREISEWERD, 2003; KARAS; KRÜGER, 2003; KNOCHENMUSS, 2003).

Figure 3. Schematic representation of MALDI ion source

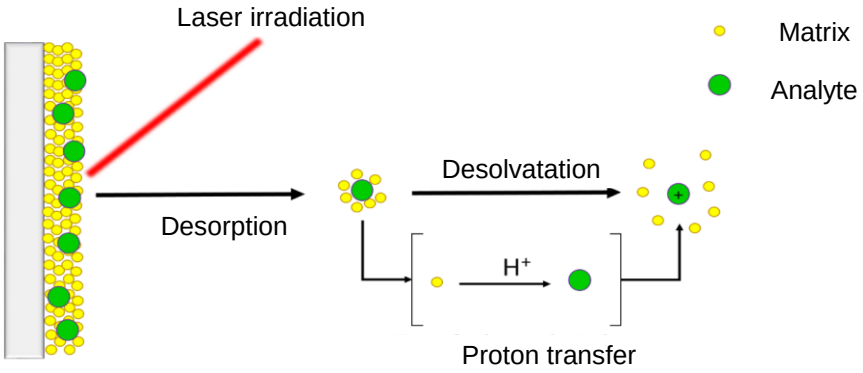

Source: (DE HOFFMANN; STROOBANT, 2007).

The choice of the matrix for MALDI is essential for ionization success once that the matrix promotes the analyte ionization/desorption, and it depends on ionization mode, molecular class, and laser absorption. This method is characterized by simple sample pre-treatment and wide tolerance to salts, buffers, and detergents (CHEN; CARROLL; BEAVIS, 1998; STUMP; FLEMING; GONG; JABER *et al.*, 2002). A list of typical MALDI matrices is presented in Table 2.

Table 2. Typical MALDI matrices for different polarities and applications

Matrix	Ionization mode	Typical application	References
DHB	Positive and negative	Drugs, lipids, peptides, oligosaccharides	(MONTINI; CROCOLL; GLEADOW; MOTAWIA *et al.*, 2020)
CHCA	Positive	Drugs, peptides, oligonucleotides	(BEAVIS; CHAUDHARY; CHAIT, 1992)
9AA	Negative	Lipids, drugs, nucleotides	(ANGELINI; VITALE; PATIL; COCCO *et al.*, 2012)
DAN	Negative and positive	Amino acids, lipids	(ELLIS; BROWN; IN HET PANHUIS; BLANKSBY *et al.*, 2013)
Sinapic acid	Positive	Proteins, polypeptides	(LEE; YEOH; OMAR; PUNG *et al.*, 2021)
2-mercaptobenothiazole	Positive	Lipids	(GARATE; FERNÁNDEZ; LAGE; BESTARD-ESCALAS *et al.*, 2015)
TCNQ	Positive	Designer drugs	(DE ALMEIDA; PINTO; DOS SANTOS; DE SOUZA *et al.*, 2019)

DHB: 2,5-dihydroxybenzoic acid; CHCA: α-cyano-4-hydroxycinnamic acid; 9AA: 9-aminoacridine; DAN: 1,5-diaminonaphthalene; TCNQ: 7,7,8,8-tetracyanoquinodimethane.

The matrix also minimizes the analyte damage from the laser ablation, absorbing most of the incident energy and enhancing the energy transference efficiency from the laser to the analyte. This enhancement makes MALDI one of the most sensitive and universal techniques once the matrix absorbs the laser and not the analyte (HOSSEINI; MARTINEZ-CHAPA, 2017). Even though the MALDI matrix selection is based on the laser wavelength, the analyte class and molecular mass can also affect the mass spectra. Therefore, they must meet several requirements simultaneously, such as strong absorption at the emission wavelength of the laser, low enough mass to be sublimable, vacuum stability, ability to promote analyte ionization, solubility in solvents compatible with analyte/sample, lack of chemical reactivity, and the crystallization between the matrix and analyte should be as homogeneous as possible (LEOPOLD; POPKOVA; ENGEL; SCHILLER, 2018).

Consequently, MALDI can systematically analyze a tissue cryo-section evenly covered by a matrix in defined space intervals. This makes it possible to correlate a specific ion's intensity with its origin region. If all spectra were positioned on coordinated *x* and *y* axis, and the intensity of each ion related to the *z-axis*, it is possible to translate these intensities into a color-code, generating a visual contrast. This principle is known as MALDI mass spectrometry imaging (MALDI-MSI).

For the MALDI-MSI assay, the MALDI matrix is applied over the sample surface, and then, a focused laser beam is directed to the sample surface, which moves in steps to scan the sample according to the intended lateral resolution of the system. The laser pulses desorb/ionize the material located in the laser focus. The matrix absorbs the laser energy and promotes the analyte ionization and desorption. The mass spectra obtained after the analysis is transformed into a grayscale value and plotted according to the pixel map at the position currently interrogated by the laser beam. Therefore, the image for a specific *m/z* peak can be created by displaying the peak's intensity into a color-code in every pixel (HILLENKAMP; PETER-KATALINIC, 2013).

Comparing DESI-MSI and MALDI-MSI, both techniques provide spatial information with high chemical specificity of analytes in a sample. MALDI and DESI operate in different ionization techniques, consequently they have some unique advantages. Imaging experiments with MALDI generate high spatial resolution (pixel size < 10 µm), while DESI often works with 100 µm pixel size (HE; PU; WANG; ZHANG *et al.*, 2022). MALDI has de advantage of high spatial resolution, Spengler's group reported a MALDI imaging at a resolution of 1.4 µm using an atmospheric pressure MALDI source (KOMPAUER; HEILES; SPENGLER, 2017).

Another MALDI advantage is the capability of spatial evaluation of high molecular weight analytes, such as proteins (LEINWEBER; TSAPRAILIS; MONKS; LAU, 2009). On the other hand, DESI has as advantages the absence of ion suppression by matrix peaks, and the simplest sample preparation for mass spectrometry imaging (HE; PU; WANG; ZHANG *et al.*, 2022).

MALDI imaging has been reported in the detection of lipid biomarkers in cancer diseases (HOLZLECHNER; EUGENIN; PRIDEAUX, 2019), especially in melanoma (NABI; MAMUN; ISLAM; HASAN *et al.*, 2021), prostate cancer (BUSZEWSKA-FORAJTA; POMASTOWSKI; MONEDEIRO; KRÓL-GÓRNIAK *et al.*, 2022), colon cancer (GARATE; MAIMÓ-BARCELÓ; BESTARD-ESCALAS; FERNÁNDEZ *et al.*, 2021), and oral cancer (BEDNARCZYK; GAWIN; CHEKAN; KURCZYK *et al.*, 2019).

Noh and co-workers 2019 (NOH; KIM; PARK; KIM *et al.*, 2019) evaluated the chronic kidney disease and renal-aging-related changes in lipid levels. The authors state that sphingolipids and arachidonic acid play a key role in the kidney aging metabolism once their spatial distribution is altered during aging. Mas and co-workers, 2020 (MAS; TORRO; FERNÁNDEZ; BEC *et al.*, 2020) used MALDI-MSI to evaluate highly similar colorectal tumors. The authors report that the tumor microenvironment is heterogeneous due to the cancer cell clonal evolution and microenvironment composition, and differences due to genetic variations between patients suffering of the same pathology. The authors developed an advanced multivariate data processing pipeline based on partial least-square discriminant analysis (PLS-DA) for classification of similar colorectal tumors. The study reports high levels of correct classification (sensitivity: 0.92; specificity: 0.77).

Klein and co-workers, 2019 (KLEIN; KANTER; KULBE; JANK *et al.*, 2019) employed MALDI imaging for classification of epithelial ovarian cancer subtypes. The authors state that MALDI imaging technique alongside with linear discriminant analysis, support vector machines, and neutral networks and convolutional neural networks was efficient for classification of four subtypes of epithelial ovarian cancer by means of proteomic studies.

The literature also reports studies about investigating lipid profile changes in mice brain under a high fat diet (SIGHINOLFI; CLARK; BLANC; COTA *et al.*, 2021). The authors reported a slight variation of PC 38:5 and PC 40:5 between obese mice and controls for the LC-MS/MS positive ion mode. They also reported that phosphatidylserine (PS 36:1 and PS 38:1) and PI 34:1 and PI 36:1 varied between the two mice groups. These results were corroborated by MALDI-MSI assays, where all lipid variations were overexpressed in diet-induced obese mice.

Moreover, some matrix improvements have been reported to enhance MALDI-MSI sensibility and image resolution, such as the use of Michler's ethylketone as a negative ion matrix for lipid analysis (SHI; HU; HAO; WU *et al.*, 2022), *N*-phenyl-2-naphthylamine as the matrix for small-molecule metabolites imaging (LIU; ZHOU; WANG; XIONG *et al.*, 2018), and 3-aminophtalhydrazide (also known as luminol) as a dual-polarity matrix for detection and imaging of 159 and 207 metabolites in mouse brain on positive, and negative ion mode respectively (LI; SUN; GORDON; GE *et al.*, 2019).

The matrix application is a critical step for MALDI-MSI, since the matrix must desorb and ionize sample components. An extraction procedure occurs when the matrix interacts with the sample surface, incorporating the analytes into the matrix crystals. Therefore, the matrix crystal size must be as uniform as possible, and the analyte migration should be limited, preserving the spatial integrity of the sample. (RÖMPP; SPENGLER, 2013).

The matrix can be applied onto the sample surface by spraying a concentrated matrix solution, which can be performed in a heated chamber (dry spray), or it can be performed at room temperature (wet spray). Another matrix application method includes matrix sublimation and subsequent recrystallization, which provides smaller crystals and a better uniformity in crystal size when compared to spray methods, with MALDI imaging spatial resolution at 1 – 2 µm (RÖMPP; SPENGLER, 2013). Many matrix application systems are commercially available, operating by means of dry spray, wet spray (e.g. ImagePrep – Bruker Daltonics, Germany; and iMatrixSpray – Tardo Gmbh, Switzerland).

High mass resolution combined with high spatial resolution of 7 µm was performed in a Fourier-transform ion-cyclotron-resonance mass spectrometer (FT-ICR-MS), but the sensitivity was not sufficient (KOESTLER; KIRSCH; HESTER; LEISNER *et al.*, 2008). The spatial resolution must be compatible with the laser focus diameter in MALDI-MSI. Mass spectrometry imaging assays of low abundant molecules with high spatial resolution often leads to low sensitivity, since there are not enough analytes in the defined special area to be desorbed and analyzed (RÖMPP; GUENTHER; SCHOBER; SCHULZ *et al.*, 2010). Regarding image resolution, the spatial and image resolution will be the same if no oversampling is observed during the MSI assay. To check if the oversampling is present in a MALDI-MSI assay, an optical image of the tissue covered with MALDI matrix must be evaluated, and the adjacent ablation spots must be well-spaced at a distance of the spatial resolution (e.g. 20 µm between adjacent ablation spots, and 20 µm between of spatial resolution).

The development of high mass resolving instruments provided more accuracy and sensitivity for current metabolomics techniques. Instruments such as Q-TOF, TripleTOF and

FT-ICR-MS have been widely used in high-mass resolution metabolomics studies (DUSHIANTHAN; POSTLE, 2021; OYENIYI; SORGI; GARDINASSI; AZEVEDO *et al.*, 2022). Time-of-flight analyzers can reach up to 80,000 resolution power, while the FT-ICR-MS equipment can reach up to 1,000,000 resolution power. Furthermore, high mass resolution is required for shotgun lipidomics due to the lack of chromatographic separation, the high mass resolution increases the confidence of analysis (ZÜLLIG; KÖFELER, 2021).

2 OBJECTIVES

2.1 General Objective

Development and analytical performance evaluation of lipid extraction in samples stored in TRIzol® solution for the lipid study of OSCC gingiva tissue conserved in TRIzol® by direct infusion mass spectrometry and lipid distribution comparison of fresh frozen tumor and healthy tissues by MALDI-MSI.

2.2 Specific Objectives

- ❖ Development and analytical performance evaluation of an extraction procedure of lipids in samples stored in TRIzol® solution;
- ❖ Application of the developed extraction method in human gingiva samples;
- ❖ Extract analyses by direct infusion mass spectrometry in both positive and negative ion mode;
- ❖ Statistical evaluation of lipid profile changes between the healthy and cancer group;
- ❖ Evaluation of lipid distribution in cancer regions by MALDI-MSI.

3 MATERIALS AND METHODS

3.1 Materials

TRIzol® solution was acquired from Invitrogen (Cergy Pontoise, France). 2,5-dihydroxybenzoic acid (DHB), 1,5-diaminonaphthalene (DAN), 1,2-diheptadecanoyl-sn-glycero-3-phosphocholine (PC 17:0/17:0) (> 99%), 4′,6-diamidino-2-phenylindole (DAPI), Fluoromount-G^{TM}, caffeine-(trimethyl-^{13}C) (99%), trifluoroacetic acid (≥99%) were acquired from Sigma Aldrich (Massachusetts, USA). Pre-column cartridge SecurityGuardTM ULTRA (UHPLC C18, 2,1 mm i.d.) was acquired from Allcrom (São Paulo, Brazil). Chloroform (99,8%) was acquired from Synth (São Paulo, Brazil). Methanol (>99.9%), acetonitrile (>99.9%), and isopropanol (>99.9%) were acquired from Tedia (Ohio, USA). Ultra-purified water was prepared in an MS2000 system (Gehaka, São Paulo, SP, Brazil). Tissue-Tek optimal cutting temperature (OCT) was acquired from Sakura Finetek USA, Inc. (California, USA).

For the analytical performance evaluation of the extraction procedure, pig's tongue samples were used as a biological matrix. The tongues were acquired in the local butcher market in Goiânia-GO, Brazil, right after the slaughter and immediately frozen at -80 °C.

3.2 OSCC and healthy gingiva sampling

The healthy and OSCC diagnosed gingiva samples were kindly donated by the Faculdade de Odontologia of Universidade Federal de Goiás, in collaboration with Professor Dra. Nádia do Lago Costa, and Professor Dr. Virgílio Moreira Roriz.

The OSCC tissues (n = 20) were collected during the lesion biopsy procedure, and healthy gingiva (n = 10) were collected during the extraction of totally impacted third molars (approximately 5 x 5 x 5 mm). The gingival tissues were collected using sterile Punch Keyes (6 mm i.d.), weighted, and immediately stored in TRIzol® solution at a rate of 1 mL of TRIzol® for each 100 mg gingival tissue (for lipid extraction) and frozen at -80 °C. The sample for MALDI-MSI (n = 1) was fresh-frozen at -80 °C. Before the sample collection, the patients signed the free-consent form (Attachment I). The samples were collected following the ethical principles of Universidade Federal de Goiás (Ethical committee n° 19414019.7.0000.5083 – Attachments 1 and 2), and they were submitted to standard tests for diagnosis confirmation at Faculdade de Odontologia.

Patients with clinical diagnosis for OSCC were recruited, attended, and diagnosed at Centro Goiano de Doenças de Boca da Faculdade de Odontologia da Universidade Federal de Goiás (CGDB-FO-UFG – from Portuguese: Mouth Disease Center in Goiás in Dentistry

Faculty of Federal University of Goiás). The inclusion criteria were patients clinically healthy (healthy group) attended in routine surgical clinic of Faculdade de Odontologia – Universidade Federal de Goiás for extraction of totally impacted third molars, older than 18 years old. Regarding the OSCC patients, the inclusion criteria were patients older than 18 years old, with a primary diagnosis for OSCC, and lesion size bigger than 1 cm to do not compromise the histopathological evaluation. The exclusion criteria were previously treated patients (chemotherapy, radiotherapy, etc.), relapsed lesions, and OSCC and healthy patients with comorbidities, such as autoimmune disease, HIV-positives, altered renal function, congestive heart failure, active infection, and a positive diagnosis for hepatitis.

3.3 TRIzol® lipid extraction in pig's tongue

The lipid extractions were performed on pig's tongue for analytical performance evaluation. Therefore, a solution of pig's tongue in TRIzol® was prepared in the proportion of 1 mL of TRIzol® for each 100 mg of the tongue, and then, the mixture tongue+TRIzol® was homogenized in an Ultra Turrax Homogenizer T25 (IKA, Campinas, Brazil). Therefore, 200 µL of chloroform were added for each 1 mL of tongue solution in TRIzol®. The solution was homogenized by vortex for 1 min and centrifuged at 1500 *g*, 4 °C for 10 min.

A three-phase system was formed, composed of an upper layer (aqueous phase containing RNA), a protein pellet, and a lower layer (organic phase I, composed mostly of lipids in chloroform). Moreover, an aliquot of 250 µL of the organic phase I was taken, PC (17:0/17:0) was added in a concentration range from 300 to 2000 ng mL^{-1}. Caffeine-(trimethyl-^{13}C) was added as internal standard (IS) at a concentration of 800 ng mL^{-1}, and an adapted Bligh & Dyer extraction, as reported by Barbosa and co-workers, 2022 (OYENIYI; SORGI; GARDINASSI; AZEVEDO *et al.*, 2022), was performed on it.

For the adapted Bligh & Dyer extraction methodology, 500 µL of methanol and 200 µL of ultrapurified water were added to 250 µL of the organic phase I in a conic vial. The solution was then vortexed for 1 min and centrifuged at 1500 *g*, 4 °C for 10 min, and another 250 µL of chloroform and 250 µL of ultrapurified water were added to the centrifuged solution. The system was then vortexed for 1 min and centrifuged one more time at 1500 *g*, 4 °C for 10 min. Another three-phase system was formed (aqueous phase, protein pellet, and organic phase II). The organic phase II was collected in a vial flask, and 500 µL of chloroform were added into the mixture of the aqueous phase and protein pellet to enhance the extraction efficiency. This solution was then vortexed and centrifuged again as described above, and the resulting organic phase (organic phase III) was collected and mixed with the organic phase II.

The mixture of organic phases II and III was evaporated in a SpeedVac Concentrator (Savant SPD131DDA, Thermo Scientific – Massachusetts, USA), and the dried extract was resuspended in 200 µL of methanol. The same extraction was performed using a pig's tongue homogenized in methanol for comparison with extraction using TRIzol® solution. The whole extraction process is illustrated in Figure 4.

Figure 4. Workflow for the total extraction of lipids in samples homogenized in TRIzol® solution

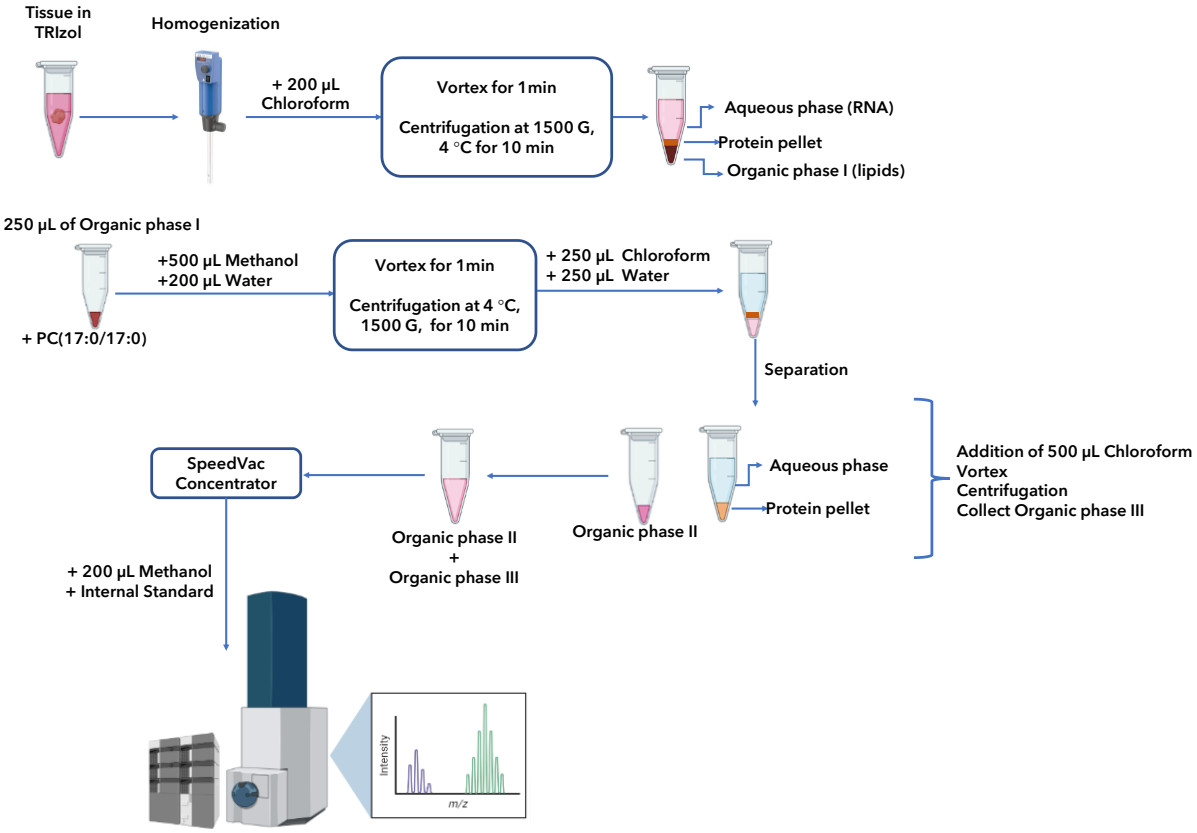

Source: Own authorship.

The gingiva samples were prepared as described above in the Faculdade de Farmácia of Universidade de São Paulo, Ribeirão Preto. However, the internal standards used for this procedure were PC 17:0, PE 17:0, PG 17:0 PS 17:0, and Cer 17:0 at a concentration of 100 ng mL^{-1}, and a mixture of isopropanol:acetonitrile:methanol:water (3:3:3:1) with ammonium formate at 5 x 10^{-4} mol L^{-1} was used to resuspend the dried extracts.

3.4 Mass spectrometry analysis for lipid extracts in pig's tongue

The extracted pig's tongue samples were analyzed by direct infusion mass spectrometry (MS). A liquid chromatographer (Shimadzu LC-20AD) was used as an automatic injector into

the mass spectrometer at a methanol flow rate of 300 µL min^{-1}, a sample volume of 40 µL, sample tray temperature at 4 °C and a pre-column cartridge SecurityGuardTM ULTRA (UHPLC C18, 2,1 mm i.d.) were used, with 10 minutes of acquisition time. No carry over between the analyses was observed, once the samples were completely eluted after 4 minutes. The mass spectrometry analyses were performed in a Bruker Daltonics micrOTOF III (Bremen, Germany) with an electrospray ion source (ESI) in positive ion mode. The parameters used for the MS analysis were capillary voltage 4 kV, nebulizer 1.0 Bar, dry temperature 200 °C, and end plate offset 500 V.

3.5 Analytical performance evaluation

The analytical performance of the extraction in TRIzol® proposed in this study was investigated. Linearity was evaluated by an analytical curve using replicates (n = 5) of PC (17:0/17:0) at 330, 500, 800, 1100, 1400, 1700, and 2000 ng mL^{-1} *versus* the extracted ion chromatogram (EIC) area and treated by the ANOVA statistical technique. Caffeine-(trimethyl-^{13}C) was used as the internal standard (IS) at the concentration level of 800 ng mL^{-1}. The ratio between the EIC area of PC (17:0/17:0) and IS was used as an analytical response.

Intraday precision (P%), accuracy (A%), and absolute recovery (R%) were determined using quintuplicate essays of the proposed method of samples at 800, 1400, and 2000 ng mL^{-1} as shown in Equations 1 – 3.

$$P\% = \frac{STD}{ACe} . 100 \qquad \textbf{Equation 1}$$

$$A\% = \frac{ACe - TC}{TC} . 100 \qquad \textbf{Equation 2}$$

$$R\% = \frac{SSC - NSSC}{SC} . 100 \qquad \textbf{Equation 3}$$

Where STD means the standard deviation in the concentrations determined experimentally, ACe corresponds to the average experimental concentration between the replicates, TC stands for theoretical concentration, SSC corresponds to the spiked sample concentration, NSSC to the non-spiked sample concentration, and SC means the spiked concentration (BERNARDO; DA SILVA; QUEIROZ; VAZ *et al.*, 2019).

The limits of detection (LOD) and quantification (LOQ) were experimentally determined with diluted concentrations of PC (17:0/17:0) up to the signal-to-noise ratio of about 3.3 and 10, respectively. The matrix effect (ME%) was evaluated in three concentration levels (800, 1400, 2000 ng mL^{-1}) and was estimated as described by Equation 4.

$$ME\% = \left(\frac{RAC}{RCC}\right) . 100 \qquad \textbf{Equation 4}$$

where RAC means the response (ratio between EIC PC (17:0/17:0) and IS areas) in the analytical curve (extraction performed in the presence of TRIzol®), and RCC means the response (ratio between EIC PC (17:0/17:0) and IS areas) in calibration curve (extraction method using methanol as TRIzol® replacement).

3.6 Mass spectrometry analysis for lipid extracts in gingiva samples

The lipid extracts in gingiva samples were analyzed on an AB Sciex TripleTOF 5600+ (California, USA) equipped with an ESI ion source in both negative and positive ion mode in MS/MS^{All} assays with a mass range from *m/z* 200 – 1200 Da, with 50 ms accumulation time and mass resolution of 35,000 at *m/z* 956. The MS/MSAll analysis automatically acquire MS/MS spectra with a precursor selection window of 1 Da for the selected mass range, providing 100% MS/MS spectra coverage for the whole mass range scanned. The parameters for positive ion mode were spray voltage, 5 kV; turbo ion spray temperature, 100 °C; nebulizer gas, 30 psi; turbo-gas, 30 psi; curtain gas, 20 psi; declustering potential, 80 V; collision energy, 46 eV. The parameters for negative ion mode were spray voltage, -4.5 kV; turbo ion spray temperature, 100 °C; nebulizer gas, 30 psi; ; turbo-gas, 30 psi; curtain gas, 20 psi; declustering potential, -80 V; collision energy, -50 eV; accumulation time 0.200 s.

3.7 Data processing

The mass spectra for the extracts in gingiva samples were processed on AB Sciex PeakView software version 2.2, and peak annotation was performed on AB Sciex LipidView software version 1.2 considering the full scan spectra and the fragmentation spectra (error < 10 ppm). For the negative ion mode analysis, the *m/z* peaks were annotated regarding free fatty acids, methyl esters, ethyl esters, cholesterol esters, and ceramides. For the positive ion mode, the *m/z* peaks were annotated regarding sphingolipids, mono/di/triacylglicerides, and phospholipids. Therefore, the raw data was converted to .mzML using the ProteoWizard

software (CHAMBERS; MACLEAN; BURKE; AMODEI *et al.*, 2012) and uploaded to the Global Natural Product Social Network (GNPS) for peak annotation confirmation (WANG; CARVER; PHELAN; SANCHEZ *et al.*, 2016).

The raw data were also exported to .txt files using the PeakView software and processed on MatLab R2020a for multivariate calculations. A threshold of 3% (relative intensity) was applied for data reduction/noise subtraction. The mass spectra acquired on MS/MS^{All} analysis were organized in an $X_{(n,m)}$ matrix, with n = 26 and 29 samples placed in the rows (negative and positive ion mode, respectively), and the m = 1000 *m/z* peaks (for both positive and negative ion mode) were the independent variables in the columns, and the values in this matrix were the peak intensities for each *m/z* peak. The PLS-DA was used to build the classification model (once the sample groups were already known) for both types of gingiva, healthy and confirmed with OSCC ones. The data were separated into training (67%) and test (33%) sets using the Kennard and Stone algorithm ((KENNARD; STONE, 1969)) for each class. Random cross-validation was applied, where splits were set at 10% of the training set. Autoscaling was applied as pre-treatment in both OSCC and healthy gingiva analysis sets. All calculations were performed in Matlab R2020a (Math Works, Natick, USA).

Ordered predictors selection adapted for classification models (OPSDA) (ROQUE; CARDOSO; PETERNELLI; TEÓFILO, 2019; WARTHA; DE AGUIAR PORTO; TOMAZ; ROQUE *et al.*, 2022) was performed to find more interpretative variables and improve the classification methods, enhancing specificity and selectivity. The classification methods were evaluated regarding sensitivity, specificity, and classification error as presented in Equations 5 to 7.

$$\text{Sensitivity} = \frac{\text{TP}}{\text{TP+FN}} \qquad \textbf{Equation 5}$$

$$\text{Specificity} = \frac{\text{TN}}{\text{TN+FP}} \qquad \textbf{Equation 6}$$

$$\text{Error} = \frac{\text{FP+FN}}{\text{TP+TN+FP+FN}} \qquad \textbf{Equation 7}$$

Where TP is the true positive, TN the true negative, FP is the false positive, and FN false negative.

3.8 MALDI-MSI

In the first phase of this study, an exchange Ph.D. fellowship was funded by Coordenação de Aperfeiçoamento de Pessoal de Nível Superior (CAPES – n°

88881.361841/2019-01), and the training on MALDI-MSI technique was performed under the supervision of Prof. Dr. Christian Janfelt, at the Toxicology and Drug Metabolism Group – University of Copenhagen. The gingiva samples were shipped from Brazil to Denmark, but the shipping took longer than expected, and all tissue samples arrived defrosted at the destination. Therefore, the defrosted tissues were for MALDI-MSI protocol practicing.

The gingiva tissue for both OSCC and healthy group fresh frozen at -80 °C were embedded on OCT and mounted on a Leica CM3050 S Cryostat (Leica Microsystems A/S, Germany) for cryosectioning at -21 °C and 10 µm thickness. Therefore, the tissue slices were transferred to indium tin oxide (ITO) glass slides and stored at -80 °C for MALDI assays.

The glass slides were dried under a vacuum for 10 min, and the MALDI matrix was applied to them (DHB for positive ion mode and DAN for negative ion mode). DHB solution 30 mg mL^{-1} in methanol:water (70:30) with 1% of trifluoroacetic acid or DAN solution 3.3 mg mL^{-1} in methanol:water (90:10) were sprayed over the tissue slice at a flow rate of 300 µL min^{-1} and nebulizer gas at 2 bar using an in-house sprayer. During the matrix covering, the glass slide was kept under rotation at 300 rpm, using an in-house spin coater built as described by Blaskievicz and co-workers, 2021 (BLASKIEVICZ; SOARES; MASCARO, 2021). The matrix application system is shown in Figure 5.

Figure 5. In-house matrix application system with electronic speed control

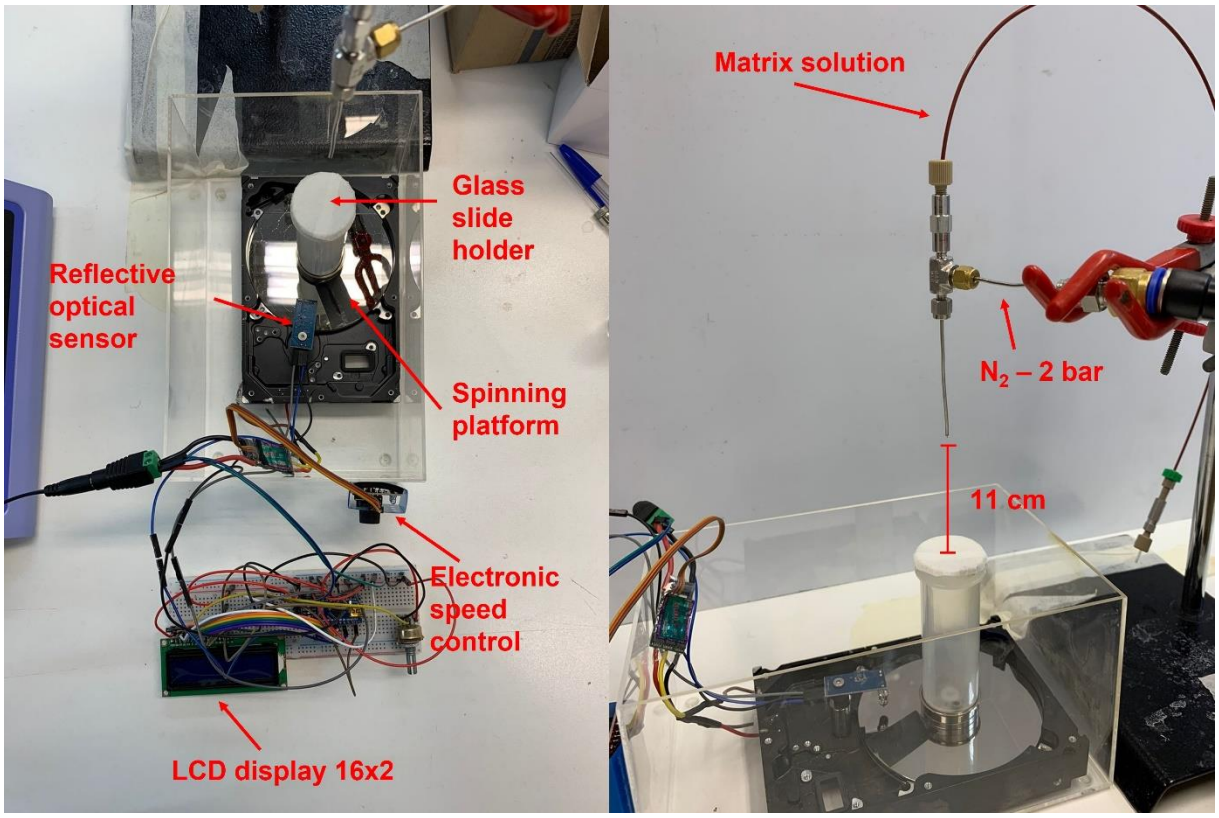

Source: Own authorship.

The MALDI-MSI assays were performed using positive and negative ion mode on a Fourier-transform ion cyclotron resonance mass spectrometer (FT-ICR-MS) 7 T solariX 2xR (Bruker Daltonics, Bremen, Germany) equipped with commercially available MALDI ion source with YAG laser (355 nm wavelength). The MALDI parameters for both positive and negative ion modes are described in Table 3, and they were optimized for the best average intensity in the mass spectra. The magnitude-mode spectra were acquired with a 1 MW transient size, 2 ω detection with 1 scan in the mass range from 150 to 1200 Da, and mass resolving power of 100,000@*m/*z404.93123.

Table 3. MALDI source parameters for both positive and negative ion mode for gingiva samples imaging

Parameters	Positive ion mode	Negative ion mode
Laser power	60%	50%
Laser shots	210	210
Frequency	1000 Hz	1000 Hz
Plate offset	100 V	-100 V
Deflector plate	220 V	-220 V
Data reduction factor	99%	99%
Lock mass	409.055408	311.130220

The MALDI images were acquired with a pixel size of 50 µm, and no oversampling was observed between adjacent ablation spots. The mass spectra were processed on flexImaging 5.0 (Bruker Daltonics, Bremen, Germany), normalized by total ion current (TIC) using a bin width of 0.001 Da.

3.9 Histological staining

The histological staining was performed following the DAPI protocol according to the manufacturer's instructions. The glass slides with tissue cryosections were washed three times with phosphate buffer solution (PBS) (0.1 mol L^{-1}. pH 7.4) for 10 min each. Then, the slides were covered with DAPI solution (1 µg mL^{-1} in PBS) for 15 min and washed three times again with PBS for 10 min. After washing, the slides were mounted with Fluoromount-G^{TM} and left to rest overnight, protected from the light, and then analyzed by confocal microscopy.

The confocal microscopy was performed at Laboratório Multiusuário de Avaliação de Moléculas, Células e Tecidos (LabCel) at Escola de Medicina Veterinária e Zootecnia – Universidade Federal de Goiás. The tissue slices were analyzed on a confocal microscope TCS

SP8 DMi8 (Leica Microsystems A/S, Germany) equipped with HC PL APO 10x/0.40 objective. The product generated by the reaction with DAPI probe was excited with diode laser 405 at 410 nm, and the measured fluorescence emission intensity at 360 nm.

4 RESULTS AND DISCUSSION

4.1 Mass spectrometry analysis of TRIzol® lipid extractions from pig's tongue

The lipid extracts for pig's tongue were directly infused into the micrOTOF III mass spectrometer in positive ion mode using the LC automatic injector. The peak annotation was performed by exact mass with mass error below 25 ppm. The extracts presented contents of phosphocholines (PC), ceramides (Cer), phosphoethanolamines (PE), betaine lipids (diacylglyceryl hydroxymethyltrimethyl-β-alanine – DGTA), lysophosphatidic acid (LPA), and phosphoserine (PS), as shown in Figures 6 and 7.

Figure 6. MS spectra for extraction performed in TRIzol® (full scan (a) and zooming (b)). The internal standard (800 ng mL^{-1}) is the blue mark, and the PC (17:0/17:0) (2000 ng mL^{-1}) is the green mark in the full scan spectrum

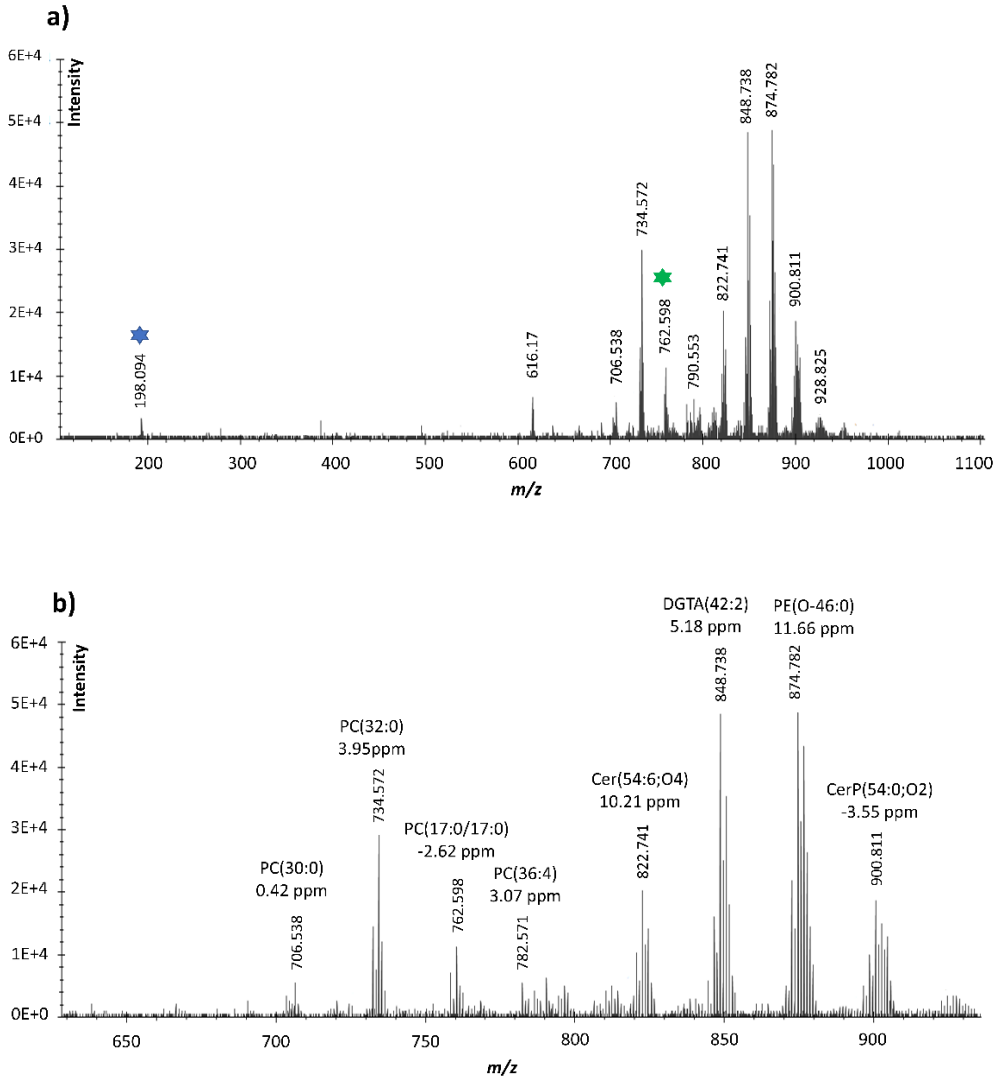

Source: Own authorship.

Figure 7. MS spectra for extraction performed in methanol (full scan (a) and zooming (b)). The internal standard (800 ng mL^{-1}) is the blue mark, and the PC (17:0/17:0) (2000 ng mL^{-1}) is a green mark in the full scan spectrum

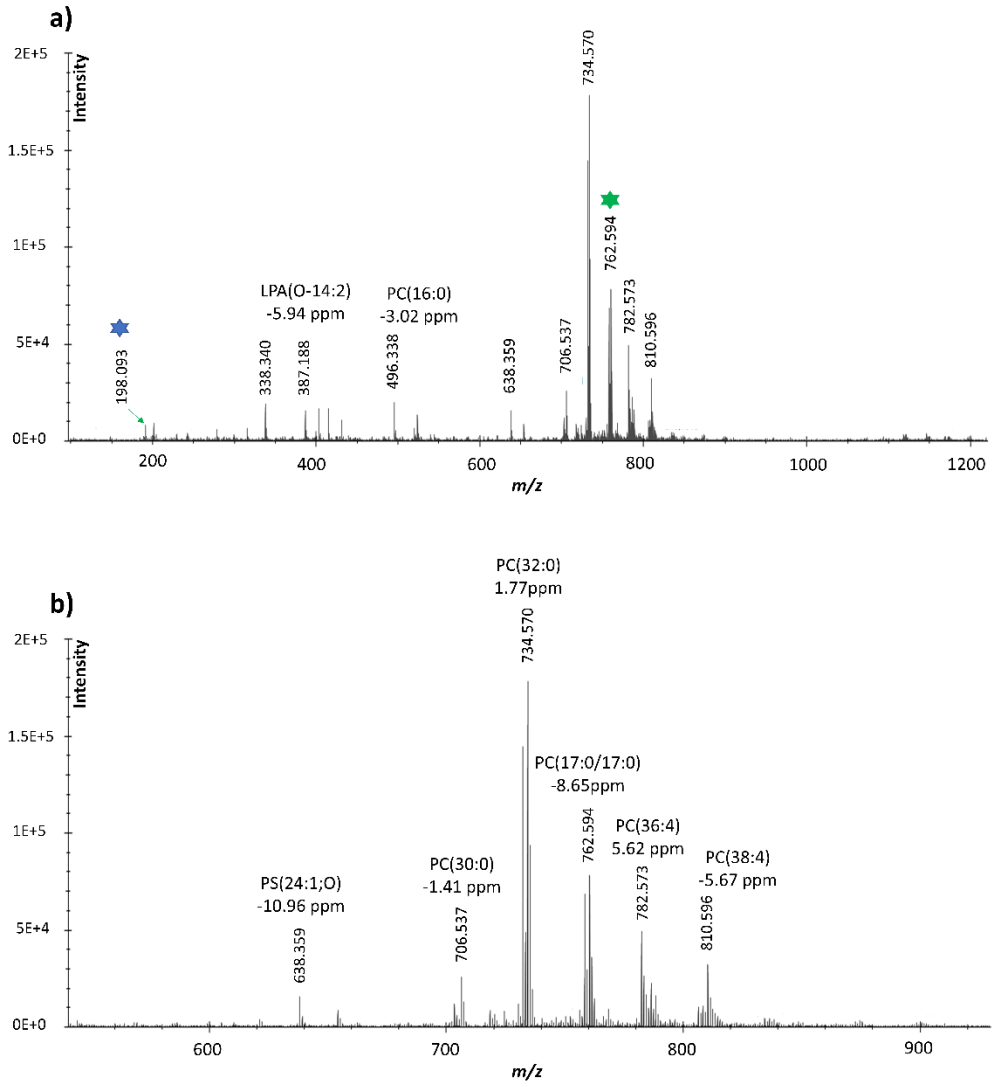

Source: Own authorship.

Comparing the Figures 6a. and 7a., it is possible to observe that spectrum intensity in the extractions performed in methanol was higher than the spectrum intensity for extractions using TRIzol®. However, the extractions in TRIzol® presented a significant enhancement in the spectral signal considering the mass range from 800 to 1000 Da. This is interesting once the lipids intensities were improved when compared with the intensities in the methanolic extracts spectra. To the best of our knowledge, this effect could be due to the phenol content present in the TRIzol® that promotes better extraction efficiency for lipids with a molecular mass higher than 700 Da. The TRIzol® solution is used for mRNA extraction and promotes cellular lysis, which is clearly observed when the tissue is being homogenized. The tissue instantly crumbles

during this process, and the homogenized solution becomes more viscous. On the other hand, when methanol is used for tissue homogenization, the resulting solution remains with small tissue pieces that did not completely crumble.

Both extraction methods were able to extract PC contents from the biological matrix. TRIzol® extraction stands out regarding lipids with higher molecular weight (mass range 600-1000 Da) and low abundant lipids, such as ceramides (ULMER; JONES; YOST; GARRETT *et al.*, 2018), were efficiently extracted and detected. Moreover, PE and DGTA were also present in the TRIzol® extraction and absented in the classic extraction using methanol. The extraction performed in methanol stands out regarding lipids with lower molecular weight, such as PA and PC, in the mass range of 300-500 Da. However, in the present study, the extractions in methanol only presented contents of PCs and PAs, which represents lower information regarding important lipids that already have been related to many diseases, such as Cer in cancer research (MARKOWSKI; BŁACHNIO-ZABIELSKA; GUZIŃSKA-USTYMOWICZ; MARKOWSKA *et al.*, 2020; SCALINCI; LUGARESI; SCOROLLI; RALLI *et al.*, 2020), and betaine role in inflammatory response (ZHAO; HE; WU; LI *et al.*, 2018).

Regarding the mass spectrometry analysis of lipid extracts, high resolution mass spectrometry based on Fourier-transform (Q-Exactive hybrid quadrupole-Orbitrap, and FT-ICR-MS) or quadrupole-time of flight instruments providing selectivity for the analysis at the cost of sensitivity and time of analysis (SCHUHMANN; THOMAS; ACKERMAN; NAGORNOV *et al.*, 2017; SCHWUDKE; SCHUHMANN; HERZOG; BORNSTEIN *et al.*, 2011; WANG; WANG; HAN; HAN, 2016). As previously reported (LIEBISCH; BINDER; SCHIFFERER; LANGMANN *et al.*, 2006; LIEBISCH; DROBNIK; LIESER; SCHMITZ, 2002), shotgun lipidomics using a syringe or a HPLC pump with isocratic flow combined with an autosampler (also called loop injection) minimizes sample carryover from previous injections, which is a drawback of the classical “continuous infusion” when a lot of samples are subjected to analysis sequentially. The loop injection requires a minimal amount of sample and mobile phase, since 5 to 50 µL of sample solution can be submitted to a nanoflow rate. Loop injection without chromatographic separation also provides speed, automation, and is suitable all the analysis. According to Hsu, 2018 (HSU, 2018), this method coupled to high resolution/tandem mass spectrometry provides a very simple and robust setup for lipidomic analysis. In the present study, no carryover effects were observed between the analysis.

Podechard and co-workers, 2018 (PODECHARD; DUCHEIX; POLIZZI; LASSERRE et al., 2018) reported that the TRIzol® lipid extraction protocol has several benefits compared to the classical methods. At first, it reduces time and reagent consumption, and most

importantly, this protocol reduces the amount of sample required for multiomics assays. In this thesis, it was observed an easier tissue homogenization process using TRIzol®, as well as the extraction/analysis of low abundant lipids. Moreover, this extraction protocol allows transcriptomics and lipidomics assays from the same biological sample.

4.2 Analytical performance

Sample preparation is one of the most important steps to the successful analyses of lipids in biological samples by mass spectrometry. For this reason, the lipid extraction protocol using TRIzol® solution was submitted to analytical performance evaluation. The linearity was evaluated in analytical curves using the PC (17:0/17:0) concentration *versus* the ratio between the EIC area for PC (17:0/17:0) over the EIC area for the IS and processed by ANOVA statistical technique of lipid extractions performed in TRIzol® solution, and methanol (Table 4). The method was linear in a concentration range from the LOQ to 2000 ng mL^{-1}, with $R^2 > 0.99$. Once the p-values in ANOVA for the extractions performed in TRIzol® and methanol were lower than 0.05, it is possible to conclude that the slopes in the linear regression for both analytical curves are significantly different from zero.

The limits of detection and quantification were experimentally determined as described in the Methods section by diluted solutions up to the signal-to-noise ratio about 3 for LOD, and 10 for the LOQ. The extraction protocol using TRIzol® solution presented lower values for LOD and LOQ than the extraction performed in methanol, which means that the proposed method in this thesis presents good sample cleanup and consequently results in a more sensitive protocol for lipid extractions than the classic extraction performed in methanol.

Table 4. Linear regression, determination coefficient (R^2), LOD and LOQ, and their respective p-value in the ANOVA test for lipid extractions performed in TRIzol® and methanol

Extraction method	Linear regression (LOD:2000 ng mL^{-1})	R^2	LOD (ng mL^{-1})	LOQ (ng mL^{-1})	ANOVA p-value
TRIzol®	y = 0.0188x + 0.3385	0.9927	110	330	5.32E-09
Methanol	y = 0.0083x + 9.5071	0.9911	160	475	2.84E-07

R^2: determination coefficient; LOD: limit of detection; LOQ: limit of quantification.

The precision and accuracy for both extractions were evaluated in intra and inter-day assays performed in quintuplicate at three concentration levels: 800, 1400, and 2000 ng mL^{-1}. The results for precision, accuracy, and recovery are in accordance with the values described

by the Food and Drug Administration (FDA) and the Brazilian National Health and Surveillance Agency (ANVISA), precision and accuracy values below 15%, and recovery values ranging from 80 to 120% (SWARTZ; KRULL, 2018), Table 5.

Table 5. Intra and inter-day precision, accuracy, and absolute recovery of the lipid extraction performed in quintuplicate assays using TRIzol® reagent

Homogenate Solvent	Concentration (ng mL^{-1})	Precision (%)		Accuracy (%)		Absolute Recovery (%)
		Intra-day	Inter-day	Intra-day	Inter-day	
TRIzol®	800	3	5	-8	-10	92
	1400	2	1	3	2	103
	2000	2.	2	2	3	102
Methanol	800	8	6	2	1	102
	1400	5	2	-1	-2	98
	2000	3	2	4	2	104

The ME can be evaluated by comparing the parallelism between the analytical curve of TRIzol® samples and the calibration curve in methanol (ZHOU; YANG; WANG, 2017) or calculation of recovery values by adding standard solutions to real pieces (STEINER; KRSKA; MALACHOVÁ; TASCHL *et al.*, 2020). As described in the Methods section, the ME was estimated by Equation 4. For the three concentration levels evaluated here (800, 1400, and 2000 ng mL^{-1}), the ME estimation was 96, 104, and 102%, respectively. It is possible to conclude that no matrix effect was observed in these analyses since the calculated values ranged from 80 to 120% (RAPOSO; BARCELÓ, 2021). In addition, the absolute recovery values for both curves are sufficiently high enough (92 – 104 - Table 5), which means that the response of the proposed method cannot be significantly affected by the sample matrix; in this case, the solvent for homogenate preparation prior to extraction. Additionally, since the TRIzol® solution promotes cellular lysis for RNA extraction, we also can conclude that the cellular components present in the TRIzol® homogenate do not significantly affect the lipid response in the mass spectra when comparing to the methanolic homogenate.

Many studies on total lipid extractions are reported in the literature for optimizing the solvent extraction ratios in well-established protocols. Ulmer and co-workers, 2018 (ULMER; JONES; YOST; GARRETT *et al.*, 2018) optimized sample-to-extraction solvent ratios in Folch, Bligh & Dyer, and Matyash methods for lipid extractions in human plasma. The authors claimed that Bligh & Dyer and Folch methods yielded higher peak areas regardless of the solvent extraction volume. In contrast, Matyash methods require larger extraction solvent volumes to yield comparable results. The authors also stated that the 1:20 sample to extraction

solvent ratio resulted in higher extraction efficiency (for liquid matrices), where some low abundant lipids (such as ceramides and phosphoinositides) were better extracted. Comparing the sample-to-extraction solvent in Bowden's study, the authors used a proportion of 5% (v/v) for liquid biological matrices. In the present study, a ratio of 10 (% wt.) was used, and equivalent results were achieved.

Wang and co-workers 2017 (WANG; WANG; LI; HOU *et al.*, 2017) performed a lipid extraction from plasma for lipid profiling and diagnostic biomarkers for oral squamous cell carcinoma. The authors do not state a name for their extraction protocol; however, it is quite like the Matyash method, using methanol, water, and MTBE. Their study extracted glycerophosphoglycerols (PGs), PCs, PEs, LPAs, Cers, and sphingomyelin (SM). However, the authors did not report any quantification assay or analytical parameter data. In the present study, the analytical performance for the TRIzol® lipid extraction is reported; most lipid species represent PCs, as reported by Wang's study. Sorvina et al., 2018 (SORVINA; BADER; CAPORALE; CARTER *et al.*, 2018) used the Folch method for lipid extraction in prostate cancer cell lines. The authors used LC-MS/MS and analyzed free cholesterol, cholesteryl esters, PC, PE, SM, and gangliosides. In addition, the methodology presented in this thesis allows the possibility of transcriptomics assays since the RNA is extracted with TRIzol® in the first extraction step, as reported by Podechard et al. 2018 (PODECHARD; DUCHEIX; POLIZZI; LASSERRE *et al.*, 2018).

Wang and co-workers, 2016 (WANG; WANG; HAN; HAN, 2016) emphasized that is difficult to achieve good recovery values for every lipid class, leading to an inaccurate measurement of the lipid content in a sample. Aiming to minimize this effect, at least one internal standard should be added to quantify a specific lipid class of interest.

4.3 Mass spectrometry in lipid extracts of gingiva samples and data analysis

The mass spectrometry assays of lipid extracts in gingiva samples were performed in a TripleTOF using an ESI ion source in both negative and positive ion mode in MS/MS^{All} assays with a mass range from *m/z* 200 – 1200 Da, as described in the Materials and Methods section. A comparison of the full scan of OSCC and healthy samples are presented on Figure 8.

The lipid extracts exhibited differences in the intensity values and *m/z* peaks. The OSCC group presented higher intensity values than the healthy one, as well as *m/z* peaks there are absent in the healthy group. This pattern was observed in both positive and negative ion modes.

The PLS-DA with OPSDA model were applied to the processed data for classification in two groups, OSCC, and Healthy group. To this aim, the raw mass spectra were converted

from .wiffi to .txt files by the AB Sciex PeakView. Therefore, a 3% absolute intensity threshold was applied to the data and submitted to MatLab R2020a software for chemometric analyses. Sensitivity, specificity, and classification errors were calculated for both groups. The parameters for classification using the models of PLS-DA with OPSDA for positive and negative ion modes are presented in Table 6.

Figure 8. Full scan mass spectra for positive (a) and negative (b) ion mode of lipid extracts in OSCC and healthy gingiva tissue stored in TRIzol® solution

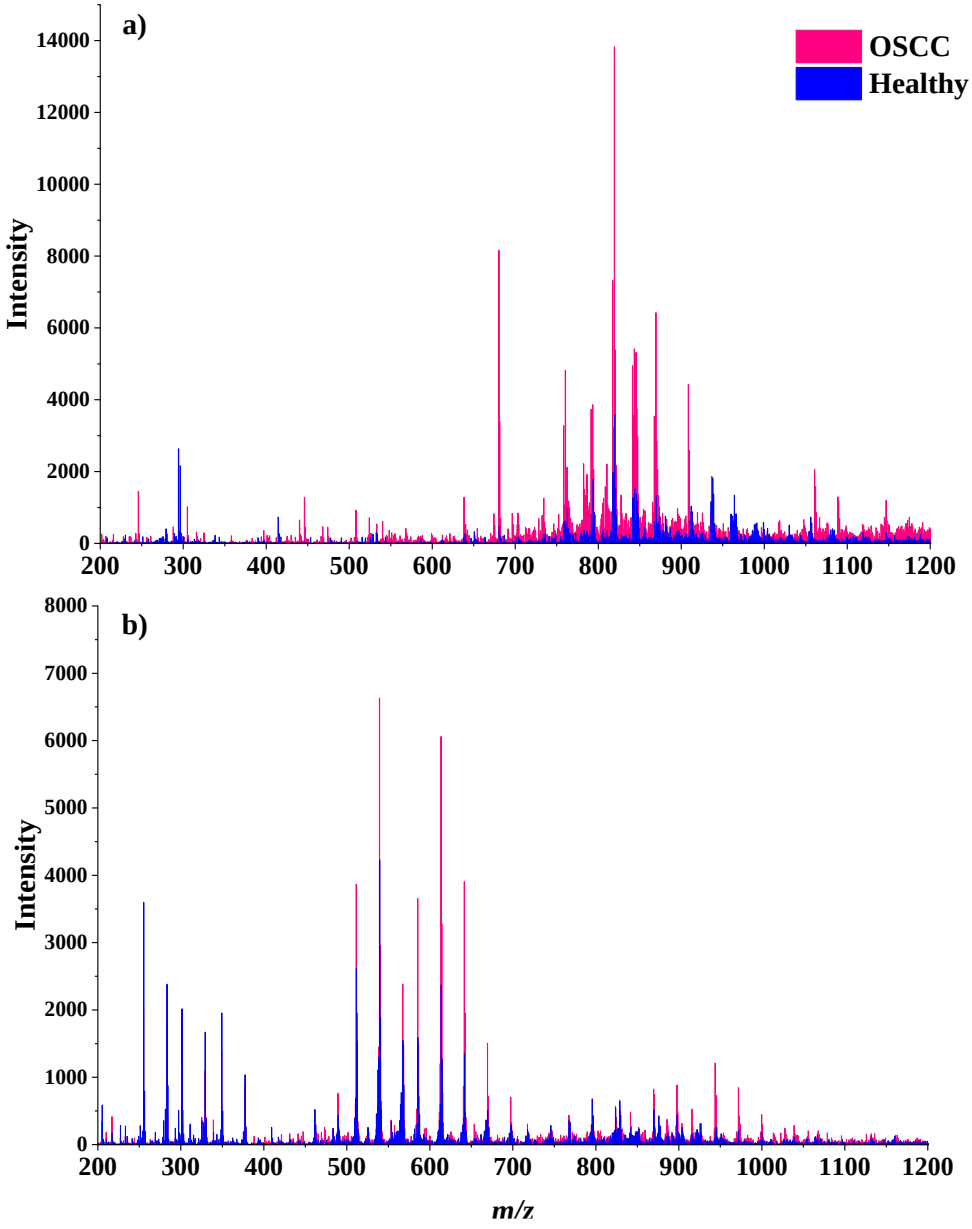

Source: Own authorship.

Table 6. Classification parameters for PLS-DA with OPSDA model for negative and positive ion mode

		Negative ion mode		**Positive ion mode**	
		Healthy	**OSCC**	**Healthy**	**OSCC**
	Samples	9	17	9	20
	n/v	8		9	
	nvars	15	15	20	15
	Vec	NAS		REG	
Training	Sensitivity	1.000	1.000	1.000	1.000
	Specificity	1.000	1.000	1.000	1.000
	Error	0.000	0.000	0.000	0.000
Test	Sensitivity	1.000	1.000	1.000	1.000
	Specificity	1.000	1.000	1.000	1.000
	Error	0.000	0.000	0.000	0.000

n/v: number of latent variables; nvars: number of selected variables; vec: informative vector; NAS: net analyte signal; REG: regression coefficient.

It is possible to observe that all samples were classified correctly in their respective groups (error = 0, sensitivity and specificity = 1.000). The samples were classified in relation to the OSCC classification. The threshold is determined by using a normal probability density function, and Bayers decision (PÉREZ; FERRÉ; BOQUÉ, 2009), all samples above the dashed line (threshold) are classified as OSCC group, and all the samples below the threshold do not belong to this class/group (Figure 9).

Figure 9. OSCC and healthy group classification for negative (a) and positive ion mode (b)

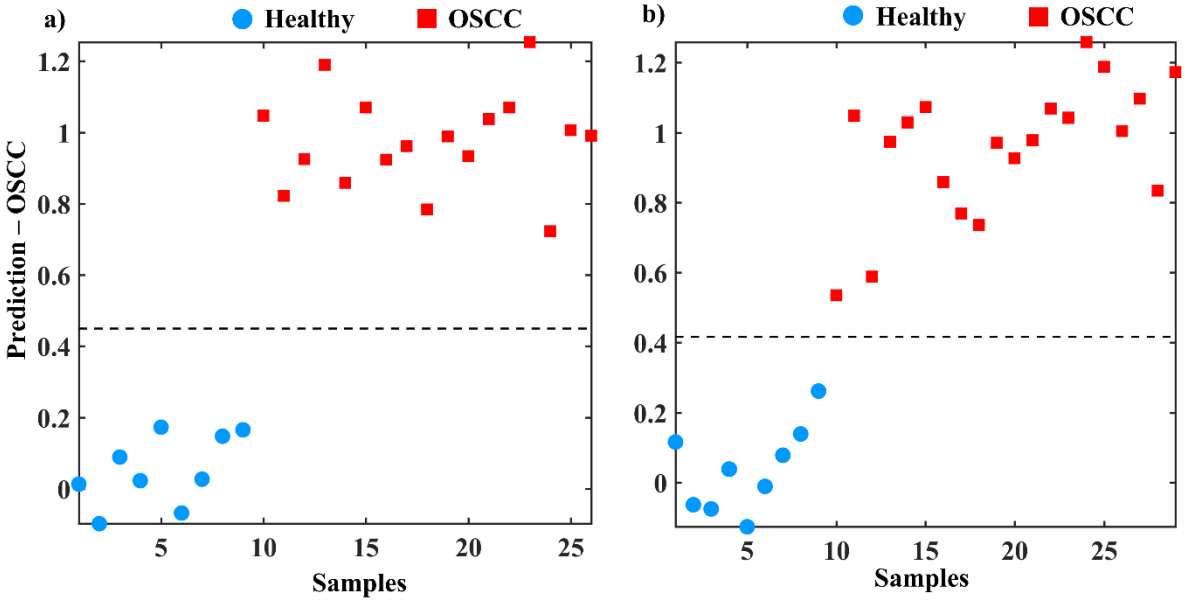

Source: Own authorship.

The selected variables (*m/z* peaks) for classification were normalized in importance, from 0 (less important) to 1 (most important). The selected variables with importance greater than 0.7 were selected for peak annotation. Importance graphs for the selected variables in the OPSDA model were built and are presented on Figure 10.

Figure 10. Importance of selected variables by OPSDA for negative (a) and positive ion mode (b)

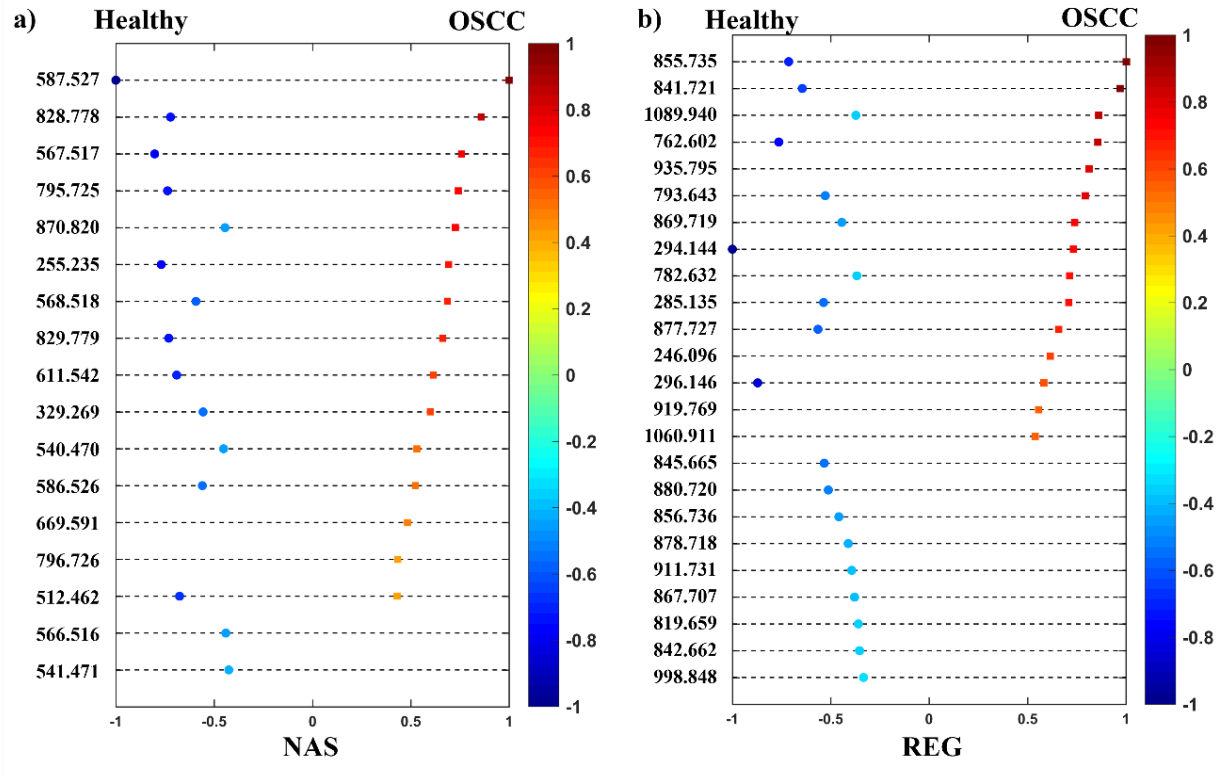

Source: Own authorship.

As presented on Figure 10 few variables were not selected for both classes. Therefore, some variables are responsible for classification of OSCC or healthy group only. The darker red the variable is, the more important it is to classify a sample in the OSCC group. The same happens with blue spots, the darker the blue, the more important for classifying the healthy samples. The same *m/z* peak can be selected for both OSCC and healthy classification, this is due to the up and down-regulation of the lipid balance.

Moreover, the selected *m/z* peaks for OSCC classification were annotated using the LipidView software, and the results were confirmed at GNPS platform. Table 7 presents the annotation for the selected peaks for OSCC classification.

Table 7. Peak annotation for the most important variables in OPSDA for OSCC classification

Negative ion mode					
Healthy group			**OSCC group**		
m/z	**Lipid**	**Error ppm**	***m/z***	**Lipid**	**Error ppm**
567.517	CE (12:0) $[M-H]^-$	4.05	828.778	ACer (54:2;O_2) $[M-H]^-$	-4.10
255.235	FA (16:0) $[M-H]^-$	12.53	567.517	CE (12:0) $[M-H]^-$	4.05
795.725	CE (26:0;O_2) $[M-H]^-$	1.76	795.725	CE (26:0;O_2) $[M-H]^-$	1.76
828.778	ACer (54:2;O_2) $[M-H]^-$	-4.10	255.235	FA (16:0) $[M-H]^-$	12.53
611.542	CE (14:0;O) $[M-H]^-$	1.80	611.542	CE (14:0;O) $[M-H]^-$	1.80
512.462	Cer (30:0;O) $[M+Formate]^-$	-12.48	329.269	FA (18:0) $[M+Formate]^-$	-2.12
586.526	Cer (38:4;O_2) $[M-H]^-$	9.38	540.470	Cer (32:1;O_4) $[M-H]^-$	12.21
329.269	FA (18:0) $[M+Formate]^-$	-2.12	586.526	Cer (38:4;O_2) $[M-H]^-$	9.38
540.470	Cer (32:1;O_4) $[M-H]^-$	12.21	669.591	CE (16:0) $[M+Formate]^-$	12.39
566.516	Cer (34:1;O) $[M+Formate]^-$	1.06	512.462	Cer (30:0;O) $[M+Formate]^-$	-12.48
Positive ion mode					
Healthy group			**OSCC group**		
m/z	**Lipid**	**Error ppm**	***m/z***	**Lipid**	**Error ppm**
762.602	PC (34:0) $[M+H]^+$	1.70	855.735	TG (52:4) $[M+H]^+$	-10.05
855.735	TG (52:4) $[M+H]^+$	-10.05	841.721	SM (44:2;O_2) $[M+H]^+$	6.29
841.721	SM (44:2;O_2) $[M+H]^+$	6.29	762.602	PC (34:0) $[M+H]^+$	1.70
877.727	PE (44:0) $[M+NH_4]^+$	-11.16	935.795	TG (58:6) $[M+H]^+$	-11.97
845.665	PG (O-42:2) $[M+H]^+$	2.36	793.643	PE (38:0) $[M+NH_4]^+$	0.12
793.643	PE (38:0) $[M+NH_4]^+$	0.12	869.719	PC (O-42:4) $[M+NH_4]^+$	9.66
880.720	PC (O-44:4) $[M+H]^+$	5.22	782.632	PG (O-36:0) $[M+NH_4]^+$	6.52
856.706	PC (O-42:2) $[M+H]^+$	-10.97	877.727	PE (44:0) $[M+NH_4]^+$	-11.16
869.719	PC (O-42:4) $[M+NH_4]^+$	9.66			
878.718	HexCer (46:4;O_3) $[M+NH_4]^+$	11.38			
911.731	PC (44:4) $[M+NH_4]^+$	10.75			
867.707	HexCer (44:4;O_3) $[M+NH_4]^+$	4.38			
782.632	PG (O-36:0) $[M+NH_4]^+$	6.52			
819.659	TG (50:8) $[M+H]^+$	11.35			
842.662	PC (40:2) $[M+H]^+$	-1.54			

CE: cholesterol ester; FA: fatty acid; ACer: 1-0-acyl ceramide; Cer: ceramide; PC: glycerolphosphocholine/phosphocholine; TG: tri(acyl/alkyl)glycerol; SM: sphingomyelin; PE: glycerolphosphoethanolamine/phosphoethanolamine; HexCer: hexosyl-ceramide; PG: glycerophosphoglycerol.

In Table 7, some lipids are responsible for OSCC and healthy group classification. This happens when a lipid is up or downregulated in both groups, e.g. LysoPC(14:0) was found

down-regulated, while SM(36:1) was found up-regulated in plasma samples from OSCC patients (WANG; WANG; LI; HOU *et al.*, 2017). Therefore, the presence or absence of some lipid species is significant for sample classification.

As presented on Figure 10, few lipids are responsible only for OSCC group classification, such as CE (16:0) and TG (58:6) for negative and positive ion mode, respectively. However, both OSCC and healthy groups contain most of the lipids described in Table 7, which could suggest a disfunction on this lipid balances in the tumor presence. More information about lipid classes differentiation is presented on the next subtopic "**4.4 MALDI-MSI**".

As reported by Broadfield and co-workers, 2021 (BROADFIELD; PANE; TALEBI; SWINNEN *et al.*, 2021), tumors undergo metabolic transformations to sustain proliferation, avoid cell death and seed in secondary organs. The FA synthesis is upregulated in tumors, which provides phospholipids for cellular membranes to sustain proliferation, but also provides lipid mediators with important roles. Bian *et al.*, 2020 reported that tumor cells activate lipolysis in adipocytes to produce free fatty acids, which can be secreted and taken up by cancer cells sustaining rapid tumor growth.(BIAN; LIU; MENG; XING *et al.*, 2020)

Ponnusamy and co-workers, 2010 (PONNUSAMY; MEYERS-NEEDHAM; SENKAL; SADDOUGHI *et al.*, 2010) reported that ceramides are the central molecules for sphingolipid metabolism, that generally mediates antiproliferative responses, apoptosis induction, senescence modulation and/or autophagy. Sphingolipids are often related to inflammatory responses and have been used for the development of sphingolipid-base cancer therapeutics (SANKALA; HAIT; PAUGH; SHIDA *et al.*, 2007; SWANTON; MARANI; PARDO; WARNE *et al.*, 2007; VISENTIN; VEKICH; SIBBALD; CAVALLI *et al.*, 2006).

4.4 MALDI-MSI

The MALDI-MSI assays performed at University of Copenhagen were not considered in this study, once there was no control under the samples' defrosting. However, some chemical images were generated for practicing only. During this period, the MALDI sample preparation was optimized regarding embedding medium, tissue slice thickness (25 and 30 µm), distance between the matrix sprayer and the sample (8 and 11 cm), matrix solution volume applied to the tissue slices (150 and 300 µL) and magnetic stirring (300 and 600 rpm). The best results were achieved using 25 µm thickness, sprayer at the distance of 11 cm from the sample, application of 300 µL of matrix solution at 300 rpm. The chemical images generated in these conditions were plotted using the MSiReader software, and they are presented in Figure 11 alongside with the hematoxylin/eosin staining.

As it can be observed in Figure 11, the MALDI images in defrosted samples did not present great resolution, once many black pixels are observed along the tissue. Regarding the hematoxylin/eosin staining image, no morphological difference is observed, which could indicate the tissue degradation due to defrosting.

Figure 11. Positive ion mode MALDI-MSI for ions *m/z* 760.58500 and 524.37100, colocalization (*m/z* 760.58500 in red, and 524.37100 in green), and hematoxylin/eosin staining for OSCC sample defrosted during the shippment to Denmark

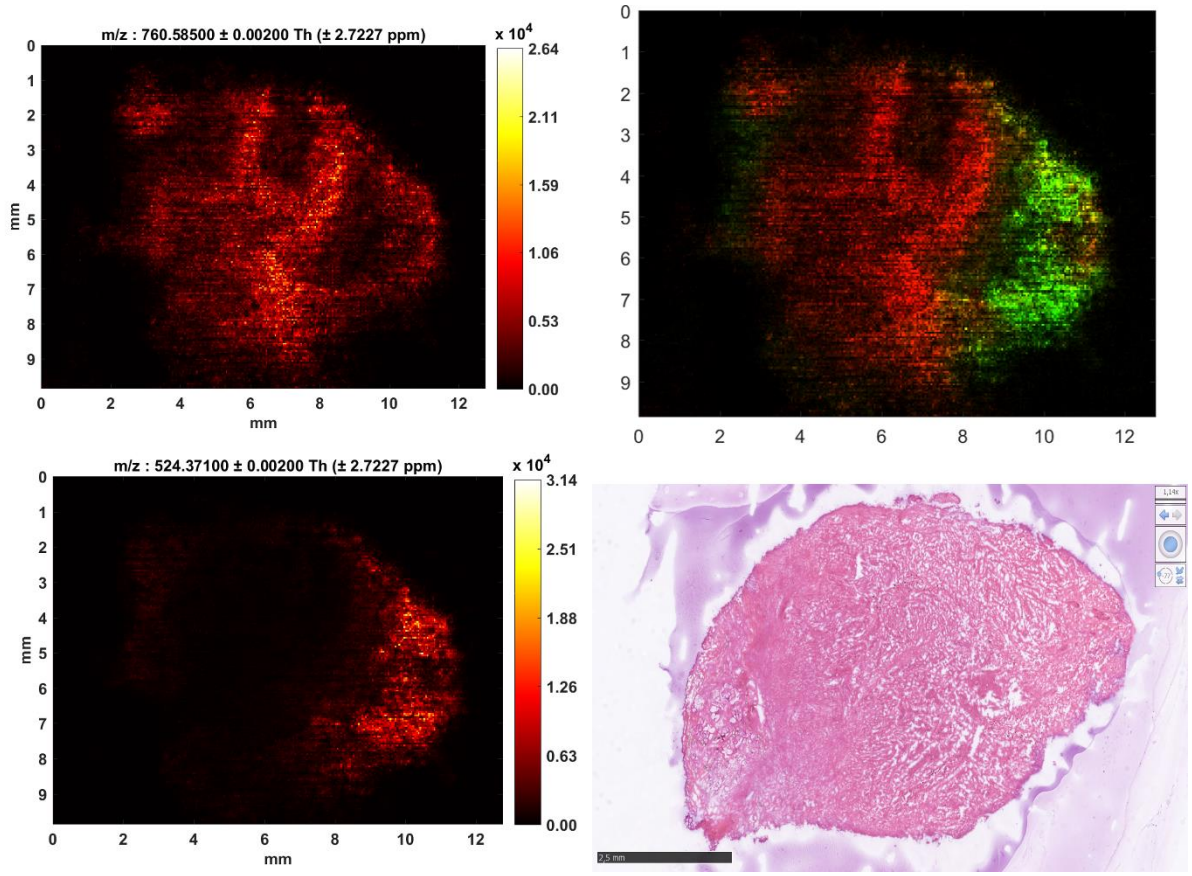

Source: Own authorship.

MALDI-MSI assays were performed aiming to visualize where the lipids responsible for OSCC classification were located along the tissue slice, which can provide information about the chemical distribution of OSCC lipids. Therefore, information about where the lipid is overexpressed or suppressed inside the tissue is provided in a visual image.

The MALDI-MSI assays were performed in positive and negative ion mode on a Bruker Daltonics 7 T solariX 2xR FT-ICR-MS. The data were acquired with a 1 MW transient size, 2 ω detection with 1 scan in the mass range from 150 to 1200 Da, and 50 µm pixel size.

Figure 12. Negative ion mode MALDI-MSI and DAPI imaging of OSCC and healthy slices for the most important variables selected by the OPSDA model

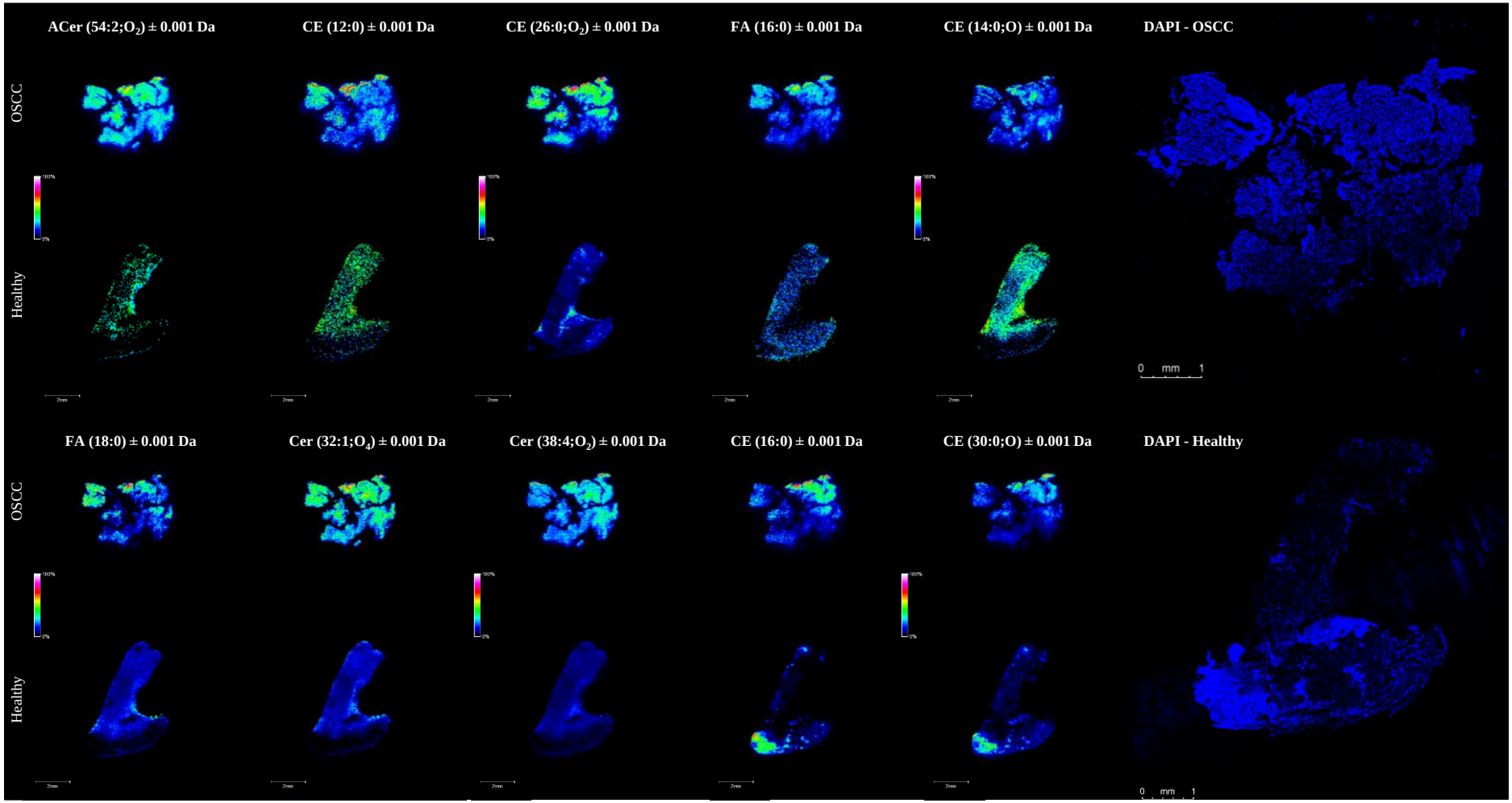

Source: Own authorship.

Figure 13. Positive ion mode MALDI-MSI and DAPI imaging of OSCC and healthy slices for the most important variables selected by the OPSDA model

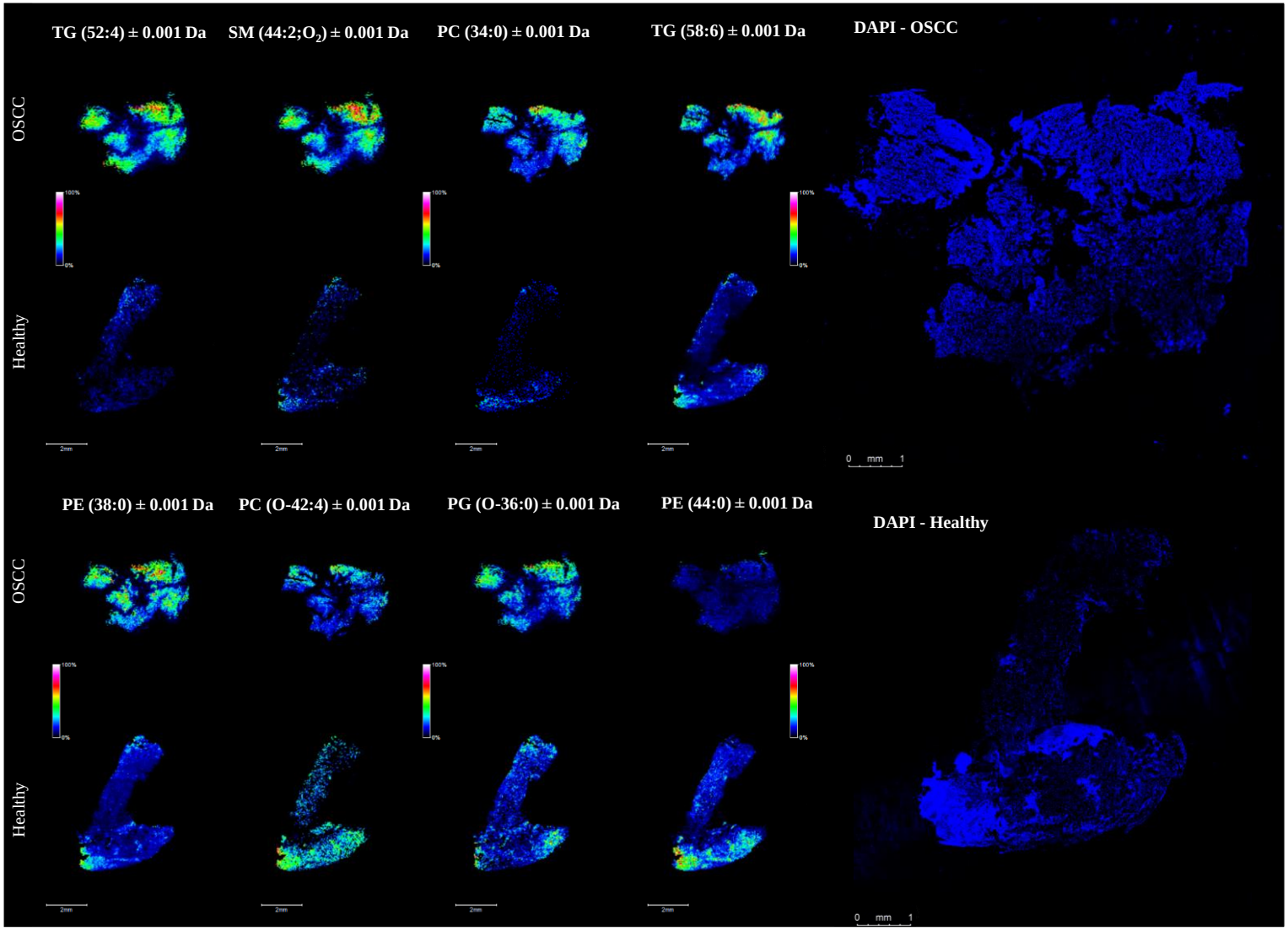

Source: Own authorship.

The chemical images were generated for the most important peaks selected by the OPSDA model (Table 6) using the flexImaging software for OSCC classification, and the lipid distribution of these species were compared to their location in the healthy tissue slices. The MALDI images are presented on Figures 12 and 13 alongside with DAPI imaging confocal microscopy.

DAPI is a fluorescent stain widely used for nuclear DNA visualization (TARNOWSKI; SPINALE; NICHOLSON, 1991), and can provide visual information about the differences between histological slices. In this thesis, DAPI imaging was performed for morphological evaluation of gingiva tissue and a correlation between MALDI images was stablished. Histological images produced by the DAPI staining provide information about cell nucleus such as: size, distribution, and agglomeration. In the Figures 12 and 13, the DAPI imaging shows structural differences between the OSCC and healthy group. Comparing both groups, the OSCC structure is irregular compared to the healthy tissue, it is also observed the presence of more nucleus in the OSCC. Regarding the healthy tissue, two light blue regions are observed in the bottom part of the slide, what could be caused by the presence of blood in the tissue since it was immediately frozen, right after the surgery. As previously reported in the literature, an increasing in the nuclear area and perimeter are observed in OSCC tissue due to rapid and abnormal growth of neoplastic cells (NANDINI; SUBRAMANYAM, 2011). The authors also stated that nuclear area and perimeter increase gradually with the increasing grades of carcinomas. It is also observed that the OSCC tissue is in total, tumor with no healthy area surrounding the cancer tissue, which can be seen in the MALDI images.

The MALDI-MSI revealed differences in the molecular distribution of lipids along the tissue. For both negative and positive ion mode, almost all lipids selected by the OPSDA model, where the lipids were very abundant in the OSCC tissue, and nearly absent in the healthy tissue, except for the PE (44:0) in the positive MALDI-MSI, in which the lipid was more abundant in the healthy tissue. These results are in accordance with Wang's study, 2017 (WANG; WANG; LI; HOU *et al.*, 2017), in which the disfunction of PC, PE, Cer, SM and PG classes in plasma were correlated to OSCC in different stages.

According to Röhrig and Schulze, 2016 (RÖHRIG; SCHULZE, 2016) the FA biosynthesis is increased as a response to the high metabolic demand of cancer cells. This upregulation on FA synthesis is crucial for cancer development and progression. The authors report that deregulated FA synthesis contributes to cancer progression on many levels, not only for generation of building blocks for membrane synthesis during cell growth, being closely connected to the cell division process.

The rapid growth and high proliferation of cancer cells requires large amount of lipids as building blocks for cellular membranes. This effect has been highlighted by the observation of expression and activity of enzymes that act in the phospholipid's synthesis, such as choline kinase. Phospholipids have been found increased in tumors from several tissues, correlating with poor prognosis (SANTOS; SCHULZE, 2012).

Cheng and co-authors, 2016 (CHENG; BHUJWALLA; GLUNDE, 2016) reported that all cancers tested so far display abnormal choline and ethanolamine phospholipid metabolism. Phospholipids are essential to form bilayer structures of all cellular membranes, and the upregulation on the FA biosynthesis promoted the phospholipid metabolism. As observed in the figures 12 and 13, the FA content is upregulated, and consequently the phospholipid content is upregulated as well in the OSCC tissue.

Regard the sphingolipid content of the OSCC tissue, ceramides are a precursor for the sphingolipid biosynthesis. In the Figure 13, the positive ion mode MALDI imaging revealed the spatial localization of SM (44:2;O_2) in the tumor tissue. This sphingomyelin was found more abundant in the OSCC group when compared to the healthy one. According to Tallima and co-workers, 2021 (TALLIMA; AZZAZY; EL RIDI, 2021), ceramides and sphingolipids are important signaling molecules for cancer biology, including apoptosis, cell proliferation, cell migration, senescence and inflammation. The authors also reported that abnormal increase in SM content in membranes reduces membrane fluidity and permeability, and increases its rigidity and strength, which promotes loss of contact inhibition and self-control mechanisms, decreasing cell to cell communication, reducing or inhibiting cell surface molecules expression and signaling pathway coordination (TALLIMA; AZZAZY; EL RIDI, 2021).

According to Perrotti and co-workers, 2016 (PERROTTI; ROSA; CICALINI; SACCHETTA *et al.*, 2016), glycerophospholipids *e.g.* PC, PG, PE, PI etc., are responsible for various functions regulations such as adhesion, migration, apoptosis and signal transduction. Moreover, cholesterol esters play important role in cellular signal transduction governing carcinogenesis, drug resistance, and metastasis pathways (SHARMA; AGNIHOTRI, 2019). The lipids found in this thesis are in accordance with Dickinson's study, 2020 (DICKINSON; SARASWAT; JOENVÄÄRÄ; AGARWAL *et al.*, 2020), where several lipid classes were investigated in OSCC samples. The authors claim that glycerophospholipids are dysregulated in OSCC tissue, highlighting PC and PE as the most increased lipid classes in tumor tissue, consequently, the fatty acids alterations (mono- and unsaturated) in these phospholipids were most increased in tumor samples. Cholesterol levels were also found upregulated in OSCC

tissue in Dickinson's study. The authors reported that the cholesterol levels found in their study suggested deregulation of the usually tightly controlled cholesterol homeostasis.

The methods presented in this thesis are promising for lipid extraction and lipid profile evaluation aiming to differentiate disease from healthy samples. The lipid extraction protocol described here can be applied to extraction in a wide range of biological matrices, such as saliva, hair, whole blood, plasma, serum, and tissues, keeping the TRIzol® solution-to-sample ratio about 1 mL of TRIzol® for each 100 mg of sample. As presented in this thesis, the extraction protocol was successful for total lipid extraction in gingiva tissue, being precise and accurate for total lipid evaluation in OSCC samples, extracting RNA, phospholipids, cholesterol esters, fatty acids, ceramides, sphingolipids and triacylglicerides in a single workflow, allowing transcriptomics and lipidomics analyses using the same biological sample.

MALDI-MSI is a versatile tool for lipid distribution evaluation in tissue samples, corroborating with classical histological images. MALDI allows lipidomic studies with a minimum sample preparation (cryosectioning and matrix application) compared to the lipid extraction protocol. In the other hand, the lipid extraction protocol allows transcriptomic and lipidomic assays from the sample biological sample, which cannot be reached by MALDI.

The results presented in this thesis provide a new way to evaluate differences between two groups of samples (tumor and healthy). However, it is important to highlight that the number of samples in both groups should be increased for a better evaluation.

5 CONCLUSION

In summary, the present study reports a reliable, accurate and precise methodology for simultaneous extraction of RNA and lipids from the same sample. The transcriptomic analyses were not performed since they have been already reported in the literature. The methodology presented here was evaluated regarding analytical parameters often used for methods validation. Intra and inter-day precision, accuracy and absolute recovery are in accordance with the FDA and Brazilian Health and Surveillance Agency regulations, and the matrix effect was not significant in the analyses. It is important to highlight the need of extraction RNA and lipids from the same sample, once some diseases are exceedingly rare, and there are not many samples available for academic research. The methodology described here could enhance the data output using the same number of samples that only a lipidomics assay would require.

Regarding the MALDI-MSI analyses, it is possible to conclude that the most important lipids selected by the OPSDA for OSCC classification were present only, or mostly in the cancer samples while in the healthy tissue these lipids were extremely low abundant. Moreover, evaluating the DAPI staining, the OSCC sample presented higher concentration of nucleus compared to the healthy ones, what can suggest that the cancer cells grow indefinitely infiltrating the surrounding areas. Consequently, comparing the MALDI-MSI images with the DAPI staining, it is possible to conclude that the OSCC sample was in total tumor, no healthy tissue surrounded the tumor area. The lipid classes selected by OPSDA as the most important for OSCC group classification are in accordance with the data reported in the literature, suggesting that the extraction methodology reported here, and the MALDI-MSI as confirmation technique are adequate for this purpose.

The data reported in this thesis open doors for several new experimental studies. The lipids responsible for the OSCC classification could be determined in less invasive samples, such as saliva, and new extractive phases could be developed for these specific lipids' determination. However, the number of gingiva samples should be increased for a more representative set of samples, since only 20 OSCC samples were used in this study. The authors believe that a greater number of samples could lead to new biomarker candidates, as well as incorporating OSCC samples in different stages to classify each one of them regarding the lipid content. Moreover, the authors hope that the data reported here aids the cancer patients in the clinical departments, enhancing the diagnosis/prognosis for the best treatment success.

REFERENCES

ABATI, S.; BRAMATI, C.; BONDI, S.; LISSONI, A. *et al.* Oral cancer and precancer: A narrative review on the relevance of early diagnosis. **International Journal of Environmental Research and Public Health**, 17, n. 24, 2020.

ABBAS, I.; NOUN, M.; TOUBOUL, D.; SAHALI, D. *et al.* Kidney lipidomics by mass spectrometry imaging: A focus on the glomerulus. **International Journal of Molecular Sciences**, 20, n. 7, p. 1623, 2019.

ALI, K. Oral cancer - the fight must go on against all odds…. **Evidence-Based Dentistry**, 23, n. 1, p. 4-5, 2022.

ALVES, A. M.; DIEL, L. F.; LAMERS, M. L. Macrophages and prognosis of oral squamous cell carcinoma: A systematic review. **Journal of Oral Pathology & Medicine**, 47, n. 5, p. 460-467, 2018.

ANGELINI, R.; VITALE, R.; PATIL, V. A.; COCCO, T. *et al.* Lipidomics of intact mitochondria by MALDI-TOF/MS. **J Lipid Res**, 53, n. 7, p. 1417-1425, Jul 2012.

AWAN, K. H.; HEGDE, R.; CHEEVER, V. J.; CARROLL, W. *et al.* Oral and pharyngeal cancer risk associated with occupational carcinogenic substances: Systematic review. **Head & Neck**, 40, n. 12, p. 2724-2732, 2018.

BEAVIS, R. C.; CHAUDHARY, T.; CHAIT, B. T. α-Cyano-4-hydroxycinnamic acid as a matrix for matrixassisted laser desorption mass spectromtry. **Organic Mass Spectrometry**, 27, n. 2, p. 156-158, 1992.

BEDNARCZYK, K.; GAWIN, M.; CHEKAN, M.; KURCZYK, A. *et al.* Discrimination of normal oral mucosa from oral cancer by mass spectrometry imaging of proteins and lipids. **Journal of Molecular Histology**, 50, n. 1, p. 1-10, 2019.

BERNARDO, R. A.; DA SILVA, L. C.; QUEIROZ, M. E. C.; VAZ, B. G. *et al.* Lab-made solid phase microextraction phases for off line extraction and direct mass spectrometry analysis: Evaluating the extraction parameters. **Journal of Chromatography A**, 1603, p. 23-32, 2019.

BIAN, X.; LIU, R.; MENG, Y.; XING, D. *et al.* Lipid metabolism and cancer. **Journal of Experimental Medicine**, 218, n. 1, p. e20201606, 2020.

BLASKIEVICZ, S.; SOARES, L.; MASCARO, L. Um spin coater artesanal baseado em lixo eletrônico: uma alternativa versátil e de baixo custo. **Química Nova**, 2021.

BLIGH, E. G.; DYER, W. J. A rapid method of total lipid extraction and purification. **Canadian Journal of Biochemistry and Physiology**, 37, n. 8, p. 911-917, 1959.

BRAVI, F.; BOSETTI, C.; FILOMENO, M.; LEVI, F. *et al.* Foods, nutrients and the risk of oral and pharyngeal cancer. **Br J Cancer**, 109, n. 11, p. 2904-2910, Nov 26 2013.

BRAY, F.; FERLAY, J.; SOERJOMATARAM, I.; SIEGEL, R. L. *et al.* Global cancer statistics 2018: GLOBOCAN estimates of incidence and mortality worldwide for 36 cancers in 185 countries. **CA: A Cancer Journal for Clinicians**, 68, n. 6, p. 394-424, 2018.

BROADFIELD, L. A.; PANE, A. A.; TALEBI, A.; SWINNEN, J. V. *et al.* Lipid metabolism in cancer: New perspectives and emerging mechanisms. **Developmental Cell**, 56, n. 10, p. 1363-1393, 2021.

BUSZEWSKA-FORAJTA, M.; POMASTOWSKI, P.; MONEDEIRO, F.; KRÓL-GÓRNIAK, A. *et al.* New approach in determination of urinary diagnostic markers for prostate cancer by MALDI-TOF/MS. **Talanta**, 236, p. 122843, 2022.

CARRERAS-TORRAS, C.; GAY-ESCODA, C. Techniques for early diagnosis of oral squamous cell carcinoma: Systematic review. **Medicina Oral Patología Oral y Cirugia Bucal**, p. e305-e315, 2015.

CHAMBERS, M. C.; MACLEAN, B.; BURKE, R.; AMODEI, D. *et al.* A cross-platform toolkit for mass spectrometry and proteomics. **Nature Biotechnology**, 30, n. 10, p. 918-920, 2012.

CHEN, X.; CARROLL, J. A.; BEAVIS, R. C. Near-ultraviolet-induced matrix-assisted laser desorption/ionization as a function of wavelength. **Journal of the American Society for Mass Spectrometry**, 9, n. 9, p. 885-891, 1998.

CHENG, M.; BHUJWALLA, Z. M.; GLUNDE, K. Targeting phospholipid metabolism in cancer. **Frontiers in Oncology**, 6, 2016. Review.

CHHONKER, Y. S.; KANVINDE, S.; AHMAD, R.; SINGH, A. B. *et al.* Simultaneous quantitation of lipid biomarkers for inflammatory Bowel disease using LC–MS/MS. **Metabolites**, 11, n. 2, p. 106, 2021.

CHI, A. C.; DAY, T. A.; NEVILLE, B. W. Oral cavity and oropharyngeal squamous cell carcinoma-an update. **CA: A Cancer Journal for Clinicians**, 65, n. 5, p. 401-421, 2015.

CHU, Y.-H.; KAO, S.-W.; TANTOH, D. M.; KO, P.-C. *et al.* Association between fine particulate matter and oral cancer among Taiwanese men. **Journal of Investigative Medicine**, 67, n. 1, p. 34, 2019.

CODY, R. B.; MCALPIN, C. R.; COX, C. R.; JENSEN, K. R. *et al.* Identification of bacteria by fatty acid profiling with direct analysis in real time mass spectrometry. **Rapid Communications in Mass Spectrometry**, 29, n. 21, p. 2007-2012, 2015.

DE ALMEIDA, C. M.; PINTO, F. E.; DOS SANTOS, N. A.; DE SOUZA, L. M. *et al.* Designer drugs analysis by LDI(+), MALDI(+) and MALDI(+) imaging coupled to FT-ICR MS. **Microchemical Journal**, 149, p. 104002, 2019.

DE HOFFMANN, E.; STROOBANT, V. **Mass spectrometry: principles and applications**. 3rd ed. England: John Wiley & Sons, Ltd, 2007. 978-0-470-03310-4.

DICKINSON, A.; SARASWAT, M.; JOENVÄÄRÄ, S.; AGARWAL, R. *et al.* Mass spectrometry-based lipidomics of oral squamous cell carcinoma tissue reveals aberrant cholesterol and glycerophospholipid metabolism - A pilot study. **Transl Oncol**, 13, n. 10, p. 100807, 2020.

DIKOVA, V.; JANTUS-LEWINTRE, E.; BAGAN, J. Potential non-invasive biomarkers for early diagnosis of oral squamous cell carcinoma. **Journal of Clinical Medicine**, 10, n. 8, p. 1658, 2021.

DREISEWERD, K. The desorption process in MALDI. **Chemical Reviews**, 103, n. 2, p. 395-425, 2003.

DU, P.; HU, T.; AN, Z.; LI, P. *et al.* Simultaneous quantitative determination of arachidonic acid and cascade metabolites in rat serum by UPLC-MS/MS: application for longitudinal metabolomics of anlotinib. **The Analyst**, 145, n. 14, p. 4972-4981, 2020.

DUSHIANTHAN, A.; POSTLE, A. Methodology to detect oxidised phospholipids and their relevance in disease. **Biochemical Society Transactions**, 49, n. 3, p. 1241-1250, 2021.

ELLIS, S. R.; BROWN, S. H.; IN HET PANHUIS, M.; BLANKSBY, S. J. *et al.* Surface analysis of lipids by mass spectrometry: more than just imaging. **Prog Lipid Res**, 52, n. 4, p. 329-353, Oct 2013.

ENGELS, E. A. Epidemiologic perspectives on immunosuppressed populations and the immunosurveillance and immunocontainment of cancer. **American Journal of Transplantation**, 19, n. 12, p. 3223-3232, 2019.

FERNANDES, H. J. R.; PATIKAS, N.; FOSKOLOU, S.; FIELD, S. F. *et al.* Single-cell transcriptomics of Parkinson's disease human in vitro models reveals dopamine neuron-specific stress responses. **Cell Reports**, 33, n. 2, p. 108263, 2020.

FERRARI, E.; PEZZI, M. E.; CASSI, D.; PERTINHEZ, T. A. *et al.* Salivary cytokines as biomarkers for oral squamous cell carcinoma: A systematic review. **International Journal of Molecular Sciences**, 22, n. 13, p. 6795, 2021.

FOLCH, J.; LEES, M.; STANLEY, G. H. S. A simple method for the isolation and purification of total lipides from animal tissues. **Journal of Biological Chemistry**, 226, n. 1, p. 497-509, 1957.

GARATE, J.; FERNÁNDEZ, R.; LAGE, S.; BESTARD-ESCALAS, J. *et al.* Imaging mass spectrometry increased resolution using 2-mercaptobenzothiazole and 2,5-diaminonaphtalene matrices: application to lipid distribution in human colon. **Analytical and Bioanalytical Chemistry**, 407, n. 16, p. 4697-4708, 2015.

GARATE, J.; MAIMÓ-BARCELÓ, A.; BESTARD-ESCALAS, J.; FERNÁNDEZ, R. *et al.* A drastic shift in lipid adducts in colon cancer detected by MALDI-IMS exposes alterations in specific K^+ channels. **Cancers**, 13, n. 6, p. 1350, 2021.

GREEN, F. M.; SALTER, T. L.; GILMORE, I. S.; STOKES, P. *et al.* The effect of electrospray solvent composition on desorption electrospray ionisation (DESI) efficiency and spatial resolution. **The Analyst**, 135, n. 4, p. 731, 2010.

GUALTERO, D. F.; SUAREZ CASTILLO, A. Biomarkers in saliva for the detection of oral squamous cell carcinoma and their potential use for early diagnosis: A systematic review. Acta Odontologica Scandinavica. : Taylor and Francis Ltd. 74**:** 170-177 p. 2016.

HE, M. J.; PU, W.; WANG, X.; ZHANG, W. *et al.* Comparing DESI-MSI and MALDI-MSI mediated spatial metabolomics and their applications in cancer studies. **Frontiers in Oncology**, 12, 2022-July-18 2022. Review.

HILLENKAMP, F.; PETER-KATALINIC, J. **MALDI MS. A practical guide to instrumentation, methods and applications**. Wiley-Blackwell, 2008/10/01 2013. 480 p., v. 4). 1618-2650.

HOFFMANN, F.; UMBREIT, C.; KRÜGER, T.; PELZEL, D. *et al.* Identification of proteomic markers in head and neck cancer using MALDI–MS imaging, LC–MS/MS, and immunohistochemistry. **PROTEOMICS – Clinical Applications**, 13, n. 1, p. 1700173-1700173, 2019.

HOLZLECHNER, M.; EUGENIN, E.; PRIDEAUX, B. Mass spectrometry imaging to detect lipid biomarkers and disease signatures in cancer. **Cancer Reports**, 2, n. 6, 2019.

HOSSEINI, S.; MARTINEZ-CHAPA, S. O. Principles and mechanism of MALDI-ToF-MS analysis. *In*: HOSSEINI, S. e MARTINEZ-CHAPA, S. O. (Ed.). **Fundamentals of MALDI-ToF-MS Analysis: Applications in Bio-diagnosis, Tissue Engineering and Drug Delivery**. Singapore: Springer Singapore, 2017. p. 1-19.

HSU, F.-F. Mass spectrometry-based shotgun lipidomics – a critical review from the technical point of view. **Analytical and Bioanalytical Chemistry**, 410, n. 25, p. 6387-6409, 2018.

HU, C.; DUAN, Q.; HAN, X. Strategies to improve/eliminate the limitations in shotgun lipidomics. **PROTEOMICS**, 20, n. 11, p. 1900070, 2020.

HUSS, R. Tissue-based biomarkers. **Advances in pharmaceutical cell therapy: principles of cell-based biopharmaceuticals**, p. 408, 2015.

ISLAM, S. R.; MANNA, S. K. Lipidomic analysis of cancer cell and tumor tissues. *In*: **Cancer Metabolism**: Springer, 2019. p. 175-204.

JENKINSON, C. P.; GÖRING, H. H. H.; ARYA, R.; BLANGERO, J. *et al.* Transcriptomics in type 2 diabetes: Bridging the gap between genotype and phenotype. **Genomics Data**, 8, p. 25-36, 2016.

KANEKO, H.; ITOH, H.; KIRIYAMA, H.; KAMON, T. *et al.* Lipid profile and subsequent cardiovascular disease among young adults aged <50 years. **The American Journal of Cardiology**, 142, p. 59-65, 2021.

KARAS, M.; KRÜGER, R. Ion formation in MALDI: The cluster ionization mechanism. **Chemical Reviews**, 103, n. 2, p. 427-439, 2003.

KENNARD, R. W.; STONE, L. A. Computer aided design of experiments. **Technometrics**, 11, n. 1, p. 137-148, 1969/02/01 1969.

KLEIN, O.; KANTER, F.; KULBE, H.; JANK, P. *et al.* MALDI-Imaging for classification of epithelial ovarian cancer histotypes from a tissue microarray using machine learning methods. **Proteomics - Clinical Applications**, 13, n. 1, p. 1700181-1700181, 2019.

KNOCHENMUSS, R. A quantitative model of ultraviolet matrix-assisted laser desorption/ionization including analyte ion generation. **Analytical Chemistry**, 75, n. 10, p. 2199-2207, 2003.

KOESTLER, M.; KIRSCH, D.; HESTER, A.; LEISNER, A. *et al.* A high-resolution scanning microprobe matrix-assisted laser desorption/ionization ion source for imaging analysis on an ion trap/Fourier transform ion cyclotron resonance mass spectrometer. **Rapid Communications in Mass Spectrometry**, 22, n. 20, p. 3275-3285, 2008.

KOMPAUER, M.; HEILES, S.; SPENGLER, B. Atmospheric pressure MALDI mass spectrometry imaging of tissues and cells at 1.4-μm lateral resolution. **Nat Methods**, 14, n. 1, p. 90-96, Jan 2017.

LEE, L. T.; WONG, Y. K.; HSIAO, H. Y.; WANG, Y. W. *et al.* Evaluation of saliva and plasma cytokine biomarkers in patients with oral squamous cell carcinoma. **International Journal of Oral and Maxillofacial Surgery**, 47, n. 6, p. 699-707, 2018.

LEE, P. Y.; YEOH, Y.; OMAR, N.; PUNG, Y.-F. *et al.* Molecular tissue profiling by MALDI imaging: recent progress and applications in cancer research. **Critical Reviews in Clinical Laboratory Sciences**, 58, n. 7, p. 513-529, 2021.

LEINWEBER, B. D.; TSAPRAILIS, G.; MONKS, T. J.; LAU, S. S. Improved MALDI-TOF imaging yields increased protein signals at high molecular mass. **Journal of the American Society for Mass Spectrometry**, 20, n. 1, p. 89-95, 2009.

LEOPOLD, J.; POPKOVA, Y.; ENGEL, K. M.; SCHILLER, J. Recent developments of useful MALDI matrices for the mass spectrometric characterization of lipids. **Biomolecules**, 8, n. 4, 2018.

LI, B.; SUN, R.; GORDON, A.; GE, J. *et al.* 3-Aminophthalhydrazide (Luminol) as a matrix for dual-polarity MALDI MS imaging. **Analytical Chemistry**, 91, n. 13, p. 8221-8228, 2019.

LIEBISCH, G.; BINDER, M.; SCHIFFERER, R.; LANGMANN, T. *et al.* High throughput quantification of cholesterol and cholesteryl ester by electrospray ionization tandem mass spectrometry (ESI-MS/MS). **Biochim Biophys Acta**, 1761, n. 1, p. 121-128, Jan 2006.

LIEBISCH, G.; DROBNIK, W.; LIESER, B.; SCHMITZ, G. High-throughput quantification of lysophosphatidylcholine by electrospray ionization tandem mass spectrometry. **Clin Chem**, 48, n. 12, p. 2217-2224, 2002.

LIU, H.; WANG, S.; LIN, J.-M.; LIN, Z. *et al.* Investigation of the lipidomic changes in differentiated glioblastoma cells after drug treatment using MALDI-MS. **Talanta**, 233, p. 122570, 2021.

LIU, H.; ZHOU, Y.; WANG, J.; XIONG, C. *et al. N*-phenyl-2-naphthylamine as a novel MALDI matrix for analysis and in situ imaging of small molecules. **Analytical Chemistry**, 90, n. 1, p. 729-736, 2018.

LIU, Y.; TAN, Y.-r.; SUN, W.-w.; JU, W.-t. *et al.* Identification of SCARA5 as a potential biomarker for oral squamous cell carcinoma using MALDI-TOF-MS analysis. **PROTEOMICS - Clinical Applications**, 12, n. 5, p. 1700180-1700180, 2018.

MA, X.; FERNÁNDEZ, F. M. Advances in mass spectrometry imaging for spatial cancer metabolomics. **Mass Spectrometry Reviews**, 2022.

MACÍAS-GARCÍA, D.; PERIÑÁN, M. T.; MUÑOZ-DELGADO, L.; JIMENEZ-JARABA, M. V. *et al.* Serum lipid profile among sporadic and familial forms of Parkinson's disease. **npj Parkinson's Disease**, 7, n. 1, 2021.

MARKOWSKI, A. R.; BŁACHNIO-ZABIELSKA, A. U.; GUZIŃSKA-USTYMOWICZ, K.; MARKOWSKA, A. *et al.* Ceramides profile identifies patients with more advanced stages of colorectal cancer. **Biomolecules**, 10, n. 4, p. 632, 2020.

MAS, S.; TORRO, A.; FERNÁNDEZ, L.; BEC, N. *et al.* MALDI imaging mass spectrometry and chemometric tools to discriminate highly similar colorectal cancer tissues. **Talanta**, 208, p. 120455, 2020.

MATTHIESEN, R.; LAUBER, C.; SAMPAIO, J. L.; DOMINGUES, N. *et al.* Shotgun mass spectrometry-based lipid profiling identifies and distinguishes between chronic inflammatory diseases. **EBioMedicine**, 70, p. 103504, 2021/08/01/ 2021.

MATYASH, V.; LIEBISCH, G.; KURZCHALIA, T. V.; SHEVCHENKO, A. *et al.* Lipid extraction by methyl-*tert*-butyl ether for high-throughput lipidomics. **Journal of Lipid Research**, 49, n. 5, p. 1137-1146, 2008.

MONTINI, L.; CROCOLL, C.; GLEADOW, R. M.; MOTAWIA, M. S. *et al.* Matrix-assisted laser desorption/ionization-mass spectrometry imaging of metabolites during sorghum germination. **Plant Physiology**, 183, n. 3, p. 925-942, 2020.

NABI, M. M.; MAMUN, M. A.; ISLAM, A.; HASAN, M. M. *et al.* Mass spectrometry in the lipid study of cancer. **Expert Review of Proteomics**, 18, n. 3, p. 201-219, 2021.

NANDINI, D.; SUBRAMANYAM, R. Nuclear features in oral squamous cell carcinoma: A computer-assisted microscopic study. **Journal of Oral and Maxillofacial Pathology**, 15, n. 2, p. 177-181, May 1, 2011 2011. Original Article.

NOH, S. A.; KIM, S.-M.; PARK, S. H.; KIM, D.-J. *et al.* Alterations in lipid profile of the aging kidney identified by MALDI imaging mass spectrometry. **Journal of Proteome Research**, 18, n. 7, p. 2803-2812, 2019.

OJO, O.; OJO, O. O.; ZAND, N.; WANG, X. The effect of dietary fibre on gut microbiota, lipid profile, and inflammatory markers in patients with type 2 diabetes: A systematic review and meta-analysis of randomised controlled trials. **Nutrients**, 13, n. 6, p. 1805, 2021.

OOI, K.-L. M.; VACY, K.; BOON, W. C. Fatty acids and beyond: Age and Alzheimer's disease related changes in lipids reveal the neuro-nutraceutical potential of lipids in cognition. **Neurochemistry International**, 149, p. 105143, 2021.

OYENIYI, E. A.; SORGI, C. A.; GARDINASSI, L. G.; AZEVEDO, L. F. *et al.* Phospholipids modifications, genotoxic and anticholinesterase effects of pepper fruit (*Dennettia tripetala* G. Baker) extract in Swiss mice. **Food and Chemical Toxicology**, 165, p. 113189, 2022.

PARK, J. K.; COFFEY, N. J.; LIMOGES, A.; LE, A. The heterogeneity of lipid metabolism in cancer. *In*: LE, A. (Ed.). **The heterogeneity of lipid metabolism in cancer**. Cham: Springer International Publishing, 2018. p. 33-55.

PÉREZ, N. F.; FERRÉ, J.; BOQUÉ, R. Calculation of the reliability of classification in discriminant partial least-squares binary classification. **Chemometrics and Intelligent Laboratory Systems**, 95, n. 2, p. 122-128, 2009.

PERROTTI, F.; ROSA, C.; CICALINI, I.; SACCHETTA, P. *et al.* Advances in lipidomics for cancer biomarkers discovery. **International Journal of Molecular Sciences**, 17, n. 12, 2016.

PODECHARD, N.; DUCHEIX, S.; POLIZZI, A.; LASSERRE, F. *et al.* Dual extraction of mRNA and lipids from a single biological sample. **Scientific Reports**, 8, n. 1, 2018.

PONNUSAMY, S.; MEYERS-NEEDHAM, M.; SENKAL, C. E.; SADDOUGHI, S. A. *et al.* Sphingolipids and cancer: ceramide and sphingosine-1-phosphate in the regulation of cell death and drug resistance. **Future Oncol**, 6, n. 10, p. 1603-1624, Oct 2010.

RAJ, A. T.; PATIL, S.; GUPTA, A. A.; RAJKUMAR, C. *et al.* Reviewing the role of human papillomavirus in oral cancer using the Bradford Hill criteria of causation. **Disease-a-Month**, 65, n. 6, p. 155-163, 2019.

RAPOSO, F.; BARCELÓ, D. Challenges and strategies of matrix effects using chromatography-mass spectrometry: An overview from research versus regulatory viewpoints. **TrAC Trends in Analytical Chemistry**, 134, p. 116068, 2021.

RÖHRIG, F.; SCHULZE, A. The multifaceted roles of fatty acid synthesis in cancer. **Nature Reviews Cancer**, 16, n. 11, p. 732-749, 2016.

RÖMPP, A.; GUENTHER, S.; SCHOBER, Y.; SCHULZ, O. *et al.* Histology by mass spectrometry: Label-free tissue characterization obtained from high-accuracy bioanalytical imaging. **Angewandte Chemie - International Edition**, 49, n. 22, p. 3834-3838, 2010.

RÖMPP, A.; SPENGLER, B. Mass spectrometry imaging with high resolution in mass and space. **Histochemistry and Cell Biology**, 139, n. 6, p. 759-783, 2013.

ROQUE, J. V.; CARDOSO, W.; PETERNELLI, L. A.; TEÓFILO, R. F. Comprehensive new approaches for variable selection using ordered predictors selection. **Analytica Chimica Acta**, 1075, p. 57-70, 2019.

SANKALA, H. M.; HAIT, N. C.; PAUGH, S. W.; SHIDA, D. *et al.* Involvement of sphingosine kinase 2 in p53-independent induction of p21 by the chemotherapeutic drug doxorubicin. **Cancer Res**, 67, n. 21, p. 10466-10474, 2007.

SANTOS, C. R.; SCHULZE, A. Lipid metabolism in cancer. **FEBS Journal**, 279, n. 15, p. 2610-2623, 2012.

SCALINCI, S.; LUGARESI, M.; SCOROLLI, L.; RALLI, M. *et al.* Neuroprotective role of phosphoserine in primary open-angle glaucoma patients. **European Review for Medical and Pharmacological Sciences**, 24, n. 19, p. 9780-9786, 2020.

SCHUHMANN, K.; THOMAS, H.; ACKERMAN, J. M.; NAGORNOV, K. O. *et al.* Intensity-independent noise filtering in FT MS and FT MS/MS spectra for shotgun lipidomics. **Anal Chem**, 89, n. 13, p. 7046-7052, 2017.

SCHWUDKE, D.; SCHUHMANN, K.; HERZOG, R.; BORNSTEIN, S. R. *et al.* Shotgun lipidomics on high resolution mass spectrometers. **Cold Spring Harbor Perspectives in Biology**, 3, n. 9, p. a004614-a004614, 2011.

SHARMA, B.; AGNIHOTRI, N. Role of cholesterol homeostasis and its efflux pathways in cancer progression. **The Journal of Steroid Biochemistry and Molecular Biology**, 191, p. 105377, 2019.

SHI, Y.; HU, H.; HAO, Q.; WU, R. *et al.* Michler's ethylketone as a novel negative-ion matrix for the enhancement of lipid MALDI tissue imaging. **Chemical Communications**, 58, n. 5, p. 633-636, 2022.

SHRESTHA, B.; SRIPADI, P.; RESCHKE, B. R.; HENDERSON, H. D. *et al.* Subcellular metabolite and lipid analysis of *Xenopus laevis* eggs by LAESI mass spectrometry. **PLoS ONE**, 9, n. 12, p. e115173, 2014.

SIGHINOLFI, G.; CLARK, S.; BLANC, L.; COTA, D. *et al.* Mass spectrometry imaging of mice brain lipid profile changes over time under high fat diet. **Scientific Reports**, 11, n. 1, p. 19664, 2021.

SIVADASAN, P.; GUPTA, M. K.; SATHE, G.; SUGHEENDRA, H. V. *et al.* Salivary proteins from dysplastic leukoplakia and oral squamous cell carcinoma and their potential for early detection. **Journal of Proteomics**, 212, 2020.

SORVINA, A.; BADER, C. A.; CAPORALE, C.; CARTER, E. A. *et al.* Lipid profiles of prostate cancer cells. **Oncotarget**, 9, n. 85, p. 35541-35552, 2018.

STEINER, D.; KRSKA, R.; MALACHOVÁ, A.; TASCHL, I. *et al.* Evaluation of matrix effects and extraction efficiencies of LC-MS/MS methods as the essential part for proper validation of multiclass contaminants in complex feed. **Journal of Agricultural and Food Chemistry**, 68, n. 12, p. 3868-3880, 2020.

STUMP, M. J.; FLEMING, R. C.; GONG, W. H.; JABER, A. J. *et al.* Matrix-assisted laser desorption mass spectrometry. **Applied Spectroscopy Reviews**, 37, n. 3, p. 275-303, 2002.

SUN, G.; CAO, Y.; WANG, P.; SONG, H. *et al.* miR-200b-3p in plasma is a potential diagnostic biomarker in oral squamous cell carcinoma. 2018.

SUNG, H.; FERLAY, J.; SIEGEL, R. L.; LAVERSANNE, M. *et al.* Global Cancer Statistics 2020: GLOBOCAN Estimates of incidence and mortality worldwide for 36 cancers in 185 countries. **CA: A Cancer Journal for Clinicians**, 71, n. 3, p. 209-249, 2021.

SURMA, M. A.; HERZOG, R.; VASILJ, A.; KLOSE, C. *et al.* An automated shotgun lipidomics platform for high throughput, comprehensive, and quantitative analysis of blood plasma intact lipids. **European Journal of Lipid Science and Technology**, 117, n. 10, p. 1540-1549, 2015.

SWANTON, C.; MARANI, M.; PARDO, O.; WARNE, P. H. *et al.* Regulators of mitotic arrest and ceramide metabolism are determinants of sensitivity to paclitaxel and other chemotherapeutic drugs. **Cancer Cell**, 11, n. 6, p. 498-512, Jun 2007.

SWARTZ, M. E.; KRULL, I. S. **Analytical method development and validation**. 1st Edition ed. CRC Press, 2018. 9781315275161.

TAKÁTS, Z.; WISEMAN, J. M.; GOLOGAN, B.; COOKS, R. G. Mass spectrometry sampling under ambient conditions with desorption electrospray ionization. **Science**, 306, n. 5695, p. 471-473, 2004.

TALLIMA, H.; AZZAZY, H. M. E.; EL RIDI, R. Cell surface sphingomyelin: key role in cancer initiation, progression, and immune evasion. **Lipids in Health and Disease**, 20, n. 1, p. 150, 2021/10/31 2021.

TARNOWSKI, B. I.; SPINALE, F. G.; NICHOLSON, J. H. DAPI as a useful stain for nuclear quantitation. **Biotech Histochem**, 66, n. 6, p. 297-302, 1991.

ULMER, C. Z.; JONES, C. M.; YOST, R. A.; GARRETT, T. J. *et al.* Optimization of Folch, Bligh-Dyer, and Matyash sample-to-extraction solvent ratios for human plasma-based lipidomics studies. **Analytica Chimica Acta**, 1037, p. 351-357, 2018.

UNSIHUAY, D.; SU, P.; HU, H.; QIU, J. *et al.* Imaging and analysis of isomeric unsaturated lipids through online photochemical derivatization of carbon–carbon double bonds**. **Angewandte Chemie**, 133, n. 14, p. 7637-7641, 2021.

VALDES-MORA, F.; HANDLER, K.; LAW, A. M. K.; SALOMON, R. *et al.* Single-cell transcriptomics in cancer immunobiology: The future of precision oncology. **Frontiers in Immunology**, 9, 2018-November-12 2018. Review.

VISENTIN, B.; VEKICH, J. A.; SIBBALD, B. J.; CAVALLI, A. L. *et al.* Validation of an anti-sphingosine-1-phosphate antibody as a potential therapeutic in reducing growth, invasion, and angiogenesis in multiple tumor lineages. **Cancer Cell**, 9, n. 3, p. 225-238, 2006.

WANG, J.; HAN, X. Analytical challenges of shotgun lipidomics at different resolution of measurements. **TrAC Trends in Analytical Chemistry**, 121, p. 115697, 2019.

WANG, L.; GANLY, I. The oral microbiome and oral cancer. Clinics in Laboratory Medicine. : W.B. Saunders. 34**:** 711-719 p. 2014.

WANG, L.; WANG, X.; LI, Y.; HOU, Y. *et al.* Plasma lipid profiling and diagnostic biomarkers for oral squamous cell carcinoma. **Oncotarget**, 8, n. 54, p. 92324-92332, 2017.

WANG, M.; CARVER, J. J.; PHELAN, V. V.; SANCHEZ, L. M. *et al.* Sharing and community curation of mass spectrometry data with Global Natural Products Social Molecular Networking. **Nature Biotechnology**, 34, n. 8, p. 828-837, 2016.

WANG, M.; WANG, C.; HAN, R. H.; HAN, X. Novel advances in shotgun lipidomics for biology and medicine. **Progress in Lipid Research**, 61, p. 83-108, 2016.

WANG, Y.; HINZ, S.; UCKERMANN, O.; HÖNSCHEID, P. *et al.* Shotgun lipidomics-based characterization of the landscape of lipid metabolism in colorectal cancer. **Biochimica et Biophysica Acta (BBA) - Molecular and Cell Biology of Lipids**, 1865, n. 3, p. 158579, 2020.

WARTHA, C. A.; DE AGUIAR PORTO, N.; TOMAZ, A. C.; ROQUE, J. V. *et al.* Classification of sugarcane genotypes susceptible and resistant to the initial attack of sugarcane borer *Diatraea saccharalis* using epicuticular wax composition. **Phytochemistry**, 199, p. 113175, 2022.

WIRKA, R. C.; PJANIC, M.; QUERTERMOUS, T. Advances in transcriptomics: Investigating cardiovascular disease at unprecedent resolution. **Circulation Research**, 122, n. 9, p. 1200-1220, 2018.

WU, Z.; ZHANG, Q.; LI, N.; PU, Y. *et al.* Comparison of critical methods developed for fatty acid analysis: A review. **Journal of Separation Science**, 40, n. 1, p. 288-298, 2017.

XU, Y.; LI, H.; HAN, Y.; WANG, T. *et al.* A simple and rapid method for extraction and measurement of circulating sphingolipids using LC–MS/MS: a targeted lipidomic analysis. **Analytical and Bioanalytical Chemistry**, 414, n. 6, p. 2041-2054, 2022.

YAMADA, M.; KITA, Y.; KOHIRA, T.; YOSHIDA, K. *et al.* A comprehensive quantification method for eicosanoids and related compounds by using liquid chromatography/mass spectrometry with high speed continuous ionization polarity switching. **Journal of Chromatography B**, 995-996, p. 74-84, 2015.

YANG, J.; WANG, Z. Y.; HUANG, L.; YU, T. L. *et al.* Do betel quid and areca nut chewing deteriorate prognosis of oral cancer? A systematic review, meta-analysis, and research agenda. **Oral Diseases**, 27, n. 6, p. 1366-1375, 2021.

ZHANG, Y.; HE, J.; HE, B.; HUANG, R. *et al.* Effect of tobacco on periodontal disease and oral cancer. **Tob Induc Dis**, 17, p. 40, 2019.

ZHAO, G.; HE, F.; WU, C.; LI, P. *et al.* Betaine in inflammation: mechanistic aspects and applications. **Frontiers in Immunology**, 9, p. 1070, 2018.

ZHOU, W.; YANG, S.; WANG, P. G. Matrix effects and application of matrix effect factor. **Bioanalysis**, 9, n. 23, p. 1839-1844, 2017.

ZÜLLIG, T.; KÖFELER, H. C. High resolution mass spectrometry in lipidomics. **Mass Spectrometry Reviews**, 40, n. 3, p. 162-176, 2021.

ATTACHMENT 1 - PARECER CONSUBSTANCIADO – COMITÊ DE ÉTICA EM PESQUISA UFG

UFG - UNIVERSIDADE FEDERAL DE GOIÁS

PARECER CONSUBSTANCIADO DO CEP

DADOS DO PROJETO DE PESQUISA

Título da Pesquisa: Estratégias para a determinação de biomarcadores de interesse oncológico em fluidos biológicos

Pesquisador: ANDREA RODRIGUES CHAVES

Área Temática:

Versão: 5

CAAE: 19414019.7.0000.5083

Instituição Proponente: Universidade Federal de Goiás - UFG

Patrocinador Principal: Financiamento Próprio

DADOS DO PARECER

Número do Parecer: 4.363.512

Apresentação do Projeto:

Título da Pesquisa: Estratégias para a determinação de biomarcadores de interesse oncológico em fluidos biológicos. Pesquisador Responsável: ANDREA RODRIGUES CHAVES. Virgílio Moreira Roriz; JOSE GONCALVES DA SILVA; Nádia do Lago Costa.

O presente estudo visa a identificação, quantificação e estudo de distribuição de IL-1, IL-6, IL-17, IFN, TNF e lipídeos em amostras de gengiva, saliva e plasma de pacientes diagnosticados com câncer de boca. Para tanto, o projeto contará com uma equipe interdisciplinar, composta por pesquisadores da área química e odontológica. O proponente do projeto, Prof. Dra. Andréa Rodrigues Chaves (UFG-GO), assim como o pesquisador integrante Prof. Dr. Bruno José G. da Silva (UFPR-PR) apresentam experiência no desenvolvimento e validação analítica de metodologias para análises de fármacos em fluidos biológicos empregando métodos de separação. O Prof. Dr. Boniek Gontijo Vaz (UFG-GO), tem desenvolvido métodos de análises por espectrometria de massas, especialmente os que utilizam fontes de ionização ambiente. A Profa. Dra. Nadia do Lago Costa e o Prof. Dr. Virgilio M. Roriz, têm se dedicado ao estudo de câncer de boca, patologia, imunidade tumoral, carcinoma espinocelular.

Objetivo da Pesquisa:

Desenvolvimento de dispositivos específicos e de baixo custo para determinação de citocinas e lipídeos em amostras de fluido biológico de pacientes em unidades de terapia intensiva.

Endereço: Pró-Reitoria de Pesquisa e Inovação - Agência UFG de Inovação, Alameda Flamboyant, Qd. K, Edifício K2
Bairro: Campus Samambaia, UFG **CEP:** 74.690-970
UF: GO **Município:** GOIANIA
Telefone: (62)3521-1215 **E-mail:** cep.prpi@ufg.br

Avaliação dos Riscos e Benefícios:

Riscos: Os participantes do presente estudo, por demanda espontânea, serão atendidos no CGDB-FO-UFG para diagnóstico, tratamento ou acompanhamento de lesões de boca. Os pacientes com lesões com hipótese de diagnóstico de câncer em cavidade oral serão submetidos a biópsia incisional (pequeno fragmento da lesão) para avaliação dos aspectos microscópicos e emissão de laudo anatomopatológico. O presente estudo utilizará uma pequena parte deste fragmento removido para o diagnóstico da lesão, o qual não comprometerá o diagnóstico ou tratamento. Além desses fragmentos, saliva e sangue periférico dos pacientes serão coletadas e avaliadas. O procedimento de biópsia possui RISCO mínimo, uma vez que isto será realizado em Consultório Odontológico equipado, limpo adequadamente, com campos cirúrgicos estéril, com material cirúrgico e equipamento estéril e, realizada por cirurgiã dentista experiente. No caso de eventual complicação transoperatória, o CGDB-FO-UFG apresenta estrutura e equipe está apta para oferecer o suporte necessário ao paciente. O paciente9receberá da cirurgiã-dentista responsável e equipe todas as orientações pós-operatórias necessárias para evitar infecções e desconfortos. Os procedimentos de consulta odontológica, biópsia, coleta de saliva e sangue serão realizados em consultório reservado a fins de evitar constrangimentos. Ressalta-se que o procedimento da biópsia faz parte do procedimento de diagnóstico do paciente que procurou atendimento. Os procedimentos usados no estudo não oferecerão riscos à dignidade ou integridade física, prejuízos ou lesões aos indivíduos participantes. Porém um risco inerente ao desenvolvimento da pesquisa será o desconforto ao paciente o qual poderá ser gerado nos procedimentos de coleta de saliva e sangue e obtenção do fragmento de biópsia. Todas as informações coletadas neste estudo serão estritamente confidenciais, garantindo o sigilo, confidencialidade e a privacidade dos participantes. Os participantes não terão benefício direto, entretanto, espera-se que este estudo proporcione informações importantes sobre o curso clínico e diagnóstico do câncer de boca, com a possibilidade do seu diagnóstico por meio de uma técnica mais rápida, fácil e precisa. Além disso, o conhecimento construído a

partir desta pesquisa poderá colaborar para o entendimento dessas doenças e para a realização de novos estudos no tratamento dessas lesões, onde o pesquisador se compromete a divulgar os resultados obtidos. Os participantes dessa pesquisa também terão BENEFÍCIOS indiretos, de forma que o conhecimento construído a partir desta pesquisa possa colaborar para o entendimento e tratamento dessa doença autoimune altamente.

Benefícios: Rápido diagnostico e possibilidade de tratamento adequado.

Comentários e Considerações sobre a Pesquisa:

Trata-se de um estudo de delineamento experimental, de cunho de pesquisa de campo. A presente proposta prevê o desenvolvimento de dispositivos para análise de biomarcadores em fluido oral de pacientes para auxiliar no diagnóstico e prognóstico para câncer. Tais objetivos contribuem de forma ímpar para a comunidade e para a saúde pública.

Considerações sobre os Termos de apresentação obrigatória:

A pesquisadora responsável adequou o titulo do projeto, unificando o mesmo título do projeto entre folha de rostro e informações básica.

Havia uma solicitação para envio de amostras ao exterior, para que pudessem realizar experimentos da pesquisa; após orientação do CONEP, a intenção foi repensada e os pesquisadores desistiu do envio de amostras para o exterior.

Foi adicionado anuência do Instituto de Química e da Faculdade de Odontologia, ambos da UFG, em atendimento de pendência, o TCLE foi reestruturado, de acordo com o solicitado pelo CEP.

Conclusões ou Pendências e Lista de Inadequações:

Após análise dos documentos postados somos favoráveis à aprovação do presente protocolo de pesquisa, smj deste Comitê

Considerações Finais a critério do CEP:

Informamos que o Comitê de Ética em Pesquisa/CEP-UFG considera o presente protocolo APROVADO, o mesmo foi considerado em acordo com os princípios éticos vigentes. Reiteramos a importância deste Parecer Consubstanciado, e lembramos que o(a) pesquisador(a) responsável deverá encaminhar ao CEPUFG o Relatório Final baseado na conclusão do estudo e na incidência de publicações decorrentes deste, de acordo com o disposto na Resolução CNS n. 466/12 e Resolução CNS n. 510/16. O prazo para entrega do Relatório é de até 30 dias após o encerramento da pesquisa, previsto para novembro de 2023.

Este parecer foi elaborado baseado nos documentos abaixo relacionados:

Tipo Documento	Arquivo	Postagem	Autor	Situação
Informações Básicas do Projeto	PB_INFORMAÇÕES_BÁSICAS_DO_PROJETO_1411829.pdf	07/10/2020 17:16:50		Aceito
Recurso Anexado pelo Pesquisador	Carta_de_Encaminhamento.pdf	07/10/2020 17:15:48	ANDREA RODRIGUES CHAVES	Aceito
Projeto Detalhado	Projeto_CEP_2020.pdf	07/10/2020	ANDREA	Aceito

UFG - UNIVERSIDADE FEDERAL DE GOIÁS

Continuação do Parecer: 4.363.512

/ Brochura Investigador	Projeto_CEP_2020.pdf	17:15:05	RODRIGUES CHAVES	Aceito
TCLE / Termos de Assentimento / Justificativa de Ausência	TCLE_modificado_2020.pdf	07/10/2020 17:14:49	ANDREA RODRIGUES CHAVES	Aceito
Declaração de Instituição e Infraestrutura	ANUENCIA_DIRECAO_FO.pdf	07/10/2020 17:14:39	ANDREA RODRIGUES CHAVES	Aceito
Declaração de Instituição e Infraestrutura	Anuencia_IQ.pdf	07/10/2020 17:14:26	ANDREA RODRIGUES CHAVES	Aceito
Folha de Rosto	FolhadeRosto2020.pdf	07/10/2020 17:13:22	ANDREA RODRIGUES CHAVES	Aceito

Situação do Parecer:
Aprovado

Necessita Apreciação da CONEP:
Não

GOIANIA, 27 de Outubro de 2020

Assinado por:
João Batista de Souza
(Coordenador(a))

Endereço: Pró-Reitoria de Pesquisa e Inovação - Agência UFG de Inovação, Alameda Flamboyant, Qd. K, Edifício K2
Bairro: Campus Samambaia, UFG **CEP:** 74.690-970
UF: GO **Município:** GOIANIA
Telefone: (62)3521-1215 **E-mail:** cep.prpi@ufg.br

ATTACHMENT 2 - TERMO DE CONSENTIMENTO LIVRE E ESCLARECIDO

PROGRAMA DE PÓS-GRADUAÇÃO EM QUÍMICA
UNIVERSIDADE FEDERAL DE GOIÁS
INSTITUTO DE QUÍMICA

Bloco IQ-1, Avenida Esperança, s/n, Campus Samambaia, Goiânia -Goiás- Brasil Fone: 62 3521-1008 / 1016

TERMO DE CONSENTIMENTO LIVRE E ESCLARECIDO - TCLE

Você/Sr./Sra. está sendo convidado(a) a participar, como voluntário(a), da pesquisa intitulada "ESTRATÉGIAS PARA DETERMINAÇÃO DE BIOMARCADORES DE INTERESSE ONCOLÓGICO EM FLUIDOS BIOLÓGICOS DE PACIENTES". Meu nome é Andréa Rodrigues Chaves, sou a pesquisadora responsável e minha área de atuação é como docente do Instituto de Química da Universidade Federal de Goiás, juntamente com os professores pesquisadores Nádia do Lago Costa e Virgílio Moreira Roriz, da Faculdade de Odontologia da Universidade Federal de Goiás; Boniek Gontijo Vaz do Instituto de Química da Universidade Federal de Goiás; e Bruno José Gonçalves da Silva, do Departamento de Química da Universidade Federal do Paraná supervisionaremos esta pesquisa. Após receber os esclarecimentos e as informações a seguir, se você aceitar fazer parte do estudo, assine ao final deste documento, que está impresso em duas vias, sendo que uma delas é sua e a outra pertence ao(à) pesquisador(a) responsável. Esclareço que em caso de recusa na participação você não será penalizado(a) de forma alguma. Mas se aceitar participar, as dúvidas sobre a pesquisa poderão ser esclarecidas pelo(s) pesquisador(es) responsável(is), via e-mail (andrea_chaves@ufg.br) e, inclusive, sob forma de ligação a cobrar, através do(s) seguinte(s) contato(s) telefônico(s): (62) 98148-1337 ou (62) 3521-1094, ramal 251. Ao persistirem as dúvidas sobre os seus direitos como participante desta pesquisa, você também poderá fazer contato com o **Comitê de Ética em Pesquisa** da Universidade Federal de Goiás, pelo telefone (62)3521-1215, que é o órgão que regula todas as pesquisas envolvendo seres humanos na Universidade Federal de Goiás.

INFORMAÇÕES IMPORTANTES SOBRE A PESQUISA:

- Título: Estratégias para determinação de biomarcadores de interesse oncológico em fluidos biológicos de pacientes

- O termo de consentimento será aplicado pela Nádia do Lago Costa, professora da Faculdade de Odontologia da Universidade Federal de Goiás e pesquisadora colaboradora para a execução do presente projeto.

- Neste estudo pretendemos desenvolver e avaliar a aplicabilidade de um dispositivo para determinação de biomarcadores de interesse oncológico. O motivo que nos leva a estudar esse assunto é a demora de diagnóstico para câncer em razão da falta de exames rápidos e sem erros para toda a população, mesmo as que vivem em regiões distantes. Para tanto, as amostras serão estudadas no Laboratório de Cromatografia e Espectrometria de Massas no Instituto de Química da Universidade Federal de Goiás, onde será feita a avaliação dos biomarcadores para o câncer de gengiva e o desenvolvimento do dispositivo diagnóstico. As amostras ficarão armazenadas no LaCEM como biorrepositório até o fim da pesquisa, onde serão incineradas.
- Para participar deste estudo, você precisará doar uma amostra de saliva (5 mL), em um frasco devidamente numerado, uma amostra de sangue (2 mL) que deverá ser coletado por profissional qualificado (Enfermeiro, Farmacêutico, Biomédico, Médico ou Cirurgião-dentista) e uma amostra da sua gengiva ou tumor.

PROGRAMA DE PÓS-GRADUAÇÃO EM QUÍMICA
UNIVERSIDADE FEDERAL DE GOIÁS
INSTITUTO DE QUÍMICA

Bloco IQ-1, Avenida Esperança, s/n, Campus Samambaia, Goiânia -Goiás- Brasil Fone: 62 3521-1008 / 1016

- A coleta da saliva e sangue serão realizados nos consultórios odontológicos do Centro Goiano de Doenças da Boca da Faculdade de Odontologia da Universidade Federal de Goiás (CGDB-FO-UFG), evitando ao máximo o seu constrangimento e sem ônus de qualquer espécie ao participante da pesquisa, em todas as situações em que este dela necessite. É garantido o direito a assistência integral gratuita devido a danos diretos/ indiretos e imediatos/ tardios, pelo tempo que for necessário ao participante da pesquisa.
- A coleta do tecido (gengiva ou tumor) também serão realizados no CGDB-FO-UFG, o qual conta com consultórios odontológicos devidamente equipados. Trata-se de um procedimento invasivo, o qual é necessário para o diagnóstico final da lesão, e que parte deste material será utilizado para a pesquisa.

- Dessa forma, ao participar deste estudo o(a) Sr.(Sra.) permitirá que eu obtenha um pequeno fragmento da lesão que será removida durante a biópsia e uma pequena quantidade de saliva e sangue. Nós realizaremos alguns estudos em laboratório com esse fragmento da lesão, saliva e sangue. Portanto, o fragmento removido será processado e congelado para execução de experimentos laboratoriais futuros.

- O procedimento de biópsia dos tecidos coletados será realizado em consultórios odontológicos do CGDB, devidamente equipado, limpo adequadamente, com campos cirúrgicos estéreis, material cirúrgico e equipamento estéril e, realizada por cirurgião-dentista estomatologista (membro da equipe do CGDB). No caso de eventual complicação trans-operatória, o CGDB apresenta todos os equipamentos de primeiros socorros (dentre eles: oxigênio e medicação) e a equipe está apta para oferecer o suporte necessário ao participante da pesquisa.

- O participante da pesquisa receberá do cirurgião-dentista responsável e equipe todas as orientações pós-operatórias necessárias para evitar infecções e desconfortos. Ressalta-se que o procedimento da biópsia faz parte do procedimento de diagnóstico do participante da pesquisa que procurou atendimento no CGDB.

- O procedimento cirúrgico, para o tratamento do câncer, será realizado por um cirurgião de cabeça e pescoço (membro da equipe de cabeça e pescoço do Hospital Araújo Jorge) em centro cirúrgico do Hospital Araújo Jorge, devidamente equipado.

- Os dados obtidos nesta pesquisa poderão direcionar o tratamento e acompanhamento dos participantes da pesquisa, podendo estes serem BENEFICIADOS diretamente, uma vez que o custo da realização destas investigações moleculares é alto. Os participantes dessa pesquisa também terão BENEFÍCIOS indiretos, pois espera-se que este estudo proporcione informações importantes sobre o câncer bucal e desordens potencialmente malignas de boca, de forma que o conhecimento construído a partir desta pesquisa possa colaborar para o entendimento dessas doenças e para a realização de novos estudos no tratamento dessas lesões.

- Dessa forma, ao participar deste estudo o(a) Sr.(Sra.) permitirá que eu obtenha um pequeno fragmento da lesão que será removida durante a biópsia e uma pequena quantidade de saliva (utilização de um tubo falcon) e sangue (somente para participantes da pesquisa com câncer). Nós realizaremos alguns estudos em laboratório com esse fragmento da lesão, sangue e saliva. Portanto, a maior parte do fragmento removido será processada, congelada, registrada no laboratório de patologia e o laudo será emitido para o diagnóstico da lesão; assim como a saliva e sangue para execução de experimentos laboratoriais mediante as técnicas de RT-PCR, ELISA, citometria de fluxo, APSMALDI-MS e LC-MS/MS.

PROGRAMA DE PÓS-GRADUAÇÃO EM QUÍMICA
UNIVERSIDADE FEDERAL DE GOIÁS
INSTITUTO DE QUÍMICA

Bloco IQ-1, Avenida Esperança, s/n, Campus Samambaia, Goiânia -Goiás- Brasil Fone: 62 3521-1008 / 1016

- As amostras coletadas a partir da biópsia, bem como as amostras de saliva e sangue serão processadas e o excedente será armazenado como biorrepositório após o término da pesquisa, podendo ser utilizadas em estudos futuros.

    - O(A) Sr.(Sra.) autoriza a utilização o material coletado em toda e qualquer nova pesquisa ( ) Sim ( ) Não

    - O(A) Sr.(Sra.) quer saber de todos os resultados obtidos com a pesquisa ( ) Sim ( ) Não

    - O(A) Sr.(Sra.) quer ser informado de toda e qualquer nova pesquisa a ser realizada, e de quando o material for destruído ( ) Sim ( ) Não

( ) Declaro ciência de que os meus dados coletados podem ser relevantes em pesquisas futuras e, portanto, autorizo a guarda do material em banco de dados e/ou biobancos e biorrepositórios.

( ) Declaro ciência de que os meus dados coletados podem ser relevantes em pesquisas futuras, mas não autorizo a guarda do material em banco de dados e/ou biobancos e biorrepositórios, que poderá ocorrer a transferência do material biológico do biorrepositório para o biobanco, após a sua aprovação pelo sistema CEP/Conep.

- A participação do Sr.(Sra.) nesta pesquisa não traz complicações legais. Os procedimentos adotados obedecem aos Critérios da Ética em Pesquisa com Seres Humanos conforme Resolução no. 466/12 do Conselho Nacional de Saúde. Um risco inerente ao desenvolvimento da pesquisa será o desconforto ao participante da pesquisa o qual poderá ser gerado nos procedimentos de coleta de saliva e obtenção do fragmento de biópsia. Todas as informações coletadas neste estudo serão estritamente confidenciais, garantindo o sigilo, confidencialidade e a privacidade dos participantes.

- **O(A) Sr.(Sra.) não terá nenhum tipo de despesa para participar desta pesquisa, bem como nada será pago por sua participação.**
- A sua participação é **voluntária** e a recusa em participar **não acarretará qualquer penalidade ou modificação na forma em que é atendido**.

- **Ao aceitar participar dessa pesquisa, o(a) Sr.(Sra.) autoriza o pesquisador responsável a ter acesso às informações contidas em seu prontuário. Tal ação é necessária para avaliação da elegibilidade do candidato a participante da pesquisa. Tais informações serão tratadas estrita confidencialidade, garantindo o sigilo, e a privacidade dos participantes.**

- A sua participação no referido projeto não acarretará nenhum tipo de pagamento ou gratificação financeira. Mas caso necessário, você tem o direito de pleitear indenização em caso de reparação de danos imediatos ou futuros.

- Para sua participação não serão necessárias nenhum tipo de intervenção e tratamentos adicionais, bem como métodos alternativos.

- O projeto terá duração de 48 meses, mas sua participação será apenas durante a aplicação deste **TERMO DE CONSENTIMENTO LIVRE E ESCLARECIMENTO**.

- Todas as informações coletadas neste estudo são estritamente **CONFIDENCIAIS**. Somente o(a) pesquisador(a) e o(a) orientador(a) terão conhecimento dos dados.

PROGRAMA DE PÓS-GRADUAÇÃO EM QUÍMICA
UNIVERSIDADE FEDERAL DE GOIÁS
INSTITUTO DE QUÍMICA

Bloco IQ-1, Avenida Esperança, s/n, Campus Samambaia, Goiânia -Goiás- Brasil Fone: 62 3521-1008 / 1016

- **O(A) Sr.(Sra.) possui a garantia expressa de liberdade de não aceitação, bem como de retirar o consentimento, sem qualquer prejuízo da continuidade do acompanhamento/tratamento usual.**

- Os resultados da pesquisa estarão a sua disposição quando finalizada, nas formas de dissertação, tese e artigos científicos. Seu nome ou material que indique sua participação não serão divulgados sem a sua permissão, ou do responsável por você. Os dados e instrumentos utilizados na pesquisa ficarão arquivados com o pesquisador responsável por um período de cinco anos, e após esse tempo serão destruídos.

- Este termo de consentimento encontra-se impresso em duas vias, sendo que uma cópia será arquivada pelo pesquisador responsável, e a outra será fornecida a você.

- TODAS AS PÁGINAS DESTE TERMO DEVERÃO SER RUBRICADAS PELO PESQUISADOR RESPONSÁVEL OU PESSOA POR ELE DELEGADA, E PELO PARTICIPANTE DA PESQUISA OU RESPONSÁVEL LEGAL.

1.2 Consentimento da Participação da Pessoa como Participante da Pesquisa:

Eu, ..., abaixo assinado, concordo em participar do estudo intitulado "ESTRATÉGIAS PARA DETERMINAÇÃO DE BIOMARCADORES DE INTERESSE ONCOLÓGICO EM FLUIDOS BIOLÓGICOS DE PACIENTES". Informo ter mais de 18 anos de idade, e destaco que minha participação nesta pesquisa é de caráter voluntário. Fui, ainda, devidamente informado(a) e esclarecido(a), pelos pesquisadores responsáveis Andréa Rodrigues Chaves e Nádia do Lago Costa, sobre a pesquisa, os procedimentos e métodos nela envolvidos, assim como os possíveis riscos e benefícios decorrentes de minha participação no estudo. Foi-me garantido que posso retirar meu consentimento a qualquer momento, sem que isto leve a qualquer penalidade. Declaro, portanto, que concordo com a minha participação no projeto de pesquisa acima descrito.

Goiânia, ... de ..... de .....

_____	_____
Assinatura por extenso do(a) participante	Assinatura por extenso do(a) pesquisador(a) responsável

Testemunhas em caso de uso da assinatura datiloscópica

PROGRAMA DE PÓS-GRADUAÇÃO EM QUÍMICA
UNIVERSIDADE FEDERAL DE GOIÁS
INSTITUTO DE QUÍMICA

Bloco IQ-1, Avenida Esperança, s/n, Campus Samambaia, Goiânia -Goiás- Brasil Fone: 62 3521-1008 / 1016

	_____
	_____

Presenciamos a solicitação de consentimento, esclarecimento sobre a pesquisa e aceite do sujeito em participar.

Testemunhas (não ligadas à equipe de pesquisadores)

_____ Testemunha 1

_____ Testemunha 2

ATTACHMENT 3 – CURRICULUM LATTES – RICARDO ALVES BERNARDO

Currículo Lattes

Ricardo Alves Bernardo

Endereço para acessar este CV: **http://lattes.cnpq.br/4470407084894434**

Última atualização do currículo em 25/07/2022

Resumo informado pelo autor

Possui graduação em Química Industrial pela Universidade Federal de Goiás (2015) e mestrado em Química Analítica pela Universidade Federal de Goiás (2017). Foi professor substituto do Instituto Federal Goiano - Campus Ceres (2017-2018) e atualmente é aluno de Doutorado do Programa de Pós-Graduação do Instituto de Química da UFG, com período sanduíche no Department of Pharmacy da The Faculty of Health and Medical Science - University of Copenhagen.
(Texto informado pelo autor)

Nome civil

Nome Ricardo Alves Bernardo

Dados pessoais

Nascimento 17/04/1993 - Trindade/GO - Brasil

CPF 035.589.361-40

Formação acadêmica/titulação

2018 Doutorado em Química.
Universidade Federal de Goiás, UFG, Goiania, Brasil
com **período sanduíche** em University of Copenhagen (Orientador: Christian Janfelt)
Título: Estratégias para determinação de biomarcadores de interesse oncológico em fluidos biológicos de pacientes
Orientador: Andréa Rodrigues Chaves
Bolsista do(a): Coordenação de Aperfeiçoamento de Pessoal de Nível Superior

2015 - 2017 Mestrado em Química.
Universidade Federal de Goiás, UFG, Goiania, Brasil
Título: Aplicações forenses do Probe Electrospray Ionization Mass Spectrometry (PESI-MS) com filmes de polipirrol, Ano de obtenção: 2017
Orientador: Andréa Rodrigues Chaves
Co-orientador: Boniek Gontijo Vaz
Bolsista do(a): Coordenação de Aperfeiçoamento de Pessoal de Nível Superior

2011 - 2015 Graduação em Química Industrial.
Universidade Federal de Goiás, UFG, Goiania, Brasil
Título: Formulações de Anfotericina B em sistemas de liberação nanoestruturados com propriedades mucoadesivas
Orientador: Emilia Celma de Oliveira Lima

Atuação profissional

1. Universidade Federal de Goiás - UFG

Vínculo institucional

2012 - 2015 Vínculo: Voluntário , Enquadramento funcional: Aluno de Iniciação Científica , Carga horária: 20, Regime: Parcial

2. Sun Pharmaceuticals Industries Ltd - SUN PHARMA

Vínculo institucional

2015 - 2015 Vínculo: Estagiário , Enquadramento funcional: Analista no Controle de Qualidade , Carga horária: 30, Regime: Parcial

3. Instituto Federal Goiano - IF Goiano

Vínculo institucional

2017 - 2018 Vínculo: Servidor público , Enquadramento funcional: Professor Substituto , Carga horária: 40, Regime: Integral

Atividades

02/2018 - 07/2018 Graduação, Licenciatura em Química

Disciplinas ministradas:
Físico-Química Experimental 2 , Oficinas de Práticas Pedagógicas em Físico-Química , Termodinâmica

02/2018 - 07/2018 Ensino médio

Especificação:
Química para 2° Ano do Curso Técnico em Agropecuárea Integrado ao Ensino Médio , Química para 2° Ano do Curso Técnico em Meio Ambiente Integrado ao Ensino Médio , Trabalho de Curso para 3° Ano do Curso Técnico em Meio Ambiente Integrado ao Ensino Médio

10/2017 - 12/2017 Ensino médio

Especificação:
Química para 2° Ano do Curso Técnico em Agropecuárea Integrado ao Ensino Médio , Química para 2° Ano do Curso Técnico em Informática Integrado ao Ensino Médio , Química para 1° Ano do Curso Técnico em Meio Ambiente Integrado ao Ensino Médio

10/2017 - 12/2017 Graduação, Licenciatura em Química

Disciplinas ministradas:
Físico-Química de Soluções

Producão

Produção bibliográfica

Artigos completos publicados em periódicos

1. **BERNARDO, RICARDO ALVES**; SOUSA, JEAN CARLOS PEREIRA; GALLIMBERTI, MATHEUS; JUNIOR, FERNANDO BARBOSA; VAZ, BONIEK GONTIJO; CHAVES, ANDRÉA RODRIGUES
A fast and direct determination of bisphenol S in thermal paper samples using paper spray ionization mass spectrometry. Environmental Science and Pollution Research. JCR, v.28, p.57288 - 57296, 2021.

2. TAVARES, LUDMYLA; **BERNARDO, RICARDO**; DE OLIVEIRA, ANSELMO; VAZ, BONIEK; CHAVES, ANDREA
Novel Method for the Extraction of Cocaine from Oral Fluid by Means of Disposable Pipette Modified with Restricted Access Material. JOURNAL OF THE BRAZILIAN CHEMICAL SOCIETY. JCR, v.32, p.2235 - 2244, 2021.

3. MACHADO, LUCAS S.; SOARES, FRANCIELLE Q.; MARTINS, RAFAEL O.; **BERNARDO, RICARDO A.**; CARDOSO, ALESSANDRA T.; RUGGIERO, MARÇAL A.; RABELO, DENILSON; SOUZA, PAULO SÉRGIO; CHAVES, ANDRÉA R.
Polypyrrole monolithic extraction phase: from conventional to miniaturized sample preparation techniques. JOURNAL OF CHROMATOGRAPHY A. JCR, v.1651, p.462260 - , 2021.

4. ROSA FERNANDES, ALINE; **ALVES BERNARDO, RICARDO**; CARLOS PEREIRA SOUSA, JEAN; DE CASTRO GEORG, RAPHAELA; GONTIJO VAZ, BONIEK; RODRIGUES CHAVES, ANDRÉA
Restrict access material for paper spray ionization mass spectrometry: A versatile tool for catecholamines and antidepressants determination in plasma samples. MICROCHEMICAL JOURNAL. JCR, v.158, p.105245 - , 2020.

5. FERNANDES, ALINE; **BERNARDO, RICARDO**; DE CARVALHO, THAYS; VAZ, BONIEK; CHAVES, ANDRÉA
Graphene Oxides Coated Paper as a Substrate to Paper Spray Ionization Mass Spectrometry for Creatinine Determination in Urine Samples. JOURNAL OF THE BRAZILIAN CHEMICAL SOCIETY. JCR, v.30, p.1074 - 1081, 2019.

6. **ALVES BERNARDO, RICARDO**; DA SILVA, LIDYA CARDOZO; QUEIROZ, MARIA EUGÊNIA C.; GONTIJO VAZ, BONIEK; RODRIGUES CHAVES, ANDRÉA
Lab-made solid phase microextraction phases for off line extraction and direct mass spectrometry analysis: evaluating the extraction parameters. JOURNAL OF CHROMATOGRAPHY A. JCR, v.1603, p.23 - 32, 2019.

Página gerada pelo sistema Currículo Lattes em 10/08/2022 às 14:48:08.

Analytical performance evaluation of total lipid extraction using tissue samples conserved in TRIzol® solution

Ricardo Alves Bernardo[1], Charles Ivo de Oliveira Júnior[1,2], Carlos Arterio Sorgi[3], Boniek Gontijo Vaz[1], Andréa Rodrigues Chaves[1,2]

[1] Instituto de Química, Universidade Federal de Goiás, 74690-900, Goiânia, GO, Brazil
[2] Departamento de Química, Universidade Federal de Jataí, 75804-020, Jataí, GO, Brazil
3 Departamento de Química, Faculdade de Filosofia, Ciências e Letras de Ribeirão Preto, Universidade de São Paulo, 14015-130, Ribeirão Preto, SP, Brazil

Abstract

This study evaluates the analytical performance of simultaneous mRNA and lipid extraction in tissue samples preserved in TRIzol® reagent. Therefore, a solution of pig's tongue in TRIzol® was prepared, followed by Bligh & Dyer extraction and mass spectrometry analysis. The samples were spiked with internal standard (PC 17:0/17:0) in eight different concentration levels for the figure of merits evaluation. The lipid extraction in TRIzol® solution was linear in a range from 330 to 2000 ng mL^{-1}, $r^2 > 0.99$, intra and inter-day precision and accuracy ranging from -9.599 to 4.938%, and absolute recovery values ranging from 90.40 to 103.15%.

Keywords: lipid extraction, mass spectrometry, analytical performance

Introduction

Science has devoted many research to the improvement and implementation of precision medicine. In this way, the literature highlighted the need to examine data from multiple molecular platforms (henceforth referred to as multiomics data) to understand underlying disease dynamics and effectively capture clinically meaningful subgroups. The use of just one molecular information to examine the molecular pathology reduces the possibility of understanding the disease's causes or causative agents. These downstream effects are also therapeutically relevant and could be considered in precision medicine studies[1, 2].

Once the requirement for the multiomic data increases, the laboratories assays have more challenges to get higher levels of information while keeping the sample molecular integrity. The development of multiomics methods always will find the obstacle of what molecular information could express better the pathology, the answer will be chosen to be investigated in more detail[3].

Additional molecular information could be obtained using a different methodology and/or a new sample aliquot, which could be a problem for some studies. The mostly multiomics studies, which use biological samples for investigation, demand patients' samples often collected by invasive methodologies. Therefore, reducing the use of samples is always desirable for these analytical methods.

Metabolomics is often applied to the investigation of changes in metabolic pathways, in which disturbed biological systems are compared to undisturbed reference systems. Changes in lipid metabolism and/or RNA transcription can provide information about differential gene and transcript expression patterns in healthy and disease cells/tissues, such as in cancer[4, 5], neurodegenerative diseases[6-8], cardiovascular disease[9, 10], and diabetes[11, 12]. However, the workflow for sample preparation in metabolomics/lipidomics is quite different from transcriptomics, and different samples are used for both purpose[13].

The RNA extractions are based on a liquid-liquid extraction (LLE), where the biological sample is homogenized in TRIzol® solution (a mixture of phenol, water, and guanidine isothiocyanate), and then, chloroform is added for phase separation. The aqueous phase containing the RNA portion is used for transcriptomics essays, and the organic phase is discarded, as described by the manufacturer's protocol, which is a drawback since the organic phase includes lipid, metabolites, and amino acid contents.

Regarding the lipid extraction in biological samples, the Bligh & Dyer method[14] (based on LLE using water, methanol and chloroform), Folch method[15] (based on LLE using chloroform and methanol), and Matyash method (based on LLE using methanol, methyl-*tert*-butyl ether and water) are the most used protocols.

In this study, a mass spectrometry methodology based on the study of Podechard *et al*.[13] was analytical validated for total extraction of lipids in samples stored in TRIzol® solution used for RNA extractions. To this aim, the Bligh & Dyer and Podechard methodology were adapted to total lipid extraction from pig's tongue samples, and the extracted samples analyzed by direct infusion mass spectrometry.

Methods

Materials

TRIzol® solution was acquired from Invitrogen (Cergy Pontoise, France). 1,2-diheptadecanoyl-sn-glycero-3-phosphocholine (PC 17:0/17:0) (> 99%), and caffeine-(3-methy-^{13}C) (99%) were acquired from Sigma Aldrich (Massachusetts, USA). Pre-column cartridge

SecurityGuardTM ULTRA (UHPLC C18, 2,1 mm i.d.) was acquired from Allcrom (São Paulo, Brazil). Chloroform (99,8%) was acquired from Synth (São Paulo, Brazil). Methanol (>99.9%) was acquired from Tedia (Ohio, USA). Ultra-purified water was prepared in a MS2000 system (Gehaka, São Paulo, SP, Brazil).

The pig's tongue samples were acquired in the local butcher market right after the slaughter and immediately frozen at -80 °C.

Sample preparation and lipid extraction

A solution of pig's tongue in TRIzol® was prepared in the ration of 1000 µL of TRIzol® for each 100 mg of tongue, and then, the mixture tongue+TRIzol® was homogenized in an Ultra Turrax Homogenizer T25 (IKA, Campinas, Brazil). Therefore, 200 µL of chloroform were added for each 1 mL of tongue solution in TRIzol®. The resulting solution was homogenized by vortex for 1 min and centrifuged at 1500 G, 4 °C for 10 min.

A three-phase system was formed, composed by an upper layer (aqueous phase containing RNA), a protein pellet, and a lower phase (organic phase I, composed by lipids in chloroform). Moreover, an aliquot of 250 µL of the organic phase I was taken, PC (17:0/17:0) was added in eight different concentration levels, and caffeine-(3-methyl-^{13}C) was added as internal standard (IS) at a concentration of 800 ng mL^{-1}, Bligh & Dyer extraction[14] as reported by Barbosa and co-workers, 2022[16] was performed on it.

For the adapted Bligh & Dyer extraction[14], 500 µL of methanol and 200 µL of ultrapurified water were added to 250 µL of the mixture organic phase I+PC (17:0/17:0)+IS. The solution was then vortexed for 1 min, and centrifuged at 1500 G, 4 °C for 10 min, and another 250 µL of chloroform and 250 µL of ultrapurified water were added to the centrifuged solution. The system was then vortexed for 1 min and centrifuged one more time at 1500 G, 4 °C for 10 min. Another three-phase system was formed (aqueous phase, protein pellet and organic phase II). The organic phase II was collected to a vial flask, and 500 µL of chloroform were added into the remaining aqueous phase+protein pellet to enhance the extraction efficiency. This solution was then vortexed and centrifuged again as described above, and the resulting organic phase (organic phase III) was collected and mixed with the organic phase II.

The mixture of organic phases II and III was evaporated in a SpeedVac Concentrator (Savant SPD131DDA, Thermo Scientific – Massachusetts, USA), and the dried extract was resuspended in 200 µL of methanol. The same extraction was performed using pig's tongue homogenized in methanol for the comparison with extraction using TRIzol® solution. The whole extraction process is illustrated in the Figure 1.

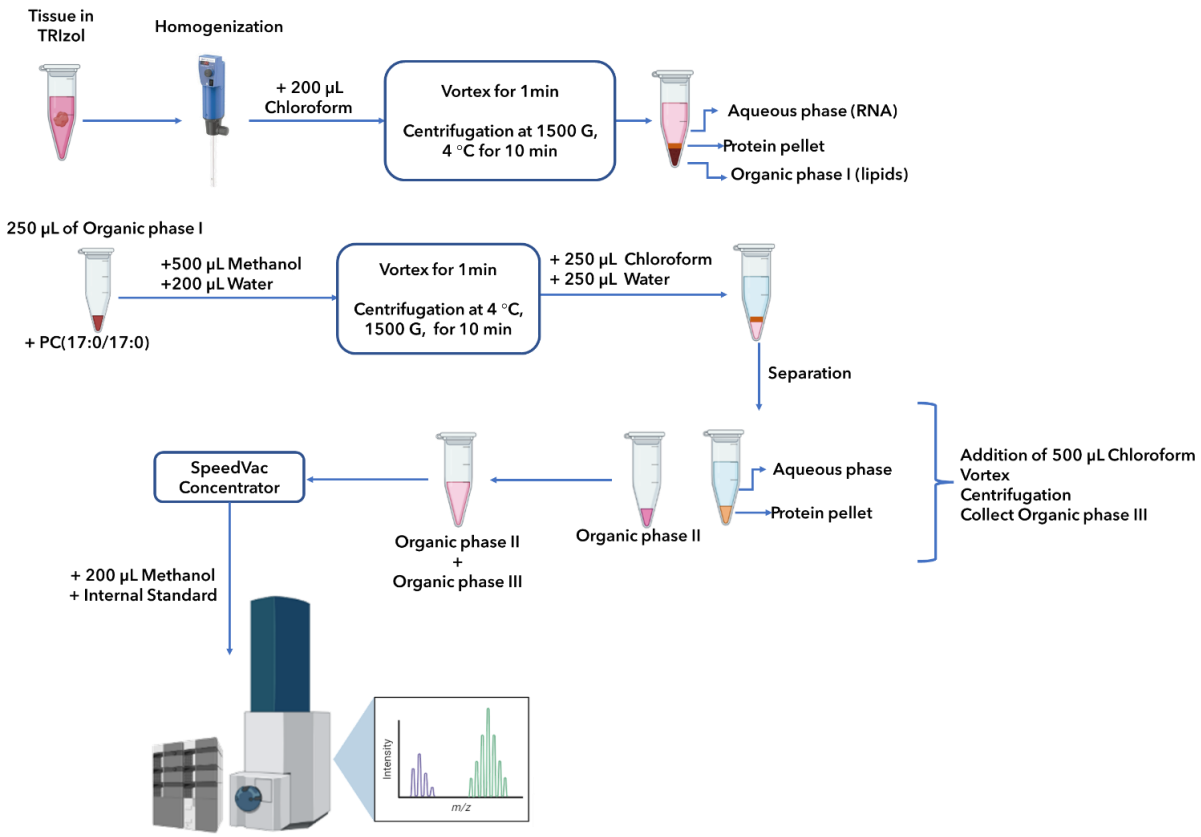

Figure 1. Workflow for the total extraction of lipids in samples homogenized in TRIzol® solution.

Mass spectrometry analysis

The extracted samples were analyzed by direct infusion mass spectrometry (MS). A liquid chromatographer (Shimadzu LC-20AD) was used as automatic injector into the mass spectrometer, at a methanol flow rate of 300 µL min^{-1}, sample volume of 40 µL, sample tray temperature at 4 °C and a pre-column cartridge SecurityGuardTM ULTRA (UHPLC C18, 2,1 mm i.d.) was used. The mass spectrometry analyses were performed in a Bruker Daltonics micrOTOF III (Bremen, Germany) with electrospray ion source (ESI) in the positive ion mode. The parameters used for the MS analysis were capillary voltage 4 kV, nebulizer 1.0 bar, dry temperature 200 °C, end plate offset 500 V.

Analytical performance

The analytical performance of the extraction in TRIzol® proposed in this study was investigated. Linearity was evaluated by an analytical curve using replicates (n = 5) of PC (17:0/17:0) at 330, 500, 800, 1100, 1400, 1700, and 2000 ng mL^{-1} *versus* the extracted ion chromatogram (EIC) area and treated by the ANOVA statistical technique. Caffeine-(3-methy-

^{13}C) was used as internal standard (IS) at concentration level of 800 ng mL^{-1}. The ratio between the EIC area of PC (17:0/17:0) and IS was used as analytical response.

Intraday precision (P), accuracy (A) and absolute recovery (R) were determined using quintuplicate essays of the proposed method of samples at 800, 1400 and 2000 ng mL^{-1} concentration levels, as shown in the Equations 1 – 3.

$$P = \frac{STD}{ACe} . 100 \qquad \textbf{Equation 1}$$

$$A = \frac{ACe - TC}{TC} . 100 \qquad \textbf{Equation 2}$$

$$R = \frac{SSC - NSSC}{SC} . 100 \qquad \textbf{Equation 3}$$

Where, STD means the standard deviation in the concentrations determined experimentally, ACe corresponds to the average experimental concentration between the replicates, TC stands for theoretical concentration, SSC corresponds to the spiked sample concentration, NSSC to the non-spiked sample concentration and SC means the spiked concentration[17].

The limits of detection (LOD) and quantification (LOQ) were experimentally determined with diluted concentrations of PC (17:0/17:0) up to the signal-to-noise ratio of about 3.3 and 10, respectively. The matrix effect (ME) was evaluated in three concentration levels (800, 1400, 2000 ng mL^{-1}) and was estimated by the ratio between the response in the analytical curve (extraction performed in the presence of TRIzol®) (B) and the response in the calibration curve (extraction method using methanol as TRIzol® replacement) (A), as described by Equation 4.

$$ME = \left(\frac{B}{A}\right) . 100 \qquad \textbf{Equation 4}$$

Results and Discussion

Lipid analysis

The lipid extracts were direct infused into the mass spectrometer in positive ion mode using the LC automatic injector. The extracts presented contents of phosphocholines (PC), ceramides (Cer), phosphoethanolamines (PE), betaines (DGTA), lysophosphatidic acid (LPA), and phosphoserine (PS), as shown in Figure 2. The peak annotation was performed using the

exact mass on LIPIDMAPS database[18]. Figures 2b, and 2c present the peak annotation with ppm error for each identified lipid.

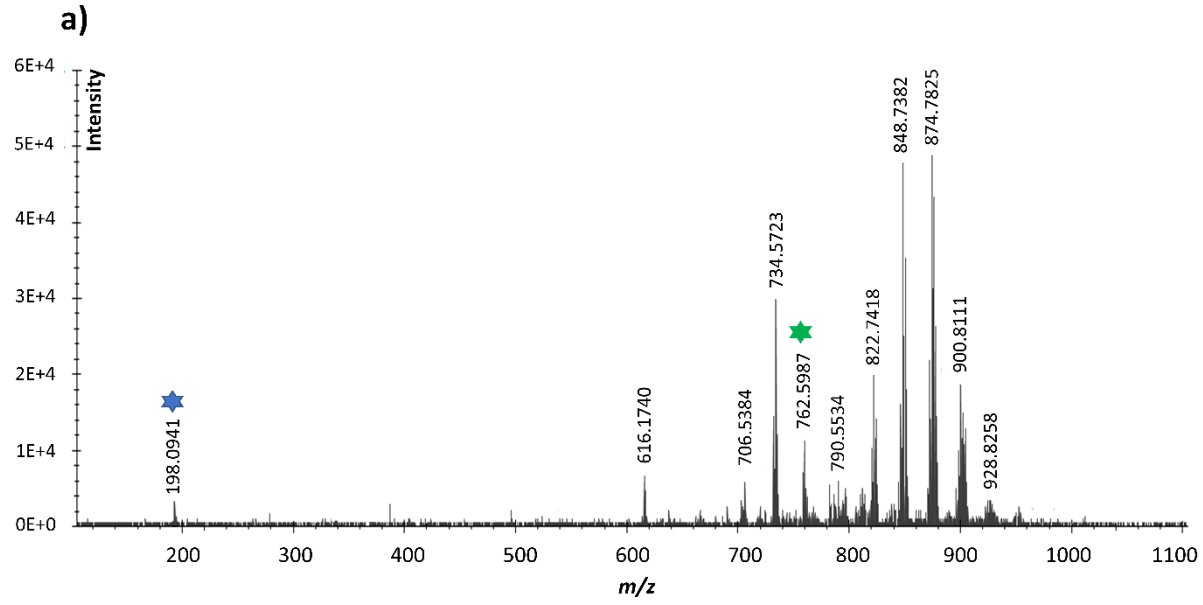

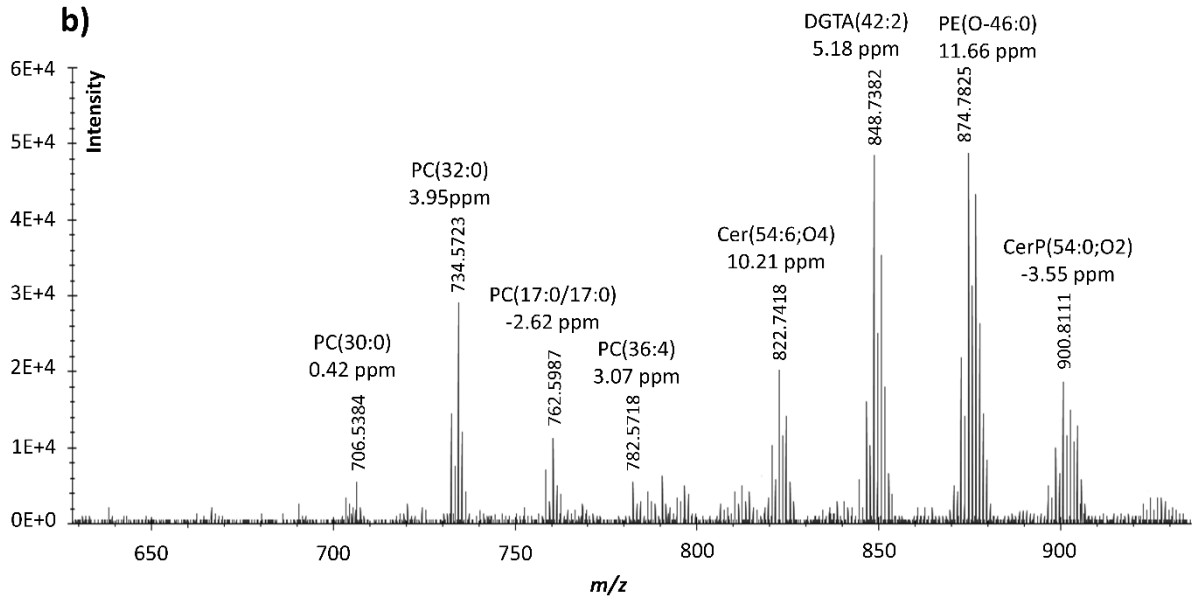

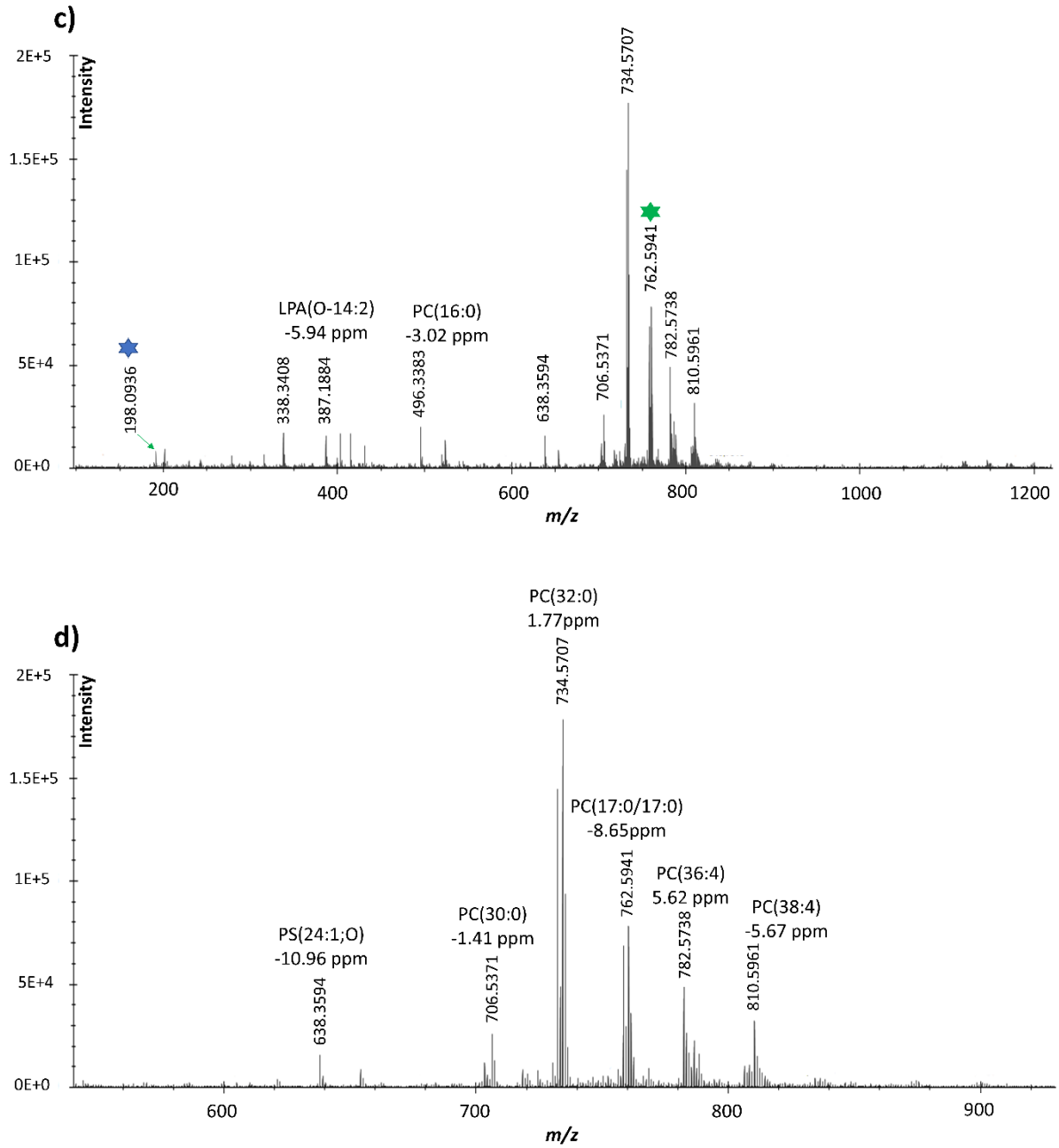

Figure 2. MS spectra for extraction performed in TRIzol® (full scan (a) and zooming (b)), and methanol (full scan (c) and zooming (d)). The internal standard (800 ng mL^{-1}) is marked with a blue star, and the PC(17:0/17:0) (2000 ng mL^{-1}) is marked with a green star in the full scan spectrum.

Comparing the Figures 2a. and 2c., it is possible to observe that spectrum intensity in methanol was higher than the spectrum intensity in TRIzol®. However, the extractions in

TRIzol® presented a significative enhancement in the spectral signal in the mass range from 600 to 1000 Da. This enhancement was not observed in the methanolic extractions.

Both extraction methods were able to extract PC contents from the biological matrix. TRIzol® extraction stands out regarding lipids with higher molecular weight (mass range 600-1000 Da), and low abundant lipids, such as ceramides[19], were efficiently extracted and detected. Moreover, PE and DGTA were also present in the TRIzol® extraction and absent in the classic extraction using methanol. The extraction performed in methanol stands out regarding lipids with lower molecular weight, such as PA and PC in the mass range of 300-500 Da. However, in the present study, the extractions in methanol only presented contents of PCs and PAs, which represents a loss of information regarding important lipids that already have been related to many diseases, such as Cer in cancer research[20], neuroprotective role of PS in patients diagnosed with glaucoma[21], and betaine role in inflammatory response[22].

Analytical performance

The linearity was evaluated in analytical curves using the PC (17:0/17:0) concentration versus the ration between the EIC area for PC (17:0/17:0) over the EIC area for the IS, and processed by ANOVA statistical technique, Table 1. The method was linear in a concentration range from the LOQ to 2000 ng mL^{-1}, with $R^2 > 0.99$. The LOD and LOQ for the extractions in TRIzol® were lower compared to the extractions in methanol, which means that the proposed method in this study was selectivity for lipid extractions allowing its extraction from samples stored in TRIzol®. The precision and accuracy for both extractions were evaluated in intra and inter-day assays. The results for precision, accuracy and recovery are in accordance with the values described by the Food and Drug Administration (FDA), precision and accuracy < 15%, and recovery values ranging from 80 to 120%[23], and are presented in Table 2.

Table 1. Linear regression, determination coefficient, LOD and LOQ, and their respective p-value in ANOVA test for lipid extractions performed in TRIzol® and methanol

Extraction method	Linear regression (LOD:2000 ng mL^{-1})	R^2	LOD (ng mL^{-1})	LOQ (ng mL^{-1})	ANOVA p-value
TRIzol®	y = 0.0188x + 0.3385	0.9927	110	330	5.32E-09
Methanol	y = 0.0083x + 9.5071	0.9911	160	475	2.84E-07

Table 2. Intra and inter-day precision, accuracy and absolute recovery of the lipid extraction performed with TRIzol® reagent

Homogenate Solvent	Contentration (ng mL^{-1})	Precision (%)		Accuracy (%)		Absolute Recovery (%)
		Intra-day	Inter-day	Intra-day	Inter-day	
TRIzol®	800	2.89	4.93	-7.62	-9.60	92.38
	1400	1.92	1.36	3.14	1.55	103.15
	2000	2.46	2.43	2.10	2.89	102.10
Methanol	800	7.99	5.77	1.76	1.00	101.76
	1400	4.95	2.12	-1.49	-1.85	98.51
	2000	3.40	2.38	4.30	2.06	104.30

The ME can be evaluated by comparing the parallelism between the analytical curve of TRIzol® samples and the calibration curve in methanol[24], or calculation of recovery values by adding standard solutions to real samples[25]. As described in the Methods section, the ME was estimated by Equation 4. The results for the three concentration levels evaluated here (800, 1400 and 2000 ng mL^{-1}) were 96.07, 103.76 and 101.69%, respectively. It is possible to conclude that no matrix effect was observed in these analyses, since the calculated values ranged from 80 to 120%[26]. In addition, the absolute recovery values for both curves are sufficiently high enough (92.38 – 104.30% - Table 2), which means that the response of the proposed method cannot be affected by the sample matrix, in this case, the solvent for homogenate preparation prior to extraction.

Method comparison

Regarding total lipid extractions, many studies are reported in the literature for optimization the solvent extraction ratios in well-stablished protocols. Bowden and co-workers, 2018[19] optimized sample-to-extraction solvent ratios in Folch, Bligh & Dyer and Matyash methods for lipid extractions in human plasma. The authors claimed that Bligh & Dyer and Floch methods yielded higher peak areas regardless the solvent extraction volume, while Matyash methods requires larger extraction solvent volumes to yield comparable results. The authors also stated that the sample to extraction solvent ratio presented higher extraction efficiency at 1:20 (for liquid matrices), where some low abundant lipids (such as ceramides and phosphoinositides) presented higher extraction efficiency. Comparing the sample-to-extraction solvent in Bowden's study, the authors used a proportion of 5% (v/v) for liquid biological matrices, and in the present study, a proportion of 10 (% wt) was used, and similar results were achieved.

Zhang and co-workers, 2017[4] performed a lipid extraction from plasma for lipid profiling and diagnostic biomarkers for oral squamous cells carcinoma. The authors do not state a name for their extraction protocol; however, it is quite similar to the Matyash method, using

methanol, water, and MTBE. In their study, glycerophosphoglycerols (PGs), PCs, PEs, LPAs, Cers, and sphingomyelin (SM) were extracted. However, the authors did not report any data about quantitation or analytical parameter. In the present study, the analytical performance for the TRIzol® lipid extraction is reported, most lipid species represent PCs, as reported by Zhang's study. Sorvina *et al.*, 2018[27] used the Folch method for lipid extraction in prostate cancer cell lines. The authors used LC-MS/MS and were able to analyze free cholesterol, cholesteryl esters, PC, PE, SM, and gangliosides. However, the authors did not report any quantitation or analytical parameter evaluation. In addition, the methodology presented in this study allows the possibility of multiomics assays, since the RNA is extracted with TRIzol® in the first extraction step, as reported by Podechard *et al.*, 2018[13], as well as proteins and small molecules, without the need of previous chromatographic separation, which provides a significant reduction in the time of analysis. Moreover, the proposed method also does not require a clean-up step for lipidomic analysis since the salt content remains in the aqueous phase.

Conclusion

A reliable, accurate and precise methodology was reported for simultaneous extraction of RNA, protein, small molecules, and lipids from the same sample. The transcriptomic analysis were not performed, since they have been already reported by Podechard *et al.*, 2018[13]. The methodology presented here was evaluated regarding analytical parameters often used for methods validation. Intra and inter-day precision, accuracy and absolute recovery are in accordance with the FDA regulation[23], and the matrix effect was not significant in the analysis.

It is important to highlight the need of extraction RNA and lipids from the same sample, once some diseases are very rare, and there are not many samples available for academic research. The methodology described here could enhance the data output using the same number of samples that only a lipidomics assay would require. Besides, the presented method allows multiomic comparison data from the same sample.

Acknowledgment

This work was funded by Conselho Nacional de Desenvolvimento Científico e Tecnológico (CNPq), Coordenação de Aperfeiçoamento de Pessoal de Nível Superior (CAPES), and Fundação de Amparo à Pesquisa do Estado de Goiás (FAPEG).

REFERENCES

(1) Ayton, S. G.; Pavlicova, M.; Robles-Espinoza, C. D.; Tamez Peña, J. G.; Treviño, V. Multiomics subtyping for clinically prognostic cancer subtypes and personalized therapy: A systematic review and meta-analysis. *Genetics in Medicine* **2022**, 24 (1), 15-25. DOI: https://doi.org/10.1016/j.gim.2021.09.006.

(2) Marabita, F.; James, T.; Karhu, A.; Virtanen, H.; Kettunen, K.; Stenlund, H.; Boulund, F.; Hellström, C.; Neiman, M.; Mills, R.; et al. Multiomics and digital monitoring during lifestyle changes reveal independent dimensions of human biology and health. *Cell Systems* **2022**, 13 (3), 241-255.e247. DOI: https://doi.org/10.1016/j.cels.2021.11.001.

(3) Nalbantoglu, S.; Karadag, A. Metabolomics bridging proteomics along metabolites/oncometabolites and protein modifications: Paving the way toward integrative multiomics. *Journal of Pharmaceutical and Biomedical Analysis* **2021**, 199, 114031. DOI: https://doi.org/10.1016/j.jpba.2021.114031.

(4) Wang, L.; Wang, X.; Li, Y.; Hou, Y.; Sun, F.; Zhou, S.; Li, C.; Zhang, B. Plasma lipid profiling and diagnostic biomarkers for oral squamous cell carcinoma. *Oncotarget* **2017**, 8 (54), 92324-92332. DOI: 10.18632/oncotarget.21289.

(5) Valdes-Mora, F.; Handler, K.; Law, A. M. K.; Salomon, R.; Oakes, S. R.; Ormandy, C. J.; Gallego-Ortega, D. Single-cell transcriptomics in cancer immunobiology: The future of precision oncology. *Frontiers in Immunology* **2018**, 9, Review. DOI: 10.3389/fimmu.2018.02582.

(6) Ooi, K.-L. M.; Vacy, K.; Boon, W. C. Fatty acids and beyond: Age and Alzheimer's disease related changes in lipids reveal the neuro-nutraceutical potential of lipids in cognition. *Neurochemistry International* **2021**, 149, 105143. DOI: 10.1016/j.neuint.2021.105143.

(7) Macías-García, D.; Periñán, M. T.; Muñoz-Delgado, L.; Jimenez-Jaraba, M. V.; Labrador-Espinosa, M. Á.; Jesús, S.; Buiza-Rueda, D.; Méndez-Del Barrio, C.; Adarmes-Gómez, A.; Gómez-Garre, P.; et al. Serum lipid profile among sporadic and familial forms of Parkinson's disease. *npj Parkinson's Disease* **2021**, 7 (1). DOI: 10.1038/s41531-021-00206-6.

(8) Fernandes, H. J. R.; Patikas, N.; Foskolou, S.; Field, S. F.; Park, J.-E.; Byrne, M. L.; Bassett, A. R.; Metzakopian, E. Single-cell transcriptomics of Parkinson's disease human in vitro models reveals dopamine neuron-specific stress responses. *Cell Reports* **2020**, 33 (2), 108263. DOI: 10.1016/j.celrep.2020.108263.

(9) Kaneko, H.; Itoh, H.; Kiriyama, H.; Kamon, T.; Fujiu, K.; Morita, K.; Michihata, N.; Jo, T.; Takeda, N.; Morita, H.; et al. Lipid profile and subsequent cardiovascular disease among young

adults aged <50 years. *The American Journal of Cardiology* **2021**, 142, 59-65. DOI: 10.1016/j.amjcard.2020.11.038.

(10) Wirka, R. C.; Pjanic, M.; Quertermous, T. Advances in transcriptomics: Investigating cardiovascular disease at unprecedent resolution. *Circulation Research* **2018**, 122 (9), 1200-1220. DOI: 10.1161/circresaha.117.310910.

(11) Ojo, O.; Ojo, O. O.; Zand, N.; Wang, X. The effect of dietary fibre on gut microbiota, lipid profile, and inflammatory markers in patients with type 2 diabetes: A systematic review and meta-analysis of randomised controlled trials. *Nutrients* **2021**, 13 (6), 1805. DOI: 10.3390/nu13061805.

(12) Jenkinson, C. P.; Göring, H. H. H.; Arya, R.; Blangero, J.; Duggirala, R.; Defronzo, R. A. Transcriptomics in type 2 diabetes: Bridging the gap between genotype and phenotype. *Genomics Data* **2016**, 8, 25-36. DOI: 10.1016/j.gdata.2015.12.001.

(13) Podechard, N.; Ducheix, S.; Polizzi, A.; Lasserre, F.; Montagner, A.; Legagneux, V.; Fouché, E.; Saez, F.; Lobaccaro, J.-M.; Lakhal, L.; et al. Dual extraction of mRNA and lipids from a single biological sample. *Scientific Reports* **2018**, 8 (1). DOI: 10.1038/s41598-018-25332-9.

(14) Bligh, E. G.; Dyer, W. J. A rapid method of total lipid extraction and purification. *Canadian Journal of Biochemistry and Physiology* **1959**, 37 (8), 911-917.

(15) Folch, J.; Lees, M.; Stanley, G. H. S. A simple method for the isolation and purification of total lipides from animal tissues. *Journal of Biological Chemistry* **1957**, 226 (1), 497-509. DOI: https://doi.org/10.1016/S0021-9258(18)64849-5.

(16) Oyeniyi, E. A.; Sorgi, C. A.; Gardinassi, L. G.; Azevedo, L. F.; Adeyemi, J. A.; Omotoso, O. T.; Faccioli, L. H.; Greggi Antunes, L. M.; Barbosa, F. Phospholipids modifications, genotoxic and anticholinesterase effects of pepper fruit (Dennettia tripetala G. Baker) extract in Swiss mice. *Food and Chemical Toxicology* **2022**, 165, 113189. DOI: https://doi.org/10.1016/j.fct.2022.113189.

(17) Bernardo, R. A.; da Silva, L. C.; Queiroz, M. E. C.; Vaz, B. G.; Chaves, A. R. Lab-made solid phase microextraction phases for off line extraction and direct mass spectrometry analysis: Evaluating the extraction parameters. *Journal of Chromatography A* **2019**, 1603, 23-32. DOI: 10.1016/j.chroma.2019.06.038.

(18) Fahy, E.; Sud, M.; Cotter, D.; Subramaniam, S. LIPID MAPS online tools for lipid research. *Nucleic Acids Research* **2007**, 35 (SUPPL.2), W606-W612. DOI: 10.1093/nar/gkm324.

(19) Ulmer, C. Z.; Jones, C. M.; Yost, R. A.; Garrett, T. J.; Bowden, J. A. Optimization of Folch, Bligh-Dyer, and Matyash sample-to-extraction solvent ratios for human plasma-based lipidomics studies. *Analytica Chimica Acta* **2018**, 1037, 351-357. DOI: 10.1016/j.aca.2018.08.004.

(20) Markowski, A. R.; Błachnio-Zabielska, A. U.; Guzińska-Ustymowicz, K.; Markowska, A.; Pogodzińska, K.; Roszczyc, K.; Zińczuk, J.; Zabielski, P. Ceramides profile identifies patients with more advanced stages of colorectal cancer. *Biomolecules* **2020**, 10 (4), 632. DOI: 10.3390/biom10040632.

(21) Scalinci, S.; Lugaresi, M.; Scorolli, L.; Ralli, M.; Greco, A.; Pantaleone, V.; Taurone, S.; Franzone, F. Neuroprotective role of phosphoserine in primary open-angle glaucoma patients. *European Review for Medical and Pharmacological Sciences* **2020**, 24 (19), 9780-9786.

(22) Zhao, G.; He, F.; Wu, C.; Li, P.; Li, N.; Deng, J.; Zhu, G.; Ren, W.; Peng, Y. Betaine in inflammation: mechanistic aspects and applications. *Frontiers in Immunology* **2018**, 9, 1070.

(23) Swartz, M. E.; Krull, I. S. *Analytical method development and validation*; CRC Press, 2018. DOI: 10.1201/9781315275161.

(24) Zhou, W.; Yang, S.; Wang, P. G. Matrix effects and application of matrix effect factor. *Bioanalysis* **2017**, 9 (23), 1839-1844. DOI: 10.4155/bio-2017-0214.

(25) Steiner, D.; Krska, R.; Malachová, A.; Taschl, I.; Sulyok, M. Evaluation of Matrix Effects and Extraction Efficiencies of LC-MS/MS Methods as the Essential Part for Proper Validation of Multiclass Contaminants in Complex Feed. *Journal of Agricultural and Food Chemistry* **2020**, 68 (12), 3868-3880. DOI: 10.1021/acs.jafc.9b07706.

(26) Raposo, F.; Barceló, D. Challenges and strategies of matrix effects using chromatography-mass spectrometry: An overview from research versus regulatory viewpoints. *TrAC Trends in Analytical Chemistry* **2021**, 134, 116068. DOI: https://doi.org/10.1016/j.trac.2020.116068.

(27) Sorvina, A.; Bader, C. A.; Caporale, C.; Carter, E. A.; Johnson, I. R. D.; Parkinson-Lawrence, E. J.; Simpson, P. V.; Wright, P. J.; Stagni, S.; Lay, P. A.; et al. Lipid profiles of prostate cancer cells. *Oncotarget* **2018**, 9 (85), 35541-35552. DOI: 10.18632/oncotarget.26222.

Bisphenol determination in UHT milk and packaging by paper spray ionization mass spectrometry

Daniel de Almeida Soares[a,b], Igor Pereira[a], Jean Carlos Pereira Sousa[a], Ricardo Alves Bernardo[a], Rosineide Costa Simas[a,c], Boniek Gontijo Vaz[a], Andréa Rodrigues Chaves[a,*]

a- Laboratório de Cromatografia e Espectrometria de Massas (LaCEM), Instituto de Química, Universidade Federal de Goiás (IQ-UFG), 74690-900, Goiânia-GO, Brazil.

b- Instituto Federal de Goiás, Campus Luziânia, Luziânia, GO, 72811-580 Brazil.

c- Escola de Engenharia – Faculdade de Química, Universidade Presbiteriana Mackenzie, São Paulo, SP, 01302-907 Brazil.

**andrea_chaves@ufg.br*

Abstract

This study evaluates the use of paper spray ionization mass spectrometry (PSI-MS) for rapid determination of bisphenol A (BPA) and bisphenol S (BPS) in UHT milk and milk packaging. The packages were analyzed by cutting the cartons into triangular shapes and submitting them to PSI-MS analysis. The milk samples were subjected to a simple liquid-liquid extraction and the supernatant was deposited onto a triangular paper that was subsequently used for PSI-MS analysis. In milk, BPS and BPA levels ranged from 60.0 to 150.8 ng mL^{-1}. The LOD and LOQ values were 1.5 and 4.8 ng mL^{-1} for BPA, and 4.8 and 16.0 ng mL^{-1} for BPS, respectively. Linearity was $R^2 > 0.98$ for both compounds. Precision values were below 20%, and recoveries close to 100%. The PSI-MS can be used as a simple, rapid, and accurate methodology to determine bisphenols in milk and milk packaging.

Keywords: *bisphenol, paper spray ionization, packaging cartons, UHT milk*

Chemical compounds studied in this article:
Bisphenol A, BPA (Pubchem CID: 6623)
Bisphenol S, BPS (Pubchem CID: 6626)

1. Introduction

Packaging is the final step in the processing of bovine milk and plays a key role in the food industry, as it helps to maintain the quality and safety of the food, protecting it from chemical, physical, and microbiological deterioration (Geueke, Groh & Muncke, 2018). However, there is a growing concern about toxicological problems arising from the interaction between packaging and milk. Packaging components such as monomers, additives, dyes, inks, and varnishes can migrate to milk and be harmful to consumer health. Many monomers, plasticizers, and additives are considered endocrine disruptors, which interfere with the production, release, transport, metabolism, binding, or elimination of natural hormones responsible for maintaining balance and regulating developmental processes (Blanco-Zubiaguirre *et al.*, 2020), (Vilarinho *et al.*, 2019), (Wang *et al.*, 2021).

Bisphenols are a group of molecules usually found in dyes, polycarbonate plastics, epoxy resins, and papers, especially recycled paper (Björnsdotter, Boer & Ballesteros-Gómez, 2017). The literature points out that this group of molecules is of concern and needs to be monitored due to its high toxicological effects. Bisphenol A (BPA; Figure S1) is the most representative analogue of the bisphenol group (García-Córcoles *et al.*, 2018) and has been associated with several adverse health effects, such as reproductive disorders (Wang *et al.*, 2015), neurotoxicity (Nagao *et al.*, 2014), metabolic disorders (Kim et al., 2019), cardiovascular diseases (Han & Hong, 2016) and cancer (Wang *et al.*, 2015), (Huang *et al.*, 2012). Bisphenol S (BPS; Figure S1) is the main substitute for BPA and has also been widely used in industry. It has estrogenic activity with potential toxicity, in addition to having greater resistance to biodegradation compared to BPA (Dualde *et al.*, 2019).

Due to the toxicological properties of bisphenols, legislative authorities have paid considerable attention to the potential migration of these compounds from packaging to food. According to the European Food Safety Authority, BPA and BPS have specific migration limits (SMLs) of 0.05 mg kg^{-1} (EU, 2018), (EFSA, 2020). For this reason, the development of analytical methods with high sensitivity and specificity that contribute to the monitoring of bisphenols in food is urgently needed. Table 1 presents some analytical methods reported in the literature for the analysis of BPA and BPS in food packaging. Liquid chromatography (LC) and gas chromatography (GC) coupled to a detector (MS, DAD, FLD, and others) are the most used, but require extensive and laborious sample preparation steps prior to instrumental analysis, consuming reagents or solvents and generating chemical waste. Therefore, analytical methods that require minimal sample preparation and consume less reagent and solvent are highly desirable.

Table 1. Literature reports on the determination of BPA and BPS in food packaging

Analyte	Matrix	Analysis	LOD/LOQ or estimated concentration	Reference
BPA	Disposable plastic materials	UPLC-TOF-MS	LOD: 0.027–0.030 μg L^{-1}	(Lian *et al.*, 2020)
BPA	Cardboard packaging material	LC-QqQ	LOD: 4 ng g^{-1}	(Blanco-Zubiaguirre *et al.* 2020)
BPA and BPS	Food-contact plastic	LC-DAD and other detectors	LOQ: 0.05 μg mL^{-1} for both	(Wang *et al.*, 2019)
BPA	Plastic baby food sample packaging	GC-MS/MS	LOQ: 0.1–1.2 ng g^{-1}	(García-Córcolez *et al.*, 2018)
BPA	Canned food	GC-LRMS	LOQ: 0.20 ng g^{-1} (food) LOQ: 20 ng L^{-1} (liquids)	(Lorber *et al.*, 2015)
BPA	Packaged food	LC-FLD	LOD: 0.1 ng mL^{-1} (canned orange) LOD: 0.3 ng mL^{-1} (milk)	(Xu *et al.*, 2011)
BPA	Packaging for water and beverages products	GC-MS	0.022–0.030 ng g^{-1} (PET bottle) 0.0585–0.32 ng g^{-1} (metal can)	(Cao and Popovic, 2018)

A technique that fulfils the aforementioned requirements is paper spray ionization mass spectrometry (PSI-MS). In PSI-MS, a small volume of sample is deposited onto a triangular paper, a high voltage is applied, then the solvent is added, and charged droplets from the sample are sprayed towards a mass spectrometer inlet (Zhang *et al.*, 2012). The analyses are usually fast as they only require a previous preparation of a sample extract. In addition, the sample itself (e.g., leaf vegetables or food packaging) can be cut into a triangle shape and analyzed by PSI-MS. This technique has been used for several purposes, such as for quantification of pesticides in tomatoes (Moura, *et al.*, 2020), identification of counterfeit blended Scottish whiskies (Teodoro, *et al.*, 2017), determination of flavanone-O-glycosides in citrus beverages (Mazzotti *et al.*, 2021), analysis of theobromine, theophylline, and caffeine in cocoa products and drugs (Bartella, *et al.*, 2019), and determination of bisphenol A and its analogues in some food packaging such as water bottles, energy drink bottles, and plastic cups (Chen *et al.*, 2017). However, PSI-MS has never been used to analyze bisphenols in milk and milk packaging.

Therefore, this work investigates the utility of PSI-MS to analyze BPA and BPS in milk and milk packaging. Minimal sample preparation was used in all analyses. The packages were cut into triangular shapes and directly analyzed by PSI-MS. The milks were submitted to a

simple extraction process, and the extract was deposited onto a triangular paper and analyzed by PSI-MS. Figures of merit such as linearity, limit of detection (LOD), limit of quantification (LOQ), precision, and recovery were evaluated.

2. Materials and Methods

2.1. Chemicals and materials

Methanol (≥99%) was acquired from the Tedia Company Ltda (Farfield, USA). Ammonium hydroxide (28%), bisphenol A (≥99%) and bisphenol S (≥98%) were acquired from Sigma-Aldrich (St Louis, USA). Whatman #1 chromatographic paper (11 μm pores) was acquired from Whatman International Ltd. (Maidstone, UK). Milk samples (n = 18) were purchased from a local supermarket (Goiânia, Brazil) in 6 different brands with different batches for each sample and different locations of production. All the samples were within the expiration date.

2.2. PSI-MS

A Thermo Scientific LTQ XL linear ion trap mass spectrometer (San Jose, USA) was used. A three-dimensional in-house mobile platform was used to position the tip of the paper (or packaging) in front of the mass spectrometer inlet at 4 ± 0.25 mm (Figure S2). The mobile platform contains three micrometers *x*, *y*, and *z* settings that remained stable for analyses. The 4 mm distance between the PSI substrate and the MS inlet is already well studied in the literature (Moura, *et al.*, 2020), and it is reported that distances smaller than 4 mm lead to electrical discharge, and greater than 7 mm of lead to signal loss. The Selected reaction monitoring (SRM) was used to monitor the analytes, using the transition of *m/z* 227→212 for BPA and 249→185 for BPS. Carryover effect was evaluated between each analysis by adding methanol (0.1% ammonium hydroxide) onto the paper or packaging sample and checking for the absence of analyte signals. The optimized instrumental parameters were: negative ion mode; scan time: 0.30 s; source voltage: 4 kV; capillary temperature: 250 °C; capillary voltage: 10 V; tube lens: 50 V; collision energy: 32 eV; maximum injection time: 100 ms; microscans: 2. A high-resolution Q-Exactive Orbitrap mass spectrometer (Thermo Scientific, San Jose, USA) was employed to confirm the identities of the analytes, and the optimized instrumental parameters were: negative ionization mode; spray voltage: 5 kV; capillary temperature: 275 °C; s-lens RF level: 50%.

2.3. Analysis of milk packaging

The milk packaging samples were cut into equilateral triangular shapes with 1.5 cm sides. Fifty microliters of methanol (0.1% ammonium hydroxide) were used as spray solvent. To estimate the concentrations of BPA and BPS, packaging samples that did not show any signals of BPA and BPS (these samples were previously analyzed by PSI-MS to ensure the absence of compounds) were spiked with 1 and 10 ng mL^{-1} of each analyte and analyzed by PSI-MS. The signal intensities obtained were then compared with those obtained from packaging samples containing BPA and BPS.

2.4. Analysis of milk samples

A volume of 1 mL of methanol with 0.1% ammonium hydroxide was added to 1 mL of milk. The mixture was vortexed (Vortex, Gehaka AV-1, São Paulo, Brazil) and then centrifuged at 7000 rpm, 15 °C, for 5 min (Sorvall Legend X1R centrifuge, Thermo Scientific). The supernatant was collected and deposited onto a triangular chromatographic paper (1.5-cm sides) which was submitted to PSI-MS analysis.

2.5. Analytical performance

Figures of merit such as linearity, LOD, LOQ, precision, and recovery were evaluated for the PSI-MS analysis of BPA and BPS in milk samples. Linearity was investigated through calibration curves constructed with concentrations ranging from 50 to 500 ng mL^{-1} for BPA and from 50 to 400 ng mL^{-1} for BPS. The LOD and LOQ were obtained by the following equations:

$$LOD = \frac{(3{,}3.sB)}{m}$$

$$LOQ = \frac{(10.sB)}{m}$$

where sB is the standard deviation of 10 blank measurements, and *m* is the slope of the calibration curve. Precision and recovery were determined using intra-day (n = 5) and inter-day (n = 3) assays at 75, 175, and 375 ng mL^{-1}. The precision was calculated by:

$$CV = \left(\frac{SD}{AEC}\right).100$$

where CV is the coefficient of variation, AEC is the average experimental concentration and SD is the standard deviation. The recovery was calculated by:

$$Rec(\%) = \left(\frac{AC}{NC}\right).100$$

where AC is the analyzed concentration and NC is the nominal (spiked) concentration.

3. Results and Discussion

3.1. Optimization of PSI-MS

Initial experiments were performed to investigate the MS/MS transitions of the BPA and BPS analytes. A 2000 ng mL^{-1} methanolic solution (50 µL) of BPA and BPS was analyzed by PSI-MS/MS, and the results are shown in Figure 1. The fragmentation mechanism for BPA and BPS are already well known and detailed in the scientific literature (Zhao *et al.*, 2016). The fragment ions at *m/z* 212 and *m/z* 185 (BPA and BPS, respectively) were selected to be monitored in subsequent analyses.

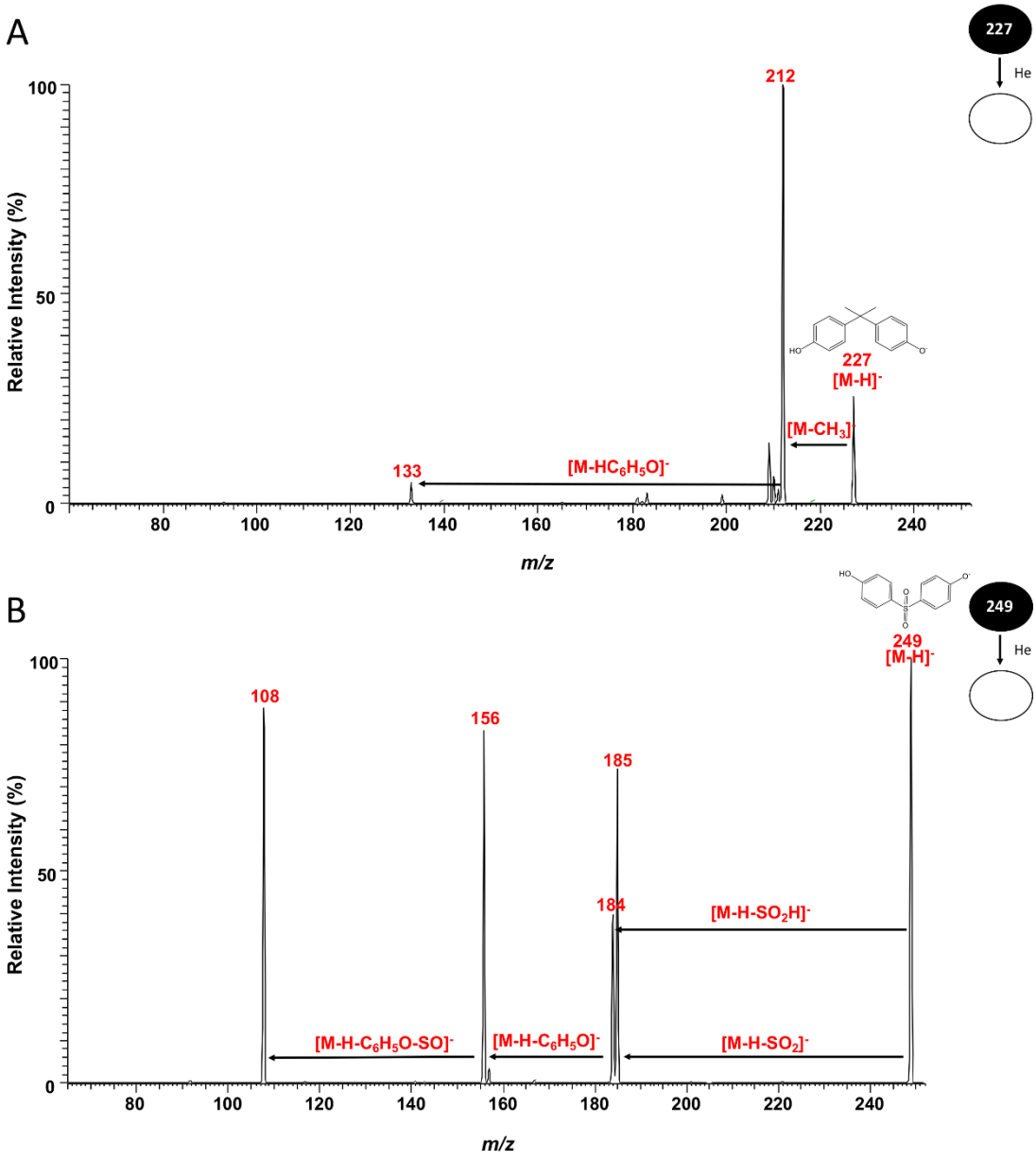

Figure 1. PSI-MS/MS spectra of (a) BPA (b) BPS. The analyses were performed using chromatographic papers spiked with standard solutions (2000 ng mL^{-1}) of BPA and BPS.

A typical total ion chromatogram (2 min acquisition) from MS/MS analysis of BPA and BPS is shown in Figure S3. Although the signal intensity lasts longer than 2 min, the highest intensity is obtained during the first 30 s. Thus, the subsequent PSI-MS analyses were performed acquiring 30 s in order to speed up the analysis protocol.

Carryover experiments were also performed to verify the need for cleaning between analyses. A volume of 50 µL of methanol (0.1% ammonium hydroxide) was applied onto the substrate between analysis, and the signal intensities of BPA and BPS were monitored. No BPA and BPS signals were detected in this experiment, demonstrating no carryover effect. Thus, the subsequent analyses were performed without the need for a cleaning step between each analysis.

3.2. PSI-MS analysis of milk packaging

To estimate the amount of BPA and BPS in milk packaging samples, carton samples were spiked with 1 or 10 ng mL^{-1} of each compound and analyzed by PSI-MS. Signal intensities were compared with those obtained from real samples. The results are presented in Figure 2, which shows the results obtained with five milk packaging samples from different brands (samples 1 to 5) and also with two samples from the same batch (samples 6 and 7). The compounds were also confirmed using a high-resolution mass spectrometer, in which BPA was detected at *m/z* 227.10794 ($[M-H]^-$; error = 1.304 ppm) and BPS at *m/z* 249.02290 ($[M-H]^-$; error = 1.294 ppm).

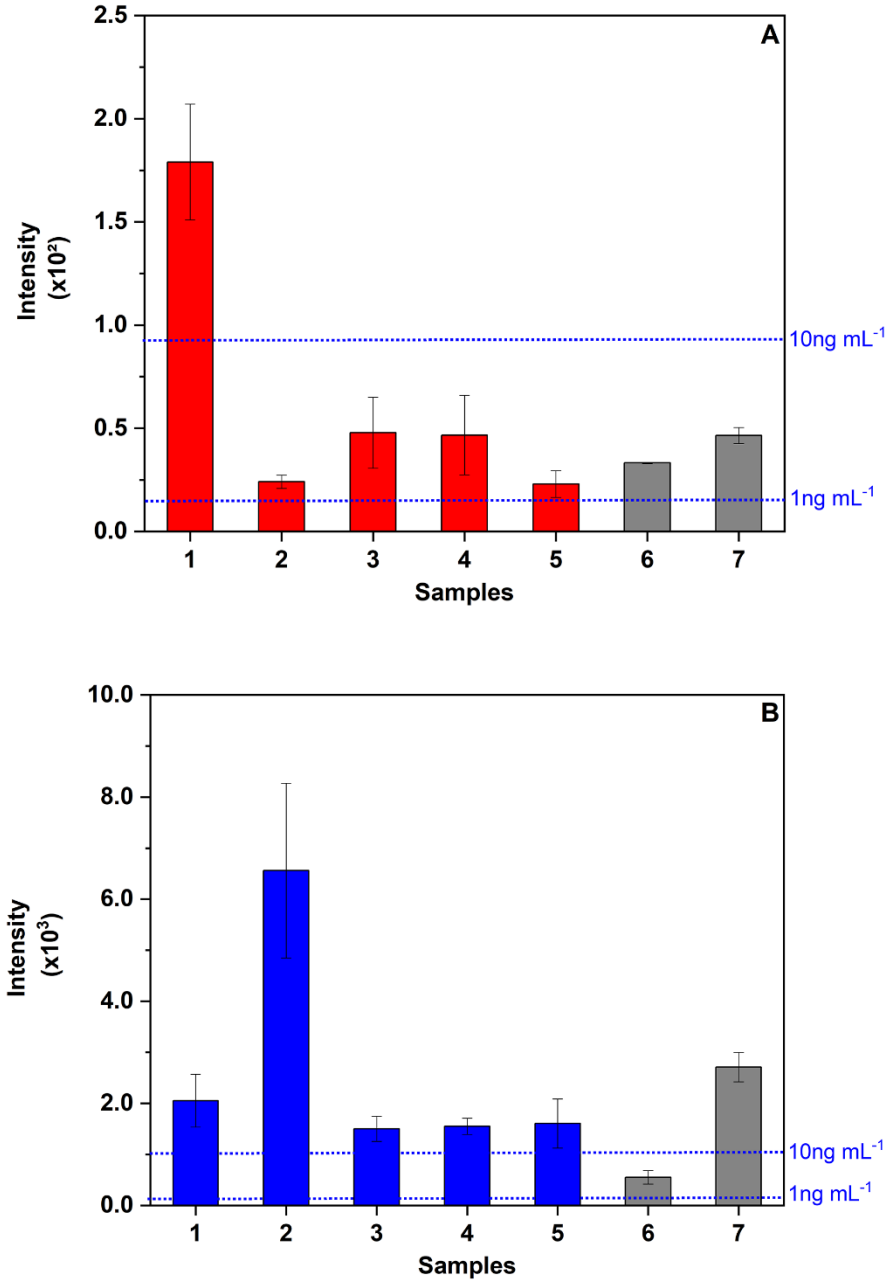

Figure 2. BPA (a) and BPS (b) ion intensities obtained from the PSI-MS analysis of milk packaging samples from different brands (samples 1 to 5) and from the same manufacturing batch (samples 6 and 7). The dotted lines indicate the ion intensities obtained with BPA and BPS at 1 or 10 ng mL^{-1}. Each sample was analyzed in replicates (n = 5).

Among all samples, the highest concentration of BPA was detected in sample 1 and the highest concentration of BPS was detected in sample 2. In general, the BPS concentration was higher than 10 ng mL^{-1} in all samples except sample 6, while the BPA concentration was higher

than 10 ng mL^{-1} only in sample 1. Both compounds were detected above of 1 ng mL^{-1} in all samples.

The analyses of packages from samples 6 and 7 were performed with the purpose of verifying whether there are significant differences in bisphenol concentrations between milk packaging samples of the batch. The results showed coefficients of variation for BPA of 0.98% for sample 6, and 8.30% for sample 7. Regarding the BPS, the coefficients of variation were 23.73% for sample 6, and 10.65% for sample 7, which may suggest heterogeneity in the concentrations of BPA and BPS between milk packaging from the same brand and batch.

Chen *et al*. (2017) used PSI-MS to analyze BPA, BPS, BPF, and BPAF in various food packaging such as paper cups, baby bottles, mineral water bottles, energy drink bottles, and plastic cups. The authors claim that the method was more effective than the conventional LC-MS in terms of simplicity, speed, and the possibility of high-throughput analysis. As it was observed here, the PSI-MS technique seems to be more feasible than LC-MS for BPA and BPS compound determination in different matrices.

3.3. PSI-MS analysis of milk samples

The milk was submitted to a simple liquid-liquid extraction, and the supernatant was collected and analyzed by PSI-MS. Figures of merit such as linearity, LOD, LOQ, precision, and recovery were evaluated. Linearity was achieved with $R^2 > 0.98$ for both compounds with the calibration curves constructed at concentrations ranging from 50 to 500 ng mL^{-1} for BPA and from 50 to 400 ng mL^{-1} for BPS (Figure 3). The LOD and LOQ were determined to be 1.5 and 4.8 ng mL^{-1} for BPA, and 4.8 and 16.0 ng mL^{-1} for BPS, respectively. These results are within a range of concentration often reported for LODs and LOQs in bisphenol analyses using chromatographic methods, as shown in Table 1.

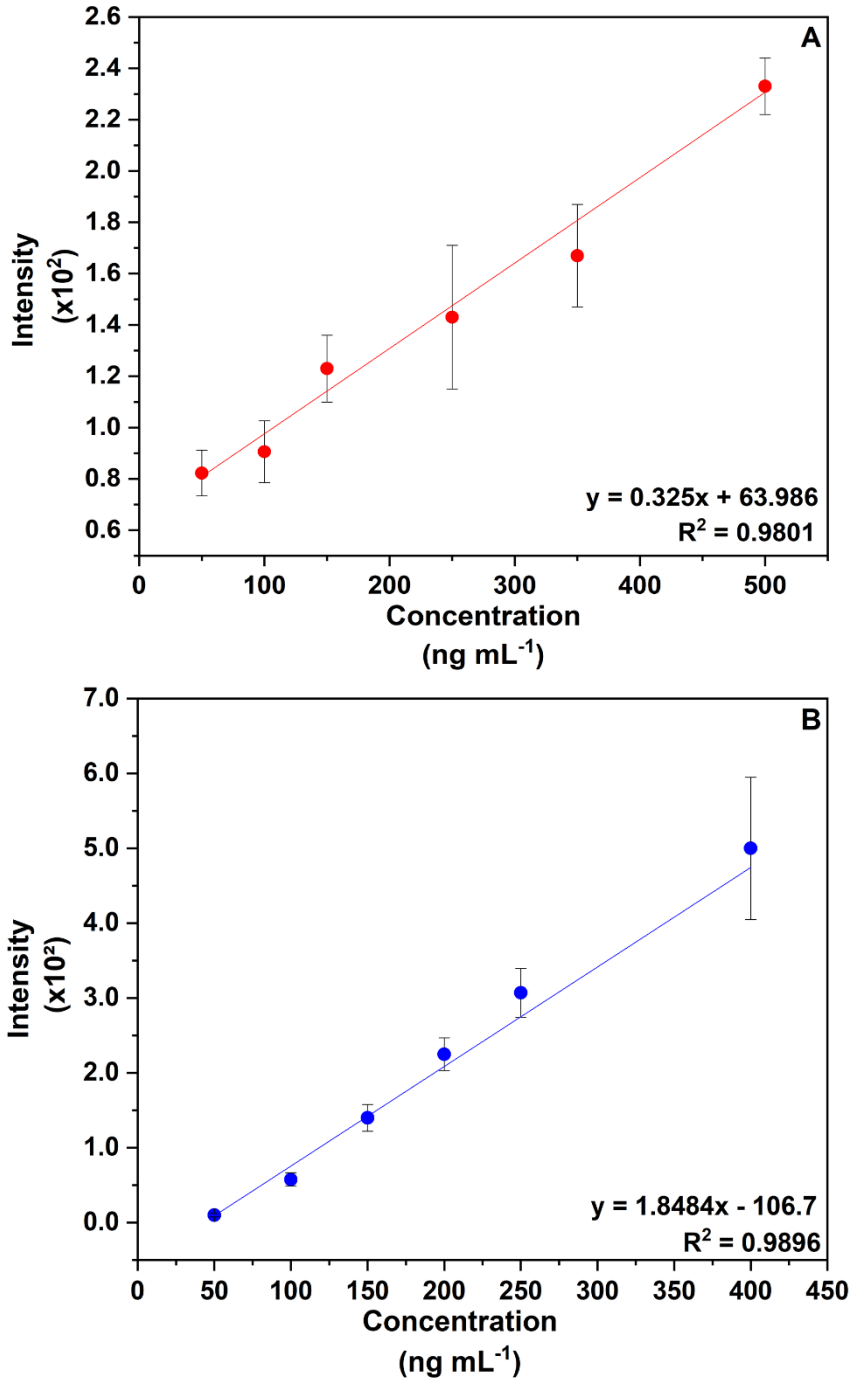

Figure 3. Calibration curves of (a) BPA (50-500 ng mL^{-1}) and (b) BPS (50-400 ng mL^{-1}) obtained by PSI-MS. Error bars show the standard deviation of replicate measurements (n = 3).

Precision (coefficient of variation) and recovery were evaluated at three concentration levels (75, 175, and 375 ng mL^{-1}) using intra-day and inter-day assays. The results are shown in Table 2. Precision values were below 20% and recoveries ranged from 74 to 112%.

Table 2. Figures of merit obtained from the PSI-MS analysis of BPA and BPS in UHT milk samples

Analyte		Nominal concentration (ng mL^{-1})	Analyzed concentration (ng mL^{-1})	SD[a] (%)	CV[b] (%)	Recovery (%)
BPA	Intra-day (n = 5)	75.0	66.9	10.6	15.8	89
		175.0	163.1	16.4	10.1	93
		375.0	366.2	31.1	8.5	98
	Inter-day (n = 3)	75.0	75.4	14.3	18.9	100
		175.0	159.5	16.9	10.6	91
		375.0	401.4	34.6	8.6	107
BPS	Intra-day (n = 5)	75.0	84.0	11.1	13.2	112
		175.0	155.8	9.2	5.9	89
		375.0	312.9	29.7	9.5	89
	Inter-day (n = 3)	75.0	80.3	10.6	13.2	107
		175.0	143.3	15.0	10.5	82
		375.0	278.8	22.2	8.0	74

[a]Standard deviation. [b]Coefficient of variation.

Posteriorly, the PSI-MS technique was applied to quantify BPA and BPS in milk samples purchased from a local supermarket. The results are shown in Figure 4. Both compounds were detected in all samples, except for BPS in sample 6. All samples analyzed showed average concentrations around 60.0 ng mL^{-1} for BPS and 77.6-150.8 ng mL^{-1} for BPA.

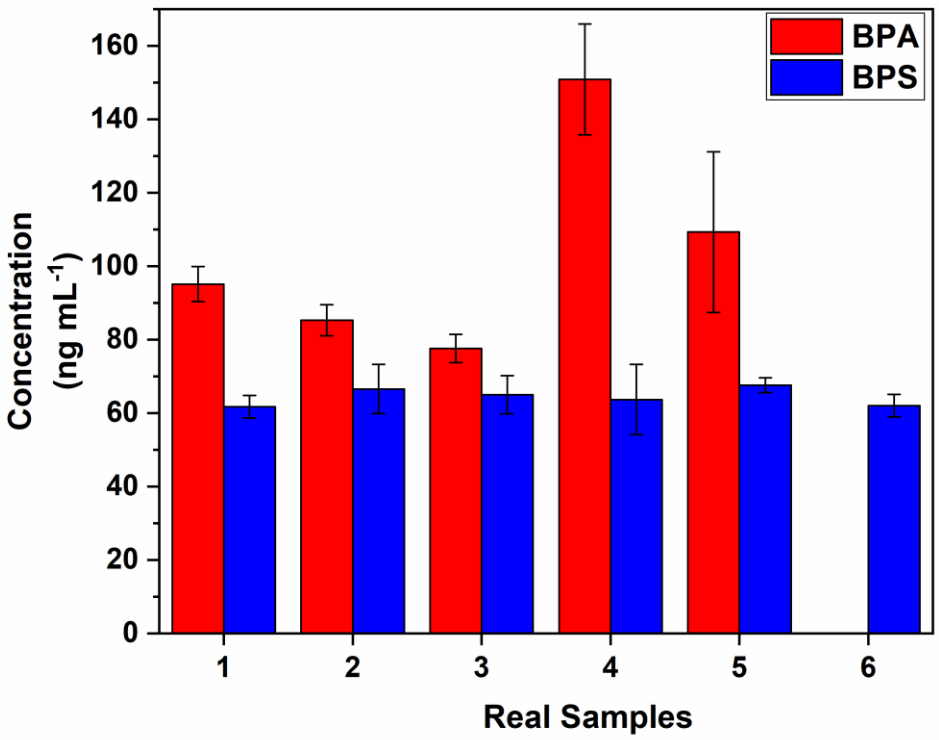

Figure 4. BPA and BPS concentrations in commercially available milk samples.

Based on Table 3, the parallelism test for both BPA and BPS presented P value >0,05, which indicates that no matrix effect is observed once there is no significant difference between the slopes for chromatographic paper and packaging. Due to this, the analytical responses for BPA and BPS are not affected by the substrate in PSI technique.

Table 3. Matrix effect estimated by the parallelism test between the analytical curve in chromatographic paper and packaging

BPA			
Substrate	**Linear Regression**	**R^2**	**Parallelism test**
Chromatographic paper	y = 50.75x - 2599	0.9713	P = 0.8120
Packaging	y = 52.04x – 546.7	0.9922	
BPS			
Substrate	**Linear Regression**	**R^2**	**Parallelism test**
Chromatographic paper	y = 10.44x – 218.01	0.9902	P = 0.1439
Packaging	y = 12.28x – 395.49	0.9804	

Methods for the simultaneous determination of BPA and BPS in UHT milk are not trivial, and reports in the literature are scarce. Some studies report the determination of bisphenols using laborious analytical techniques, which depend on sample cleanup and chromatographic separation before analyte detection. For example, Ding *et al*. (2019) determined traces of bisphenols (BPA, BPB, BPAP, BPAF) in milk using effervescent reaction-assisted dispersive solid-phase extraction (mETDSE /Ni@N-GrTs) followed by HPLC with fluorescence detection. Grumetto et al. (2013) analyzed five bisphenols (BPA, BPB, BPF, BPFDGE, BPADGE) in commercial milk packed in plastic bottle. The authors employed SPE as sample pre-treatment and analyzed the extracts by HPLC with fluorescence detection. According to the authors, out of 68 samples, BPA was detected in 16 of them, with concentrations ranging from 10 to 48 ng mL^{-1}.

As shown in this work, PSI-MS is a useful technique for analyzing BPA and BPS in milk and milk packaging. The easy-to-use and less demanding features of PSI-MS provide rapid determination of bisphenols in samples, which is traditionally accomplished by more complex, expensive, and demanding techniques, such as chromatography coupled to a detector. It is not suggested here that PSI-MS replaces conventional chromatography methods for absolute quantification of bisphenols in milk and milk packaging, but it is expected that preliminary screening will be facilitated using a faster and simpler method.

4. Conclusions

This study demonstrated the utility of PSI-MS in determining the levels of BPA and BPS in different samples of UHT milk and milk packaging. The BPS content was higher than BPA in all milk packaging samples, while in milk samples, BPA showed higher concentrations than BPS. From a total of seven packaging samples analyzed, bisphenols were detected in all, even at low concentrations. Regarding the milk samples, out of a total of six samples, all of them showed the presence of bisphenols, except for sample 6, which did not show any BPA content. This is the first work on the determination of BPA and BPS in UHT milk and milk packaging samples using the PSI-MS technique. Considering the urgent need to develop new analytical methods for the analysis of bisphenols, this manuscript shows that these harmful compounds can be readily detected and quantified using a simple and inexpensive method, with the potential to be an alternative to conventional chromatographic methods. Future research should assess the presence of other contaminants that may be present in both packaging and food.

CRediT authorship contribution statement

Daniel de Almeida Soares: Conceptualization, Formal analysis, Investigation, Data curation, Writing – original draft, Writing – review & editing. **Igor Pereira:** Formal analysis, Conceptualization, Investigation, Data curation, Writing – review & editing. **Jean Carlos Pereira Sousa:** Formal analysis, Investigation, Data curation. **Ricardo Alves Bernardo:** Data curation, Visualization, Writing – review & editing. **Rosineide Costa Simas:** Conceptualization, Writing – review & editing, Supervision, Project administration. **Boniek Gontijo Vaz:** Funding acquisition, Supervision, Resources. **Andréa Rodrigues Chaves:** Conceptualization, Project administration, Resources, Supervision.

Declaration of Competing Interest

The authors declare that they have no known competing financial interests or personal relationships that could have appeared to influence the work reported in this paper.

Acknowledgements

This research was generously funded by CAPES, CNPq (#447927/2014-0), and FAPEG (#2018-0267001519).

5. References

1. Bartella, L. Di Donna, L., Napoli, A., Siciliano, C., Sindona, G., Mazzotti, F (2019). A rapid method for the assay of methylxanthines alkaloids: Theobromine, theophylline and caffeine, in cocoa products and drugs by paper spray tandem mass spectrometry. *Food Chemistry*. 278, 261-266. https://doi.org/10.1016/j.foodchem.2018.11.072
2. Björnsdotter, M. K., Boer, J., Ballesteros-Gómez, A. (2017). Bisphenol A and replacements in thermal paper: A review. *Chemosphere*. 182, 691-706. https://doi.org/10.1016/j.chemosphere.2017.05.070
3. Blanco-Zubiaguirre, L., Zabaleta, I., Usobiaga, A., Prieto, A., Olivares, M., Zuloaga, O., Elizalde, M. P. (2020). Target and suspect screening of substances liable to migrate from food contact paper and cardboard materials using liquid chromatography-high resolution tandem mass spectrometry. *Talanta*. 208, 120394, 1-11. https://doi.org/10.1016/j.talanta.2019.120394.
4. Cao, X., Popovic, S. (2018). Solid phase extraction of large volume of water and beverage samples to improve detection limits for GC-MS analysis of bisphenol A and four other

bisphenols. *Food Additives & Contaminants: Part A*. 2018. 35(1). 49-55. http://dx.doi.org/10.1080/19440049.2017.1382730.

5. Chen, S., Chang, Q., Yin, K., He, Q., Deng, Y., Chen, B., Liu, C., Wang, Y., Wang, L. (2017) Rapid analysis of bisphenol a and its analogues in food packaging products by paper spray ionization mass spectrometry. *Journal of Agricultural and Food Chemistry*. 65 (23), 4859-4865. https://doi.org/10.1021/acs.jafc.7b02061.
6. Ding, W., Wang, X, Liu, T., Gao, M., Qian, F., Gu, H., Zhang, Z. (2019). Preconcentration/extraction of trace bisphenols in milks using a novel effervescent reaction-assisted dispersive solid-phase extraction based on magnetic nickel-based N-doped graphene tubes. *Microchemical Journal*, 150, 104109, 1-13. https://doi.org/10.1016/j.microc.2019.104109.
7. Dualde, P., Pardo, O., Corpas-Byurgos, F., Kuligowski, J., Gormaz, M., Vento, M., Pastor, A., Yusà, V., (2019). Biomonitoring of bisphenols A, F, S in human milk and probabilistic risk assessment for breastfed infants. *Science of the Total Environment*. 668, 797–805. https://doi.org/10.1016/j.scitotenv.2019.03.024.
8. EU, 2018. Commission Regulation (EU) 2018/213. Official Journal of the European Union. https://eur-lex.europa.eu/eli/reg/2018/213/oj. Acess: 06/02/2021.
9. European Food Safety Authority (EFSA), FitzGerald, R., Loveren H. V., Civitella C., Castoldi, A. F., Bernasconi, G. (2020). Assessment of new information on Bisphenol S (BPS) submitted in response to the Decision under REACH Regulation (EC) No 1907/2006. EFSA supporting publication 2020:EN-1844. 39 pp. https://doi.org/10.2903/sp.efsa.2020.EN-1844.
10. García-Córcoles, M. T., Cipa, M., Rodríguez-Gómez, R., Rivas, A., Olea-Serrano, F., Vílchez, J. L., Zafra-Gómez, A. (2018). Determination of bisphenols with estrogenic activity in plastic packaged baby food samples using solid-liquid extraction and clean-up with dispersive sorbents followed by gas chromatography tandem mass spectrometry analysis. *Talanta*. 178, 441–448. http://dx.doi.org/10.1016/j.talanta.2017.09.067.
11. Geueke, B., Groh, K., Muncke, J. (2018). Food packaging in the circular economy: overview of chemical safety aspects for commonly used materials. *Journal of Cleaner Production*, 193, 491–505. https://doi.org/10.1016/j.jclepro.2018.05.005.
12. Grumetto, L., Gennari, O., Montesano, D., Ferracane, R., Ritieni, A., Albrizio, S., Barbato, F. (2013). Determination of Five Bisphenols in Commercial Milk Samples by Liquid Chromatography Coupled to Fluorescence Detection. *Journal of Food Protection*. 76, 9, 1590-1596. https://doi.org/10.4315/0362-028X .JFP-13-054.

13. Han, C., Hong, Y. (2016). Bisphenol A, Hypertension, and Cardiovascular Diseases: Epidemiological, Laboratory, and Clinical Trial Evidence. *Curr Hypertens Rep*. 18:11, 1-5. https://doi.org/10.1007/s11906-015-0617-2

14. Huang Y. Q., Wong C. K., Zheng J. S., Bouwman H., Barra R., Wahlström B., Neretin L., Wong M. H. (2012). Bisphenol A (BPA) in China: a review of sources, environmental levels, and potential human health impacts. *Environment International*. 42, 91–99. https://doi.org/10.1016/j.envint.2011.04.010.

15. Kim, J. K., Khan, A., Cho, S., Na, J., Lee, Y., Bang, G., Yu, W. J., Jeong, J. S., Jee, S. H., Park, Y. H., (2019). Effect of developmental exposure to bisphenol A on steroid hormone and vitamin D3 metabolism. *Chemosphere*, 237, 1-9. https://doi.org/10.1016/j.chemosphere.2019.124469.

16. Lian, L., Jiang, X., Guan, J., Qiu, Z., Wang, X., Lou, D. (2020). Dispersive solid-phase extraction of bisphenols migrated from plastic food packaging materials with cetyltrimethylammonium bromide-intercalated zinc oxide *Journal of Chromatography A*. 1612, 460666, 1-27. https://doi.org/10.1016/j.chroma.2019.460666.

17. Lorber, M., Schecter, A., Paepke, O., Shropshire, W., Christensen, K., Birnbaum, L. (2015). Exposure assessment of adult intake of bisphenol A (BPA) with emphasis on canned food dietary exposures. *Environment International*. 77. 55-62. http://dx.doi.org/10.1016/j.envint.2015.01.008.

18. Mazzotti, F., Bartella, L., Talarico, I. R., Napoli, A., Di Donna, L. (2021). High-throughput determination of flavanone-O-glycosides in citrus beverages by paper spray tandem mass spectrometry. *Food Chemistry*. 360, 130060, 1-6. https://doi.org/10.1016/j.foodchem.2021.130060

19. Moura, A. C. M., Lago, I. N., Cardoso, C. F., Nascimento, A. dos R., Pereira, I., Vaz, B. G. (2020) Rapid monitoring of pesticides in tomatoes (*Solanum lycopersicum L.)* during pre-harvest intervals by paper spray ionization mass spectrometry. *Food Chemistry*. 310, 125938, 1-6. https://doi.org/10.1016/j.foodchem.2019.125938

20. Nagao T., Kawachi K., Kagawa N., Komada M. (2014). Neurobehavioral evaluation of mouse newborns exposed prenatally to low-dose bisphenol A. *The Journal of Toxicological Sciences*. 39, 231-235. https://doi.org/10.2131/jts.39.231

21. Teodoro, J. A. R., Pereira, H. V. P., Sena, M. M., Piccin, E., Zacca, J. J., Augusti, R. (2017). Paper spray mass spectrometry and chemometric tools for a fast and reliable identification of counterfeit blended Scottish whiskies. *Food Chemistry*. 237, 1058-1064. http://dx.doi.org/10.1016/j.foodchem.2017.06.062

22. Vilarinho, F., Sendón, R., van der Kellen, A., Vaz, M. F., Silva, A. S. (2019). Bisphenol A in food as a result of its migration from food packaging. *Trends in Food Science & Technology*. 91, 33–65. https://doi.org/10.1016/j.tifs.2019.06.012.

23. Wang, L., Zhang, Z., Xu, X., Zhang, D., Wang, F., Zhang, L. (2015). Simultaneous determination of four trace level endocrine disrupting compounds in environmental samples by solid-phase microextraction coupled with HPLC. *Talanta*, 142, 97-103. http://dx.doi.org/10.1016/j.talanta.2015.04.043.

24. Wang, H., Song, S., Shao, M., Gao, Y., Yang, C., Li, Y., Wang, W., He, Y., Li, P. (2019). Determination of bisphenol analogues in food-contact plastics using diode array detector, charged aerosol detector and evaporative light-scattering detector. *Ecotoxicology and Environmental Safety*. 186, 109778, 1-7. https://doi.org/10.1016/j.ecoenv.2019.109778.

25. Wang, R., Huang, Y., Dong, S., Wang, P., Su, X. (2021). The occurrence of bisphenol compounds in animal feed plastic packaging and migration into feed. *Chemosphere*.265,129022. https://doi.org/10.1016/j.chemosphere.2020.129022.

26. Xu, Z., Ding, L., Long, Y., Xu, L., Wang, L., Xu, C., (2011). Preparation and evaluation of superparamagnetic surface molecularly imprinted polymer nanoparticles for selective extraction of bisphenol A in packed food. *Analytical Methods*, 3, 1737-1744. http://dx.doi.org/10.1039/c1ay05206c.

27. Zhang, Z., Cooks, R. G., Ouyang, Z. (2012). Paper spray: a simple and efficient means of analysis of different contaminants in foodstuffs. *Analyst*, 137, 2556. https://doi.org/10.1039/c2an35196j

28. Zhao, H., Xiang, L., Li, J., Yang, Z., Fang, J., Zhao, C., Xu, S., Cai, Z. (2016). Investigation on fragmentation pathways of bisphenols by using electrospray ionization Orbitrap mass spectrometry. *Rapid Commun. Mass Spectrom*. 30(16). 1-24. https://doi.org/10.1002/rcm.7666.

A fast and direct determination of Bisphenol S in thermal paper samples using paper spray ionization mass spectrometry

Ricardo Alves Bernardo[1], Jean Carlos Pereira Sousa[1], Matheus Gallimberti[2], Fernando Barbosa Junior[2], Boniek Gontijo Vaz[1], Andréa Rodrigues Chaves[1]*

1 Institute of Chemistry, Federal University of Goiás, 74690-900, Goiânia, GO, Brazil.

2 Faculty of Pharmaceutical Sciences of Ribeirão Preto, University of São Paulo, 14040-900, SP, Brazil.

** Corresponding author: andrea_chaves@ufg.br tel: +55 62 3521 1016 R 251*

ABSTRACT: Concerns about human health regarding the large use of bisphenol A in thermal papers have led to its replacement by bisphenol S. Analyses of bisphenols require several sample pretreatment steps, which are laborious, expensive and time-consuming. A paper spray ionization mass spectrometry (PSI-MS) was developed to detect and quantify bisphenol S in three different brands of thermal papers commercially available. Parameters such as paper size, and paper position relative to the mass spectrometer inlet were evaluated. The analyses were performed in selected ion monitoring mode on a linear ion trap mass spectrometer. The developed method presented absolute recovery values ranging from 92.2% to 109.04%, accuracy values from -1.2% to 9.0%, and inter assays precision from 1.8% to 5.6% and enabled LOD as low as 5 ng g^{-1}. The concentration of bisphenol S in all of the three brands of BPA-free thermal papers evaluated ranged from 1.36 µg g-1 to 6.77 µg g^{-1}, and the concentrarion of BPA ranged from 6.56 µg g^{-1} to 16.4 µg g^{-1} in all samples of thermal paper evaluated. The PSI-MS method described here was comparable to the conventional ones, such as liquid chromatography coupled with mass spectrometry and gas chromatography coupled with mass spectrometry described in the literature. The present study proved to be practical, fast, and efficient for the direct determination of bisphenol S in thermal papers. Furthermore, the methodology here described showed to be a promising alternative to replace the classical methods for determination of bisphenol S, due to its simplicity, and no needing of any sample pretreatment.

Keywords. Bisphenol S, thermal paper, paper spray ionization, ambient ionization, mass spectrometry

INTRODUCTION

The bisphenol belongs to a group of molecules with two hydroxyphenyl functionalities differing only by the constitution of the bond that connects the two phenol rings (Zhao *et al*. 2016). These compounds, mainly the bisphenol A [BPA, 2,2-Bis(4-hydroxyphenyl) propane], are widely used in the manufacture of polycarbonate plastics, epoxy resins, and thermal paper (Björnsdotter *et al*. 2017a). However, an increasing number of studies have shown that BPA has adverse effects on the endocrine system, including discontinuation of steroid hormones, disturbance in the development of mammary gland, and deregulation of parameters associated with obesity (Moral *et al*. 2008; Mielke *et al*. 2011; Zhang *et al*. 2011; Geens *et al*. 2012; Karrer *et al*. 2018). According to Rocha *et al*., 2015, around 98% of Brazilian thermal paper contained BPA at a concentration of up to 4.3% (wt%) (Rocha et al. 2015). Beyond that, this compound was also found in 100% of the evaluated paper samples, in a concentration range from 0.6% to 1.4% (wt%), in the United States of America, Korea, and Vietnam (Liao and Kannan 2011).

The restrictions on the use of BPA in thermal papers had led to the use of bisphenol S (BPS, 4,4'-sulfonyldiphenol) as a substitute candidate, because it has a chemical structure very similar to the BPA, containing one sulfone group in the bridge, thus being stronger than BPA in terms of acidity (Choi *et al*. 2018). Since the limitation and/or prohibition of BPA, BPS has been widely used as a thermal color developer in the production of thermal papers, protonating the structure of a colorless neutral dye present on thermal paper, transforming it into a colored cationic structure (Gontani *et al*. 2017; Oh *et al*. 2018; Wu *et al*. 2018). The European Chemicals Agency estimates that 61% of all thermal paper in European Union will be based on BPS by the year 2022 (European Chemicals Agency). Even though BPS is being widely used as BPA substitute, BPA is still the major ink developer in thermal papers. The structural representation of BPA and BPS is presented in Figure 1.

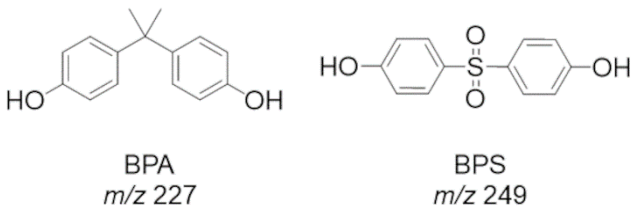

Figure 1. Structural representation for bisphenol-A (BPA) and bisphenol-S (BPS).

The use of BPS has been reported on thermal paper receipts in four countries (United States of America, Japan, Korea, and Vietnam) with 100% detection in 111 randomly collected samples, with concentrations ranging from 13.8 ng g^{-1} to 22.0 mg g^{-1} (geometric average 0.181

mg g^{-1}) (Liao *et al*. 2012). However, studies have shown that some parameters of BPS may be equally or more harmful compared to the BPA (Ahsan *et al*. 2018; Zhou 2018; Qiu *et al*. 2018; Ullah *et al*. 2019).

The bisphenols analyses are commonly performed in liquid chromatography coupled with mass spectrometry (LC-MS) (Gao *et al*. 2013; Wang *et al*. 2018; de Oliveira *et al*. 2019) and also by gas chromatography coupled with mass spectrometry (GC-MS) systems (Chen *et al*. 2017). Despite their high selectivity and sensitivity, the use of chromatographic techniques for complex sample analyses requires intensive sample pretreatment steps, such as liquid-liquid extraction (Rocha *et al*. 2016), solid phase micro-extraction (Tan *et al*. 2009), and derivatization reactions to chromatographic methods, adding costs and time to the analyses. Ambient ionization mass spectrometry has been one of the most promising techniques related to the non-need of sample pre-treatment (Harris *et al*. 2011). Among the several ion sources for ambient ionization mass spectrometry (Cooks *et al*. 2006; Forbes and Sisco 2018; Li *et al*. 2018; Lu *et al*. 2018), the paper spray ionization mass spectrometry (PSI-MS) stands out for being one of the cheapest and straightforward ion sources, allowing a quick analysis of complex samples (Cooks *et al*. 2011; Shen *et al*. 2012; Yang *et al*. 2012; Kerian *et al*. 2014; Gómez-Ríos and Pawliszyn 2014). Pereira *et al*, 2018 described the use of PSI-MS coated with molecularly printed polymers (MIP's) to enhance the specificity/selectivity in analyses for screening agrochemicals in food (Pereira *et al*. 2018).

Recently, new phenol-free ink developers had been reported in the literature as alternative to BPS and its analogous compounds, such as urea urethane compound (UU), N-(p-toluenesulfonyl)-N'-(3-p-toluenesulfonyloxyphenyl) urea (Pergafast 201), 4,4'-bis(N-carbamoyl-4-methylbenzenesulfonamide) diphenylmethane (BTUM), 4-hydroxyphenyl 4-isoprooxyphenylsulfone (D-8), and 4-hydroxy-4’-benzyloxydiphenylsulfone (BPS-MAE) (United States Environmental Protection Agency 2014; Eckardt *et al*. 2020). The Pergafast 201 and UU have been considered important non-phenolic bisphenol substitutes in the European market (Björnsdotter *et al*. 2017b). Although Pergafast 201 can be considered to be of low toxicity (Goldinger *et al*. 2015), its use has not been applied on a large scale due to its higher cost of manufacture, thus, thermal papers based on phenolic ink developers, especially BPA and BPS, are still more common and accessible in several countries (Eckardt *et al*. 2020).

In this study, a direct and fast PSI-MS method is proposed for the detection and quantification of BPS and also BPA, in commercially available thermal paper samples. The analyses were performed without any sample pretreatment or derivatization step, which had led

to a reduction in the analysis time and cost. The PSI-MS method was also compared to conventional methods for bisphenols determination.

EXPERIMENTAL

Chemicals and reagents

Methanol (99.95%), the analytical standards for BPS (4,4'-sulfonyldiphenol) (≥98%), BPA (2,2-Bis(4-hydroxyphenyl) propane) (≥98%) and ibuprofen [(RS)-2-(4-isobutylphenyl) propionic acid] (≥99%) were acquired from Sigma-Aldrich Ltda. (Rio de Janeiro, Brazil). The standards solutions were prepared in methanol and stored at -8 °C for mass spectrometry analyses. Ultra-purified water was prepared in an MS2000 system (Gehaka, São Paulo, SP, Brazil). The chromatographic paper Whatman™ 3MM CHR was acquired from Fisher Scientific Ireland Ltd. (Ballycoolen, Dublin, Ireland).

Thermal paper preparation

The BPA-free thermal papers were purchased from suppliers in the Brazilian market of three different brands on the first semester of 2019, these brands were called A, B and C. These brands are the most used BPA-free thermal papers in Brazil. The regular thermal papers (not BPA free) were collected from seven different local markets in April 2021 These seven brands were here called D, E, F, G, H, I, and J. The thermal papers were cut in equilateral triangle shape with 0.4 cm sides and weighted (average weight of 0.5 mg, and 0.069 cm^2 area). Triangular thermal papers with area larger than 0.069 cm^2 often lead to equipment contamination. After cutting the paper, 1 µL of internal standard (ibuprofen solution at 1000 ng g^{-1}) was added to the paper and allowed to dry at ambient conditions (25 °C) for 15 minutes before the analysis. Thus, they were subjected to direct analysis by PSI-MS, without needing additional preparation step. All the ten analyses were performed in quintuplicate.

Mass spectrometry analysis

The MS assays were performed using the linear ion trap LTQ XL mass spectrometer Thermo Scientific™ (Waltham, Massachusetts, USA). The triangular papers were positioned at 5-7 mm from the mass spectrometer inlet, then 20 µL of methanol was added into the paper surface to generate the electrolytic spray that guides the ions into the mass spectrometer (Figure 2). The negative ion mode was used to acquire the spectra using as scan mode the selected ion monitoring (SIM) with a ion isolation window width of 2.0 *m/z*. The following mass spectrometer parameters have been used: voltage applied to the paper -3.8 kV, capillary tension

-2.00 V, capillary temperature 275 °C and tube lens tension -38.0 V. No sweep, coating nor auxiliary gas were used. For peak annotation, MS/MS analyses, isolation width 1.0 *m/z*, normalized collision energy 30 eV, acquisition time 0.8 min were used (*m/z* 249 → 155 for BPS, *m/z* 227 → 212 for BPA, and *m/z* 205 → 161 for internal standard) on mass spectra. The MS/MS spectrum for BPS is presented on Figure 3, and the MS/MS spectrum for ibuprofen and BPA are presented on Figure S-1 and S-2, respectively, in the supplementary information.

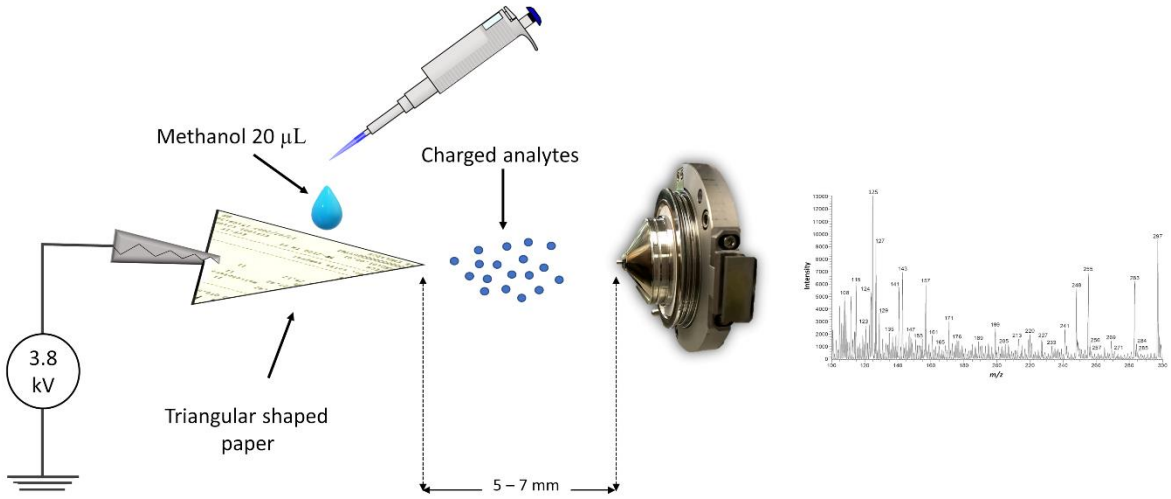

Figure 2. Schematic representation for thermal paper analysis using PSI-MS method.

Quantitative PSI-MS analyses

Chromatographic paper Whatman™ 3MM CHR was used as blank paper sample and cut into an equilateral triangle shape with a 1.5 cm edge. Therefore, 20 µL of a solution containing BPS and ibuprofen were added into the paper samples and left to dry at 25 °C for 15 min. The ibuprofen was used as an internal standard (IS) compound at a concentration of 1000 ng g^{-1} for all MS analyses. Among all available standards, this molecule showed linear responses similar to the response obtained by BPS standard curves. Besides this, the ibuprofen is not present in thermal paper samples, being impossible to be found as an interfering molecule. The analytical curve was plotted using the blank paper samples spiked with BPS+IS solution at seven concentration values 87, 100, 150, 250, 350, 450, 500 ng g^{-1}, for BPS, and at seven concentration values 13, 50, 100, 150, 250, 400, 550 ng g^{-1}, for BPA in replicates (n = 5). The linearity was evaluated through the linear regression of the area of the extracted ions current

chromatrogram (EIC), calculated within an acquisition time of 0.8 minutes, with a single application of elution solvent onto the paper surface.

The limit of detection (LOD) was determined based on the analyte signal-to-noise ratio (S/N) about 3, which means analyte signal three times higher than the equipment noise signal. The limit of quantification was determined by 10 times the ratio between the intercept standard deviation and the slope value. Inter-day precision and accuracy were also evaluated by the analytical curve using quintuplicate essays of PSI-MS of samples at 100, 200 and 500 ng g^{-1}, for the BPS, and samples at 150, 250 and 550 ng g^{-1} for BPA, as shown in Equations 1, 2 and 3.

$$\text{Accuracy}(\%) = \left(\frac{\text{AEC}-\text{TC}}{\text{TC}}\right) * 100 \quad \textbf{(1)}$$

$$\text{Precision}(\%) = \left(\frac{\text{STD}}{\text{AEC}}\right) * 100 \quad \textbf{(2)}$$

$$\text{Recovery}(\%) = \left(\frac{\text{AEC}}{\text{TC}}\right) * 100 \quad \textbf{(3)}$$

where AEC is the average experimental concentration, TC is the theoretical concentration, STD corresponds to the standard deviation in the experimental concentrations (BRASIL 2017).

The thermal paper analyses were carried out in the same arrangement as described for the chromatographic ones. The same paper size could not be applied to the commercial thermal paper analyses due to the higher bisphenols concentration in this type of paper. Trying to obtain a simple methodology for direct determination of BPA and BPS in thermal paper, the size of the paper sample was optimized, to ensure adequate sensibility to the purpose method and also keep the equipment integrity. According to this, thermal paper samples were cut in an equilateral triangle shape with 0.4 cm sides (average weight of 0.5 mg, and 0.069 cm^2 area) keeping adequate methodology sensibility and also equipment integrity. These papers could then be used for PSI-MS technique, without previous extraction and/or dilution steps.

RESULTS AND DISCUSSION

Analytical assays

The linearity of BPA and BPS analyses in the chromatographic paper using PSI-MS was determined through the linear regression in the analytical curve. The EIC area of replicates (n = 5) was used to correlate concentration and analytical response, calculated within an acquisition time of 0.8 minutes, with a single application of elution solvent onto the paper surface. The presented method showed to be linear in a concentration range from LOQ to 500 ng g^{-1}, with $R^2 = 0.9948$, intercept value -2.0317 ± 0.4721 and slope value 0.0541 ± 0.0022, for

BPS analysis. Moreover, the present method showed to be linear in a concentration range from LOQ to 550 ng g^{-1} with $R^2 = 0.9915$, intercept value 1.8914 ± 0.8222 and slope value 0.0705 ± 0.0029, for BPA analysis. The analytical curve is presented on Figure S-3, for BPS, and in the Figure S-4, for BPA, in the supplementary information. Inter-day precision and accuracy were assessed in the present study with values ranging from -1.2% and 9.0%, respectively (Table 1). The absolute recovery ranged from 92.04% to 109.04%. According to the Agência Nacional de Vigilância Sanitária (ANVISA), a regulatory Brazilian agency for health surveillance, precision, and accuracy are considered to be acceptable up to 15%, and absolute recovery must vary from 80 to 120% (BRASIL 2017). Therefore, the present study showed to be accurate and precise for BPS and also BPA determination in thermal papers.

Table 1. Inter-day precision and accuracy, absolute recovery, LOD and LOQ for BPS and BPA analysis using the PSI-MS method

BPS						
Concentration (ng g^{-1})	**Estimated concentration (ng g^{-1})**	**Precision (%)**	**Accuracy (%)**	**Absolute recovery (%)**	**LOD (ng g^{-1})**	**LOQ (ng g^{-1})**
100	92.20 ± 3. 50	3.8	7.8	92.04		
200	214.77 ± 4.08	1.9	7.4	107.40	5	87
500	508.20 ± 28.46	5.6	1.6	101.60		
BPA						
Concentration (ng g^{-1})	**Estimated concentration (ng g^{-1})**	**Precision (%)**	**Accuracy (%)**	**Absolute recovery (%)**	**LOD (ng g^{-1})**	**LOQ (ng g^{-1})**
150	163.56 ± 8.79	5.4	9.0	109.04		
250	247.09 ± 4.38	1,8	-1.2	98.84	1.9	13
550	554.23 ± 12.83	2,3	0.8	100.77		

As described in the Experimental section, the LOD was determined based on the analyte signal-to-noise ratio (S/N) about 3, in a SIM mode, where the precursor ion of BPS (*m/z* 249) was fragmented, and its specific fragment ion (*m/z* 155) was monitored. Analyses of chromatographic papers spiked with BPS solutions were performed and compared to the

analyses of blank ones (thermal papers with no BPS added). At the concentration of 5 ng g^{-1}, the BPS signal-to-noise ratio (S/N) was about 3, therefore 5 ng g^{-1} was considered to be the LOD concentration.Otherwise, at the concentration of 1.9 ng g^{-1} the BPA S/N was about 3, which was considered to be the LOD. The LOQ for the BPS analysis in BPA-free thermal paper using the PSI-MS was estimated at 87 ng g^{-1} , and 13 ng g^{-1} for BPA analysis in regular thermal paper.

PSI-MS of thermal papers

The chromatographic and thermal papers were evaluated by PSI-MS as described in the Experimental Section. The PSI-MS parameters were evaluated for high analyte desorption to better mass spectrometry conditions. To this, the paper position was optimized, where distances shorter than 5 mm often lead to electrical discharge onto the MS inlet, and distances greater than 7 mm are related to poor electrospray generation. Something similar occurs to the voltage applied during the PSI-MS. When a voltage lower than 2~3 kV is applied, the electrospray generated has poor stability and poor desorption efficiency, and if a voltage higher than 5 kV is used, it may burn the paper substrate, as described by Vaz and co-workers (Colletes *et al*. 2016).

The absence of BPA and BPS on the chromatographic paper was confirmed by PSI-MS analysis of blank chromatographic paper (Figure 3a). A high signal intensity spectrum (for *m/z* 185, specific fragment ion for BPS) was obtained with paper at 5 mm from MS inlet (Figure 3c). A high voltage (-3.8 kV) was applied between the paper and the mass spectrometer inlet, and 20 µL of methanol were added onto the paper surface to generate the electrolytic spray.

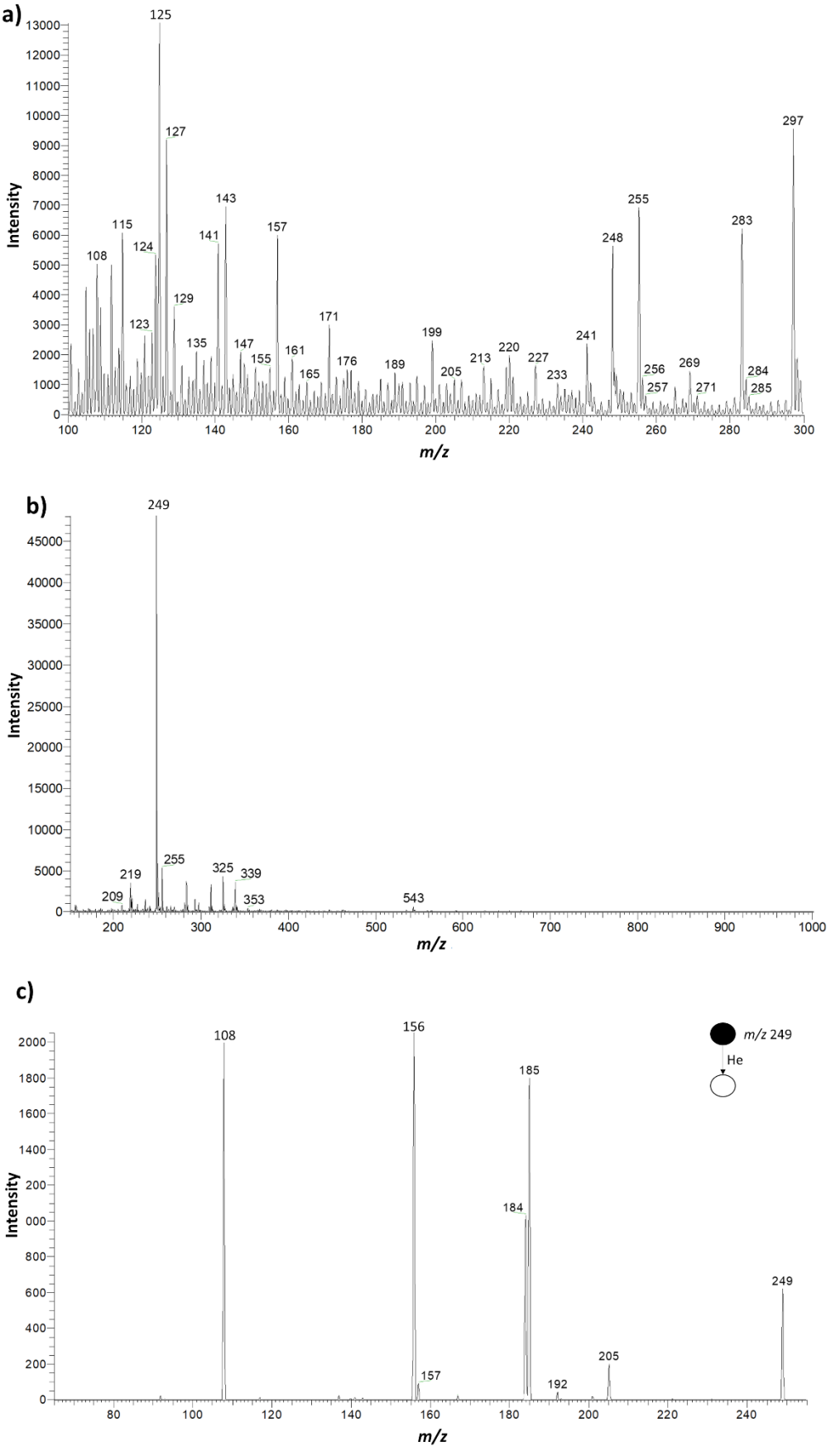
a)
Intensity
m/z
125
127
143
115
157
141
124
108
129
123
135
147
155
161
165
171
176
189
199
205
213
220
227
233
241
248
255
256
257
269
271
283
284
285
297
b)
Intensity
m/z
249
255
219
209
325
339
353
543
c)
Intensity
m/z
m/z 249
He
108
156
185
184
157
192
205
249

Figure 3. Chromatographic paper without adding the standard (a); Ionization profile of the BPS standard at 200 ng g^{-1} (b); Fragmentation profile of the precursor ion (*m/z* 249) (c).

Aiming to evaluate the capability of BPS ionization/desorption in the chromatographic paper, 20 µL of 200 ng g^{-1} BPS solution was spiked onto the paper surface. Thus, the spectrum of this evaluation is presented in Figure 3b, where it can be observed an intense peak for the *m/z* 249, which corresponds to the deprotonated analyte $[BPS\text{-}H]^-$. The attribution of *m/z* 249 for the BPS molecule was confirmed by MS/MS assay (Figure 3c), where the characteristic fragment ions for this molecule can be observed (Xie *et al*. 2018).

The EIC area was used to estimate the obtained concentration by the analytical curve linear regression equation. The dilution was considered to re-calculated the obtained concentration. The PSI-MS (-) spectra for the three different brands of thermal paper (A, B, and C) are shown in Figure 4.

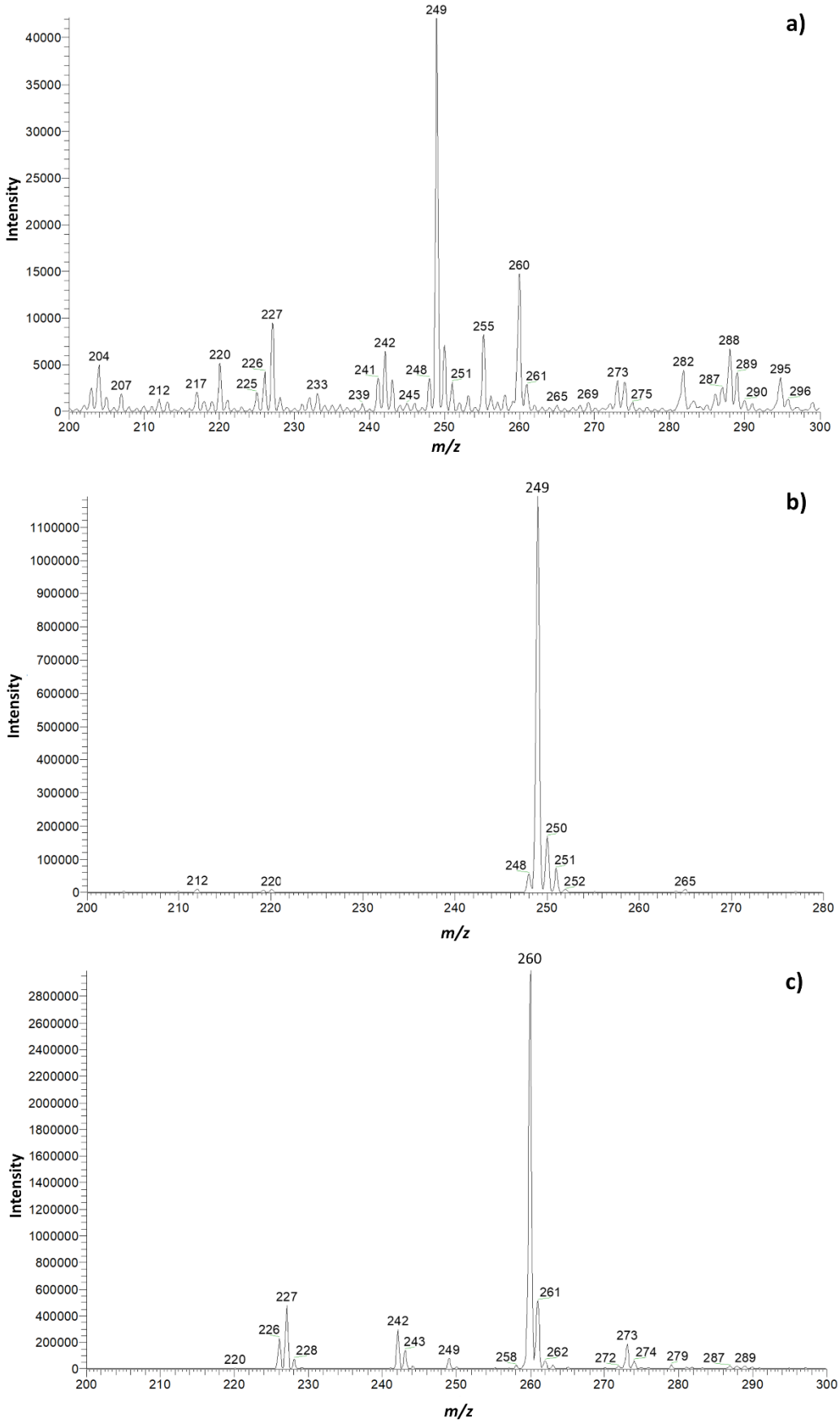
a)
Intensity
m/z
249
260
227
255
242
288
204
220
226
241
248
251
282
289
295
207
212
217
225
233
239
245
261
265
269
273
275
287
290
296
b)
Intensity
m/z
249
250
248
251
212
220
252
265
c)
Intensity
m/z
260
227
261
226
242
243
273
220
228
249
258
262
272
274
279
287
289

Figure 4. PSI-MS (-) spectra for Brand A (a); Brand B (b); Brand C (c).

Table 2. BPS content in the three commercially available BPA-free thermal papers (A, B and C), and BPA content in seven commercially available regular thermal papers (D to J)

Type of thermal paper	Brand	Bisphenol content (μg g^{-1})
BPA-free	A	6.77
	B	1.39
	C	1.36
Regular termal paper	D	16.4
	E	9.38
	F	9.62
	G	6.74
	H	6.87
	I	6.56
	J	14.0

The results pointed out a large amount of BPA and BPS in the thermal paper samples (Table 2). Furthermore, to the best of our knowledge, it currently has no limit on the maximum amount of BPS in the thermal paper by any regulatory agency. Despite the higher amount of bisphenols, large variations in its concentrations were observed among the ten commercial brands evaluated in this study. Thereby, this could represent a considerable risk especially for workers with high exposure to this type of material, such as store cashiers who stay in contact with receipts all day long, since it is an easily absorbable compound at a rate of 15.6 μg/day (Pal *et al*. 2017). The toxicological power of BPS, had been already described in the literature, being equivalent to BPA (Gayrard *et al*. 2019), which may lead to a high risk of direct and long exposure to thermal papers.

Comparison of PSI-MS method

The PSI-MS methodology for BPS determination in thermal papers proposed in this study can be compared to the results of conventional bisphenols determination methods, such as LC-MS and GC-MS. Patel's group developed a methodology for the determination of bisphenols in the thermal paper using liquid chromatography and tandem mass spectrometry (LC-MS/MS) and assisted liquid-liquid micro-extraction as a sample pretreatment step. The authors reported a LOD value of 1.25 ng g^{-1} with a recovery of 99% (Asati *et al.* 2017). Castro and coworkers proposed the determination of BPA in thermal paper samples using direct analysis in real time accurate mass spectrometry (DART-MS) technique. The authors reported

a fast and accurated methodology, however, their limits of quantification is around 40 µg g^{-1}, while in this present study, the LOD is 5 ng g^{-1} (Castro *et al.* 2019).

Table 3. Comparison of the PSI-MS method with conventional methods for bisphenol determination in thermal paper samples

Method	**Analyte**	**LOD**	**References**
DART-MS	BPA	LOQ: 40 µg g^{-1}	(Castro *et al.* 2019)
Py-GC/MS	BPA and BPS	970 ng g^{-1}	(Becerra and Odermatt 2012)
LC-MS/MS	BPA and analogs	1.25 ng g^{-1}	(Asati *et al.* 2017)
SUPRAS-LC-MS	BPS and analogs	1 ng g^{-1}	(Ballesteros-g and Rubio 2019)
Present study	BPS BPA	5 ng g^{-1} 1.9 ng g^{-1}	-

LC: liquid chromatography

DART: Direct analysis in real time

Py: Pyrolysis

GC: Gas chromatography

SUPRAS: Supramolecular solvent-based microextraction

Becerra and Ordematt reported an analytical pyrolysis gas chromatography-mass spectrometry (Py-GC/MS) method for BPA and BPS detection and quantification in thermal papers. The authors reported a correlation coefficient of 0.9984, which is very close to the R^2 value found in this study. However, the authors analyzed samples in order of mg/kg, while in the present study samples were evaluated in order for ng g-1 without any sample pretreatment, in a very short time (less than 1 minute per sample), which proofs the high sensitivity of the proposed method (Becerra and Odermatt 2012).

Gómez co-workers have optimized a new method for sample preparation of thermal papers for BPS analysis, the supramolecular solvent-based microextraction (SUPRAS) method. It consists of multi-target solvents composed of self-assembled amphiphiles, offering multiple extraction interactions (dispersion, polar, hydrophobic, etc.) (Dueñas-Mas *et al*. 2019). However, it takes time to prepare and the consumption of solvent in this technique is considerably high.

In the present study, the LOD found 1.9 ng g^{-1} and 5 ng g^{-1} for BPA and BPS respectively, with inter-day accuracy and precision up to 9.0% and 5.6%, and absolute recovery varying from 92.04% to 109.04%. Furthermore, the PSI-MS described here showed to be very sensitive, precise and accurate, even when it is compared to studies that used sample pretreatment steps and separation techniques coupled with high-resolution mass spectrometers. The proposed methodology also stands out due to its simplicity, easy handling, very low cost, minimum consumption of solvent, and analysis time extremely low compared to the classical methodologies for bisphenols determination. In this study, each analysis took about 1 min to be performed, which represents a huge analytical frequency and highlighted between other studies that describe derivatization steps and chromatographic separations.

Despite all the advantages of the present study, it is important to describe that other alternative ink developers in thermal papers should be evaluated, such as Pergafast 201, BTUM, and UU. However, the phenol-based thermal papers still dominate the Brazilian market due to their lower price compared to phenol-free thermal papers, and absence of regulations which prohibit or limit the amount of phenolic ink developers in this type of paper.

CONCLUSION

In this study, a methodology for BPS determination in thermal papers using PSI-MS was developed. The proposed method showed to be precise (<5.6%) and accurate (<7.8%), according to the ANVISA, and very sensitive, with very low limits of detection (1.9 and 5 ng g^{-1}) and limit of quantification at 13 and 87 ng g^{-1}. The PSI-MS proved to be a versatile and promising alternative for BPS determination, with no derivatization neither pretreatment steps. As long as the PSI-MS technique is a simple, fast, low cost, and easy-to-perform ion source, it can be applied in routine analysis when large amounts of samples are provided, with extremely reduced analysis time and solvent consumption, or even applied in analyses in situ using a portable mass spectrometer. The technique does not require excessive equipment conditions, such as high source temperatures, use of auxiliary gases and vacuum conditions at the source. Besides all advantages of the developed methodology, this study could contribute to BPS concentration controls and regulation, especially regarding employees with habitual exposure to thermal papers.

ACKNOWLEDGEMENT

The authors sincerely thank to Conselho Nacional de Desenvolvimento Científico e Tecnológico (CNPq), Coordenação de Aperfeiçoamento de Pessoal de Nível Superior (CAPES), and Fundação de Apoio à Pesquisa do Estado de Goiás (FAPEG).

FUNDING

This work was supported by grants from Fundação de Amparo à Pesquisa do Estado de Goiás (FAPEG) (grant numer 2018/10267001519), Conselho Nacional de Desenvolvimento Científico e Tecnológico (CNPq) (grant number 447927/2014-0), and Coordenação de Aperfeiçoamento de Pessoal de Nível Superior (CAPES) for providing financial support through scholarships.

ETHICS DECLARATIONS

Avaiability of data and materials

The datasets used and/or analysed during the current study are available from the corresponding author on reasonable request.

Competing interests

The authors declare that they have no competing interests.

Ethics approval and consent to participate

Not applicable.

Consent for publication

Not applicable.

AUTHORS CONTRIBUTION

RAB and JCPS contributed equaly to this work. They otimized all parameters for PSI-MS essays, analyse and interpreted the data for blank samples and commercial available thermal papers, and contributed to the writing process. MG, FBJ, and BGV contributed to the discussion of results. FBJ also contributed obtaining inputs to the work. ARC contributed to the conceptualization, project administration, resources, supervision and writing. All authors read and approved the final manuscript.

REFERENCES

Ahsan N, Ullah H, Ullah W, Jahan S (2018) Comparative effects of bisphenol S and bisphenol A on the development of female reproductive system in rats; a neonatal exposure study. Chemosphere 197:336–343. https://doi.org/10.1016/j.chemosphere.2017.12.118

Asati A, Satyanarayana GNV, Panchal S, et al (2017) Ionic liquid based vortex assisted liquid–liquid microextraction combined with liquid chromatography mass spectrometry for the determination of bisphenols in thermal papers with the aid of response surface methodology. J Chromatogr A 1509:35–42. https://doi.org/10.1016/j.chroma.2017.06.040

Becerra V, Odermatt J (2012) Detection and quantification of traces of bisphenol A and bisphenol S in paper samples using analytical pyrolysis-GC/MS. Analyst 137:2250–2259. https://doi.org/10.1039/c2an15961a

Björnsdotter MK, de Boer J, Ballesteros-Gómez A (2017a) Bisphenol A and replacements in thermal paper: A review. Chemosphere 182:691–706. https://doi.org/10.1016/j.chemosphere.2017.05.070

Björnsdotter MK, Jonker W, Legradi J, et al (2017b) Bisphenol A alternatives in thermal paper from the Netherlands, Spain, Sweden and Norway. Screening and potential toxicity. Sci Total Environ 601–602:210–221. https://doi.org/10.1016/j.scitotenv.2017.05.171

BRASIL (2017) RDC N. 166, de 25 de Julho de 2017,. Agência Nac Vigilância Sanitária 2017:1–21

Castro G, Rodríguez I, Ramil M, Cela R (2019) Direct analysis in real time accurate mass spectrometry determination of bisphenol A in thermal printing paper. Talanta 205:120086. https://doi.org/10.1016/j.talanta.2019.06.086

Chen S, Chang Q, Yin K, et al (2017) Rapid analysis of bisphenol a and its analogues in food packaging products by paper spray ionization mass spectrometry. J Agric Food Chem 65:4859–4865. https://doi.org/10.1021/acs.jafc.7b02061

Choi K-H, Kwon H-J, An B-K (2018) Synthesis and developing properties of functional phenolic polymers for ecofriendly thermal papers. Ind Eng Chem Res 57:540–547. https://doi.org/10.1021/acs.iecr.7b03129

Colletes TC, Garcia PT, Campanha RB, et al (2016) A new insert sample approach to paper spray mass spectrometry: A paper substrate with paraffin barriers. Analyst 141:1707–1713. https://doi.org/10.1039/c5an01954k

Cooks RG, Manicke NE, Dill AL, et al (2011) New ionization methods and miniature mass spectrometers for biomedicine : DESI imaging for cancer diagnostics and paper spray ionization for therapeutic drug monitoring. 247–267. https://doi.org/10.1039/c005327a

Cooks RG, Ouyang Z, Takats Z, Wiseman JM (2006) Ambient Mass Spectrometry. 311:

de Oliveira ML, Rocha BA, Souza VC de O, Barbosa F (2019) Determination of 17 potential endocrine-disrupting chemicals in human saliva by dispersive liquid-liquid microextraction and liquid chromatography-tandem mass spectrometry. Talanta 196:271–276. https://doi.org/10.1016/j.talanta.2018.12.067

Dueñas-Mas MJ, Ballesteros-Gómez A, Rubio S (2019) Supramolecular solvent-based microextraction of emerging bisphenol A replacements (colour developers) in indoor dust from public environments. Chemosphere 222:22–28. https://doi.org/10.1016/j.chemosphere.2019.01.095

Eckardt M, Kubicova M, Tong D, Simat TJ (2020) Determination of color developers replacing bisphenol A in thermal paper receipts using diode array and Corona charged aerosol detection—A German market analysis 2018/2019. J Chromatogr A 1609:460437. https://doi.org/10.1016/j.chroma.2019.460437

European Chemicals Agency ECHA/NR/20/22. https://echa.europa.eu/-/bisphenol-s-has-replaced-bisphenol-a-in-thermal-paper. Accessed 1 Apr 2021

Forbes TP, Sisco E (2018) Recent advances in ambient mass spectrometry of trace explosives. Analyst 143:1948–1969

Gao L, Zou J, Liu H, et al (2013) Determination of bisphenol A in thermal printing papers treated by alkaline aqueous solution using the combination of single-drop microextraction and HPLC. J Sep Sci 36:1298–1303. https://doi.org/10.1002/jssc.201201060

Gayrard V, Lacroix MZ, Gély CA, et al (2019) Jo u Pr f. Toxicol Appl Pharmacol 114845. https://doi.org/10.1016/j.taap.2019.114845

Geens T, Aerts D, Berthot C, et al (2012) A review of dietary and non-dietary exposure to bisphenol-A. Food Chem Toxicol 50:3725–3740

Goldinger DM, Demierre AL, Zoller O, et al (2015) Endocrine activity of alternatives to BPA found in thermal paper in Switzerland. Regul Toxicol Pharmacol 71:453–462. https://doi.org/10.1016/j.yrtph.2015.01.002

Gómez-Ríos GA, Pawliszyn J (2014) Development of coated blade spray ionization mass spectrometry for the quantitation of target analytes present in complex matrices. Angew Chemie - Int Ed 53:14503–14507. https://doi.org/10.1002/anie.201407057

Gontani S, Ohashi T, Miyanaga K, et al (2017) Structural comparison of two bisphenol S derivatives used as colour developers in high-performance thermal paper. Dye Pigment 139:549–555. https://doi.org/10.1016/j.dyepig.2016.12.049

Harris GA, Galhena AS, Fernández FM (2011) Ambient sampling/ionization mass spectrometry: Applications and current trends. Anal Chem 83:4508–4538. https://doi.org/10.1021/ac200918u

Karrer C, Roiss T, von Goetz N, et al (2018) Physiologically based pharmacokinetic (PBPK) modeling of the bisphenols BPA, BPS, BPF, and BPAF with new experimental metabolic parameters: Comparing the pharmacokinetic behavior of BPA with its substitutes. Environ Health Perspect 126:077002. https://doi.org/10.1289/EHP2739

Kerian KS, Jarmusch AK, Cooks RG (2014) Touch spray mass spectrometry for in situ analysis of complex samples. 2714–2720. https://doi.org/10.1039/c4an00548a

Li X, Ma W, Li H, et al (2018) Sampling and analyte enrichment strategies for ambient mass spectrometry. Anal Bioanal Chem 410:715–724. https://doi.org/10.1007/s00216-017-0658-2

Liao C, Kannan K (2011) Widespread occurrence of bisphenol A in paper and paper products: Implications for human exposure. 9372–9379

Liao C, Liu F, Kannan K (2012) Bisphenol S, a new bisphenol analogue, in paper products and currency bills and its association with bisphenol a residues. Environ Sci Technol 46:6515–6522. https://doi.org/10.1021/es300876n

Lu H, Zhang H, Chingin K, et al (2018) Ambient mass spectrometry for food science and industry. TrAC - Trends Anal. Chem. 107:99–115

Mielke H, Partosch F, Gundert-Remy U (2011) The contribution of dermal exposure to the internal exposure of bisphenol A in man. Toxicol Lett 204:190–198. https://doi.org/10.1016/j.toxlet.2011.04.032

Moral R, Wang R, Russo IH, et al (2008) Effect of prenatal exposure to the endocrine disruptor bisphenol A on mammary gland morphology and gene expression signature. J Endocrinol 196:101–112. https://doi.org/10.1677/JOE-07-0056

Official Journal of the European Union (2016) Commission Regulation (EU) 2016/2235

Oh J, Choi JW, Ahn YA, Kim S (2018) Pharmacokinetics of bisphenol S in humans after single oral administration. Environ Int 112:127–133. https://doi.org/10.1016/j.envint.2017.11.020

Pal S, Sarkar K, Nath PP, et al (2017) Bisphenol S impairs blood functions and induces cardiovascular risks in rats. Toxicol Reports. https://doi.org/10.1016/j.toxrep.2017.10.006

Pereira I, Rodrigues MF, Chaves AR, Vaz BG (2018) Molecularly imprinted polymer (MIP) membrane assisted direct spray ionization mass spectrometry for agrochemicals screening in foodstuffs. Talanta 178:507–514. https://doi.org/10.1016/j.talanta.2017.09.080

Qiu W, Yang M, Liu S, et al (2018) Toxic effects of bisphenol S showing immunomodulation in fish macrophages. Environ Sci Technol 52:831–838. https://doi.org/10.1021/acs.est.7b04226

Rocha BA, Azevedo LF, Gallimberti M, et al (2015) High levels of bisphenol A and bisphenol S in Brazilian thermal paper receipts and estimation of daily exposure. J Toxicol Environ Heal - Part A Curr Issues 78:1181–1188. https://doi.org/10.1080/15287394.2015.1083519

Rocha BA, Da Costa BRB, De Albuquerque NCP, et al (2016) A fast method for bisphenol A and six analogues (S, F, Z, P, AF, AP) determination in urine samples based on dispersive liquid-liquid microextraction and liquid chromatography-tandem mass spectrometry. Talanta 154:511–519. https://doi.org/10.1016/j.talanta.2016.03.098

Shen L, Zhang J, Yang Q, et al (2012) High throughput paper spray mass spectrometry analysis. Clin Chim Acta. https://doi.org/10.1016/j.cca.2012.10.025

Tan F, Zhao H, Li X, et al (2009) Preparation and evaluation of molecularly imprinted solid-phase microextraction fibers for selective extraction of bisphenol A in complex samples. J Chromatogr A 1216:5647–5654. https://doi.org/10.1016/j.chroma.2009.06.007

Ullah A, Pirzada M, Jahan S, et al (2019) Bisphenol A analogues bisphenol B, bisphenol F, and bisphenol S induce oxidative stress, disrupt daily sperm production, and damage DNA in rat spermatozoa: A comparative in vitro and in vivo study. Toxicol Ind Health 35:294–303. https://doi.org/10.1177/0748233719831528

United States Environmental Protection Agency (2014) Bisphenol A Alternatives in Thermal Paper. Epa 519

Wang Z, Yu J, Yao J, et al (2018) Simultaneous identification and quantification of bisphenol A and 12 bisphenol analogues in environmental samples using precolumn derivatization and ultra high performance liquid chromatography with tandem mass spectrometry. J Sep Sci 41:2269–2278. https://doi.org/10.1002/jssc.201701087

Wu L-H, Zhang X-M, Wang F, et al (2018) Occurrence of bisphenol S in the environment and implications for human exposure: A short review. Sci Total Environ 615:87–98. https://doi.org/10.1016/j.scitotenv.2017.09.194

Xie P, Zhao C, Zhao H, et al (2018) Determination of bisphenol A and bisphenol S in sacked mouse foods by liquid chromatography-tandem mass spectrometry. Int J Mass Spectrom 434:17–22. https://doi.org/10.1016/j.ijms.2018.08.011

Yang Q, Wang H, Maas JD, et al (2012) Paper spray ionization devices for direct, biomedical analysis using mass spectrometry. Int J Mass Spectrom 312:201–207. https://doi.org/10.1016/j.ijms.2011.05.013

Zhang X, Chang H, Wiseman S, et al (2011) Bisphenol a disrupts steroidogenesis in human H295R cells. Toxicol Sci 121:320–327. https://doi.org/10.1093/toxsci/kfr061

Zhao H, Xiang L, Li J, et al (2016) Investigation on fragmentation pathways of bisphenols by using electrospray ionization Orbitrap mass spectrometry. Rapid Commun Mass Spectrom 93:1901–1913. https://doi.org/10.1002/rcm.7666

Zhou D (2018) Ecotoxicity of bisphenol S to Caenorhabditis elegans by prolonged exposure in comparison with bisphenol A. Environ Toxicol Chem 37:2560–2565. https://doi.org/10.1002/etc.4214

Journal of the Brazilian Chemical Society

Graphical Abstract (GA)

GA Figure:

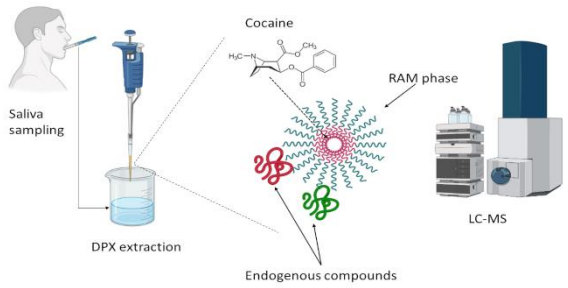

GA Text: A new reliable extractive phase for disposable pipette extraction is developed, and its performance was evaluated in extractions of cocaine in saliva samples using High Performance Liquid Chromatography coupled to Mass Spectrometry.

Novel method for the extraction of cocaine from oral fluid by means of disposable pipette modified with restricted access material

*Ludmyla S. Tavares[1], Ricardo A. Bernardo[1], Anselmo E. de Oliveira[2], Boniek G. Vaz[1], Andrea R. Chaves[1]**

[1] Laboratório de Cromatografia e Espectrometria de Massas, Instituto de Química, Universidade Federal de Goiás, Goiânia - GO, 74690-900, Brazil.

[2] Laboratory of Theoretical and Computational Chemistry, Instituto de Química, Universidade Federal de Goiás, Goiânia - GO 74690-900, Brazil.

* andrea_chaves@ufg.br (e-mail of the corresponding autor)

ORCID ID: 0000-0002-1600-1660

Abstract

This study proposes a new, efficient, and selective method for the analysis of cocaine in oral fluid. For this purpose, an extractive phase with restricted access materials (RAM) capable of extract and pre-concentrate low molecular weight analytes and simultaneously exclude macromolecules was developed for disposable pipette extraction (DPX) followed by liquid chromatography coupled to mass spectrometry (LC-MS) analyses. The proposed method was optimized using a 2^4 factorial design which pointed higher extraction efficiency under the following conditions: pH 9, 10 cycles of extraction (aspirate/dispense), 3 cycles of desorption (aspirate/dispense) and acetonitrile as desorption solvent. The DPX-RAM/LC-MS method showed linearity range from 10 to 100 ng mL^{-1} with $R^2 = 0.999$, accuracy values ranged from -0.9 to 4.3%, precision values ranged from 1.7 to 9.1% and recovery values ranged from 97.9 to 101.1%. The benefits of this method are that it can be performed in few minutes and the analytical performances, including the limit of detection (3.13 ng mL^{-1}), limit of quantitation (10 ng mL^{-1}) and linear range were found to be in agreement with other methods used for similar analysis.

Keywords: cocaine, restricted access materials, disposable pipette extraction, desorption, validation.

Introduction

Cocaine is an alkaloid derived from the Erythroxylon coca plant that grows abundantly in the Andes region of South America.[1] It can be mainly found in the cocaine hydrochloride form, a white crystalline powder, which is introduced to the human body by inhalation, ingestion or directly injected in the blood stream. Cocaine effects in human body may include topical local anesthetic, ability to block reuptake of the neurotransmitters, such as dopamine, epinephrine and serotonin.[2] Cocaine also acts as stimulant drug, being widely used for truck-drivers during long travels.[3]

Many countries in South America, and worldwide, have passed legislation dictating that individuals must provide oral fluid, blood, hair, or nail samples to renew driver's licenses, which necessitates the development of reliable methods, with high throughput, for the analysis of drugs of abuse, and their analytes, in these biological matrices.[4,5]

Among the conventional biological matrices, urine is the most commonly used matrix for the analysis and identification of drugs and toxic substances due to the high concentration of analytes present in this matrix. In addition to analyzing the parent compound, it is necessary to detect various metabolic products that are generated as the body processes these compounds before elimination in urine.[6] An alternative matrix is oral fluid, which has, high concentration of analytes in their original form before they can be metabolized.[7] Other benefits of using oral fluid as a biological matrix are that it is an easy and noninvasive matrix to collect. Thus, the collection can be performed in remote locations where there are no medical facilities available.[8]

Samples originating from biological matrices are complex due to the presence of endogenous compounds, such as proteins,[9] hormones,[10] lipids,[11] and metabolites,[12] and a clean-up and pre-concentration step must be performed before injecting in chromatographic systems.[13] Historically, liquid–liquid extraction has been used for the isolation of drugs from biological samples. More recently, many of these liquid–liquid methods have been adapted or modified to include solid-phase extractions (SPE).[14] SPE has proven to be useful for sample preparation in oral fluid drug testing because of its high recovery rates and ease of use.[15–17] In general, SPE is faster, more efficient, and more selective, and it uses less solvent than liquid–liquid extraction methods.[14,18]

Disposable pipette extraction (DPX) is a miniaturized technique based on SPE. DPX uses a small amount of adsorbent (30 mg) which is placed inside of a micropipette tip containing a filter on the bottom and it may also contain a filter at the top.[19–22] Although DPX is derived from SPE, the efficiency of extraction is based on the time of sorption equilibrium between the sample solution and the adsorbent phase, consequently, this process is not dependent on sample

flow rate. Besides that, the miniaturized design of DPX consumes smaller volumes of solvents compared to traditional SPE.[22,23]

There are a lot of commercially available phases that can be used in DPX, they are all based on chromatographic media, such as C18 and C8 microparticles, hydrophobic or ion exchange phases.[24–26] On the other hand, there are a lot of advantages of manufacturing new phases including easy preparation and control of permeability and enhancement of the selectivity.[27]

Restricted access materials (RAM) are a class of biocompatible compounds that were first reported by Desilets and co-workers in 1991.[28] In general, RAM materials are derived from silica, being widely used with chromatography techniques for the separation of compounds with lower molecular weight from complex matrices.[19] A macromolecule such as protein, is immobilized onto the silica surface, and during the extraction process, this immobilized protein acts as a barrier to endogenous compounds. Furthermore, the analytes are sufficiently small to permeate this barrier and interact with the silica surface (Figure 1). The immobilized protein present in the surface of hydrophobic RAM combines the extraction mechanism of barrier exclusion and partition. The macromolecules are excluded and interact only with the external surface of support particles, and the analytes interact with the hydrophobic interior modified with protein.[28,29]

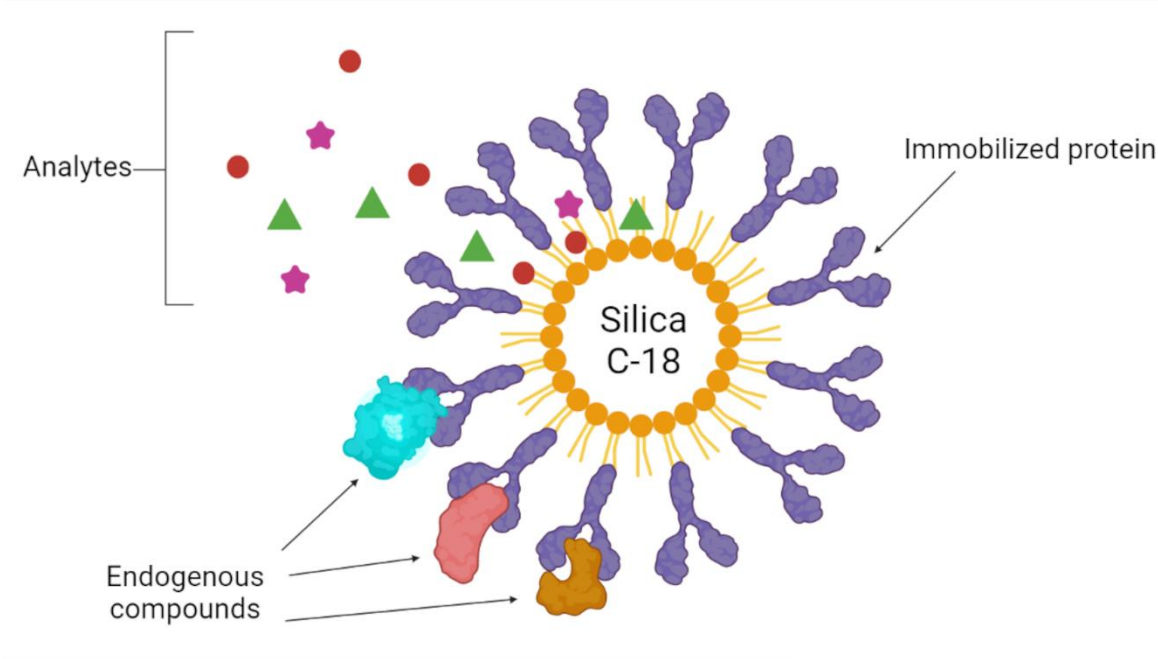

Figure 1. Extraction process of a restricted access material based on protein immobilized onto a silica C-18 surface.

In the present study, a DPX-RAM/LC-MS method was developed and applied for the analysis of cocaine in oral fluid. In addition, this work focused on developing the sorbent and optimizing the extraction conditions using a factorial design.

Experimental

Chemicals and reagents

Methanol and acetonitrile HPLC grade were acquired from J.T. Baker (Phillipsburg, USA); SPE C-18 cartridge was acquired from Supelco (São Paulo, Brazil). Sodium phosphate monobasic, sodium azide, and ammonium acetate were acquired from Mallinckrodt (Mexico City, Mexico). Benzophenone, potassium chloride, and glutaraldehyde 25% were acquired from Vetec (Rio de Janeiro, Brazil). Methacrylic acid, ethylene dimethacrylate, formic acid, potassium hydroxide, and bovine serum albumin (BSA) were acquired from Sigma Aldrich (Germany). Hydroxyethyl cellulose was acquired from Polytechno Indústrias Químicas Ltda. (São Paulo, Brazil). Calcium chloride dihydrate and magnesium chloride hexahydrate were acquired from Labsynth (Diadema, Brazil). Acetone P.A grade was acquired from Scharlau (Sentmenat, Spain). Cellulose membrane (diameter: 47 mm, and pore size: 0,45 µm) was acquired from Agilent Technologies (Germany). The water employed in this study was ultrapurified in a system Gehaka MS-2000 WFi.

The cocaine standard employed for the method optimization was kindly donated by the Polícia Civil do Estado de Goiás. In the validation step, a cocaine standard suitable for LC and GC analysis was acquired from Sigma Aldrich (USA) and kindly donated by Professor Wanderson Romão from the Chemistry Department of Universidade Federal do Espírito Santo.

RAM-BSA phase synthesis

The restrict access material adsorbent modified with bovine serum albumin (RAM-BSA) was prepared as described by Chaves *et al*, 2015.[19] An SPE cartridge containing C-18 silica was positioned in a manifold and conditioning with 3 mL of a 0.05 mol L^{-1} phosphate buffer solution (PBS) with pH 6. Then, the BSA was immobilized in the phase by treating it with 10 mL of a 2 mg mL^{-1} BSA solution for 15 min, and then, the cartridge was washed with 5 mL of ultrapurified water.

Thereafter, the cartridge was immersed with 5 mL of glutaraldehyde 25% and left to rest for 5 h. After that, 5 mL of a 1.0 mg mL^{-1} sodium azide solution was eluted through the cartridge until pH 10 was reached. The cartridge remained in rest for 2 h. Finally, the cartridge was washed with ultrapurified water for 1 h and stored in PBS 0.05 mol L^{-1} with pH 6 at the

temperature of 4° C until the use. The workflow for RAM-BSA synthesis is presented on Figure 2.

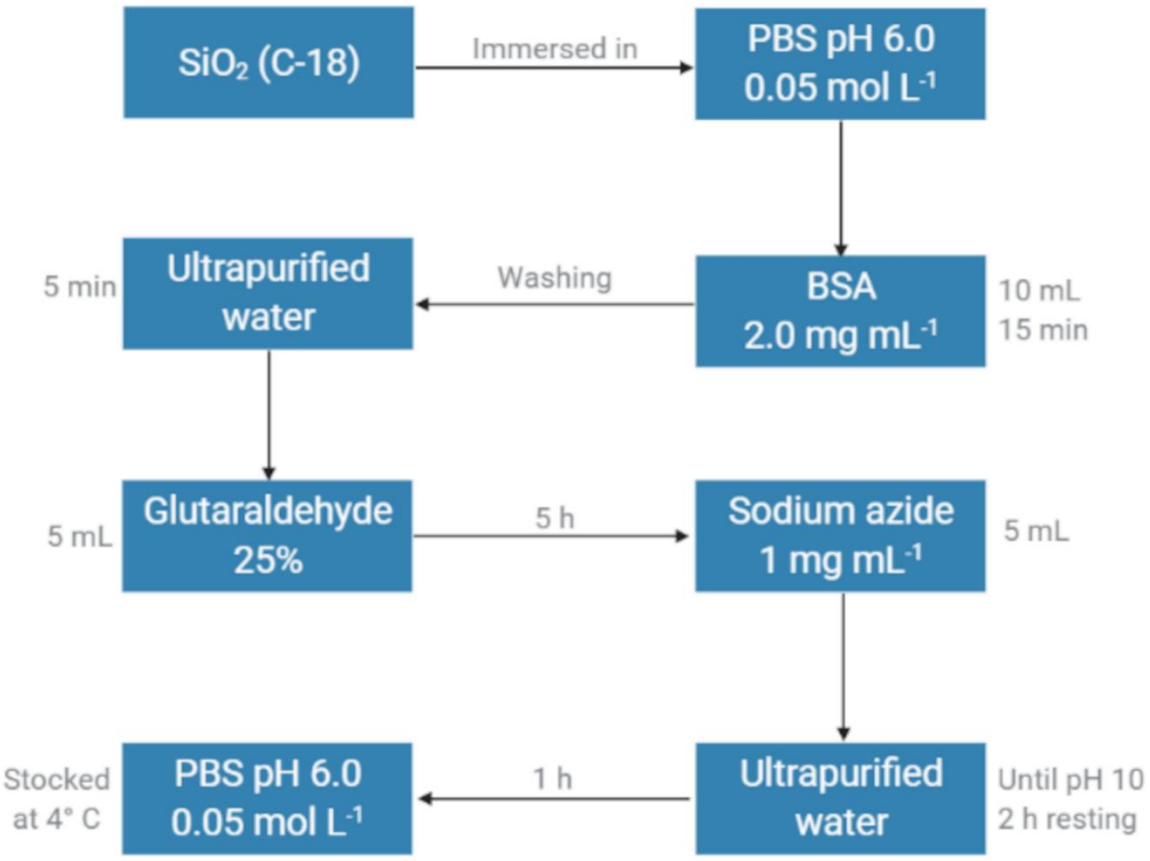

Figure 2. Schematic representation of RAM-BSA synthesis.

DPX tip preparation

In order to prepare the DPX tips, 10 mg of glass wool was set in the lower end of a 1 mL pipette tip. Then, 30 mg of RAM-BSA phase was placed inside the tip and washed with 2 mL of ultrapurified water. The DPX tips were prepared immediately before each experiment, and they were used for 10 cycles of extraction/desorption without extraction efficiency reduced (Figure 3). Between each extraction, the tip was washed twice with 1 mL of acetonitrile and twice with ultrapurified water.

Figure 3. Pipette tips with RAM phase used in the present study.

Oral fluid and synthetic saliva samples

Synthetic saliva was used during the optimization of the parameters of the DPX-RAM/LC-MS method and it was prepared by adaptation of the protocol presented by Alshali and co-workers.[30] Briefly, 0.25 g of hydroxyethyl cellulose was dissolved in 400 mL of ultrapurified water. The solution was left under magnetic stirring for 24 h in order to achieve total dissolution. Then, potassium chloride (0.625 g L^{-1}), calcium chloride dihydrate (0.166 g L^{-1}), potassium phosphate monobasic (0.326 g L^{-1}), magnesium chloride hexahydrate (0.059 g L^{-1}) and bovine serum albumin (0.00235 g L^{-1}) were added to the solution. After the dissolution of all the reagents, the pH was adjusted to 6.75 with potassium hydroxide and the volume was completed to 500 mL.

For the validation of the method, a pool of oral fluid collected from 10 nonuser volunteers was used. The authentic oral fluid samples were diluted 5 times with ultrapurified water and spiked with cocaine. The authentic oral fluid samples were collected according to Universidade Federal de Goiás ethical committee regulations. No real samples from drug users were evaluated, once the objective of this study is to present the applicability of the RAM extractive phase for DPX sample preparation steps.

Factorial design

Aiming to optimize the extraction conditions of DPX-RAM and determine the most significant parameters, a factorial design 2^k was used, where k = 4. The variables to be considered were coded as follows: a = pH, b = extraction cycles, c = desorption cycles and d = desorption solvent. The levels of each variable are presented in Table 1.

Table 1. Parameters, variables, and levels used in the factorial design 2^4

Parameter	Variable	Lower Level	Higher Level
a	pH	4	9
b	Extraction cycles	3	10
c	Desorption cycles	3	10
d	Solvent	Acetonitrile	Methanol

Following the factorial design, sixteen randomized extractions were performed in duplicate. The samples were prepared in 500 µL of synthetic saliva spiked with cocaine at the concentration of 100 ng mL^{-1} and 500 µL of buffer solution (phosphate 0.05 mol L^{-1} pH 9 or acetate 0.05 mol L^{-1} pH 4). 250 µL of sample was aspirated/dispensed 3 or 10 times in the extraction cycle using the same sample vial, then 500 µL of desorption solvent (methanol or acetonitrile) were aspirated/dispensed 3 or 10 times in a vial flask. Moreover, the extractions were performed using 10 cycles of extraction (aspirate/dispense), acetonitrile as desorption solvent in 3 cycles of desorption. It is necessary to highlight that RAM sorbents usually recommend the use between pH 5 to 9, once RAM sorbent did not exhibit good protein exclusion near to isoelectric point. For factorial design, an extreme condition was used.

Chromatographic conditions

Analysis was performed in a Shimadzu LC-20A high performance liquid chromatography with a UV-vis Shimadzu SPD-20A detector set at the wavelength of 235 nm. The separations were performed using a Phenomenex Luna C-18 (5 µm, 150 x 4.6 mm) column. The mobile phase consisted of A: 10 mM of ammonium acetate in water with 0.01% formic acid and B: acetonitrile, in isocratic mode 25:75 v/v respectively at a flow rate of 0.3 mL min^{-1}.

Experimental conditions of Mass Spectrometer

The mass spectrometer used in the DPX-RAM/LC-MS method was a micrOTOF-Q III, fabricated by Bruker (Billerica, USA). The experiments were performed in positive mode, at a flow rate of 5 L min^{-1} of drying gas, ESI source temperature of 280 °C, nebulizer pressure of 0.5 bar, the capillary voltage of 2800 V and the mode of operation was MS/MS.

Bradford test

In order to evaluate the efficiency of the RAM-BSA phase in excluding proteins and endogenous compounds, oral fluid samples were submitted to a Bradford test before and after extraction. This test was performed in a UV-vis Ultrospec 2000 spectrometer, fabricated by Pharmacia Biotech.

Concisely, the method developed by Bradford[31] involves the bounding of reagent Coomassie Brilliant Blue G-250 to the proteins present in the sample. The bounding of the Bradford's reagent to proteins promotes a change in its maximum absorption, changing from 465 nm to 595 nm, and this change is monitored by UV-Vis spectrophotometry. The protein quantification is performed through an analytical curve, using different human albumin solution concentration as a protein source.

Analytical essays

In the present study, the analytical validation parameters were evaluated as described by Agência Nacional de Vigilância Sanitária (ANVISA) in resolution RDC n° 166 of July 24th, 2017.[32] Thus, accuracy, precision, recovery, linearity, limits of detection and quantitation, and matrix effect were evaluated. In this study, no internal standard was used, because the chromatographer was coupled to a high-resolution MS system, and the DataAnalysis software version 5.0 with peak attribution error less than 3 ppm.

Results and Discussion

RAM phase synthesis

In the synthesis of the RAM phase, the 0.05 mol L^{-1} phosphate buffer solution pH 6 was employed to ensure that the BSA protein was not denatured. The solution of glutaraldehyde 25% was used to assist the stabilization of the immobilized protein, then, the sodium azide solution was added to reduce residual glutaraldehyde clusters and prevent further reactions.

After the synthesis, the RAM-BSA phase was kept in PBS solution 0.05 mol L^{-1} pH 6 in refrigerator to ensure immobilized protein integrity.[33]

Protein exclusion test

Bradford tests are commonly used in the quantitation of total proteins[31] and was used in this study to evaluate the capability of the developed RAM-BSA phase to exclude proteins. The method developed by Bradford involves the bond of the reagent Coomassie Brilliant Blue G-250 to the proteins present in the sample. The bond of the dye to the protein causes a change in the maximum absorption of the dye from 465 nm to 595 nm and this change in absorption is monitored by the UV-vis spectrometer. The protein quantitation is performed using an analytical curve built with human serum albumin standard solution. The developed analytical curve is presented below on Equation 1:

$$y = \left(\frac{X-0.0809}{0.0423}\right).10\ \mu g\ mL^{-1} \qquad \textbf{(1)}$$

Where, y is the concentration of proteins present in the sample, and X is the measurement of the spectrometer.

In this test, a sample of authentic oral fluid was prepared by diluting it 5-fold according to the developed method and divided in two aliquots, the first one was not submitted to any extraction. The second one was extracted using the DPX-RAM protocol described in this paper and then the oral fluid sample that usually is discarded after the extraction was collected to be analyzed for its protein content. Table 2 shows that the concentration of proteins present in the sample before and after the extraction are very close, proving that the RAM-BSA is in fact, excluding the endogenous compounds present in the sample.

Table 2. Bradford test to oral fluid before and after the extraction process

Sample	Measurement of spectrometer	Concentration (µg mL^{-1})
Extracted Oral Fluid	0.111	7.115
Oral Fluid without extraction	0.112	7.352

Chromatographic conditions optimization

In order to perform the analytical validation of the DPX-RAM/LC-MS method, the chromatographic conditions were evaluated employing two different columns, three mobile

phases, and two wavelengths, as shown in Table 3. The evaluated conditions were selected according to the literature.[34–38]

Table 3. Chromatographic conditions evaluated in the method's optimization

Mobile Phase	Column	Wavelength
Methanol and water 0.01% formic acid (70:30 v/v)	Agilent XDB C18 (5 µm, 150 x 4.6 mm)	235 nm
Methanol and ammonium acetate 10 mM 0.01% formic acid (70:30 v/v)	Phenomenex Luna C18 (5 µm, 150 x 4.6 mm)	200 nm
Acetonitrile and ammonium acetate 10 mM 0.01% acid formic (75:25 v/v)	Phenomenex Luna C18 (5 µm, 150 x 4.6 mm)	235 nm

The higher chromatographic efficiency was obtained with a Phenomenex Luna C-18 column, acetonitrile: 10 mmol L^{-1} ammonium acetate 0.01% formic acid (75:25, v/v) as mobile phase and wavelength of 235 nm. In this optimized condition, the retention time of cocaine standard solution at 100 ng mL^{-1} was 8.7 min. The experimental conditions of the mass spectrometer were adjusted to suit the flow rate and chromatographic conditions. The total ion chromatogram and the respective mass spectrum are presented in Figure 4.

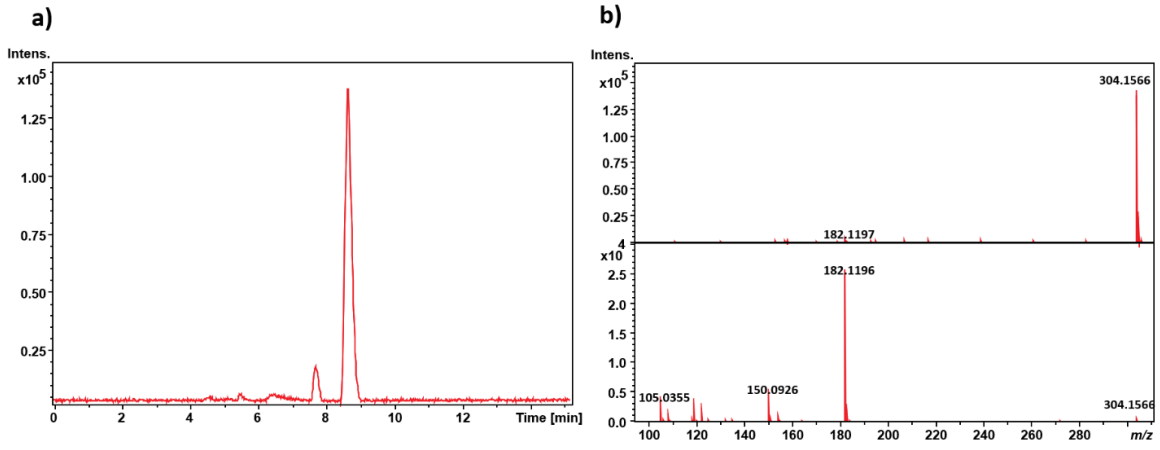

Figure 4. (a) Total ion chromatogram; (b) mass spectrum of the retention time 8.7 min on the top and its MS/MS spectrum on the bottom acquired in the optimized conditions of analysis.

Factorial design

For the optimization of the extraction using the DPX-RAM protocol a factorial design 2^k, k = 4 was employed, meaning that 4 variables were evaluated in the planning of experiments. The oral fluid samples spiked with cocaine were submitted to extraction with the DPX-RAM in duplicate in the 16 experimental conditions, and the obtained extracts were analyzed by LC-MS. Table 4 presents the performed experiments and the results in each essay in the factorial design 2^4, the responses correspond to the absolute intensity of the cocaine peak in the mass spectrum. The data were analyzed with the aid of Design-Expert software.[39]

Table 4. Absolute intensity of the cocaine peak in the MS spectrum for each essay in the factorial design 2^4. High (+) and low (-) levels according to Table 1

Experiment	pH	Extraction Cycle	Desorption Cycle	Solvent	Absolute intensity of response/peak 1	Absolute intensity of response 2
1	-	-	-	-	19448	13742
2	+	-	-	-	12785	11788
3	-	+	-	-	34895	25023
4	+	+	-	-	25287	27771
5	-	-	+	-	16593	19442
6	+	-	+	-	10206	13296
7	-	+	+	-	35123	25364
8	+	+	+	-	38005	32103
9	-	-	-	+	7479	7438
10	+	-	-	+	3052	3171
11	-	+	-	+	15527	16842
12	+	+	-	+	11691	12256
13	-	-	+	+	9179	9030
14	+	-	+	+	5992	6237
15	-	+	+	+	16916	15388
16	+	+	+	+	20047	19181

In the semi-normal distribution graph (Figure 5), the most significant effects are those that move further away from the linear model followed by the other effects. Therefore, it is observed that the most significant effects are caused by the extraction cycle at the high level and by the solvent at the low level.

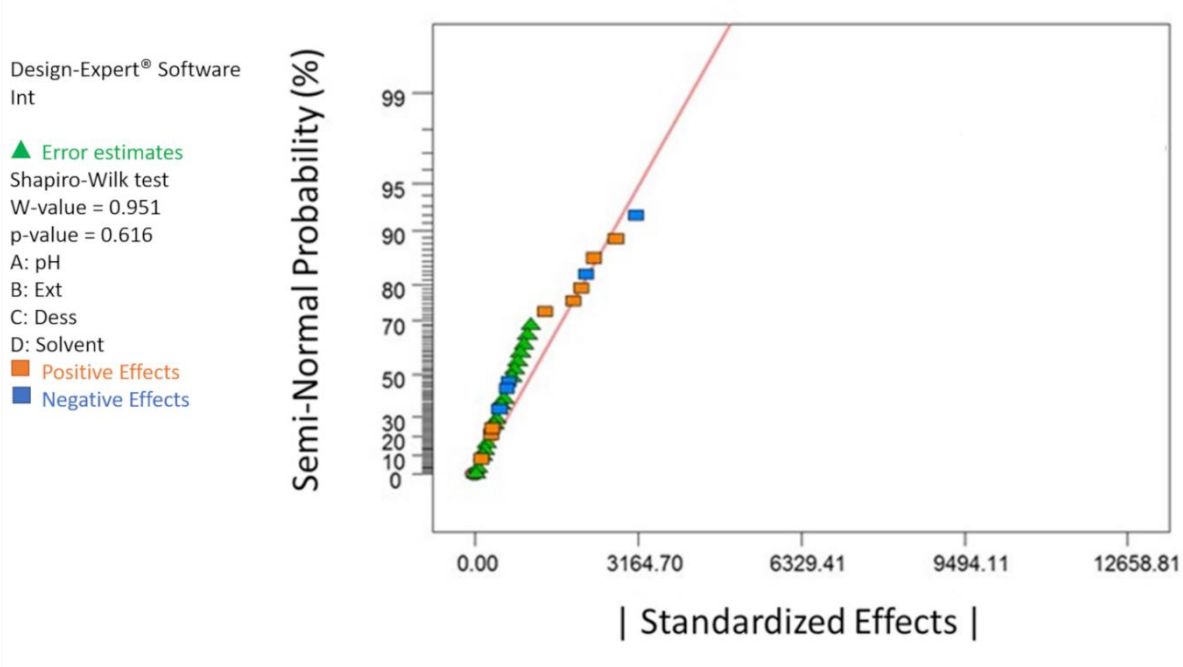

Figure 5. Graph of semi-normal distribution.

The Pareto diagram was used for a more precise analysis and it is shown in Figure 6. In this bar chart, the occurrence frequencies are ordered, from highest to lowest, allowing the best visualization of the most significant effects. There is a limit line, calculated by the t-Student test. The variables with the highest significance in the experiment should be above the limit line.

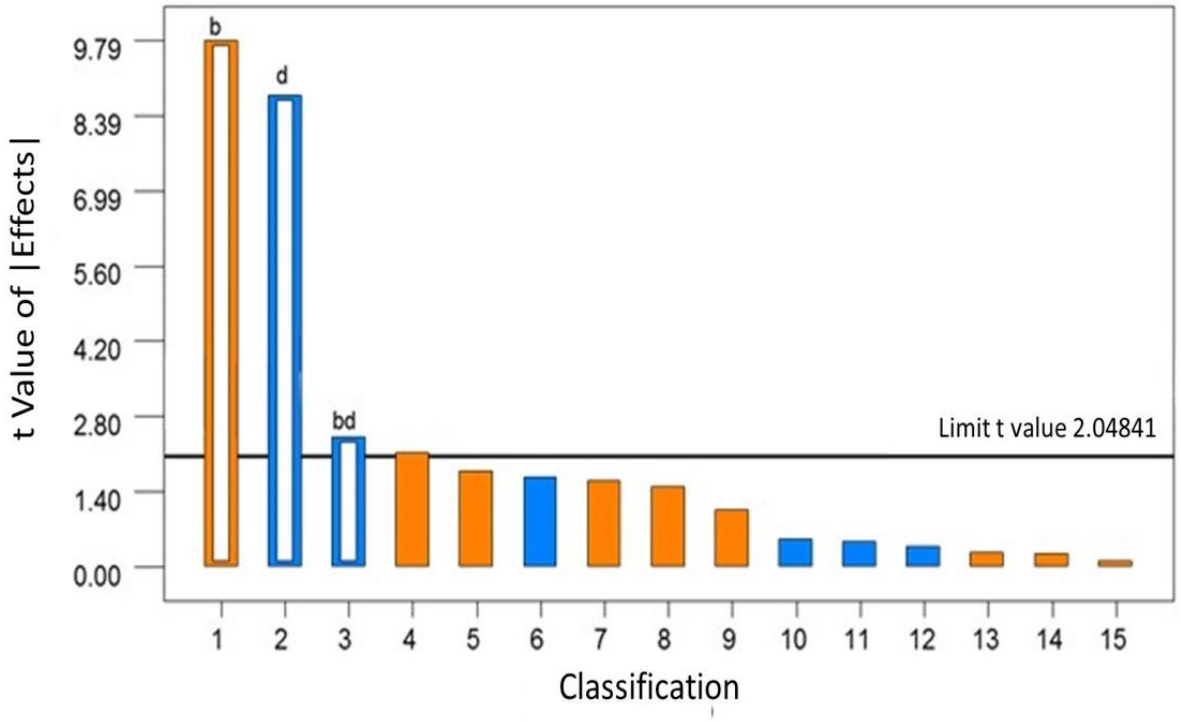

Figure 6. Pareto diagram obtained for the studied variables, where b means the number of extraction cycles, d means the solvent used to desorption, and bd means the interaction between b and d parameters. The colors orange and blue are attributed to positive and negative effects, respectively.

According to the Pareto diagram, the most significant effects are the same as those found by the graph of semi-normal distribution: extraction cycles and desorption solvent. In the diagram it is also possible to observe that the interaction effect between these two variables is significant, there is influence between the variation of one over the other. However, as this interaction effect is very close to the boundary line, its influence on extractions is smaller than when analyzing each variable separately.

In order to statistically verify the variation of experimental responses produced by the significant variables to the factorial design model, the analysis of variance (ANOVA) was used and the results are presented in Table 5.

Table 5. Analysis of variance for the significant effects, where b means the number of extraction cycles, d means the solvent used to desorption, and bd means the interaction between b and d parameters

ANOVA for the factorial design

Analysis of variance (partial sum of squares - Type III)					
Source	**Sum of Squares**	**Df**	**Square Mean**	**F value**	**p Value Prob > F**
Model	2.389E+09	3	7.963E+08	59.57	< 0.0001
B	1.282E+09	1	1.282E+09	95.90	< 0.0001
D	1.029E+09	1	1.029E+09	76.96	< 0.0001
BD	7.813E+07	1	7.813E+07	5.84	0.0224
Residual	3.743E+08	28	1.337E+07		
Error	1.451E+08	16	9.067E+06		
Total	2.763E+09	311			

B: number of extraction cycles

D: desorption solvent

BD: interaction between B and D parameters

In this type of analysis, the p values obtained equal or less than 0.05 are significant, since they show, with 95% confidence or more, that these parameters influence the extraction responses. The ANOVA, presented in Table 6, shows that the significant parameters in the Pareto diagram also have a p-value less than 0.05.

ANOVA confirms that the two main effects in the extraction with DPX-RAM are the extraction cycle and the desorption solvent, since the confidence that these parameters influence in the analysis is greater than 99.9%. As shown in the Pareto diagram, the interaction effect between these two variables is also significant, this is a secondary effect and the confidence of it influences the extraction experiments with DPX-RAM is 97.76%.

The extraction efficiency using DPX is based on the equilibrium time of sorption between the sample solution and extraction phase. In this way, the result from the factorial design illustrates that the more extraction cycles are performed the higher is the intensity of the response, which is consistent with DPX mode of operation. Also, as the affinity between the desorption solvent and the analyte increases, there is an improvement in the desorption of the retained analyte from the extractive phase. Thus, the results found that the solvent desorption influences the response generated with the DPX-RAM extraction phase are consistent with the literature. Based on this, the optimum experimental conditions for the extractions of cocaine in oral fluid by DPX-RAM is 10 cycles of extraction (aspirate/dispense) and acetonitrile as desorption solvent, following the trend of the most significant effects. However, the other two variables do not present significant influence. Thus, it was chosen to carry out the extractions

in 0.05 mol L^{-1} phosphate buffer solution of pH 9, because this pH is close to pKa of cocaine, ensuring that it is in molecular form during the extraction procedure. And finally, 3 desorption cycles (aspirate/dispense) were chosen because it is less laborious condition.

Analytical assays for DPX-RAM/LC-MS method

Linearity and linear range

The linearity of the method was demonstrated by the analytical curve constructed with cocaine in a concentration ranging from 10 to 100 ng mL^{-1}. The analytical curve was plotted using the absolute signal intensity of the mass spectrum for the most intense m/z fragment of cocaine, thus ensuring that the all of the analyzed signal comes from the fragmentation of cocaine, eliminating possible interferences in the analysis. The most common fragmentation profile of cocaine (*m/z* 304) is the loss of a benzoyl group, giving the most abundant fragment (*m/z* 182), as shown in Figure 4b.

The linearity of the standardized DPX-RAM/LC-MS method was determined using oral fluid samples (blank) spiked with cocaine at the concentrations of 10, 20, 30, 40, 50, 60, 70, 80, 90 and 100 ng mL^{-1} and each of these points were analyzed in replicates (n = 5). The evaluated range was linear with the square of the correlation coefficient greater than 0.999 (Table 6), and the coefficients of variation of the points of the analytical curve were lower than 15%, following ANVISA's regulations. Aiming to test if the linear regression model used is true, the ANOVA variance test was performed, the data obtained are presented in Table 6. As the probability of the F value is much lower than 0.05, it can be stated that the model is indeed linear.

Table 6. Linear regression and ANOVA test for the DPX-LC-MS method with their respective limit of detection (LOD), and limit of quantitation (LOQ)

Matrix	**Analyte**	**Linear Regression (LOQ:100 ng mL^{-1})**	**R^2**	**LOD (ng mL^{-1})**	**LOQ (ng mL^{-1})**
Oral fluid	Cocaine	y = 84.276x + 1055.7	0.9990	3.13	9.48
ANOVA test					
	Df	**Sum of Squares**	**Square Mean**	**F value**	**Prob > F**
Model	1	13322.54403	13322.54403	46617.20892	2.220E-16
Error	8	2.28629	0.28579		
Total	9	133424.83032			

LOD: limit of detection

LOQ: limit of quantification
Df: degrees of freedom

Limit of detection (LOD) and limit of quantitation (LOQ)

For the determination of LOD and LOQ, ten measurements of the blank sample were performed, specifically, oral fluid extracted by DPX-RAM without the presence of cocaine. Then, Equations 2 and 3 were used to perform the calculations, as described below:

$$LOD = 3.\left(\frac{STD}{a}\right) \quad \textbf{(2)}$$

$$LOQ = 10.\left(\frac{STD}{a}\right) \quad \textbf{(3)}$$

Where, STD is the standard deviation of 10 measurements of blank samples and a is the angular coefficient in the analytical curve.

The values empirically obtained were: LOD = 3.13 ng mL^{-1} and LOQ = 9.48 ng mL^{-1}. The limit of quantitation was also determined experimentally by means of the lowest concentration of cocaine that was able to be fragmented with precision and accuracy. The experimental LOQ was found to be 10 ng mL^{-1}.

Precision, Accuracy, Recovery, and Matrix Effect

In order to evaluate recovery (R), accuracy (E), intra and interday precision (P), blank samples of oral fluid spiked with standard cocaine were prepared at three concentration levels: 10, 50, and 100 ng mL^{-1}; for each concentration, the tests were performed in replicate (n = 5). Equations 4, 5 and 6, as described below, were used in the calculations, and the results can be seen in Table 7.

$$R(\%) = \frac{EC}{TC}.100 \quad \textbf{(4)}$$

$$E(\%) = \left(\frac{C-TC}{TC}\right).100 \quad \textbf{(5)}$$

$$P(\%) = \left(\frac{STD}{C}\right).100 \quad \textbf{(6)}$$

Where EC is the concentration determined experimentally, TC is the theoretical concentration, C is the average of experimental concentration and STD is the standard deviation between the concentrations measurements.

Table 7. Precision, accuracy, and recovery for cocaine analysis in oral fluid by DPX-RAM/LC-MS method

Concentration (ng mL^{-1})	Accuracy (%)	Precision (%)		Recovery (%)
		Intraday	Interday	
10,0	4.3	7.4	9.1	97.9
50,0	-0.9	2.1	2.5	100.1
100,0	0.5	1.7	2.3	101.1

The matrix effect was evaluated through the parallelism between the analytical and the calibration curve, and the intercept comparison. Both curves were built in replicate (n = 5) at the concentration levels of 10, 20, 30, 40, 50, 60, 70, 80, 90, and 100 ng mL^{-1}, were the calibration curve was composed of standard cocaine in water, and the analytical curve was composed of saliva spiked with standard cocaine. A t-test was performed to compare both intercept and slopes at the 0.05 significance level (Table 8).

Table 8. Intercept and slope comparison on t-test to evaluate matrix effect

	Estimation	Standard Deviation	t	P-value
Intercept	1055.7	651.4777	1.6205	0.1247
Concentration	84.276	10.4995	8.0267	0
CalibrationCurve	-4567.9	921.3286	-4.9579	0.0001
Concentration:Calibration Curve	431.2422	14.8486	29.0427	0
	Degree of Freedom	**Sum of Sqaures**	**F**	**P-value**
Equality of the Intercept	1	22356118.2964	24.5813	0.0001
Parallelism	1	767125504.9396	843.4787	0
Coincidence	2	2600818435.8216	1429.841	0

Since the P-value (0.0001) in the equality of intercept test is lower than 0.05, it is possible to conclude that the lines do not have the same intercept. Regarding the parallelism test, since the P-value (0) is lower than 0.05, it is possible to conclude that the lines are not parallel. In other words, the matrix effect is present in this methodology.

The evaluation of matrix effect, if it is considerable or not, can be assessed by comparing the slope of a calibration curve for standard solutions to the slope of a analytical curve matched standard solutions,[40] or calculation of the recovery values in several points of a standard calibration curve by adding the standard solution to the real sample matrix.[41] As can be seen in tables 7 and 8 the recoveries values are high enough (98-101%). Therefore, the response of the developed method cannot be affected by the sample matrix.

According to ANVISA,[32] accuracy and precision values below 15% are desirable. Recovery values close to 100% are desirable, but values between 80 and 120% are also acceptable as long as recovery is precise and accurate. In the extraction process using DPX-RAM, the influence of proteins present in oral fluid was minimized due to the ability of the adsorbent phase to exclude such interferents. In this way, satisfactory analytical recovery rates were obtained.

In the literature, there are no reports of cocaine analysis with an extraction step done with RAM phases. However, Bordin and co-workers[42] used a commercial DPX tip containing an ion exchange adsorbent phase to analyze cocaine, nicotine and their metabolites in meconium samples by GC-MS with a derivatization step. The authors obtained recovery values for cocaine between 73 and 97%. Thus, with the use of the RAM-BSA phase as the adsorbent phase for DPX and LC-MS analysis, there is no need to perform a derivatization step in addition to an increase in cocaine recovery.[42–44]

Dulaurent and co-workers reported a methodology using QuEChERS as sample preparation technique for LC-MS/MS analysis of abuse drugs in whole blood.[45] The sample preparation step was performed in 20 min, and the authors reported 3 ng mL^{-1} as LOD. Ellefsen and co-workers reported the determination of cocaine and benzoylecgonine in saliva after controlled intravenous cocaine administration.[46] The authors reported 1 ng mL^{-1} as LOD. Melanson and co-workers reported a LC-MS/MS for cocaine (LOD 2 ng mL^{-1}) and benzoylecgonine (LOD 5 ng mL^{-1}).[47] García-Valverde and co-workers modified cotton fibers with β-cyclodextrins and applied it as sorbent to cocaine and methamphetamine extraction in saliva samples.[48] Bernardo and co-workers reported the use of platinum wires coated with polypyrrole as needle for probe electrospray ionization, determining cocaine, LSD, methamphetamine and MDMA in oral fluid and urine samples.[13]

The methodology described here is sensitive, with LOD close to the ones reported in the literature (3 ng mL^{-1}). The DPX-RAM/LC-MS is also considered to be a fast technique, since the sample preparation took less than 5 min for each sample. The standardized and validated DPX-RAM/LC-MS method showed to be promising for drug determination in oral fluid and other drugs could be also analyzed.

Conclusions

In this work, a new method, DPX-RAM/LC-MS, for the analysis of cocaine in oral fluid was standardized and validated. The RAM-BSA phase used as an adsorbent in the DPX extraction, successfully excluded the interfering compounds in oral fluid, making method more selective for the analyte of interest.

According to the parameters of analytical validation, the proposed method is adequate, since its values of precision, accuracy, and recovery are within the standards established by ANVISA. The method also has a wide range of linearity and adequate R^2, LOD and LOQ values. In addition to simplicity, low cost, low solvent consumption, speed, and efficiency.

The DPX-RAM/LC-MS method showed a good range of linearity and little matrix effect, evidenced by recovery and linearity values. The developed methodology showed to be a promising tool for routine forensic analysis.

Acknowledgements

This work was supported by grants from the Coordenação de Aperfeiçoamento de Pessoal de Nível Superior (CAPES), and Conselho Nacional de Desenvolvimento Científico e Tecnológico (CNPq). The whole team involved in this work thanks professor Wanderson Romão and the Polícia Civil de Goiás, who kindly donated us the drugs standards. We also thank professor Anselmo Elcana de Oliveira for contributing to the chemometric analysis, and professor Raphaela de Castro Georg who kindly borrowed the necessary equipment for the Bradford test. We would also like to express our gratitude to Jennett Chenevert Aijala, who kindly helped in the revision process of this work.

References

1. Moreno-Artero, E.; Querol-Cisneros, E.; Rodríguez-Garijo, N.; Tomás-Velázquez, A.; Antoñanzas, J.; Secundino, F.; Pilar Gil-Sánchez, M.; España, A. ;J. Eur. Acad. Dermatology Venereol. 2018, 32, 1420.

2. Principles of Forensic Toxicology; Levine, B. S.; Kerrigan, S., Eds.; 5th ed.; Springer: Cham, Switzerland, 2020.

3. Dini, G.; Bragazzi, N. L.; Montecucco, A.; Rahmani, A.; Durando, P. ;J. Prev. Med. Hyg. 2019, 60, E124.

4. Frederick, D. L. ;Clin. Lab. Med. 2012, 32, 467.

5. Conselho Nacional de Trânsito - CONTRAN Resolução N° 517 de 29 de Janeiro de 2015 http://www.denatran.gov.br/download/Resolucoes/Resolucao5172014.pdf (accessed Jun 21, 2021).

6. Moeller, M. R.; Steinmeyer, S.; Kraemer, T. ;J. Chromatogr. B Biomed. Sci. Appl. 1998, 713, 91.

7. Dinis-Oliveira, R. J. ;Toxicol. Mech. Methods 2015, 25, 494.

8. Toyo'oka, T. ;Biol. Pharm. Bull. 2016, 39, 1397.

9. Vasconcelos, I.; Fernandes, C. ;Trends Anal. Chem. 2017, 89, 41.

10. Wudy, S. A.; Schuler, G.; Sánchez-Guijo, A.; Hartmann, M. F. ;J. Steroid Biochem. Mol. Biol. 2018, 179, 88.

11. Lísa, M.; Cífková, E.; Khalikova, M.; Ovčačíková, M.; Holčapek, M. ;J. Chromatogr. A 2017, 1525, 96.

12. Drouin, N.; Rudaz, S.; Schappler, J. ;J. Pharm. Biomed. Anal. 2018, 159, 53.

13. Bernardo, R. A.; da Silva, L. C.; Queiroz, M. E. C.; Vaz, B. G.; Chaves, A. R. ;J. Chromatogr. A 2019, 1603, 23.

14. Telepchak, M. J.; August, T. F.; Chaney, G. Forensic and Clinical Applications of Solid Phase Extraction Forensic and Clinical Applications of Solid Phase Extraction Forensic and Clinical Applications of Solid Phase Extraction ii Contents; Telepchak, M. J.; August, T. F.; Chaney, G., Eds.; Humana Press: Totowa, New Jersey, USA, 2004.

15. Soriano, T.; Jurado, C.; Menéndez, M.; Repetto, M. ;J. Anal. Toxicol. 2001, 25, 137.

16. Logan, B. K.; Stafford, D. T.; Tebbett, I. R.; Moore, C. M. ;J. Anal. Toxicol. 1990, 14, 154.

17. Piet Franke, J.; De Zeeuw, R. A. ;J. Chromatogr. B Biomed. Appl. 1998, 713, 51.

18. Hennion, M.-C. ;J. Chromatogr. A 1999, 856, 3.

19. Chaves, A. R.; Moura, B. H. F.; Caris, J. A.; Rabelo, D.; Queiroz, M. E. C. ;J. Chromatogr. A 2015, 1399, 1.

20. Fernandes, A. R.; De Souza, P. S.; De Oliveira, A. E.; Chaves, A. R. ;J. Braz. Chem. Soc. 2018, 29, 695.

21. Lehotay, S. J.; Mastovska, K.; Lightfield, A. R.; Nuñez, A.; Dutko, T.; Ng, C.; Bluhm, L. ;J. Chromatogr. A 2013, 1313, 103.

22. Pinto, M. A. L.; Queiroz, M. E. C. ;Sci. Chromatogr. 2015, 7, 101.

23. Bordin, D. C. M.; Alves, M. N. R.; de Campos, E. G.; De Martinis, B. S. ;J. Sep. Sci. 2016, 39, 1168.

24. Miyazaki, S.; Morisato, K.; Ishizuka, N.; Minakuchi, H.; Shintani, Y.; Furuno, M.; Nakanishi, K. ;J. Chromatogr. A 2004, 1043, 19.

25. Ota, S.; Miyazaki, S.; Matsuoka, H.; Morisato, K.; Shintani, Y.; Nakanishi, K. ;J. Biochem. Biophys. Methods 2007, 70, 57.

26. Hsieh, H.-C.; Sheu, C.; Shi, F.-K.; Li, D.-T. ;J. Chromatogr. A 2007, 1165, 128.

27. Mafra, G.; Spudeit, D.; Brognoli, R.; Merib, J.; Carasek, E. ;J. Chromatogr. B 2018, 1102–1103, 159.

28. Desilets, C. P.; Rounds, M. A.; Regnier, F. E. ;J. Chromatogr. A 1991, 544, 25.

29. Guardia, M. de la; Esteve-Turrillas, F. A. Handbook of smart materials in analytical chemistry. Volume I; Guardia, M. de la; Esteve-Turrillas, F. A., Eds.; 1st ed.; Wiley: Chichester, West Sussex, PO19 8SQ, UK, 2019.

30. Alshali, R. Z.; Salim, N. A.; Satterthwaite, J. D.; Silikas, N. ;J. Dent. 2015, 43, 1511.

31. Bradford, M. M. ;Anal. Biochem. 1976, 72, 248.

32. ANVISA Resolução da Diretoria Colegiada N° 166, de 25 de Julho de 2017 https://www.in.gov.br/materia/-/asset_publisher/Kujrw0TZC2Mb/content/id/19194581/do1-2017-07-25-resolucao-rdc-n-166-de-24-de-julho-de-2017-19194412 (accessed Jun 20, 2021).

33. Veronica de Lima, V.; Maria Cassiano Quezia Bezerra Cass, N. ;Quim. Nov. 2006, 29, 72.

34. D'Avila, F. B.; Pereira, A. G.; Salazar, F. R.; Ferreira, P. L.; Salazar, C. R.; Limberger, R. P.; Fröehlich, P. E. ;J. Pharm. Biomed. Anal. 2015, 103, 67.

35. Paulsen, R. B.; Wilkins, D. G.; Slawson, M. H.; Shaw, K.; Rollins, D. E. ;J. Anal. Toxicol. 2001, 25, 490.

36. Pereira, A. G.; D'Avila, F. B.; Ferreira, P. C. L.; Holler, M. G.; Limberguer, R. P.; Froehlich, P. E. ;Chromatographia 2016, 79, 179.

37. Pereira, A. G.; D'Avila, F. B.; Ferreira, P. C. L.; Holler, M. G.; Limberger, R. P.; Fröehlich, P. E. ;Anal. Methods 2014, 6, 456.

38. Scheidweiler, K. B.; Huestis, M. A. ;Anal. Chem. 2004, 76, 4358.

39. Stat-Ease, Inc.; Design-Expert®, version 13; USA, 2021.

40. Zhou, W.; Yang, S.; Wang, P. G. ;Bioanalysis 2017, 9, 1839.

41. Steiner, D.; Krska, R.; Malachová, A.; Taschl, I.; Sulyok, M. ;J. Agric. Food Chem. 2020, 68, 3868.

42. Mozaner Bordin, D. C.; Alves, M. N. R.; Cabrices, O. G.; De Campos, E. G.; De Martinis, B. S. ;J. Anal. Toxicol. 2014, 38, 31.

43. Montesano, C.; Simeoni, M. C.; Curini, R.; Sergi, M.; Lo Sterzo, C.; Compagnone, D. ;Anal. Bioanal. Chem. 2015, 407, 3647.

44. Fernández, P.; Morales, L.; Vázquez, C.; Lago, M.; Bermejo, A. M. ;J. Appl. Toxicol. 2008, 28, 998.

45. Dulaurent, S.; El Balkhi, S.; Poncelet, L.; Gaulier, J. M.; Marquet, P.; Saint-Marcoux, F. ;Anal. Bioanal. Chem. 2016, 408, 1.

46. Ellefsen, K. N.; Concheiro, M.; Pirard, S.; Gorelick, D. A.; Huestis, M. A. ;Forensic Sci. Int. 2016, 260, 95.

47. Melanson, S. E. F.; Petrides, A. K.; Khaliq, T.; Griggs, D. A.; Flood, J. G. ;J. Appl. Lab. Med. 2020, 5, 935.

48. García-Valverde, M. T.; Soriano, M. L.; Lucena, R.; Cárdenas, S. ;Anal. Chim. Acta 2020, 1126, 133.

Restrict access material for paper spray ionization mass spectrometry: A versatile tool for catecholamines and antidepressants determination in plasma samples

Aline Rosa Fernandes[1], Ricardo Alves Bernardo[1], Jean Carlos Pereira Sousa[1], Raphaela de Castro Georg2, Boniek Gontijo Vaz[1], Andréa Rodrigues Chaves[1]*

[1] Laboratório de Cromatografia e Espectrometria de Massas - Instituto de Química, Universidade Federal de Goiás, 74690-900, Goiânia, GO, Brazil.

2 Laboratorio de Bioquímica de Microorganismos – Instituto de Ciências Biológicas, Universidade Federal de Goiás, 74690-900, Goiânia, GO, Brazil.

*andrea_chaves@ufg.br

* +55 62 3521 1016 R251

Address reprint requests to Andréa Rodrigues Chaves, Laboratório de Cromatografia e Espectrometria de Massas - Instituto de Química, Universidade Federal de Goiás, 74690-900, Goiânia, GO, Brazil.

TEL +55 62 3521 1016 R251

andrea_chaves@ufg.br

Abstract: In the present study, a fast, accurate and reliable mass spectrometry methodology without any sample pretreatment step and low solvent consumption for catecholamines and antidepressants determination in plasma samples is reported. An internal surface reversed-phase restrict access material was synthesized onto a paper surface and applied to the extraction of dopamine, epinephrine, diazepam, nortriptyline, and fluoxetine from human plasma following direct desorption by paper spray mass spectrometry (PSI-MS). The developed methodology showed to be accurate, precise and linear in a concentration range from the limit of quantification to 1000 ng mL^{-1}. The limits of quantification for all analytes ranged from 1.4 to 5.3 ng mL^{-1}. According to the results, the developed methodology could be a powerful tool for drug levels monitoring in clinical or urgent care.

Keywords: Biomarkers; antidepressants; human plasma; restrict access material; paper spray ionization.

1. INTRODUCTION

The analysis of catecholamines and antidepressants in biological matrices has been increasing in recent years [1,2]. Catecholamines levels in biological fluids have been related to diseases, such as Parkinson [3], Alzheimer [4], schizophrenia [5], and hyperactivity [6]. Antidepressants are routinely used for psychiatric disorders treatment, and their prescription has been increasing in the last years. Monitoring antidepressants levels methods have been widely reported in the literature [7–9] due to the needing of a clinical therapeutic monitoring for more effective treatment and also to prevent possible adverse effects, like addiction, sedation, ataxia, vertigo, and headache [10]. Their levels were investigated by spectrophotometry [11], Fourier transform infrared spectroscopy (FT-IR) [12], Raman spectroscopy [13], chromatography [14], and fluorescence [15]. However, these analyses may suffer from interferences from the matrices and false-positive results [16].

Paper spray ionization mass spectrometry (PSI-MS) first reported by Cooks et al., 2010, is a straightforward and versatile ion source [17]. It consists of the application of a high voltage (≈ 4 kV) onto the triangular shaped paper that contains the sample. Many modifications in the paper surface have been reported aiming the enhancement of analyte signal and desorption, such as molecularly imprinted polymers [18], graphene oxides [19], carbon nanotubes [20], and labor of paraffin canals [21]. Nevertheless, for the best of our knowledge, no study of paper modified with restricted access material (RAM) has been reported.

The RAM is a class of biocompatible materials first developed by Desilets and co-workers in 1991 [22]. In general, RAM is derived from silica being widely used coupled with

a chromatographic technique for separation of low molecular weight compounds in complex matrices. The commercial phases available include hydrophobic phase of immobilized protein [23], internal surface reversed-phase (ISRP) [24], semipermeable surfaces (SPS) [25], shielded hydrophobic phases (SHP) alkyl-diol silica (ADS) and mixed function phases [22,26]. Lima and co-workers, 2006 [26], developed four different chromatographic columns with RAM phase from bovine serum albumin (BSA) and commercial stationary phases (e.g. octyl silane, octadecyl silane, phenyl silica, and cyan silica) for drug analysis in plasma. According to the authors, the protein exclusion for all columns evaluated was greater than 90%, no matter the injected volume sample [26]. Chaves and co-workers [23], developed a capillary filled with RAM phase based on silica C18 covered with BSA. The developed phase was applied to sulphonamide determination in milk samples by in-tube solid phase microextraction coupled with liquid chromatography with UV detection.

In the present study, a restrict access material was synthesized onto a paper surface and used as substrate for paper spray ionization mass spectrometry. The substrate was evaluated to the extraction of dopamine, epinephrine, diazepam, nortriptyline and fluoxetine from human plasma following by direct analyte desorption into mass spectrometer. The PSI-MS developed method was evaluated for clinical purposes.

2. EXPERIMENTAL SECTION

2.1. Materials

Epinephrine, dopamine hydrochloride, nortriptyline hydrochloride, diazepam, and fluoxetine hydrochloride were all acquired from the United States Pharmacopeia reference standard. Glycidyl methacrylate (GMA) 97%, 4,4'-bipyridine 98%, (3-aminopropyl)triethoxysilane (APTES) 99%, Whatman cellulose chromatography paper (grade 1 Chr, 0.18 mm thick) and solid phase extraction (SPE) cartridges (Silica C18) were acquired from Sigma Aldrich (Saint Louis, Missouri, USA). Silica gel was acquired from Merck (Darmstadt, Germany). Copper (II) bromide 99% ($CuBr_2$), copper (I) bromide 98% (CuBr), and ethylenediaminetetraacetic acid disodium salt dihydrate 98.5% (EDTA) were acquired from Synth (Diadema, Brazil). Methanol HPLC grade (purity ≥ 99.9%), and isopropanol HPLC grade (purity ≥ 99.9%) were acquired from J.T. Baker (Phillipsburg, USA).

The plasma sample from a patient receiving antidepressant medication (fluoxetine) was collected 8 hours after fluoxetine intake drug administration and kept in a -20 °C freezer until the analysis. The volunteer signed a free consent form to be part of the study. Blank plasma samples were collected from healthy volunteers and kept for a week at -20 °C and one freezing

drowning. The samples were collected following the ethics principles and had been approved by the Universidade Federal de Goiás' ethical committee (Comitê de Ética em Pesquisa (CEP) 056/13).

2.2. RAM phase preparation

The GMA immobilization onto silica C18 and silica gel was adapted from Wang and co-workers, 2014 protocol [24]. To this, silica was completely removed from the SPE commercial cartridge, and a solution was prepared using 0.5 g of silica (C18 or gel), 468 µL of GMA, 0.5 mg of CuBr, 0.5 mg of $CuBr_2$, and 10 mg of 4-4'-bipyridine in 10 mL of isopropanol. Therefore, the solution was kept in a nitrogen atmosphere under sonication for deoxygenation, and then, kept at 40 °C for 24 hours with magnetic stirring at 600 rpm. Thus, the modified silica particles were filtered and washed with EDTA 0.3 mol L^{-1} solution to remove Cu^{+} and Cu^{2+} residual ions.

2.3. Paper coating with RAM phase

The paper coating process was performed as described in our previous study [19]. Chromatography paper was cut in a triangular shape (1.5 cm edge) using CUTOK DC plotter (Hefei CNC Equipment Co. – Hefei, China). The triangular papers were immersed in a methanolic solution of RAM phase (5 wt.%), and then, an APTES solution (3 wt.%) was added under magnetic stirring at 600 rpm. The system was kept at this condition overnight (24 hours). Therefore, the triangular papers were dried at ambient conditions (22° C) and washed with methanol to remove synthesis residues. After that, the surface modified papers were once again dried at ambient conditions and stored in a dried atmosphere until their use.

2.4. LC-MS analysis

A method using liquid chromatography with mass spectrometer detector was developed and used as standard method to compare the proposed PSI-MS alternative method. The chromatographic analyses were performed in a Shimadzu LC-20A chromatographer with UV detector Shimadzu SPD-20A at 230 nm wavelength using Phenomenex Luna C-18 (5 µm, 150 x 4.6 mm) column. The mobile phase consisted of acetonitrile:water at 36:64 volume ratio, containing 0.01% of formic acid. The chromatographic assays were performed in 10 minutes, at 500 µL min^{-1} flow, with an oven temperature of 35° C.

The mass spectrometer used in LC-MS assays was Bruker micrOTOF-Q III (Bruker Daltonik GmbH, Bremen, Germany) with software Data Analysis 4.2. The experiments were

performed in positive mode, with sheath gas flow of 5 L min^{-1}, electrospray ionization (ESI) source temperature at 280° C, 0.5 bar of nebulizer pressure, 2.8 kV of capillary voltage.

2.5. PSI-MS analysis

The PSI-MS analyses were performed using the LCQ Fleet (Thermo Fisher Scientific, San Jose, CA, USA) equipment with software Thermo Tune Plus. The PSI-MS assays were performed in positive mode with no sheath gas, capillary temperature at 275° C, 3 kV were applied to triangular paper, the capillary voltage at 10 V, spray voltage at 4 V, tube lens voltage at 50 V. The spiked plasma samples (20 µL) were dropped over the paper surface, then left to dry under ambient condition (22 °C) for 5 minutes and positioned at 5 mm distance from the mass spectrometer inlet [27]. Therefore, 20 µL of methanol was dropped over the paper to form the electrolytic spray.

2.6. Bradford test

Aiming to evaluate the protein exclusion efficiency of the RAM developed phase, the plasma samples before and after the extraction process were submitted to the well establish Bradford test [28]. The Bradford test was performed in Pharmacia Biotech Spectrophotometer UV Ultrospec 2000, at the Instituto de Ciências Biológias of Universidade Federal de Goiás.

2.7. Analytical assays

To ensure that the proposed methodology described here is suitable for the intended use and to evaluate the reliability of the data produced, some analytical parameters were evaluated. For this purpose, blank plasma samples were spiked with standard analytical solutions of epinephrine, dopamine at 10, 600, 1000 ng mL^{-1}, and diazepam, nortriptyline, and fluoxetine at 10, 500 and 1000 ng mL^{-1}. Since the epinephrine and dopamine are endogenous catecholamines, the quantification was performed by standard addition method.

The linearity for the RAM-PSI-MS method was evaluated through the linear regression in the analytical curves in replicate (n = 5), with a range from LOQ to 1000 ng mL^{-1} for all analytes. The limit of detection (LOD) was experimentally evaluated with a diluted solution at the lowest concentration where the analytical response can be differentiated from the signal/noise ratio (S/N) (≈ 3 x S/N). The limit of quantification (LOQ) was experimentally evaluated with a diluted solution at the lowest concentration where the analytical response can be quantified with accuracy and precision below 15% (≈ 10 x S/N) is three times the signal/noise ratio.

The percentage recovery (%Recovery), intraday precision and accuracy were evaluated as the percentage coefficient of variation (%C.V.) and the percentage error (%Er), respectively. As standardized by Food and Drug Administration (FDA) [29], precision and accuracy must be lower than 15%.

3. RESULTS AND DISCUSSION

3.1. RAM phase preparation

The silica chemically bounded to octadecyl silane group, C18, is the most used reverse phase in sample pre-treatment and chromatographic separations. In 2014, Wang and co-workers [24] proposed a new RAM reverse phase based in surface-initiated atom transfer radical polymerization (SI-ATRP), where the initiator GMA was immobilized onto silica surface and then, an epoxy group from GMA is hydrolyzed to diol, creating an external hydrophilic layer that forms a diffusion barrier for proteins. In this RAM phase, the internal layer is hydrophobic due to octadecyl silane groups, which allows the RAM phase being used as a reversal phase for small hydrophobic molecules. Therefore, the RAM phase has a second surface and belongs to the ISRP support group.

The preparation of ISPR materials consists in the following procedures: (a) silica surface amination, (b) activation of amino-propylated silica with 1,6-diisocyanatehexane, (c) silica modification with alcohols polyvinylics, and (d) deactivation of isocyanate groups using hexylamine. Xu and co-workers prepared a RAM phase using ATRP method in five steps: (1) silica surface amination, (2) initiator immobilization, (3) insertion of polystyrene-divinylbenzene to form hydrophobic layers, (4) insertion of GMA group to form hydrophilic layers, and (5) epoxy hydrolysis in GMA chain [24]. In the present study, the proposed method has only three steps. First, the initiator immobilization onto the silica surface. Second, the insertion of the GMA group in the silica external surface via SI-ATRP. Third, epoxy hydrolysis to produce diol groups. This method is reported as simple and easy to be performed. Therefore, it was chosen for the RAM preparation into the paper surface for the RAM-PSI-MS method.

3.2. Chemical composition of RAM phase

The chemical composition of silica C-18 and RAM prepared as mentioned in the Experimental Section were evaluated by FT-IR. Figure S-1 in the supplementary material exhibits the infrared spectra for the silica C-18 and the silica modified with RAM phase. Comparing both spectra, the presence of a peak in 1730 cm^{-1} is observed, which is characteristic of vibrations of carbonyl stretch, indicating that GMA was successfully bonded to silica.

3.3. RAM-PSI-MS method

The RAM phase includes the extraction mechanisms of size exclusion and partition. In other words, proteins and other macromolecules present in plasma are excluded and interact only with the external surface of the RAM phase. Furthermore, the analytes interact with the hydrophobic interior of the extractive phase, and then, are desorbed with an appropriated solvent.

To evaluate RAM efficiency for the protein exclusion in PSI-MS analysis, a previous test was evaluated using plasma blank samples spiked with dopamine standard solution (1 mg L^{-1}). This solution was added into the conventional chromatographic paper, the paper coated with RAM prepared in silica C-18, and paper coated with RAM prepared in silica gel.

Figure 1 shows the PSI-MS spectra for the dopamine solution in plasma (1 mg L^{-1}). When the conventional chromatographic paper is used, the ions with mass-to-charge ratio (*m/z*) above 432 were predominant. In this substrate, the analyte signal (dopamine *m/z* 154) is suppressed by the other endogenous compounds in plasma. In the mass spectrum of RAM in silica gel, the secondary ions are the most intense. It is possible to note that molecules with higher *m/z* were excluded in the extraction process, and also the dopamine was detected. In the mass spectrum of RAM in silica C-18, the dopamine was the most abundant ion in the spectrum, and in the region with higher *m/z* ions, they were less intense.

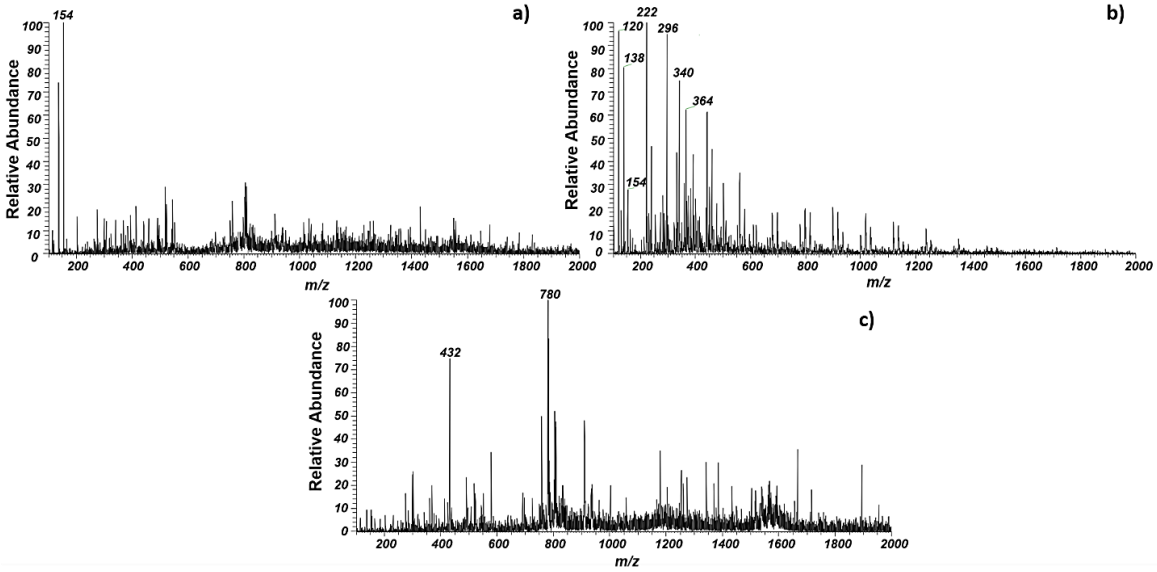

Figure 1. PSI-MS spectra for dopamine in plasma (1 mg L^{-1}) using RAM in silica C-18 (a), RAM in silica gel (b), and conventional chromatographic paper (c).

When the analysis is performed with the conventional paper without any coating, it is impossible to detect minor molecules in a complex matrix, such as plasma, by PSI-MS technique, even when the analyte concentration is considerably high (1 mg L^{-1}). Furthermore, the paper coated with RAM from silica C-18 presented higher endogenous compound exclusion and higher extraction efficiency, leading to better signal response in PSI-MS compared to the conventional paper and the RAM from silica gel. Therefore, the first one was chosen to develop and partial validation of RAM-PSI-MS method to quantify the dopamine, epinephrine, diazepam, nortriptyline, and fluoxetine in human plasma as a concept prove of the proposed method.

3.4. Bradford test

The protein quantification is performed through an analytical curve, using different human albumin solution concentration as a protein source. The analytical curve for protein quantification in the present study is presented in Equation 1.

$$Y = \frac{x-0.0809}{0.0423} \,.\, 10\ \mu g\ mL^{-1} \qquad \textbf{Equation 1}$$

where, y is the protein concentration in the sample, and x is the absorbance in the spectrophotometer.

The Bradford test was performed using plasma before and after the extraction process with RAM phase. The plasma sample, before the extraction, had a protein content of 80.34 µg mL^{-1}, and after the extraction procedure, 79.46 µg mL^{-1}. According to this, the RAM phase presented an average protein exclusion of 98.9%.

3.5. Catecholamine analysis in human plasma

The analytical curve was plotted using the abundance of *m/z* 137 produced from the collision-induced fragmentation of dopamine ($[M+H]^+$ m/z 154) versus its concentration. The same methodology was performed for epinephrine molecules.

The protonation of the most basic site of dopamine, a primary amine, produces the ion *m/z* 154. When the dopamine is submitted to fragmentation conditions, a neutral loss of NH_3 occurs due to an inductive cleavage, producing the ion *m/z* 137, as presented in Figure S-2, and the MS/MS spectrum is presented in Figure S-3 in the supplementary material.

The protonation of the hydroxyl group in epinephrine molecule produces the ion *m/z* 184, followed by a neutral loss of H_2O due to an inductive cleavage, producing the ion *m/z* 166, as shown in Figure S-4, and the MS/MS spectrum is presented in Figure S-5 in the supplementary material.

The linearity of the proposed method was evaluated using blank samples of plasma spiked with catecholamines (dopamine, epinephrine), or antidepressants (diazepam, nortriptyline, fluoxetine) at 10, 200, 400, 600, 800 and 1000 ng mL^{-1} (n = 5). The concentration range evaluated showed to be linear, with R^2 greater than 0.999 for catecholamines, and greater than 0.993 for antidepressants analyses. Diluted solutions were evaluated to determine the experimental LOD and LOQ. The linear regression parameters, R^2, and limits of detection and quantification are presented in Table 1.

Table 1. Analytical curve parameters for all analytes by RAM-PSI-MS/MS method

Analyte	Slope	Intercept	R^2	LOD ng mL^{-1}	LOQ ng mL^{-1}
Dopamine	0.1406 ± 0.0013	2.0528 ± 0.1328	0.9998	1.8	5.3
Epinephrine	0.228 ± 0.0009	7.3852 ± 0.6158	0.9998	1.2	3.6
Nortriptyline	10.809 ± 0.4700	- 339.79 ± 3.8979	0.9930	0.6	1.8
Diazepam	10.895 ± 0.0422	- 254.07 ± 3.9359	0.9929	0.5	1.4
Fluoxetine	9.2412 ± 0.3367	- 332.66 ± 2.5270	0.9943	0.7	2.0

The most reported method for the determination of dopamine in plasma samples is the LC-MS/MS. As comparative purposes, this methodology was employed using the same solutions evaluated in the RAM-PSI-MS method. The better chromatographic conditions were achieved using a column Phenomenex Luna C-18 (5 µm, 150 x 4.6 mm), the mobile phase consisted in acetonitrile:water with 0.01% of formic acid (27:63 volume ratio) and wavelength in 230 nm. In this condition, the retention time for dopamine was 2.8 minutes. The experimental conditions in the mass spectrometer were adjusted to the LC flow rate. The chromatogram and the respective MS/MS spectrum are presented in Figure 2.

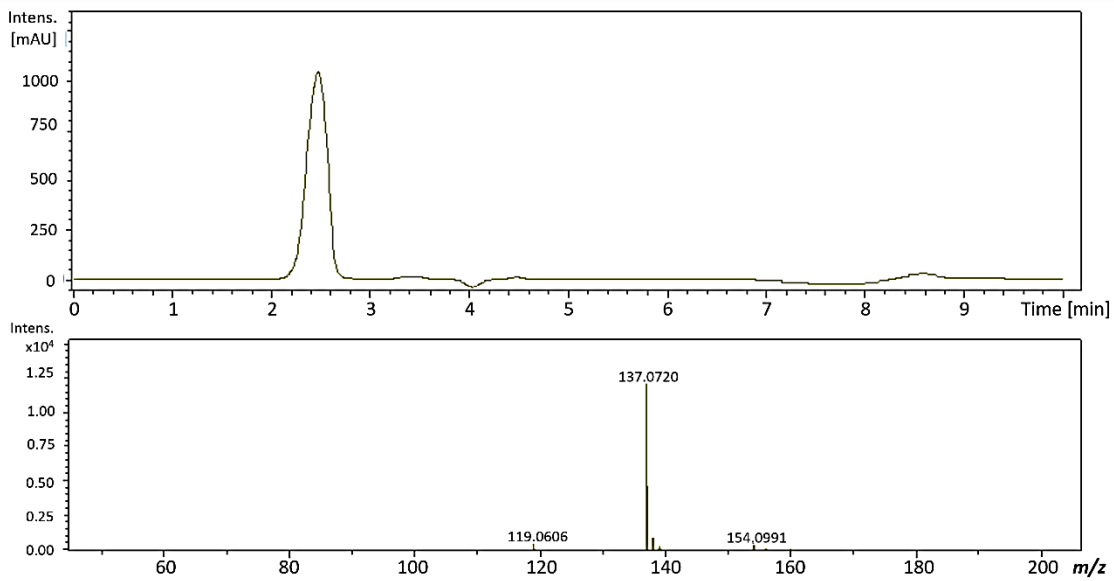

Figure 2. Chromatogram in 230 nm and ESI-MS/MS spectrum for dopamine.

The parameters for dopamine analytical curve by LC-MS/MS and RAM-PSI-MS are presented in Table 2.

Table 2. Intraday precision (%C.V.), accuracy (%Er), and relative recovery of LC-MS/MS and RAM-PSI-MS methods for dopamine analysis

	Concentration ng mL^{-1}	**%C.V.**	**%Er**	**%Recovery**
	10	13.2	14.9	85.6
LC-MS/MS	600	8.4	1.2	96.9
	1000	5.3	-1.2	99.9
	10	5.1	9.6	95.6
RAM-PSI-MS	600	2.6	1.6	97.0
	1000	1.7	1.7	99.1

3.6. Antidepressant analysis in human plasma

The determination of antidepressants is particularly important both for therapeutic monitoring and toxicological analysis. The RAM-PSI-MS was submitted to antidepressants analyses in plasma. To this study, three antidepressants of different classes were chosen:

nortriptyline, fluoxetine, and diazepam. The analytical curve for all antidepressant analyses were plotted as already described to catecholamine analysis, in the same concentration range.

The protonation of the secondary amine in the nortriptyline produces the ion *m/z* 264. This ion suffers an inductive cleavage producing the ion *m/z* 233 and a primary amine, as shown in Figure S-6, and the MS/MS spectrum is presented in Figure S-7 of supplementary material.

The diazepam has in its structure a chlorine atom, producing in the mass spectrum two peaks with a *m/z* difference of 2 Da, and the second peak (*m/z* 287) is 33% of the first one due to the isotopic pattern of chlorine. The protonation of the most basic site of diazepam produces the ions *m/z* 285 and 287. When diazepam is submitted to fragmentation conditions, a neutral loss of CO occurs due to an inductive cleavage that produces the fragment ion *m/z* 257. This ion also fragmented by sigma dissociation, producing radical chlorine and radical ion *m/z* 222 as presented in Figure S-8, and the MS/MS spectrum is presented in Figure S-9 of supplementary information.

The reaction between fluoxetine and formic acid produces the ion *m/z* 310. The fragmentation of the protonated fluoxetine produces two major fragments, the ion *m/z* 279 from the neutral loss of a primary amine, and the ion *m/z* 148 from a neutral loss of a $C_7H_5F_3O$ molecule. Figures S-10, S-11 and S-12 of supplementary information shows the fragmentation mechanism and MS/MS spectrum for fluoxetine.

The linearity of RAM-PSI-MS method for antidepressant analysis was evaluated using analytical curves plotted with the intensity of the most abundant fragment ion in the MS/MS experiment versus their concentration (10, 200, 400, 600, 800 and 1000 ng mL^{-1}) in replicate (n = 5). The linear regression parameters for antidepressant analyses are presented in Table 1.

3.7. Analytical assays for antidepressant analyses

According to the FDA, accuracy, and precision below 15%, and recovery values between 80 and 120% are desirable. The intra-day accuracy, precision, and recovery for catecholamines and antidepressants analyses in human plasma were calculated according to equations 1, 2, and 3 (Table 3).

Table 3. Precision (%C.V.), accuracy (%Er.), and relative recovery values for dopamine, epinephrine, nortriptyline, diazepam, and fluoxetine analysis using the RAM-PSI-MS/MS method

	Concentration ng mL $^{-1}$	%C.V.	%Er	%Recovery
Dopamine	10	5.1	9.6	95.6
	600	2.6	1.6	97.0
	1000	1.7	1.7	99.1
Epinephrine	10	5.8	1.9	97.5
	600	1.2	0.1	98.4
	1000	0.9	-0.8	97.5
Nortriptyline	10	13.6	10.6	98.0
	500	2.3	6.5	92.5
	1000	6.4	1.7	101.4
Diazepam	10	2.3	7.4	88.2
	500	0.9	4.6	93.6
	1000	1.0	0.6	98.4
Fluoxetine	10	1.4	12.5	92.9
	500	2.3	8.6	93.7
	1000	5.6	5.0	101.8

Shen and co-workers developed a method for nortriptyline determination in rat plasma using liquid-liquid extraction followed by liquid chromatography coupled with mass spectrometry (LLE-LC-ESI-MS) [31]. The concentration ranged from 10 to 1000 ng mL^{-1}, and LOQ at 10 ng mL^{-1}. The RAM-PSI-MS method had a LOQ six times lower than reported by Shen. Furthermore, the Shen's method spends 12.5 mL of solvent for each LC run, and 12.5 minutes, while the PSI technique is fast (about 30 seconds) and uses 20 µL for each MS run without any sample pretreatment. Therefore, the method proposed in this study showed to be faster, more sensitive and with lower solvent consumption and less residual generation when compared to the studies mentioned above.

In 2013, Liu and co-workers proposed a new technique of enhancement based in magnetic core-mesoporous shell microspheres with C8-modified interior pore-walls for the determination of diazepam in rat plasma by LC-MS [32]. They obtained a LOQ at 3 ng mL^{-1}

and LOD 0.46 ng mL^{-1}. Besides that, Liu and Shen used liquid chromatography, which makes their methods much longer and with higher solvent waste.

Oliveira and co-workers developed a liquid microextraction with two phases using hollow fiber and derivatization for gas chromatographic analysis of fluoxetine and nortriptyline in human plasma [33]. Their LOD and LOQ were 3 and 10 ng mL^{-1} for fluoxetine, while in this study 0.66 and 2.01 ng mL^{-1} was found.

Besides all the good analytical parameters performance, the proposed methodology presented here was conduct in a few seconds (less than 40 s), and the solvent consumption is insignificant when compared to chromatographic methods, which implies directly in cost reduction. The developed methodology presented promising results and should be fully validate to future clinical applications.

However, to demonstrate the developed methodology application, plasma sample from fluoxetine user patient was analyzed as described in the RAM-PSI Analysis topic in the Experimental Section. The full scan and MS/MS spectra are presented in Figure S-13 of supplementary information. In the full scan (Figure S-13 a), the fluoxetine peak (*m/z* 310) and another endogenous compounds with low molecular weight can be seen. It is important that no molecules with *m/z* higher than 369 were significantly extracted in the RAM phase, which means that the exclusion property of this extractive phase was successfully highlighted, the obtained spectrum were similar to those obtained by spiked plasma samples. The analyses were performed in replicate (n = 5) and the fluoxetine plasma concentration was estimated by analytical curve equation presented in Table 1. The concentration of fluoxetine in plasma was found at 74.3 ng mL^{-1}. According to Nixdorf and co-workers [30], the maximum concentration of fluoxetine in plasma occurs after 6-8 hours and it can ranges from 30 to 500 ng mL^{-1}. Therefore, the methodology presented in this study comes out as a fast and reliable tool for determination of catecholamines and antidepressants in complex matrices, such as plasma.

4. CONCLUSION

The RAM successfully excluded the proteins present in human plasma, at an exclusion rate of 98.9%, making the analyses more selective for the target analytes, allowing direct mass spectrometry analysis by paper spray mass spectrometry method.

According to the analytical assays, the proposed RAM-PSI-MS method is adequate, both for catecholamines and antidepressants analyses in human plasma, and its accuracy, precision, and recovery are acceptable for FDA. Besides that, the RAM-PSI-MS method

presents a wide linear range and high values for R^2, LOD, and LOQ, coupled to the method's simplicity, low-cost, minor solvent consumption, speed, and efficiency.

Comparing to the LC-MS/MS method for dopamine analysis in human plasma, the LOQ and LOD were estimated at 7.22 and 2.38 ng mL^{-1} respectively, while the RAM-PSI-MS method, these values were 5.34 and 1.76 ng mL^{-1}. Therefore, the new method proposed in this study presents lower detectability, and better accuracy, precision, and recovery values than the classical LC-MS/MS. The RAM-PSI-MS developed method does not need any additional sample pretreatment, using some microliters of solvent (about 20 µL), and is all performed in a few seconds, reducing considerably method cost. The developed methodology has been applied to real sample analysis demonstrating a good perspective to use as routine method for therapeutic drug monitoring of antidepressant drugs.

5. CONFLICTS OF INTEREST

There are no conflicts of interest to declare.

6. ACKNOWLEDGMENT

The authors sincerely thank to Conselho Nacional de Desenvolvimento Científico e Tecnológico (CNPq) and Fundação de Apoio à Pesquisa do Estado de Goiás (FAPEG).

7. REFERENCES

[1] W. Le Fang, L.J. Xia, X. Huang, X.F. Guo, J. Ding, H. Wang, Y.Q. Feng, Highly sensitive determination for catecholamines using boronate affinity polymer monolith microextraction with in-situ derivatization and HPLC fluorescence detection, Chromatographia. 81 (2018) 1381–1389. https://doi.org/10.1007/s10337-018-3592-3.

[2] K. Murtada, F. de Andrés, A. Ríos, M. Zougagh, Determination of antidepressants in human urine extracted by magnetic multiwalled carbon nanotube poly(styrene-co-divinylbenzene) composites and separation by capillary electrophoresis, Electrophoresis. 39 (2018) 1808–1815. https://doi.org/10.1002/elps.201700496.

[3] C.A. Kelm-Nelson, M.A. Trevino, M.R. Ciucci, Quantitative analysis of catecholamines in the Pink1 −/− Rat model of early-onset Parkinson's disease, Neuroscience. 379 (2018) 126–141. https://doi.org/10.1016/J.NEUROSCIENCE.2018.02.027.

[4] X. Pan, A.C. Kaminga, S.W. Wen, K. Acheampong, A. Liu, Catecholamines in Alzheimer's disease: A systematic review and network Meta-analysis, (2019). https://papers.ssrn.com/sol3/papers.cfm?abstract_id=3311844 (accessed May 6, 2019).

[5] T. Hauser, M. Moutoussis, P. Dayan, R. Dolan, F210. The role of catecholamines in information gathering, Biol. Psychiatry. 83 (2018) S320–S321. https://doi.org/10.1016/j.biopsych.2018.02.824.

[6] E. Quansah, T.S.C. Zetterström, Chronic methylphenidate preferentially alters catecholamine protein targets in the parietal cortex and ventral striatum, Neurochem. Int. 124 (2019) 193–199. https://doi.org/10.1016/j.neuint.2019.01.016.

[7] J.A. Caris, A.R. Chaves, M.E.C. Queiroz, Evaluation of solid-phase microextraction using a polythiophene film and liquid chromatography with spectrophotometric detection for the determination of antidepressants in plasma samples, J. Braz. Chem. Soc. 23 (2012) 57–64. https://doi.org/10.1590/S0103-50532012000100009.

[8] A.R. Chaves, B.H.F. Moura, J.A. Caris, D. Rabelo, M.E.C. Queiroz, The development of a new disposable pipette extraction phase based on polyaniline composites for the determination of levels of antidepressants in plasma samples, J. Chromatogr. A. 1399 (2015) 1–7. https://doi.org/10.1016/J.CHROMA.2015.04.027.

[9] A.R. Chaves, F.Z. Leandro, J.A. Carris, M.E.C. Queiroz, Microextraction in packed sorbent for analysis of antidepressants in human plasma by liquid chromatography and spectrophotometric detection, J. Chromatogr. B Anal. Technol. Biomed. Life Sci. 878 (2010) 2123–2129. https://doi.org/10.1016/j.jchromb.2010.06.023.

[10] J. Read, J. Williams, Adverse effects of antidepressants reported by a large international cohort: Emotional blunting, suicidality, and withdrawal effects, Curr. Drug Saf. 13 (2018) 176–186. https://doi.org/10.2174/1574886313666180605095130.

[11] H. Montaseri, H. Khajehsharifi, S. Yousefinejad, UV determination of epinephrine, uric acid, and acetaminophen in pharmaceutical formulations and some human body fluids using multivariate calibration, Quim. Nova. 37 (2014) 1404–1409. https://doi.org/10.5935/0100-4042.20140206.

[12] Z. Gerelkhuu, D. Jung, B. The Huy, S.M. Tawfik, M.L. Conte, E.D. Conte, Y.I. Lee, Highly selective and sensitive detection of catecholamines using NaLuGdF4:Yb3+/Er3+ upconversion nanoparticles decorated with metal ions, Sensors Actuators, B Chem. 284 (2019) 172–178. https://doi.org/10.1016/j.snb.2018.12.135.

[13] C.X. Shi, Z.P. Chen, Y. Chen, Q. Liu, R.Q. Yu, Quantification of dopamine in biological samples by surface-enhanced Raman spectroscopy: Comparison of different calibration models, Chemom. Intell. Lab. Syst. 169 (2017) 87–93. https://doi.org/10.1016/j.chemolab.2017.09.006.

[14] M. V Gorbunova, S. V Gutorova, D.A. Berseneva, V. V Apyari, V.D. Zaitsev, S.G. Dmitrienko, Y.A. Zolotov, Spectroscopic methods for determination of catecholamines: A mini-review, Appl. Spectrosc. Rev. 54 (2018) 631–652. https://doi.org/10.1080/05704928.2018.1470980.

[15] M. Iacomino, M.L. Alfieri, O. Crescenzi, M. D'Ischia, A. Napolitano, Unimolecular variant of the fluorescence turn-on oxidative coupling of catecholamines with resorcinols, ACS Omega. 4 (2019) 1541–1548. https://doi.org/10.1021/acsomega.8b02778.

[16] H. Emms, G. Farah, B. Shine, C. Boot, B. Toole, M. McFadden, L. Lam, Z.Q. Ou, G. Woollard, H. Madhavaram, C. Kyle, A.B. Grossman, Falsely elevated plasma metanephrine in patients taking midodrine, Ann. Clin. Biochem. 55 (2018) 509–515. https://doi.org/10.1177/0004563218755817.

[17] J. Liu, H. Wang, N.E. Manicke, J.M. Lin, R.G. Cooks, Z. Ouyang, Development, characterization, and application of paper spray ionization, Anal. Chem. 82 (2010) 2463–2471. https://doi.org/10.1021/ac902854g.

[18] L.S. Tavares, T.C. Carvalho, W. Romão, B.G. Vaz, A.R. Chaves, Paper Spray Tandem Mass Spectrometry Based on Molecularly Imprinted Polymer Substrate for Cocaine Analysis in Oral Fluid, J. Am. Soc. Mass Spectrom. 29 (2018) 566–572. https://doi.org/10.1007/s13361-017-1853-2.

[19] A.R. Fernandes, R.A. Bernardo, T.C. de Carvalho, B.G. Vaz, A.R. Chaves, Graphene oxides coated paper as a substrate to paper spray ionization mass spectrometry for creatinine determination in urine samples, J. Braz. Chem. Soc. 30 (2019) 1074–1081. https://doi.org/10.21577/0103-5053.20190007.

[20] S. Chiang, W. Zhang, Z. Ouyang, Paper spray ionization mass spectrometry: recent advances and clinical applications, Expert Rev. Proteomics. 15 (2018) 781–789. https://doi.org/10.1080/14789450.2018.1525295.

[21] T.C. Colletes, P.T. Garcia, R.B. Campanha, P. V. Abdelnur, W. Romão, W.K.T. Coltro, B.G. Vaz, A new insert sample approach to paper spray mass spectrometry: A paper substrate with paraffin barriers, Analyst. 141 (2016) 1707–1713. https://doi.org/10.1039/c5an01954k.

[22] C.P. Desilets, M.A. Rounds, F.E. Regnier, Semipermeable-surface reversed-phase media for high-performance liquid chromatography, J. Chromatogr. A. 544 (1991) 25–39. https://doi.org/10.1016/S0021-9673(01)83976-5.

[23] A.R. Chaves, M.E. Costa Queiroz, In-tube solid-phase microextraction with molecularly imprinted polymer to determine interferon alpha 2a in plasma sample by high performance

liquid chromatography, J. Chromatogr. A. 1318 (2013) 43–48. https://doi.org/10.1016/j.chroma.2013.10.018.

[24] C. Wang, M. Li, H. Xu, Y. Wei, Preparation of an internal surface reversed-phase restricted-access material for the analysis of hydrophobic molecules in biological matrices, J. Chromatogr. A. 1343 (2014) 195–199. https://doi.org/10.1016/J.CHROMA.2014.03.074.

[25] H. Xu, C. Wang, Y. Wei, A boronate affinity restricted-access material with external hydrophilic bottlebrush polymers for pretreatment of cis-diols in biological matrices, Chinese Chem. Lett. 29 (2018) 521–523. https://doi.org/10.1016/j.cclet.2017.08.056.

[26] N.M. Cassiano, V. V. Lima, R. V. Oliveira, A.C. de Pietro, Q.B. Cass, Development of restricted-access media supports and their application to the direct analysis of biological fluid samples via high-performance liquid chromatography, Anal. Bioanal. Chem. 384 (2006) 1462–1469. https://doi.org/10.1007/s00216-005-0253-9.

[27] Q. Yang, H. Wang, J.D. Maas, W.J. Chappell, N.E. Manicke, R.G. Cooks, Z. Ouyang, Paper spray ionization devices for direct, biomedical analysis using mass spectrometry, Int. J. Mass Spectrom. 312 (2012) 201–207. https://doi.org/10.1016/j.ijms.2011.05.013.

[28] M.M. Bradford, A rapid and sensitive method for the quantitation of microgram quantities of protein utilizing the principle of protein-dye binding, Anal. Biochem. 72 (1976) 248–254. https://doi.org/10.1016/0003-2697(76)90527-3.

[29] U.S.D. of H. and H. Services, Analytical Procedures and Methods Validation for Drugs and Biologics Guidance for Industry Analytical Procedures and Methods Validation for Drugs and Biologics - Guidance for Industry, 2015. https://www.fda.gov/files/drugs/published/Analytical-Procedures-and-Methods-Validation-for-Drugs-and-Biologics.pdf.

[30] L.A. Marques, T.T. Nakahara, T. Bervelieri Madeira, M. Bortholazzi Almeida, A. Maffei Monteiro, M. de Almeida Silva, E. Carrilho, L.G. Piccoli de Melo, S.L. Nixdorf, Optimization and validation of an SBSE-HPLC-FD method using laboratory-made stir bars for fluoxetine determination in human plasma, Biomed. Chromatogr. 33 (2019) e4398. https://doi.org/10.1002/bmc.4398.

[31] Y. Shen, R.H. Zhu, H. De Li, Y.W. Liu, P. Xu, Validated LC-MS (ESI) assay for the simultaneous determination of amitriptyline and its metabolite nortriptyline in rat plasma: Application to a pharmacokinetic comparison, J. Pharm. Biomed. Anal. 53 (2010) 735–739. https://doi.org/10.1016/j.jpba.2010.04.031.

[32] X. Liu, Y. Yu, Y. Li, S. Ning, T. Liu, F. Li, G. Duan, Restricted access magnetic core-mesoporous shell microspheres with C8-modified interior pore-walls for the determination of

diazepam in rat plasma by LC-MS, Talanta. 106 (2013) 321–327. https://doi.org/10.1016/j.talanta.2012.11.015.

[33] A.F.F. Oliveira, E.C. de Figueiredo, Á.J. dos Santos-Neto, Analysis of fluoxetine and norfluoxetine in human plasma by liquid-phase microextraction and injection port derivatization GC-MS, J. Pharm. Biomed. Anal. 73 (2013) 53–58. https://doi.org/10.1016/j.jpba.2012.04.006.

Journal of the Brazilian Chemical Society

Graphical Abstract (GA)

GA **Figure:**

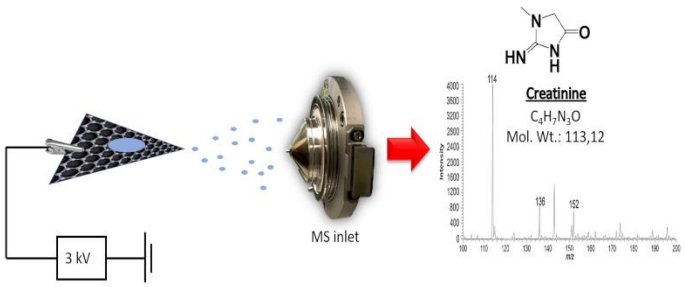

GA Text: A fast and reliable methodology for creatinine determination in urine samples using graphene oxide paper by Paper Spray Ionization Mass Spectrometry.

Graphene oxides coated paper as a substrate to Paper Spray Ionization Mass Spectrometry for creatinine determination in urine samples

Aline Rosa Fernandes[a], Ricardo Alves Bernardo[a], Thays Colletes de Carvalho[a],Boniek Gontijo Vaz[a], Andréa Rodrigues Chaves[a]*

[a]Laboratório de Cromatografia e Espectrometria de Massa (LaCEM), Instituto de Química, Universidade Federal de Goiás. Goiânia, Goiás, Brasil. CEP:74690-900, phone: +55-62-35211094

* andrea_chaves@ufg.br

Abstract

Paper spray ionization (PSI) is a promising analytical tool for direct analysis in mass spectrometry (MS). However, this technique usually uses chromatographic paper, which rarely accomplishes a stable MS signal and could vary with the sample matrix effect. In the present study, the application of graphene oxides (GO) was scrutinized as modifier paper substrate for PSI-MS methods. The developed substrate efficiency was evaluated towards creatinine determination in urine samples. The GO-PSI-MS developed method for creatinine in urine samples showed linearity in the range of 0.1 to 3.4 ppm with $R^2 = 0.9991$. The precision was evaluated and the values were between 1.1 to 6.8% and the accuracy above 96.8%. The LOD and LOQ were 0.05 ppm and 0.17 ppm respectively. The GO-PSI developed was compared to conventional chromatographic paper for PSI-MS methods, and the results showed that the modify paper with GO, bolster method linearity, precision, and LOQ values.

Keywords: paper spray ionization, graphene oxide, creatinine, urine, mass spectrometry.

Introduction

Introduced in 2010 by Wang et al.,[1] paper spray ionization mass spectrometry (PSI-MS) is a new ambient mass spectrometry technique for qualitative and quantitative analysis of complex matrices, presented to be the simplest as possible compared to desorption electrospray (DESI) and direct analysis in real time (DART).[1] Since then, a plethora of publication employing PSI technique has been explored for different applications, mainly to analyze directly samples of blood, urine, saliva, tissues, cell cultures, water, and bacteria.[2-12] Moreover, other elements, such as wick microporous polymers,[13] wooden toothpicks,[14] plant leaves (leaf spray), or other vegetable materials were also employed as both sample and substrate.[15]

The PSI-MS methods involve directly loading the sample onto a triangular paper, which is moistened with an organic solvent and placed in front of a mass spectrometer inlet. The spray of the charged microdroplets is formed by applicating a high voltage (usually 1~5 kV) on the opposite side of the paper tip, and desolvation occurs without any sheath gas.[16] The PSI-MS mechanism of ion formation is similar to electrospray ionization (ESI) process. Briefly, the strong electric field at the sharp tip of the paper results in the formation of an electrolytic spray in Taylor's cone shape, which consists of a plume of charged droplets. After the desolvation, the ions are evaporated to the gas phase.

Some parameters for PSI had been investigated by Cooks and co-workers, [16] and had been previously demonstrated in the literature, such as paper geometry,[17] onset voltage for spray generation efficiency.[18] Despite this, MS signal stability is impaired due to the low conductivity of paper, desorption solvent evaporation on the paper, results in the variance of the produced spray.[16]

Graphene oxide (GO) is a single-atom-thick and two-dimensional carbon material produced by oxidation of graphite, containing oxygen functional groups, such as epoxides, phenol hydroxyls, and carboxylic groups.[19,20] The oxygenated framework of GO not only

facilitates better conductivity and signal stability but also allows noncovalent interaction with diols, amine functional groups, and phenyls in biomolecules through electrostatic interaction, π–π stacking, and hydrogen bonding to enable recognizing of biomolecules with detectable specificity.[21,22] Recently, GO has attracted considerable attention due to it is extraordinary electronic, optical, and thermal properties in comparison to other nanomaterials.[23] Remarkable properties of GO, such as large surface area, good water dispersibility and biocompatibility, facile surface modification and low manufacturing cost, make it a promising material for biotechnology and biosensor application.[24-30] The aforementioned attributes become GO a potential material to modify paper surface for PSI-MS application. Wei and co-workers described in 2018 a procedure to immobilize GO onto nylon membrane to analyze highly toxic disinfectants in liquid samples and fish meat.[29] The authors reported an enhance in selectivity and sensitivity for the MS quantification due to the thin layer of GO. To the best of our knowledge, this is the first report regarding the use of GO chemically immobilized onto the paper surface for PSI-MS methods.

Creatinine is an important biochemical parameter to correctly determine the urinary excretion rate of endogenous and exogenous compounds.[31] Accurate creatinine determination is essential for diagnosis and treatment of renal diseases, thyroid malfunction and muscle disorders.[32-33] The creatinine quantification in urine in clinical laboratories is routinely performed by the Jaffe method or by enzymatic methods, which may suffer from interference like bilirubin, proteins, ketones, and glucose. Thus, it is an essential development efficient, quick and more reliable interference-free methods.[34-35] Besides this, creatinine structure is a good molecule model for mass spectrometric method, due to their good ionization efficiency and well related fragmentation profile in MS/MS experiments.

In this study, GO was chemically immobilized onto a chromatographic paper surface and employed as a substrate for PSI-MS method for creatinine determination in urine samples.

The developed GO-PSI-MS method was also evaluated to health check for creatinine levels in real urine samples.

Experimental

Materials

Creatinine (purity ≥ 98%), uric acid (purity ≥ 99%), ~~and~~ graphite (purity ≥ 99.99%), and potassium bromide (KBr purity ≥ 99%) were obtained from Sigma-Aldrich (St. Louis, Missouri, USA). Methanol (HPLC grade 99.9%, Vetec Fine Chemicals LTDA, Duque de Caxias, RJ, Brazil) was used to moisten the blotter for the ionization process. Formic acid (purity ≥ 98%, Sigma-Aldrich Chemicals, St. Louis, MO, US) was used for the PSI(+)-MS measurements.

Synthesis of graphene oxide

GO was synthesized from natural graphite powder based on Hummer's and Offeman's protocol.[19] Briefly, $KMnO_4$ was slowly added into a mixture of graphite, $NaNO_3$, and H_2SO_4 in an ice bath, then the mixture was transferred to a 35 °C water bath and stirred for about 1 hour. After that, 100 mL water was added, and the suspension was stirred for 30 min at 90 °C to oxidize graphite. Next, water and H_2O_2 (30 wt%) solution were added respectively to terminate the reaction. Then the product was filtered and washed with 1 mol L^{-1} HCl and water two times, respectively. At last, the obtained brown solid was dried at 60 °C for 24 hours.

Preparation of GO-modified paper

Paper triangles were cut from chromatography paper using a CUTOK DC craft cutting plotter (Hefei CNC Equipment Co. Hefei, China). The paper triangles had an angle of 38° and an area of ~60 mm2 (base width = 9 mm, height = 13.2 mm). The paper triangles were immersed in suspension of graphene oxide in methanol 5 wt% under constant magnetic stirring and then

an aminopropyltrietoxysiloxane (APTS) 3 wt% solution of was added. The calculated mass of GO deposited in the paper surface was about 9.15 mg. The wet triangular paper was let dry overnight (24h). Afterward, the papers were washed with 1 mL of methanol and dried at room temperature.

GO-Paper characterization

To evaluate the morphological properties of the developed modified paper a Scanning Electron Microscope (SEM) (Jeol, JSM-6610 Thermo scientific, with EDS). The paper samples were cut in square shape (0.5 x 0.5 cm) and directly analyzed in the equipment without any sample preparation.

Fourier-Transform Infrared Spectroscopy (FT-IR) analysis of the developed graphene oxides and graphite samples was performed by NSS Spectral spectrophotometer PerkinElmer, model Spectrum 400, using a pellet of graphene oxide or graphite sample in KBr (1 wt%) mixture.

Synthetic urine

For the optimization and analytical validation assays, synthetic urine was used. The synthetic urine was prepared by dissolving 3.333 g L^{-1} of urea (CH_4N_2O), 0.050 g L^{-1} of uric acid ($C_5H_4N_4O_3$), 0.177 g L^{-1} of creatinine ($C_4H_7N_3O$), 1.000 g L^{-1} of chloride (Cl^-), 1.000 g L^{-1} of potassium (K^+), 0.025 g L^{-1} of phosphate (PO_4^{3-}), 0.300 g L^{-1} of sulfate (SO_4^{2-}), 0.025 g L^{-1} of calcium (Ca^{2+}), 0.0167 g L^{-1} of magnesium (Mg^{2+}), 0.167 g L^{-1} of sodium (Na^+), 0.025 g L^{-1} of ammonium (NH_4^+), and 0.167 g L^{-1} of carbonates (CO_3^{2-}) in 1 L of ultra-purified water.[36] These salts were obtained from Dinâmica (São Paulo, Brazil).

Paper spray

The procedure for preparation and analysis with GO-paper spray is represented in Figure 1.

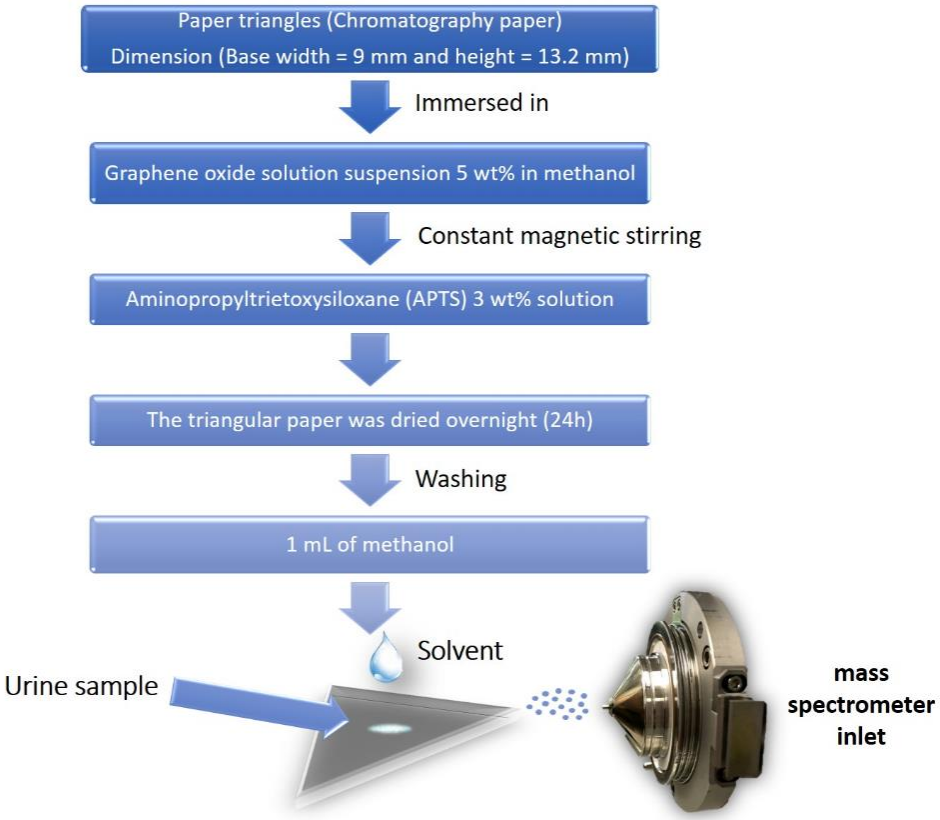

Figure 1. Schematic representation of GO synthesis and GO-PSI-MS arrangement.

Paper spray was performed using a 3D Ion Trap mass spectrometer (LCQ Fleet™, Thermo Scientific™) with the following instrumental parameters. A spray voltage, capillary voltage, and tube lens offset were set at 0, and the capillary temperature at 275 °C, positive ion mode was employed. The paper triangle was held about 5–10 mm from the MS inlet. After, with the aid of a micropipette, 10 µL of urine sample was directly spiked on the GO-paper surface, and then, 10 µL ~~acid solvent~~ (0.1% formic acid in methanol) was added to enhance creatinine ionization.[37] After that, a high voltage (3.0 kV) was applied to the paper to generate an electrospray, and mass spectra were recorded. All assays were performed in triplicate.

Quantitative PS-MS analyses

Samples were prepared using ten standard-spiked synthetic urine samples with concentrations in the range from 0.1 to 3.4 ppm of creatinine. For the analytical curves, was used the intensity of *m/z* 88 creatinine fragment integrated in 30 seconds of spray, both for GO-Modified paper and Chromatographic paper. The limit of detection (LOD) was defined as the minimum detectable concentration of spiked samples with a signal/noise relation upper than three. Similarly, the limit of quantitation (LOQ) was defined for an S/N ratio above ten. Precision, accuracy and absolute recovery were evaluated in three concentration levels (0.1; 1.4 and 3.4 ppm) performed in replicates (n = 5). Accuracy (Acc%) is a measure of how near the concentration experimentally determined is to the theoretical concentration. Its values were calculated by comparing the concentrations of analytes added to the synthetic urine samples and the determined concentration by the analytical curve, as described in Equation 1. The absolute recovery (Rec%) measures the efficiency of an extraction/desorption procedure in an analytical method within a limit of variation. Its values were calculated comparing the peak intensity of the most abundant fragment ion of extracted creatinine from the synthetic urine with those at the same concentration in standard solutions of the analyte, as described in Equation 2.

$$\mathrm{Acc}(\%) = \left[\frac{\mathrm{CDE}-\mathrm{TC}}{\mathrm{TC}}\right].100 \qquad \text{Equation 1.}$$

$$\mathrm{Rec}(\%) = \left[\frac{\mathrm{CDE}}{\mathrm{TC}}\right].100 \qquad \text{Equation 2.}$$

Where, CDE is the concentration determined experimentally, and TC is the theoretical concentration.

Urine samples

Urine samples were collected from healthy volunteers and kept for four days at 2–8 °C

and one freezing drowning. The samples were collected following the ethics principles and had been approved by the University Ethical Committee (CEP 056/13).

Results

The biological fluids, like urine, present many endogenous compounds and salts, which could results in several problems in ESI techniques.

Chemical modification onto paper surface could improve selective and desorption/ionization of PSI-MS methods, as shown in the literature.[38,39]. Thereby, graphene oxides could enhance the conductivity of paper substrate resulting in better MS signal.

Characterization of graphene oxide

The synthesized graphene oxides were characterized by FT-IR analysis. The Fig. 2 shows the FT-IR spectrum of graphite (a) and GO (b), comparing to the graphite FT-IR spectrum, the GO presents the strong characteristic peak at 3318 cm^{-1} for –O-H (υ O-H), 1724 cm^{-1} for –C=O (υ C=O), C-O-C (υ C-O-C) at 1350 cm^{-1} and –C-O (υ C-O) at 1100 cm^{-1} indicating that GO possessed rich oxygen-containing groups including hydroxyl and carboxyl groups (Fig. 1 (b)), while graphite spectrum (Fig. 1 (a)) presents only the 1612 cm^{-1} for aromatic- C=C (υ C=C) and the peak 3318 cm^{-1} for –O-H (υ O-H). The peak at 1612 cm^{-1} for aromatic- C=C (υ C=C) is due to the skeletal vibrations of not oxidized graphitic domains. The data obtained were very similar to those presented by Chen et al.,[40] that developed a cheap, massively scalable, fast and easy method for the preparation of graphene oxide and reduced nanoplatelets of graphene oxide. The basic strategy was the preparation of graphite oxide from graphite through reaction with benzoyl peroxide (BPO), complete exfoliation of GO on graphene oxide sheets, followed by in situ reductions of reduced graphene oxide nanoplatelets.

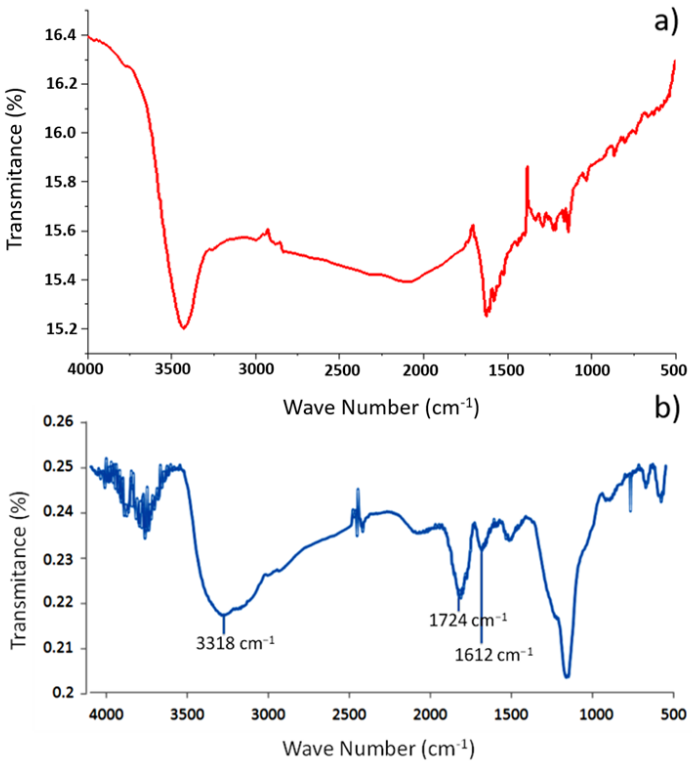

Figure 2. FT-IR spectrum of graphite (a) and graphene oxides samples (b).

A triangular shaped cellulosic paper was modified with GO synthesized as mentioned in experimental section 2.3. The modified GO paper was evaluated by scanning electron microscopy (SEM).

Figure 3 shows the SEM image of the GO-modified paper. It is possible to note in Fig. 3, the presence of small agglomerates of particles immobilized into the pores of the chromatographic paper present in its entire structure, which is not observed in the native chromatographic paper.

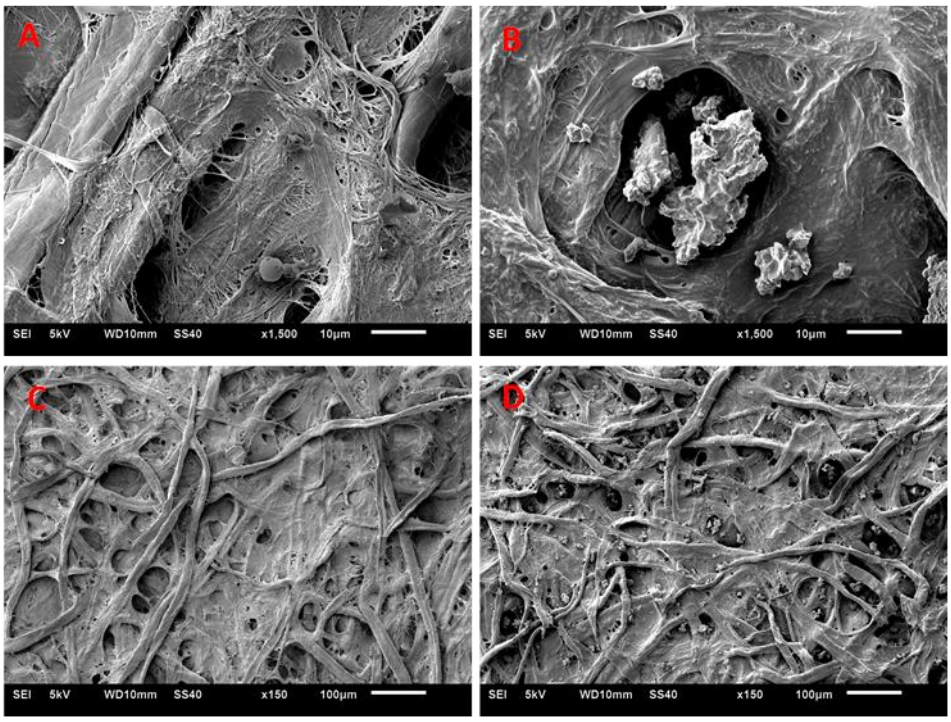

Figure 3. SEM images of Chromatographic paper [A (x1500), C (x150)]; and GO-Modify paper [B (x1500), D (x150)].

Paper spray properties of GO-modified paper

The effects of spray voltage on GO-PSI-MS in positive ion mode were evaluated. Cooks and co-workers reported the use of 4.5 kV to promote the spray formation through PSI-MS.[18] Due to the electronic properties of GO, an adequate efficiency and precision were obtained using 3.0 kV as spray potential. So 3.0 kV was used because satisfactory ionization efficiency was observed.

In order to demonstrate the applicability of GO-modified paper on PSI-MS method, was analyzed creatinine in urine samples. Creatinine is a good model molecule; it presents a well-related MS profile and its structure seems to be interesting for others similar drugs and proteins studies. The comparison between the mass spectrum of GO-modified paper and chromatographic paper in synthetic urine samples demonstrated that the first one increased the stability of spray (Figure 4).

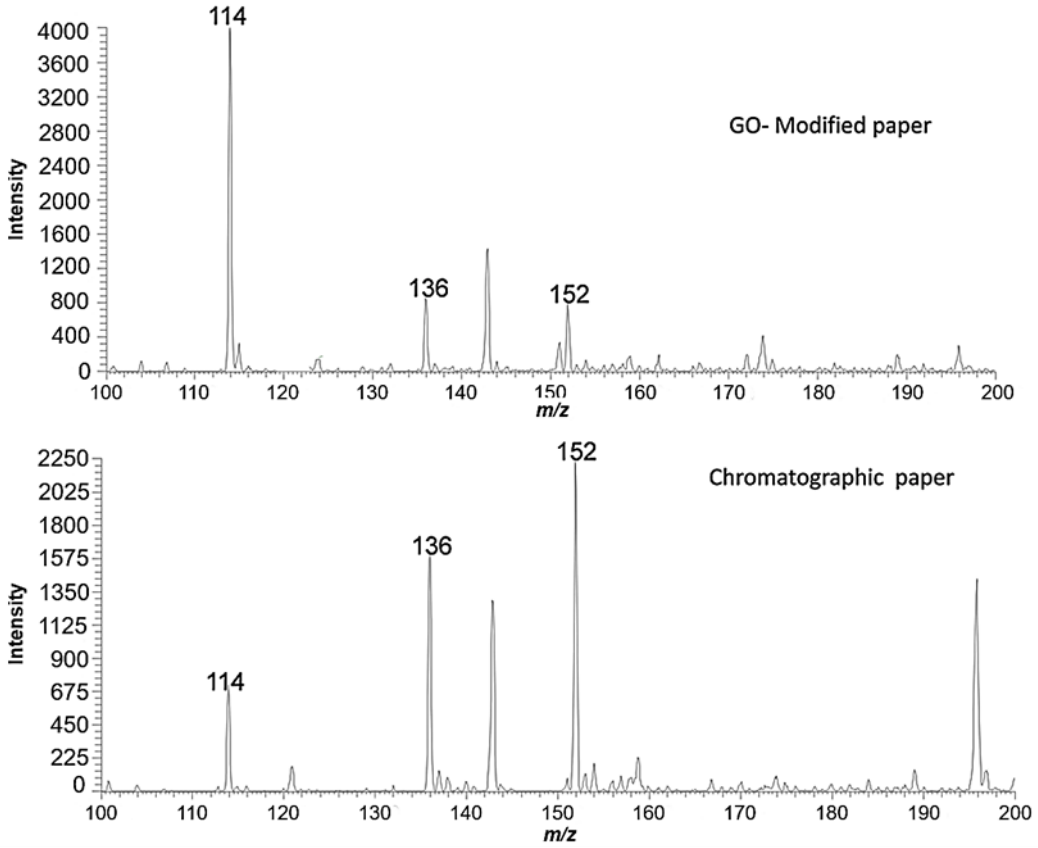

Figure 4. PSI(+)MS of creatinine for GO-Modify paper (A) and chromatographic paper (B). *m/z* 114 = $[M+H]^+$, *m/z* 136 = $[M+Na]^+$; *m/z* 152 = $[M+K]^+$.

PSI ionization is ESI-based, this technique is usually incompatible with traditional buffers and nonvolatile salts,[41–45] with even their small amounts sometimes affecting electrospray stability and significantly suppressing analyte signals, resulting in poor S/N ratios (ionization suppression). Therefore, the salt-induced ionization suppression in PSI-MS cannot be ignored.

Avoiding the salt-induced ionization suppression is very important to achieve highly sensitive PSI-MS quantitative analysis. Although a number of desalting methods have been established for HPLC/ESI-MS, such as on-line electrodialysis, off-line gel filtration, solid-phase extraction, microdialysis, and multistage electrolysis, they are difficult to implement and are seldom used in PSI-MS. Thus, developing new desalting strategies is important for PSI-MS.

Urine is a biological matrix composed largely of ions (Cl^-, K^+, PO_4^{3-}, SO_4^{2-}, Ca^{2+}, Mg^{2+}, Na^+, NH_4^+, CO_3^{2-}).[40] In GO-PSI-MS creatinine analyses, protonated creatinine ion presents a higher intensity compared to its sodium and potassium adducts ion signal, whereas using chromatographic paper protonated creatinine signal intensity is less than half, as shown in Figure 4. The real samples analysis showed the same spectrum profile. The PSI(+) mass spectrum of creatinine in real samples is shown in Figure 5. Note that it was detected as protonated molecule $[M + H]^+$ of *m/z* 114 and as sodium and potassium adducts, $[M+Na]^+$ of *m/z* 136 and $[M+K]^+$ of *m/z* 152, respectively.

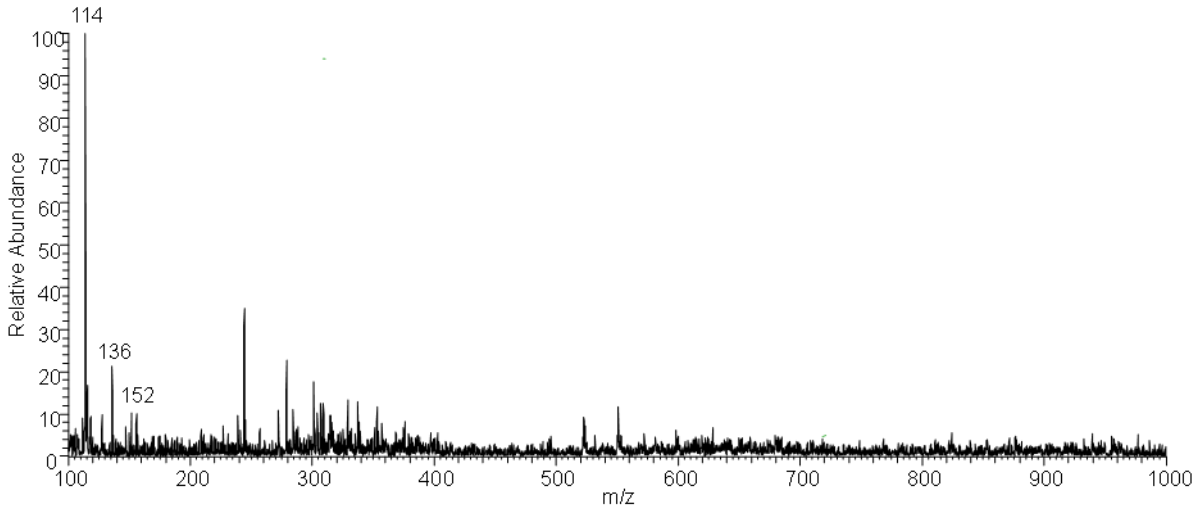

Figure 5. PSI(+)MS of creatinine in urine real samples, *m/z* from 100 to 1000.

Using chromatographic paper the detection ability of the method is reduced due to a decrease in the analyte signal, as result higher detection limit (LOD) could be observed. The ratio of ions, precision, linearity, and quantification may be affected due to the variability of the matrix effect between samples. All of these factors can lead to a false negative in positive samples since the method was developed for creatinine and not for adducts.[44]

The chemical structure of the analyte was confirmed by its fragment ions in Collision Induced Dissociation Experiments (CID) as previously described in the literature and PSI(+)-MS/MS dissociation.[46] The MS/MS spectrum is shown in Figure S1 of supplementary material creatinine (*m/z* 114) is characterized by the loss of CO leading to the formation of the $[C_3H_8N_3]^+$

ion with *m/z* 86.

Additionally, modifying the paper with a graphene oxide film increases MS spray time. The spray time using chromatographic paper showed a decrease in 1.2 minutes while the spray using GO-modified paper showed stable until 2.0 minutes. Besides this, the efficiency decreases abruptly for the chromatographic paper, this decrease is slower for GO-modified paper even after 2.0 minutes. Graphene oxide has several functional groups, such as epoxy, hydroxyl, and carbonyl, in its basal planes and edges. These groups exhibit hydrophilic properties, polar groups, retaining for longer the solution applied to the paper, making elution to the mass spectrometer slower.[24-31] Figure S2 into supplementary material shows the total ion chromatograms for chromatographic paper and GO-modified paper, both applied to PSI-MS creatinine in urine samples analysis.

Quantification of creatinine in urine.

The linearity of the PSI-GO/MS method for creatinine determination in urine samples was assessed by the analytical curve (Figure S3 in the supplementary material). The analytical curve was constructed using the absolute intensity of the fragment ion, *m/z* 86, as a function of concentration. The method showed linear between 0.1 to 3.4 ppm with $R^2 = 0.9991$. The limit of quantification (LOQ) and limit of detection (LOD) was determined based on S/N higher than 10 and 3 respectively. According to the obtained results the LOQ was 0.17 ppm and LOD 0.05 ppm.

The developed GO-PSI-MS method was compared with the chromatographic paper, in three concentrations levels (0.1, 1.4 and 3.4 ppm). These obtained values are shown in Table 1. The GO-PSI-MS developed method presented accuracy over 96.8% in the range of all analyzed concentrations. The interday precision was presented by the coefficient of variation (CV%) and the values were lower than 6.8%. For unmodified chromatographic paper, the results were

acceptable only at concentrations greater than 1.0 ppm with accuracy of 102.4%.

Table 1. Inter-day precision, accuracy and absolute recovery of the PSI-MS method for creatinine using modify paper and chromatographic paper

PSI substrate	Concentration (ppm)	Precision (%)	CV*	Accuracy (%)	Absolute recovery (%)
GO-Modified paper	0.1	6.8		4.5	96.8
	1.4	4.2		1.3	99.5
	3.4	1.1		0.1	100.9
Chromatographic paper	1.0	9.6		10.1	102.4
	1.4	9.2		8.8	96.4
	3.4	8.8		8.9	102.7

*Coefficient of variation

Kwon et al. developed a method for the analysis of creatinine in urine using liquid chromatography-tandem mass spectrometry, obtaining values of LOQ and LOD of 10 and 3 ppm respectively. While the developed method here presented LOQ of 0.17 ppm and LOD of 0.05 ppm, with of precision and accuracy. In addition, there is a fact that the PSI-MS technique is a faster analysis and almost no solvent consumption when compared to the LC-MS technique that demands a considerable time of chromatographic run.[47]

Real urine samples

To evaluate the proposed method for clinical use, the described protocol was applied to the analysis of urine samples healthy volunteers. Twenty-four samples were analyzed, and the creatinine concentrations found in these samples ranged from 0.9 to 3.6 ppm.

The PSI-GO-MS developed method for creatinine in urine samples analysis, showed to be a potential tool for clinical determination, exhibiting great accuracy and specificity when compared to conventional methods for creatinine determination.

Conclusion

In this study, graphene oxide was synthesized and immobilized into cellulose paper surface, and afterward the developed substrate was used to PSI-MS method for creatinine determination in urine samples.

The GO-PSI-MS developed method is based on simple ionization, besides being easy to perform, fast, and powerful outdoors technique that can be used for high-performance analysis. The technique does not require sheath gas, heating or materials for analysis of samples and sample preparation for complex samples, such as urine, and does not suffer from interferences compared to the traditional methods for creatinine analysis. GO considerable improve spray stability and results in the lower limit of quantification when compared to chromatographic paper (conventional substrate).

The developed method showed adequate accuracy (lower than 4.5 %), precision (lower than 6.8 %) and LOQ (0.1 ppm) values. Real urine samples were subject to GO-PSI-MS analysis to creatinine biomonitoring levels, the results showed the adequate performance of the developed method for clinical purposes.

Supplementary Information

The supplementary material for this study (total ion chromatograms, GO-PSI-MS/MS spectrum and analytical curve) are avaiable free of charge at http://jbcs.sbq.org.br as a PDF file.

Acknowledgments

This work was supported by grants from Conselho Nacional de Desenvolvimento Científico e Tecnológico (CNPq- 447927/2014-0). The authors thank the Grupo de Métodos Eletroforéticos (GME) da Universidade Federal de Goiás for donating of creatinine standard solution.

Compliance with Ethical Standards

All procedures performed involving human participants were in accordance with the ethical standards of the institutional and national research committee and with the 1964 Helsinki

Declaration and its later amendments or comparable ethical standards.

The authors have declared no conflict of interest.

References

1. Wang, H.; Liu, J.; Cooks, R. G.; Ouyang, Z.; *Angew. Chem.* **2010**, *122*, 889.

2. Espy, R. D.; Manicke, N. E.; Ouyang, Z.; Cooks, R. G.; *Analyst* **2012**, *137*, 2344.

3. Lin, C. H.; Liao, W. C.; Chen, H. K.; Kuo, T.; *Bioanalysis*. **2014**, *2*, 199.

4. Hamid, A. M.; Jarmusch, A. K.; Pirro, V.; Pincus, D. H.; Clay, B. G.; Gervasi, G.; Cooks, R. G.; *Anal. Chem.* **2014**, *86***,** 7500.

5. Espy, R. D.; Teunissen, S. F.; Manicke, N. E.; Ren, Y.; Ouyang, Z.; Van, A. A.; Cooks, R. G.; *Anal. Chem.* **2014**, *86*, 7712.

6. Zhang, C., Manicke, N. E.; *Anal. Chem.* **2015**, *87*, 6212.

7. Liu, W.; Wang, N.; Lin, X.; Ma, Y.; Lin; J. M.; *Anal. Chem.* **2014**, *87*, 7128.

8. Jjunju, F. P. M.; Maher, S.; Damon, D. E.; Barrett, R. M.; Syed, S. U.; Heeren, R. M. A.; Taylor, S.; Badutawiah; A. K.; *Anal. Chem.* **2016**, *88*, 1391.

9. Deng, J. W.; Yang, Y. Y.; *Anal. Chim. Acta*. **2013**, *785*, 82.

10. Su, Y.; Wang, H.; Liu, J. J.; Wei, P.; Cooks, R. G.; Ouyang, Z.; *Analyst.* **2013**, *138*, 4443.

11. Li, A.; Wei, P.; Hsu, H. C.; Cooks, R. G.; *Analyst.* **2013**, *138*, 4624.

12. Liu, J. J.; Gu, Z. X.; Yao, S. Z.; Zhang, Z. H.; Bo, C.; *J. Pharm. Biomed. Anal.* **2016**, *124*, 93.

13. Tepper G.; Kessick, R.; *Appl. Phys. Lett.* **2009**, *94*, 084196.

14. Hu, B.; So, P. K.; Chen, H.; Yao, Z. P; *Anal. Chem.* **2011**, *83*, 8201.

15. Maa, Q.; Bai, H.; Li, W.; Wang, C.; Cooks, R. G.; Ouyang, Z.; *Talanta.* **2015**, *142*, 190.

16. Manicke, N. E.; Yang, Q.; Wang, H.; Oradu, S.; Ouyang, Z.; Cooks, R. G.; *Int. J. Mass Spectrom.* **2011**, *300*, 123.

17. Wang, H.; Manicke, N. E.; Yang, Q.; Shi, L. R.; Cooks, R. G.; Ouyang, Z.; *Anal. Chem.* **2011**, *83*, 1197.

18. Zhang, Z.; Cooks, R. G.; Ouyang, Z.; *Analyst*. **2012**, *137*, 2556.

19. Gao, Y.; Qin, C.; Qiao, Z.; Wang, B.; Li, W.; Zhang, G.; Chen, R.; Xiao, L.; Jia. S.; *Carbon*. **2015**, *93*, 843.

20. Dreyer, D. R.; Todd, A. D.; Bielawski, C. W.; *Chem. Soc. Rev*. **2014**, *43*, 5288.

21. Upadhyay, R. K.; Soin, N.; Bhattacharya, G.; Saha, S.; Barman, A.; Roy, S. S.; *Mater.Lett.* **2015**, *160*, 355.

22. Krishnamoorthy, K.; Ramadoss, A.; Kim, S. J.; *Sci. Adv. Mater.* **2013**, *5*, 406.

23. Park, J. H.; Park, J. M.; *Surf. Coat. Technol.* **2014**, *254*, 167.

24. Hu, X. B.; Yu, Y.; Hou, W. M.; Zhou, J. E.; Song, L.; *Appl. Surf. Sci.* **2013**, *273*, 118.

25. Rasuli, R.; Mokarian, Z.; Karimi, R.; Shabanzadeh, H.; Abedini, Y.; *Thin Solid Films.* **2015**, *589*, 364.

26. Hu, X. B.; Yu, Y.; Zhou, J. E.; Song, L.; *Nano.* **2014**, *9*, 1450037.

27. Zanin, H.; Saito, E.; Ceragioli, H. J.; Baranauskas, V.; Corat, E. J.; *Mater. Res. Bull.* **2014**, *49*, 487.

28. Kou, L.; Gao, C.; *Nanoscale*. **2011**, *3*, 519.

29. Wei, S. C.; Fan, S.; Lien, C. W.; Unnikrishnan, B.; Wang, Y. S.; Chu, H. W.; Huang, C. C.; Hsu, P. H.; Chang, H. T.; *Anal. Chim. Acta*. **2018**, *1003*, 42.

30. Zanin, H.; Saito, E.; Marciano, F. R.; Ceragioli, H. J.; Granato, A. E. C.; Porcionatto, M.; *J. Mater. Chem. B*. **2013**, *1*, 4947.

31. Araújo, W. R.; Salles, M. O.; Paixão, T. R. L. C.; *Sens. Actuators B Chem.* **2012**, *173*, 847.

32. Koncki, R.; *Trends Anal. Chem.* **2008**, *27*, 304.

33. Bhagavan. N. V.; *Medical Biochemistry*, 4th ed.; Harcourt Academic Press: Orlando, USA, 2002.

34. Myers, G. L.; Miller, W. G.; Coresh, J.; Fleming, J.; Greenberg, N.; Greene, T.; *Clin. Chem.* **2006**, *52*, 5.

35. Randviir, E. P.; Banks, C. E.; *Sensors and Actuators B.* **2013**, *183*, 239.

36. Dbira, S.; Cañizares, P.; Rodrigo, M. A.; *J. Electroanal. Chem.* **2015**, *744*, 62.

37. Mendes, T. P. P.; Pereira, I.; Ferreira, M. R.; Chaves, A. R.; Vaz, B. G.; *Anal. Meth.* **2017**, *9*, 6117.

38. Zargar, T.; Khayamian, T.; Jafori, M. T.; *J. Pharmac. Biomed. Anal.* **2017**, *132*, 232.

39. Zheng, Y.; Wang, Q.; Wang, X.; Chen, Y.; Wang, X.; Zhang, X.; Bai, Z.; Han, X.; Zhang, Z.; *Anal. Chem.* **2016**, *88(14)*, 7005.

40. Chen, J.; Hu, Y.; Shi, M.; Lu, X.; Qin, C.; Li, C.; Ye, M.; *Chem. Mater.* **2009**, *21*, 3514.

41. Annesley, T. M.; *Clin. Chem.* **2003**, *49*, 1041.

42. Fujii, T.; *Mass Spectrom. Rev.* **2000**, *19*, 111.

43. Furey, A.; Moriarty, M.; Bane, V.; Kinsella, B.; Lehane, M.; *Talanta.* **2013**, *115*, 104.

44. Liu, A. C.; Lin, T. Y.; Su, L. W.; Fuh, M. R.; *Talanta.* **2008**, *75*, 198.

45. Antignac, J. P.; Wasch, K.; Monteau, F.; De Brabander, H.; Andre, F.; Le Bizec, B.; *Anal Chim Acta.* **2005**, *529*, 129.

46. Nicolardi, S.; van der Burgt, Y. E. M.; Codée, J. D. C.; Wuhrer, M.; Hokke, C. H.; Chiodo, F.; *ACS Nano*. **2017**, 11, 8257.

47. Kwon, W.; Kim, J. Y.; Suh, S.; Kyo, M.; *Forensic Sci. Int.* **2012**, 221, 57.

Lab-made solid phase microextraction phases for off line extraction and direct mass spectrometry analysis: evaluating the extraction parameters

Ricardo Alves Bernardo[1], Lidya Cardozo da Silva[1], Maria Eugênia C. Queiroz2, Boniek Gontijo Vaz[1], Andréa Rodrigues Chaves[1]*

[1] Instituto de Química, Universidade Federal de Goiás, 74690-900, Goiânia, GO, Brazil.

[2] Departamento de Química, Faculdade de Filosofia Ciências e Letras de Ribeirão Preto, Universidade de São Paulo, 14040-903, Ribeirão Preto, SP, Brazil

Email: *andrea_chaves@ufg.br

tel: +55-62-3521-1016 R 251

ABSTRACT

The analyses of drugs and metabolites in complex matrices have been widely studied in recent years. However, due to high levels endogenous compounds and matrix complexity, these analyses require a sample pre-treatment step. To this aim, two lab-made extractive phases were integrated to probe electrospray ionization mass spectrometry (PESI-MS) technique for direct analysis of illicit drugs in biological fluids and phorbol esters in *Jatropha curcas* extract. The polypyrrole (PPy) phase was electropolymerized onto a platinum wire surface by cyclic voltammetry. The molecularly imprinted polymer (MIP) was synthesized and adhered onto a stainless-steel needle with epoxy resin. The PPy-PESI-MS method showed to be linear in a concentration range from 1 to 500 µg L^{-1}, with accuracy values between -2.1 and 14%, and precision values between 0.8 and 10.8%. The MIP-PESI-MS method showed to be linear in a concentration range from 0.92 to 30 mg L^{-1}, with accuracy values between -1.6 and -15.26%, and precision values between 4.06 and 13.49%.

Keywords: solid phase microextraction, mass spectrometry, probe electrospray ionization, illicit drugs, phorbol esters

1. INTRODUCTION

A tendency in analytical laboratories has been the development of an accurate, precise and robust miniaturized low-cost methods [1]. Mass spectrometry is gaining interest in laboratories due to the high selectivity for the target analyte, especially to high resolution mass spectrometers [2,3]. Recently, the most used ionization source for mass spectrometry is the electrospray ionization (ESI-MS) [4,5]. However, this technique commonly requires sample pretreatment steps due to clogging problems and ionic suppression effects for analytes in complex matrices [6,7].

The probe electrospray ionization mass spectrometry (PESI-MS) is an ESI-based technique. It was first proposed by Hiraoka *et al*., 2007 [8], and consists of high voltage (≈ 2 – 3 kV) application on a wet metallic probe with the sample. The ionization process in PESI is quite similar to the electrospray ionization mass spectrometry (ESI-MS). Both PESI and ESI ensure reliable mass spectrometry analysis [9–11], but sensitivity can be improved aiming to determine analytes at trace levels, a mass spectrometer was used with modified PESI as an ion source.

Janusz Pawliszyn *et al*., 1987 [12], first reported the solid phase microextraction (SPME) technique to pretreat samples in a shorter time, with little or no solvent use. SPME is a miniaturized system that uses a very small amount of sample, and consists in an extraction phase supported on the probe. In general, the commercial SPME phases are supported on fused silica rods that are fragile. Besides, it has a limited number of commercial extraction phases and exhibits low conductivity, which is difficult to use as a probe for PESI-MS methods [13].

Polypyrrole (PPy) seems to be a promising extractive phase with which to coat the

metallic probe for PESI-MS analysis. PPy is a conductive biodegradable polymer that can be formed by chemical or electrochemical synthesis over various surfaces with different shapes and sizes. PPy promotes intermolecular interactions like acid-base, π-π, dipole-dipole, hydrophobic, hydrogen bonding, and exchanges between the polymer film and the analytes [14–19]. The literature highlighted the PPy coating as an extraction phase media in different techniques and samples, such as solid phase microextraction (SPME) for drug analysis in plasma samples, and in-tube SPME to antidepressants analysis in biological fluids [14]. Also, PPy was coated on fused silica capillaries for determination of β-blockers in urine and serum samples [20]. Besides the intermolecular interactions with analytes, the conductivity of PPy coated metallic probes could promote an enhancing in the spray formation, what results in better analyte desorption.

Furthermore, molecularly imprinted polymers (MIPs) mimics a specific site of identification using a target molecule, known as template, and have been widely used as extractive phase, biomimetic sensors, subtract for solid phase extraction (SPE), and affinity support in the recognition of target molecules [21]. The main synthetic route for MIPs is the polymerization of functional monomers in the presence of the template and a cross-linker. After the polymerization process, the MIP's template completely removed, therefore, specifics sites for the target molecule recognition remains in the polymer structure [22]. MIPs are reported as adsorbent to sampling, extraction and analyte enrichment substrate for ambient MS analyses in the literature, e.g. for detection of pesticides from water [23], and fruits [24], also for drug analysis in biological and environmental samples [25].

The aim of this research was to integrate the sample pretreatment step to PESI-MS applying SPME phases, such as: PPy and MIP. To avoid cracking and low conductive problems, common in commercial SPME phases, platinum and stainless-steel wire were employed. The proposed SPME-PESI-MS methods were evaluated for offline extraction and quantification of

cocaine, lysergic acid diethylamide (LSD), methamphetamine (MA) and 3,4-Methylenedioxymethamphetamine (MDMA) in oral fluid and urine samples; phorbol esters in *Jatropha curcas* leaves.

2. EXPERIMENTAL SECTION

2.1 Materials

Methanol (99.9%) was acquired from TEDIA (Fairfield, OH, USA). Sodium perchlorate (98%), and acetic acid (99.8%) were acquired from Acros Organics (Somerville, NJ, USA). Cocaine, diethylamide lysergic acid (LSD), methamphetamine (MA), 3,4 methylenedioxymethamphetamine (MDMA), pyrrole monomer (98%), acetonitrile (99.9%), formic acid (98%), ammonium hydroxide (28-30%), phorbol 12-myristate 13-acetate (PMA) (98%), phorbol 12,13-diacetate (PDA) (99%), sodium dodecyl sulfate (SDS) (98.5%), ethanol (99.5%), tetraethoxysilane (TEOS) (98%), and aminopropyltriethoxysilane (APTES) (98%) were acquired from Sigma Aldrich (São Paulo, SP, Brazil). Solid phase extraction cartridge C-18 was acquired from Supelco (São Paulo, Brazil). Ultrapurified water was prepared by MS2000 equipment (Gehaka, São Paulo, SP, Brazil).

The SPME commercial phases of polydimethylsiloxane/divinylbenzene (PDMS/DVB 65 µm) and carboxen (CAR 75 µm) were acquired from Supelco (Bellefonte, PA, USA). Drug standards were acquired from Sigma Aldrich (São Paulo, SP, Brazil) by the professor Wanderson Romão, from Universidade Federal do Espírito Santo, and generous given to us.

Three samples of toxic leaves and three non-toxic leaves from different Jatropha curcas genotypes were provided by Embrapa Agroenergia (Brasília, Brazil). Toxic genotypes were identified as 113F, 199F and 259F; non-toxic samples were identified as 169F, 170F and 183F.

2.2 Sample Preparation

The stock solution of drug standards was prepared in pool, at a concentration of 1 mg L^{-1} in 25 mL of blank biological fluids and diluted with matrix to a concentration range from 1 to 500 µg L^{-1} in 1.5 mL vials.

The blank samples of oral fluids and urine samples were donated from healthy volunteers not exposed to any drugs or medicine, after appropriate sanitisation of the area and before the first meal of the day. These studies were performed in accordance with the World Medical Association's "Ethical principles for medical research involving human and animal subjects".

To prepare the leaves extracts 100 mg of each leaf were placed into microcentrifuge tubes where 1.0 mL of methanol was added. The flasks were placed into ultrasonic bath for 10 min, and then the supernatant was separated. The methanol addition and ultrasonic bath steps were repeated twice to obtain approximately 3 mL of methanolic extract from each sample.

2.3 Electropolymerization

The pyrrole electropolymerization was carried out in the Omnimetra potentiostat/galvanostat instrument model PG-3901, with PG39A software. To this process, a three-electrode electrochemical cell was used, where the reference electrode was an Ag/AgCl electrode, the auxiliary electrode was a 10 cm platinum wire (0.5 mm in diameter) and the working electrode consisted in a 3 cm platinum wire (0.5 mm in diameter). The surfaces of platinum wires were previously washed with nitric acid for 15 min, and then polished with steel sponges and finally washed with methanol in an ultrasonic bath for 15 minutes.

The electropolymerization was carried out as described by Chaves *et al.* [13]. The PPy film was deposited on the surface of the working electrode. The electrolytic solution consisted in 0.1 mol L^{-1} of sodium perchlorate and 0.01 mol L^{-1} of pyrrole monomer in 25 mL of acetonitrile. The potential range from 0 to 1.2 V was applied at a scan rate of 50 mV s^{-1}. The

number of cycles for the electropolymerization process was evaluated in 5, 10, 15, and 25 cycles to ensure higher extraction/desorption efficiency.

2.4 MIP synthesis and needle modification

For the MIP synthesis, 5.9 mmol of TEOS, 12.8 mmol of ultra-purified water, 0.03 mmol of HCl and 6.8 mmol of ethanol were added into a Falcon tube. The mixture was stirred and allowed to stand for 24 hours. After this, another solution containing 1.4 mmol of APTES, 3.5 mmol of SDS and 616.2 mmol of the analytical standard PMA were added. The second solution was stirred, added to the first one and allowed to stand for 24 hours. Later, the PMA used as template was removed with methanol in a Soxhlet extractor for 48 hours.

In addition, a non-molecularly imprinted polymer (NIP) was also synthesized for purposes of comparing the morphology and performance of the polymers used in the extraction of the target compounds in the leaves extracts.

The synthesized polymers were used to modify the needle. By means of an epoxy resin, 1 cm from the tip of stainless-steel rods, of 4 cm long and 0.6 cm in diameter, were coated with the polymers.

2.5 Scanning Electron Microscopy and Atomic Force Microscopy

The morphological characterization of PPy films, MIP and RAM were evaluated by Scanning Electron Microscopy (SEM) using a JSM – 6610 (JEOL Ltd., Tokyo, Japan) instrument with 10 kV as its accelerating potential.

2.6 Extraction Parameters

The analyte extraction was performed similarly to the SPME method. According to this, the intrinsic SPME variables, such as: number of cycles during the electropolymerization,

extraction pH and time, were evaluated aiming the best extraction efficiency using the developed PPy-SPME probe. Thus, the coated probe was immersed in solutions of samples (pH 3.4, 6.9 and 10.6) for 5, 15, 30, and 40 minutes under magnetic stirring at a rate of 1200 rpm [13]. The temperature of 25 °C and 40 °C were also evaluated for better extraction efficiency.

The pH of spiked matrices was adjusted to 3.4, 6.9 and 10.6 with acetic acid and ammonium hydroxide solution to perform the extraction and then, the MS peaks intensity was evaluated for each illicit drug. After the extraction, the coated probe was rinsed with purified water and positioned in front of the mass spectrometer for analyte ionization/desorption.

Aiming to promote the reusability of PPy-SPME probes, a washing step was evaluated. After each extraction, the probes were washed in triplicate with 5 mL of methanol under magnetic stirring, 1200 rpm. The washing step was evaluated through the absence of analytes in MS experiments, where no analyte peaks were detected.

The developed PPy-PESI-MS method was compared to the commercial SPME phases applied in the PESI-MS method. Two commercial phases were evaluated, carboxen and polydimethylsiloxane-divinylbenzene (PDMS/DVB), both have fused silica as support.

2.7 Optimization of MIP-SPME Probe Analysis

In order to obtain higher extraction and ionization/desorption efficiency, the covered probes were submitted to tests. Therefore, the probes were immersed in 1.5 mL of sample for 20 min under magnetic stirring at 1200 rpm followed by washing step, so the drying time was evaluated by put the probes to dry at room temperature of 22 °C for 1, 2, 3, and 4 hours. Also, aiming to reduce the dry time, the probes were put in oven at 40 °C for 0.5, 1, 1.5, and 2 hours and the results were compared. Also, using the same extraction parameters and the optimized dry time of 30 min in oven, the need for magnetic stirring during the extraction and wash before drying was evaluated and the resulting MS spectra were compared.

Finally, to obtain higher extraction efficiency of the MIP-SPME probe the extraction time was evaluated. Thus, the coated probe was immersed in 1.5 mL of sample solutions for 10, 20, 30, and 40 min, in sequence, the probes were washed with ultra-purified water and put to dry in oven at 40 °C for 30 min to comparing the obtained MS spectra.

2.8 MIP-SPME Probe Analysis

MS analyses were carried out in full scan mode followed by CID experiments to confirm the attribution of the detected ion to phorbol molecule. In the same way, MS analyses by NIP SPME-PESI and traditional PESI were also performed for comparison purposes.

The MS experiments were conducted in positive mode using a claw to apply the voltage of 3.5 kV at the probes to generate electrospray. No sheath, sweep, and auxiliary gases were needed. To conduce CID experiments, He was used as collision gas with 20 eV energy. The ion source parameters were 38 V of capillary voltage, 275 ºC of capillary temperature, and 110 V lens voltage.

In order to evaluate the extractive capacity of the method, MS analyses with MIP and NIP SPME-PESI and traditional PESI were performed. The extraction was carried out by immersion of the needles in 1.5 mL of the methanolic extracts for 20 min under magnetic stirring at 1200 rpm followed by washing with ultra-purified water and drying for 4 hours at room temperature of 22 °C.

2.9 Mass Spectrometry Conditions

The MS analysis were performed in tandem mode on a Thermo LCQ Fleet with software Thermo Tune Plus. For all phases evaluated here, the coated probe was positioned at 5-7 mm from the mass spectrometer inlet, at an angle of 90°, and a high voltage (3 kV for PPy, and 3.5 kV for MIP and NIP) was applied to generate the PESI (+) mass spectra, without the needing

of auxiliary, sheath or sweep gas flow, capillary voltage of 30 V, capillary temperature of 275 °C, and tube lens voltage of 50 V. For the analytical curve plot, it was used the intensity of the specific fragment ion with 30 seconds of acquisition time for each analyte *versus* their concentration at μg L^{-1}.

All SPME-PESI-MS analyses were performed in SRM mode. Therefore, the cocaine analysis was monitored the transition from the ion $[M+H]^+$ (*m/z* 304) → *m/z* 182 (Figure S 1) with collision energy of 30 eV; for LSD analysis, was monitored the transition from $[M+H]^+$ (*m/z* 324) → *m/z* 223 (Figure S 2) with collision energy of 30 eV; for MA analysis, was monitored the transition from $[M+H]^+$ (*m/z* 150) → *m/z* 119 (Figure S 3) with collision energy of 25 eV; for MDMA analysis, was monitored the transition from $[M+H]^+$ (*m/z* 194) → *m/z* 163 (Figure S 4) with collision energy of 25 eV; and for phorbol esters analysis, was monitored the transition from $[M+H]^+$ (*m/z* 311) → *m/z* 293 with collision energy of 20 eV.

A solution consisted by methanol with 0.1% of formic acid was used on the coated probes to improve analyte ionization/desorption, as shown in Figure 1. The dropping system was settled almost in contact with the coated probe (<1 mm) to avoid the influence of high voltage on methanol solution.

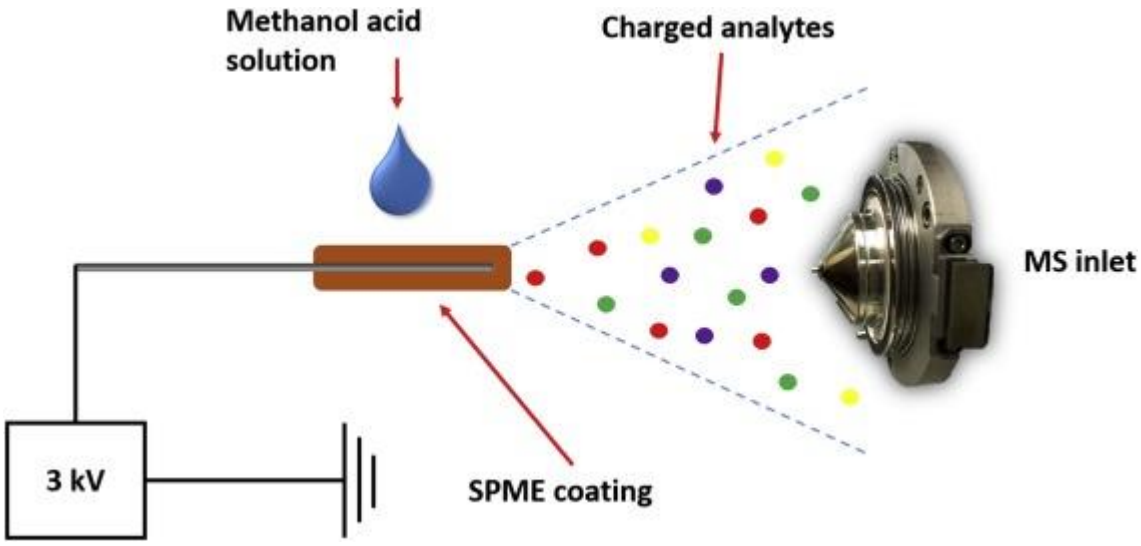

Figure 1. Scheme of SPME-PESI-MS method with addiction of methanol 0.1% acid formic

solution at a flow rate of 40 µL min^{-1} dropping over the 1 cm of SPME coating.

2.10 Analytical essays

Aiming to evaluate some analytical parameters, such as: intra and inter-day accuracy and precision, absolute recovery, limit of detection (LOD) and limit of quantification (LOQ), the SPME-PESI-MS method developed was performed with blank matrices spiked with standard solutions at concentration range from 1 to 500 µg L^{-1}.

The linearity was evaluated through the linear regression of peak intensity (y) of the specific fragment ion for each analyte on mass spectra *versus* analyte concentration (x, µg L^{-1}). The analytical curves were plotted using 8 concentration values LOQ, 5, 50, 100, 200, 300, 400 and 500 µg L^{-1}, in replicate analysis (n = 5), and treated by the ANOVA statistical technique.

Intra and inter-day accuracy and precision were determined by analytical curves using quintuplicate essays of the SPME-PESI-MS method of samples at 1, 200 and 500 µg L^{-1}, as shown in equations 1 to 3.

$$P(\%) = \frac{STD}{AEC} . 100 \qquad \textbf{Eq. 1}$$

$$A\ (\%) = \frac{AEC - TC}{TC} . 100 \qquad \textbf{Eq. 2}$$

$$Re = \left(\frac{SSC - NSSC}{SC}\right) . 100 \qquad \textbf{Eq. 3}$$

where P is the precision, STD corresponds to the standard deviation of the experimental concentrations, AEC corresponds to the average experimental concentration, A is the accuracy, TC corresponds to the theoretical concentration, Re is the absolute recovery, SSC corresponds to the spiked sample concentration, NSSC corresponds to the non-spiked sample concentration and SC is the spiked concentration [26,27].

The LOD and LOQ were theoretical, as shown in equations 4 and 5, and experimentally determined. Experimentally, the LOD and LOQ were determined based on the analytes signal-to-noise ratio (S/N) about 3.3 for LOD and 10 for LOQ.

$$LOD = 3.3 \left(\frac{STDB}{\alpha}\right) \qquad \textbf{Eq. 4}$$

$$\mathrm{LOQ} = 10\left(\frac{\mathrm{STDB}}{\alpha}\right) \qquad \textbf{Eq. 5}$$

where STDB means the standard deviation of ten measurements of blank samples, and α is the angular coefficient found by the linear regression in the analytical curves [28].

Recovery values were calculated comparing the peak intensity of the most abundant fragment ion of extracted drugs from the matrices with those at the same concentration in standard solutions of the drugs [27].

3. RESULTS AND DISCUSSION

3.1 Electropolymerization process

The polypyrrole probe was electrochemically prepared on the platinum wire, using cyclic voltammetry. During this process, as the number of cycles increases, the thickness of the prepared films also increases, meaning that this process could result in better extraction efficiency. The voltammogram area could be related to electrodeposited film area [29]; accordingly, the PPy films prepared with 25 electropolymerization cycles exhibited a higher area compared to 5, 10, and 15 cycles [30]. According to SPME extraction process, extraction efficiency is based on analytes and phases equilibrium [17]. Therefore, it is expected that a thicker film could improve the extraction capability of PPy-SPME probes [31]. Even though, using 25 cycles PPy-SPME probes, when the high voltage (3 kV) is applied, the coating was completely peeled off from the needle. This behavior was also observed on the SPME probes of 10 and 15 cycle. Therefore, the probe prepared in 5 voltammetric cycles was selected to perform all of the extractions, once at 5 cycles, the coated probe performed about 60 extractions before some degradation effect.

3.2 Scanning Electron Microscopy and Atomic Force Microscopy

The SPME developed probes was submitted to scanning electron microscopy and atomic force microscopy analysis. The images were obtained with an acceleration potential of 10 kV and a magnification of 10000 for PPy phase, and acceleration potential of 10 kV and magnification of 3000 for MIP phase (Figure 2 A and B). The electrodeposition parameters directly influence PPY morphology. The slower the scan ratio, the higher the film porosity. The potential applied must be closer to the potential of pyrrole oxidation, producing small granules and increasing the surface area, as exhibited in Figure 2A. When the potential applied is higher

than the potential of pyrrole oxidation, large granules are formed, reducing the contact surface, thus directly affecting the analyte extraction efficiency [15].

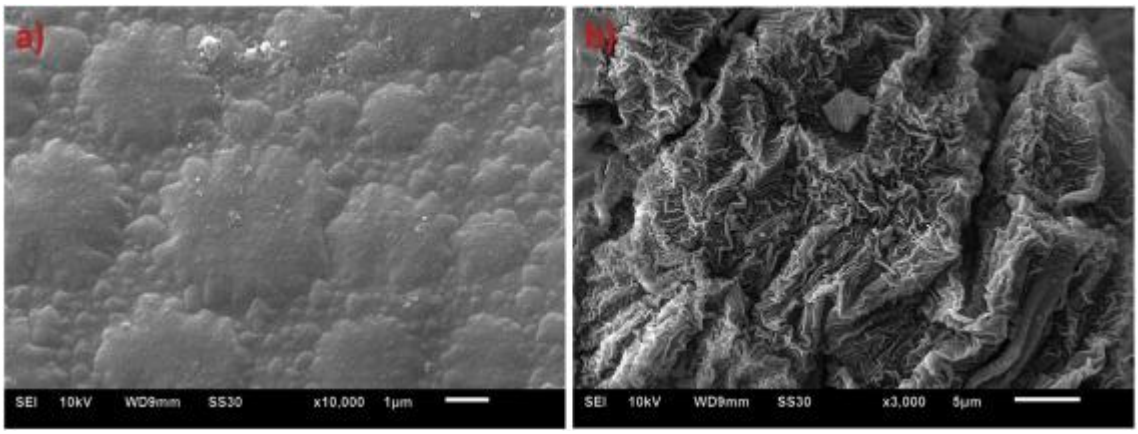

Figure 2. SEM image of SPME PPy extraction phase (A) and SPME MIP extraction phase (B). The MIP morphology can be verified via SEM analyses. As seen in Figure 2 B, macropores structures and cavities are observed on the polymer surface. The presence of cavities can be explained by the MIPs synthesis that involves the formation of a complex between the template molecule and the monomer followed by template elimination that creates selective sites on the polymer surface [22]. Besides this, according to Comarck and Elorza (2004), the macroporous polymers are mechanically stable and preferable in MIP synthesis [32].

3.3 Extraction parameters

PPy and MIP-SPME probes were used for direct analysis using PESI-MS of cocaine, LSD, MDMA and MA from oral fluid and urine, and phorbol esters in *J. curcas* extract respectively. Some intrinsic SPME variables such as time of extraction, temperature and pH were evaluated aiming to improve the extraction efficiency for the analytes in complex matrices. The extraction temperature influences the mass transfer rate and analyte partition coefficient [33]. The temperature of 25 °C was chosen for all extractions to improve the reuse of the developed probe, once the PPy synthetized here does not exhibit good thermal stability [13], and to avoid degradation of *J. curcas* extract. However, by heating the sample solution to 40 °C, the extraction equilibrium was reached in 10 minutes, and as results of this heating, the probe could not be reused as huge damage to the probes was observed.

The extraction efficiency with PPy decreases as the pH of the solution also decreases. As described by Wu and Pawliszyn [17], pH values below 5.0 are not desirable for the extraction of basic analytes (such as cocaine, LSD, MA and MDMA) using PPy as extractive phase. As consequence, at this pH value, the drugs (pKa values from 7.8 to 10.2) are partially

or totally in the ionic form and there is an electrostatic repulsion between basic analytes and the PPy film in low pH values, where analytes and PPy are positively charged. To evaluate the pH solution influence on the extraction process with PPY-SPME probe, the samples pH values were adjusted to pH 3.4, 6.9 and 10.6. According to the results, the samples in pH 6.9 showed better extraction efficiency and were selected to perform the following extractions.

The extraction time was evaluated at 5, 15, 30 and 40 minutes. A higher MS signal intensity was achieved within 40 minutes of extraction at 25°C with the magnetic stirring of the solution at 1200 rpm to improve analyte diffusion to the extractor phase. However, no equilibrium condition was achieved prior to 40 minutes. Times above 40 minutes have not been employed because this could result in longer analysis time, which is a great disadvantage for analytical methods. Although, 40 minutes is a relatively longer extraction time, the extraction procedure could be performed in batch. It is possible to perform many extractions at the same time, in different vial flasks, using different probes. In the present study, 12 extraction probes were used at the same time. Each probe was reused for about 60 extractions without a significant reduction in method sensitivity.

To evaluate the extractive capacity of the synthesized polymers the signal intensities of the target ion was compared in MS/MS spectra by analyses with the MIP and NIP SPME-PESI and traditional PESI in Figure 3. The lower signal intensities observed in PESI-MS analyses can be attributed to ionic suppression effect since in this method the probe is not covered with an extractive phase. Also as expected, the MIP SPME-probe provided the higher increase in the relative abundance of the target ion. Comparing with the NIP, the results indicate that the printed cavities in the MIP surface present selectivity. For this reason, its use is promising to promote extraction of phorbol esters directly from the ionization probe.

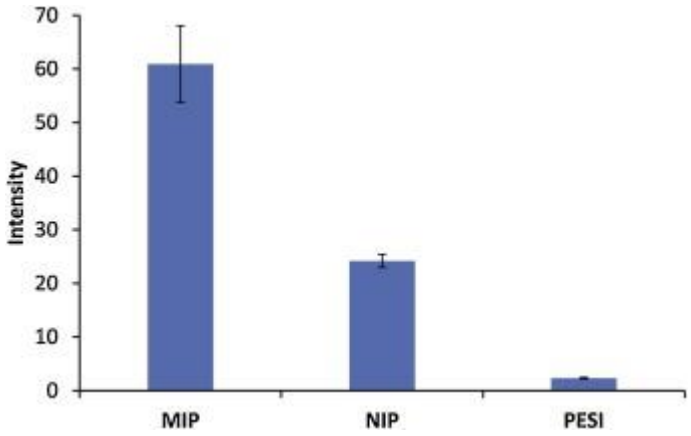

Figure 3. Intensities of the fragment ion of m/z 293 obtained in MS/MS spectra using MIP and NIP-SPME Probe, and traditional PESI in positive mode. Error bars show the standard deviation of the analyses made in triplicate.

During the method development, we observe the need to dry the covered probes before the MS analyses. As shown in Figure 4 (a), under the room temperature of 22 ºC, the efficiency of the extractive phases is improved with the long dry time achieving best results after 4 h. However, the need for such drying time can make method impracticable. Thus, the probes were put in an oven at 40 °C to reduce the drying time. As seen in Figure 4 (b), enough sensibility was obtained with drying about 30 min at 40 °C. The decrease in the signal intensity with the longer dry time in the oven may be associated with degradation due to thermal instability of the phorbol molecules.

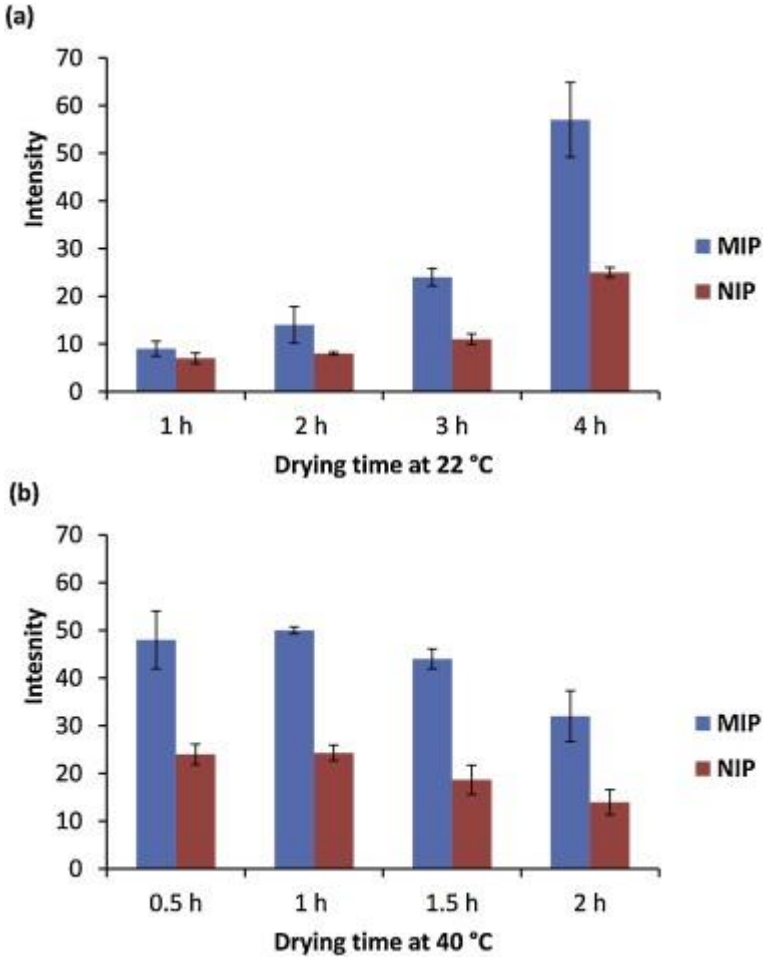

Figure 4. Relative abundances obtained in mass spectra for the fragment ion of *m/z* 293 in function of drying time using MIP and NIP-SPME-PESI (+) - MS in SRM mode. (A) Drying

at 22 °C and (B) drying at 40 °C. Error bars show the standard deviation of the analyses made in triplicate.

In the standard method, the magnet stirring at 1200 rpm was applied to facilitate the adsorption of the analytes in the polymers. Also, the covered Probes were washed after the extraction step for removing the non-target components present in the complex sample. Therefore, tests were done to evaluate how the absence of magnetic stirring during the extraction and the washing step affect the performance of the covered Probes. As noted in Figure 5, in absence of magnetic stirring the analyte adsorption is less efficient. However, the more significant loss in performance was observed in analyses without the wash step due to ionic suppression caused by the other components present in the complex sample that were not removed.

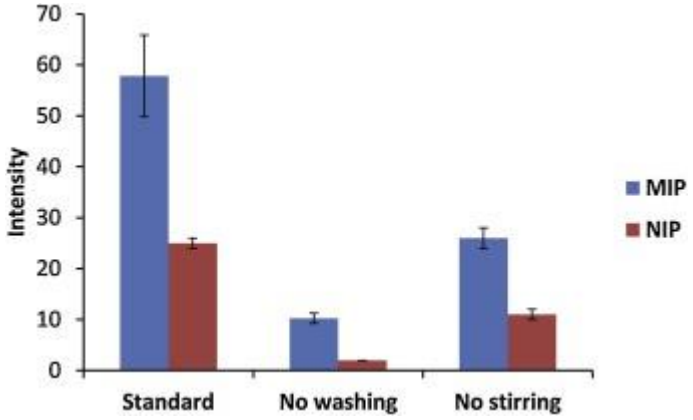

Figure 5. The intensities obtained by the standard method and analyses by covered-Probes without washing step, and magnetic stirring during extraction. Error bars show the standard deviation of the analyses made in triplicate. Intensities of the fragment ion of *m/z* 293 in MIP and NIP-SPME-PESI (+) MS/MS spectra was monitored.

Tests were done with the MIP and NIP-SPME probe in order to obtain higher extraction and ionization/desorption efficiency in the detection of the target phorbol ion directly from the *J. curcas* methanolic extracts. Therefore, the extraction time was evaluated by the immersion of the coated-probe in 1.5 mL of the methanolic extracts under magnetic stirring at 1200 rpm for 10, 20, 30, and 40 min. Figure 6 showed the comparison of MIP and NIP-SPME probe extraction performance by the evaluation of signal intensities of the *m/z* 293 in function of the extraction time. For the MIP-SPME probe, the shorter extraction time provided the higher ion intensity, and for the NIP-SPME probe, the relative abundance remains about 10%. Than higher

extraction time, than the competition phase effects between analyte and matrix interferents (Fig. 6). Therefore, the best PDA extraction time by MIP in *J. curcas* methanolic extract was 10 minutes.

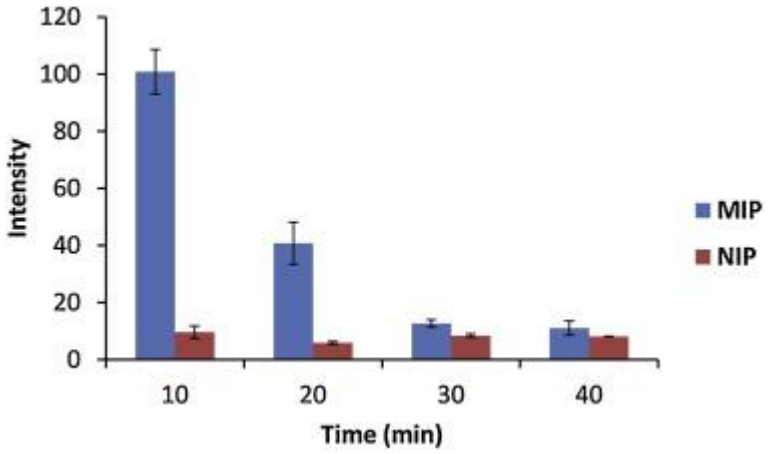

Figure 6. The fragment ion of *m/z* 293 in function of extraction time using MIP and NIP-SPME-PESI (+) - MS in SRM mode. Error bars show the standard deviation of the analyzes made in triplicate.

As Li et al. 2008 reported, salt can promote the reduce of solute solvation, enhancing the SPME extraction process, but it is followed by some problems such as irreversible adsorption onto the extractive phase, porous obstruction and corrosion of metallic support for electropolymerized fibres [33]. Salt is generally more dangerous for MS coupled with ESI methods, as it is usually related to precipitation in mass spectrometer canals and capillaries promoting clogging problems; therefore, it should be avoided. Thus, this parameter was not evaluated for the PPY-SPME PESI-MS and MIP-PESI-MS developed methods.

3.4 PESI-MS

The SPME-PESI(+) mass spectrum for all of analytes are shown below (Figure 7). In Figure 7, the illicit drugs can be observed in their protonated form: MA *m/z* 150; MDMA *m/z*: 194; Cocaine *m/z*: 304; and LSD *m/z*: 324. The other ratio mass-charge detected on the spectrum was derived from endogenous compounds in urine and oral fluids.

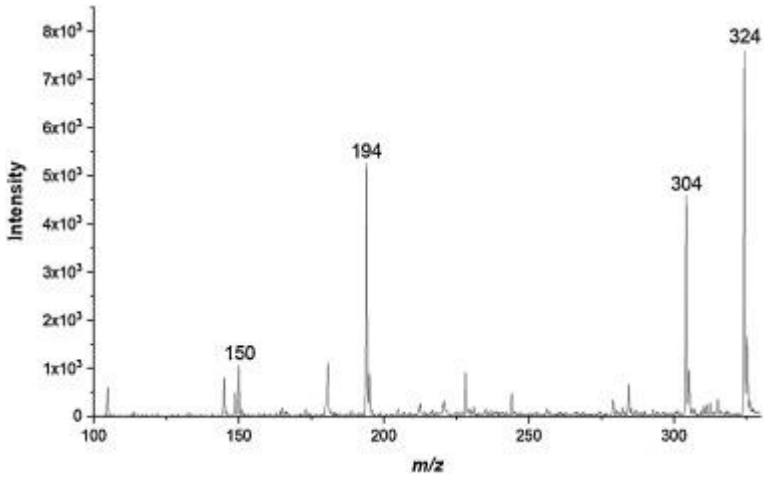

Figure 7. Mass spectrum for cocaine (*m/z* 304), LSD (*m/z* 324), methamphetamine (*m/z* 150) and MDMA (*m/z* 194) by SPME-PESI-MS method.

The SPME-PESI-MS method has a powerful sensitivity, as it promotes easy analyte desorption, and reduces ion suppression effect and adduct formation [8–11]. All MS analyses were performed in tandem mode, and the analytical curves were plotted using the intensity of the specific fragment ion versus analyte concentration. In this study, the specific fragment ion coincided with the most abundant fragment ion.

Toxic and non-toxic samples of *J. curcas* leaves were provided by Embrapa Agroenergy. The ion 4,9,12-trideoxyphorbol of *m/z* 311 was verified in all toxic samples. This ion is commonly referred to as the main degradation product of phorbol esters [34,35]. Figure 8 shows the results of CID experiments using the MIP SPME-Probe where its typical fragmentation pattern is observed by a loss of a water molecule and a ketone group.

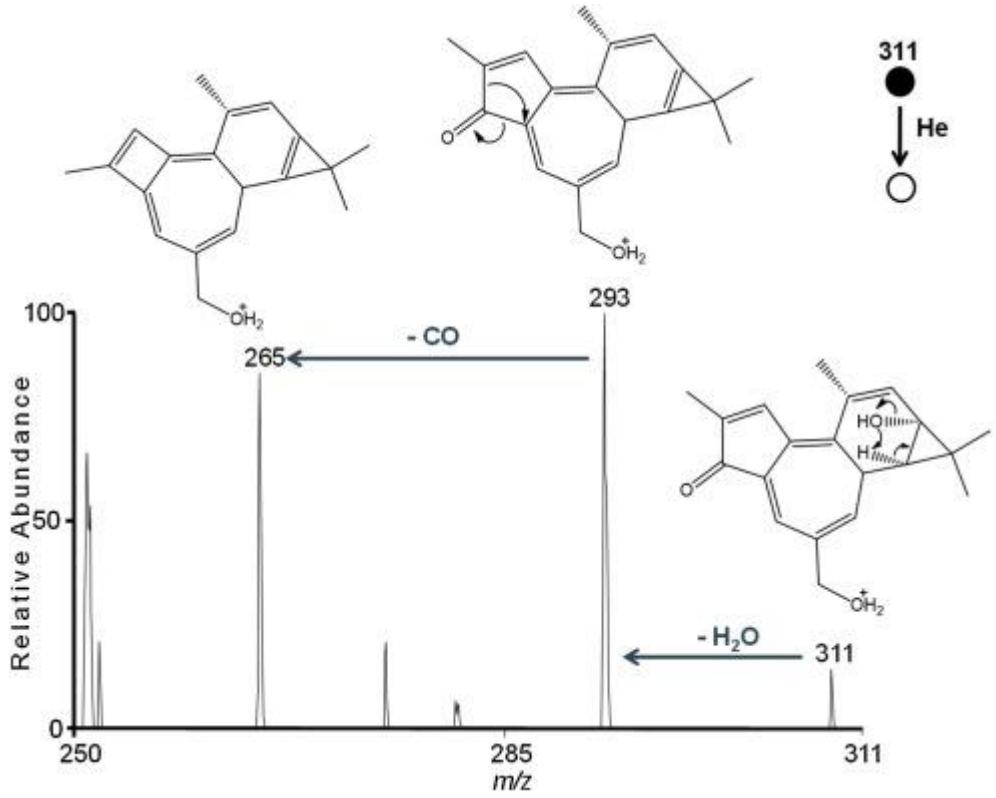

Figure 8. MIP SPME-PESI (+) MS/MS spectrum and proposed fragmentation mechanism for the ion 4,9,12-trideoxiforbol of *m/z* 311.

In CID experiments, the 4,9,12-trideoxyphorbol exhibited the characteristic loss of one water molecule leading to the formation of the *m/z* 293 as the most abundant ion. As the experiments were performed in a low-resolution mass spectrometer, the experiments were done in SRM mode, and the intensities of the ion 293 were monitored.

The MIP covered-PESI provided extraction of target analyte and analysis directly from the ionization source, consequently, the method enabled the detection of the 4,9,12-trideoxyphorbol directly from the methanolic extracts of *J. curcas* leaves. Moreover, by the method optimization, higher extraction efficiency was obtained and results in better accuracy and precision values. Figure 9 shows the MS spectra comparison after optimization between the MIP and NIP covered-PESI and conventional PESI-MS method. As noted, the use of the optimized MIP covered-Probe to promote direct extraction provides the largest signal magnitude. This behaviour could be related to adequate enrichment of target molecule in the polymer layer that leads to efficient ionization/desorption by PESI and minimizes ion suppression effects that are routinely observed in the conventional PESI.

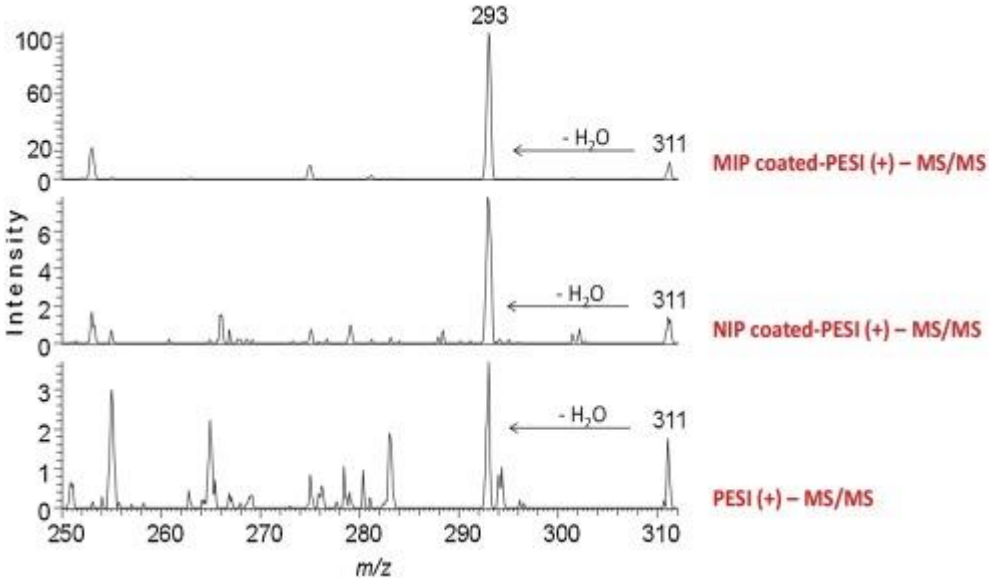

Figure 9. Mass spectra comparing intensities after optimizations of the fragment ion of *m/z* 293 obtained in CID experiments using MIP and NIP SPME-Probe, and conventional PESI in positive mode.

All analytical curves were performed in replicate (n = 5), evaluating 7 concentrations and processed by the ANOVA statistical technique [28,36]. The linearity for each analyte was evaluated through the respective analytical curve. The regression equation and their respective correlation coefficients for all analytes, the LOQ and LOD, were theoretically estimated (T) as described in the material section. It was also experimentally determined (from 0.5 to 10 µg L-1) by performing the SPME-PESI-MS method with diluted solutions until the equipment does not detect, or quantify the analytes with satisfactory precision and accuracy. These values are presented in Table 1.

Table 1. Linear regression for the SPME-PESI-MS method with their respective limit of detection (LOD), limit of quantification (LOQ) and ANOVA P value

Drug	Matrix	Linear Regression (LOQ:500 µg L^{-1})	r^2	LOD µg L^{-1}	LOQ µg L^{-1}	ANOVA P value
Cocaine	Oral Fluids	y = 0.4474x + 3.3652	0.995	0.61	2.05	7.13E-07
	Urine	y = 0.0752x + 2.6171	0.999	2.65	8.78	2.69E-09
LSD	Oral Fluids	y = 0.4516x - 3.9886	0.997	0.28	0.92	1.19E-07
	Urine	y = 0.0496x + 0.4381	0.999	1.47	4.90	8.35E-09
MA	Oral Fluids	y = 0.0425x + 0.1394	0.998	1.33	4.45	1.11E-07
	Urine	y = 0.0118x - 0.0376	0.997	1.46	5.02	1.28E-07

MDMA	Oral Fluids	y = 0.1791x + 8.1192	0.994	0.51	1.69	1.16E-06
	Urine	y = 0.0199x + 0.2743	0.999	1.31	4.23	2.60E-08
PDA	*J. curcas* leaves extract	y = 1.8099x + 7.3950	0.997	0.28E3	0.92E3	1.40E-07

Diethylamide lysergic acid – LSD

Methamphetamine – MA

3,4 methylenedioxymethamphetamine – MDMA

Phorbol 12,13-diacetate – PDA

The precision and accuracy for both PPy-PESI-MS and MIP-PESI-MS were evaluated in intra and interday assays. The results are shown in the Table 2 for PPy-SPME-PESI-MS, and Table 3 for MIP-PESI-MS.

Table 2. Precision and recovery for PPY SPME-PESI-MS developed method

Drug	**Matrix**	**Concentration µg L^{-1}**	**Intra-day**		**Inter-day**		**Recovery (%)**
			Precision (%) n = 5	**Accuracy (%) n = 5**	**Precision (%) n = 5**	**Accuracy (%) n = 5**	
Cocaine	Oral Fluids	1	8.9	8.5	9.6	5.2	108.5
		350	3.2	2.8	2.5	0.8	102.8
		500	3.0	-2.4	1.5	0.4	97.6
	Urine	1	10.8	5.7	3.2	5.6	105.7
		350	2.8	-2.1	1.6	0.2	97.9
		500	2.0	-1.7	0.8	0.1	98.3
LSD	Oral Fluids	1	6.4	7.5	3.0	3.8	107.5
		350	2.2	-1.0	2.6	-0.3	99.0
		500	1.7	0.7	2.6	1.2	100.7
	Urine	1	9.4	11.9	5.8	13.7	111.7
		350	1.9	-0.4	0.9	0.01	99.6
		500	2.6	-0.6	1.6	-0.6	99.4
MA	Oral Fluids	1	4.0	14.0	9.2	13.5	114.0
		350	3.8	1.0	1.8	0.2	101.0
		500	2.7	-0.1	3.0	0.1	99.9
	Urine	1	7.5	7.8	7.5	7.9	107.8
		350	1.9	-0.2	1.8	-0.01	99.8
		500	1.9	-0.5	1.0	0.7	99.5
MDMA	Oral Fluids	1	6.1	4.2	9.3	8.0	104.2
		350	3.1	0.7	4.2	1.4	100.7
		500	2.5	-0.3	1.6	-0.2	99.7
	Urine	1	9.0	6.2	7.2	5.1	106.2
		350	2.4	-0.2	1.4	-0.4	99.8
		500	1.9	-0.2	2.0	0.6	99.7

Table 3. Precision and recovery values for MIP-PESI-MS developed method

Drug	Matrix	Concentration mg L^{-1}	Intra-day		Inter-day		Recovery (%)
			Precision (%) n = 5	Accuracy (%) n = 5	Precision (%) n = 5	Accuracy (%) n = 5	
PDA	*J.curcas* leaves extract	5.00	13.49	-1.60	7.78	12.77	112.8
		15.00	7.72	-11.70	4.35	-15.26	88.3
		25.00	9.37	10.73	4.06	5.65	110.7

The capacity of extraction/desorption in the PPy SPME-PESI-MS method was compared to commercial SPME phases (carboxen,and PDMS) applied to PESI-MS. The experiment was evaluated performing the same optimized extraction described in this study, only changing the probes. The signal response in the mass spectrometer presented a large amount of ions from PPy compared to carboxen and PDMS/DVB. The PPy SPME phase synthesised here, presented thicker coating when comparing to the commercial SPME phases. This can be related to a better extraction efficiency, since the extractive phase volume is higher than carboxen and PDMS/DVB. Comparing PPy with carboxen, the first one promoted a spray with better stability for 0.42 min, while the second one promoted a stable spray for only 0.12 min. As described by Niu *et al.* [37], PDMS is a non-electrical conductor polymer, and PESI-MS using the PDMS/DVB probe did not promote the high voltage electrical field necessary to form the spray; therefore, no ions reached the detector.

3.5 Method comparison

Many methodologies for drug analysis in biological fluids and phorbol esters in plant derivates have been reported. Guardia and co-workers in 2018 developed a methodology for cocaine extraction from saliva based on magnetic molecularly imprinted polymers for selective determination by ion mobility spectrometry. The authors declared a total procedure time about 16 minutes, and the cocaine was successfully extracted in a linear range from 35 to 560 µg L^{-1}. The authors also reported a LOD of 4 µg L^{-1} and LOQ, 6 µg L^{-1} [38]. Biziuk and co-workers in 2018 determined amphetamine-types stimulants, such as MA and MDMA, by gas chromatography-tandem mass spectrometry. They reported the use of derivatization agents, and the chromatography essays had as longer retention time 8.37 minutes [39].

The PPy-SPME-PESI-MS methodology proposed here has linear range from 1 to 500 µg L^{-1} for four abuse drugs in saliva and urine. The LOQ and LOD reported here are similar to those found in the literature [38,39]. Futhermore, PPy-SPME-PESI-MS can be performed in batch and then analysed in the MS system (each analysis in MS system takes less than 1 minute

to be performed); no derivatization step is required for analyte determination, reducing time of analysis and method's cost.

The differentiation of toxic and non-toxic *J. curcas* genotypes can be performed by monitoring the phorbol esters, but such molecules are unstable and difficult to detect. Therefore, the differentiation of toxic and non-toxic *J. curcas* is usually performed from the seeds using laborious methods of extraction and separation [34,35]. In this context, MIP-PESI-MS was developed as an alternative to perform such task by the analyses of unusual matrices, such as leaves, in addition to making the process faster because the analyses can be performed before the cultivar produces seeds. The developed probe enabled detection of PEs with limits of detection and quantification in μg mL^{-1} range as reported in the literature for PEs determination in leaves and seeds of *J. curcas* by HPLC-MS analysis, and HPLC-UV [34,40].

Pawliszyn and co-workers in 2014, developed the coated blade spray (CBS) methodology for analyses of diazepam and cocaine in plasmas samples. The CBS uses a blade as solid support similarly for the SPME phase. However, according to the authors, it requires higher amount of sample compared to the SPME-PESI proposed here [41].

SPME phases developed here exhibited better sensitivity and MS response compared to the commercial phases. The SPME-PESI-MS seems to be a powerful tool for a wide range of analytes determination, and also can be applied for in situ analyses when coupled to portable mass spectrometers. The homemade phases can be applied to in vivo extractions, as demonstrated in the literature [42].

4. CONCLUSION

Polypyrrole films were electrodeposited in platinum wire, and MIP was synthetized and adhered in stainless steel needle for application in PESI-MS. The PPy film morphology showed a roughened surface, which is responsible for the adequate capacity of extraction/desorption of the film since the analytes adsorb mainly on the film's surface. The MIP showed better extractive efficiency compared to the NIP. The SPME-PESI-MS method has shown efficiency in the SPME extraction and direct analysis of illicit drugs and phorbol esters in complex matrices. The results for LOQ and LOD accompanied by the analytical evaluation results confirm that SPME-PESI-MS increases the sensitivity, excluding the classical problems of ESI-MS. This method is a promising alternative to conventional techniques due to easy extraction during the sampling process and analysis without the need for any pre-treatment process.

5. ACKNOWLEDGEMENT

Doctoral Thesis – Ricardo Alves Bernardo

This work was supported by grants from Fundação de Amparo à Pesquisa do Estado de Goiás (FAPEG), Coordenação de Aperfeiçoamento de Pessoal de Nível Superior (CAPES), and Conselho Nacional de Desenvolvimento Científico e Tecnológico (CNPq). The whole team involved in this work thanks professor Wanderson Romão and Polícia Federal do Espírito Santo, who kindly donated the drugs standards, and Embrapa Agroenergia (Brasília, Brazil), which kindly yielded the *J. curcas* samples. We also thank to Universidade de São Paulo for the loan of the potentiostat/galvanostatic equipment used here.

6. REFERENCES

[1] K. Cai, R. Yang, Y. Wang, X. Yu, J. Liu, Super fast detection of latent fingerprints with water soluble CdTe quantum dots, Forensic Sci. Int. 226 (2013) 240–243. doi:10.1016/j.forsciint.2013.01.035.

[2] R. Gottardo, D. Sorio, M. Ballotari, F. Tagliaro, First application of Atmospheric-Pressure Chemical Ionization Gas Chromatography Tandem mass spectrometry to the determination of cannabinoids in serum, J. Chromatogr. A. (2019). doi:10.1016/j.chroma.2019.01.041.

[3] M. Pan, P. Xiang, Z. Yu, Y. Zhao, H. Yan, Development of a high-throughput screening analysis for 288 drugs and poisons in human blood using Orbitrap technology with gas chromatography-high resolution accurate mass spectrometry, J. Chromatogr. A. (2018). doi:10.1016/j.chroma.2018.12.022.

[4] A. Illiano, V. Arpino, G. Pinto, A. Berti, V. Verdoliva, G. Peluso, P. Pucci, A. Amoresano, Multiple Reaction Monitoring Tandem Mass Spectrometry Approach for the Identification of Biological Fluids at Crime Scene Investigations, Anal. Chem. 90 (2018) 5627–5636. doi:10.1021/acs.analchem.7b04742.

[5] D. Zhang, H. Bi, B. Liu, L. Qiao, Detection of Pathogenic Microorganisms by Microfluidics Based Analytical Methods, Anal. Chem. (2018) acs.analchem.8b00399. doi:10.1021/acs.analchem.8b00399.

[6] K. Lipponen, S. Tähkä, T. Sikanen, V. Jokinen, A. Tatikonda, S. Franssila, R. Kostiainen, T. Kotiaho, Thiol-ene micropillar array electrospray ionization platform for zeptomole level bioanalysis, Analyst. 142 (2017) 2552–2557. doi:10.1039/c7an00544j.

[7] M. Del Mar Gómez-Ramos, Ł. Rajski, A. Lozano, A.R. Fernández-Alba, The evaluation of matrix effects in pesticide multi-residue methods: Via matrix fingerprinting using liquid chromatography electrospray high-resolution mass spectrometry, Anal. Methods. 8 (2016) 4664–4673. doi:10.1039/c6ay00436a.

[8] K. Hiraoka, K. Nishidate, K. Mori, D. Asakawa, S. Suzuki, Development of probe electrospray using a solid needle, Rapid Commun. Mass Spectrom. 21 (2007) 3139–3144. doi:10.1002/rcm.3201.

[9] L.C. Chen, K. Nishidate, Y. Saito, K. Mori, D. Asakawa, S. Takeda, T. Kubota, H. Hori, K. Hiraoka, Characteristics of Probe Electrospray Generated from a Solid Needle, (n.d.). doi:10.1021/jp803730x.

[10] M.K. Mandal, L.C. Chen, Z. Yu, H. Nonami, R. Erra-Balsells, K. Hiraoka, Detection of protein from detergent solutions by probe electrospray ionization mass spectrometry (PESI-MS), J. Mass Spectrom. 46 (2011) 967–975. doi:10.1002/jms.1977.

[11] S. Saha, M.K. Mandal, K. Hiraoka, Direct detection of trace level illicit drugs in human body fluids by probe electrospray ionization mass spectrometry (PESI-MS), Anal. Methods. 5 (2013) 4731. doi:10.1039/c3ay41117f.

[12] J. Pawliszyn, S. Liu, Sample introduction for capillary gas chromatography with laser desorption and optical fibers, Anal. Chem. 59 (1987) 1475–1478. doi:10.1021/ac00137a024.

[13] A.R. Chaves, G. Chiericato Júnior, M.E.C. Queiroz, Solid-phase microextraction using poly(pyrrole) film and liquid chromatography with UV detection for analysis of antidepressants in plasma samples, J. Chromatogr. B. 877 (2009) 587–593. doi:10.1016/J.JCHROMB.2008.12.070.

[14] A.R. Chaves, G. Chiericato Júnior, M.E.C. Queiroz, Solid-phase microextraction using poly(pyrrole) film and liquid chromatography with UV detection for analysis of antidepressants in plasma samples, J. Chromatogr. B Anal. Technol. Biomed. Life Sci. (2009). doi:10.1016/j.jchromb.2008.12.070.

[15] T. Patois, B. Lakard, S. Monney, X. Roizard, P. Fievet, Characterization of the surface properties of polypyrrole films: Influence of electrodeposition parameters, Synth. Met. 161 (2011) 2498–2505. doi:10.1016/J.SYNTHMET.2011.10.003.

[16] T. V Vernitskaya, O.N. Efimov, Polypyrrole: a conducting polymer; its synthesis, properties and applications, Russ. Chem. Rev. 66 (1997) 443–457. doi:10.1070/RC1997v066n05ABEH000261.

[17] J. Wu, J. Pawliszyn, Solid-phase microextraction based on polypyrrole films with different counter ions, Anal. Chim. Acta. 520 (2004) 257–264. doi:10.1016/J.ACA.2004.05.019.

[18] Jingcun Wu, and W. M. Mullett, J. Pawliszyn*, Electrochemically Controlled Solid-Phase Microextraction Based on Conductive Polypyrrole Films, (2002). doi:10.1021/AC025595Q.

[19] J. Wu, J. Pawliszyn, Preparation and applications of polypyrrole films in solid-phase microextraction, J. Chromatogr. A. 909 (2001) 37–52. doi:10.1016/S0021-9673(00)01025-6.

[20] J. Wu, H.L. Lord, J. Pawliszyn, H. Kataoka, Polypyrrole-coated capillary in-tube solid phase microextraction coupled with liquid chromatography-electrospray ionization mass spectrometry for the determination of ?-blockers in urine and serum samples, J. Microcolumn Sep. 12 (2000) 255–266. doi:10.1002/(SICI)1520-667X(2000)12:4<255::AID-MCS10>3.0.CO;2-J.

[21] L.S. Tavares, T.C. Carvalho, W. Romão, B.G. Vaz, A.R. Chaves, Paper Spray Tandem Mass Spectrometry Based on Molecularly Imprinted Polymer Substrate for Cocaine Analysis in Oral Fluid, J. Am. Soc. Mass Spectrom. 29 (2018) 566–572. doi:10.1007/s13361-017-1853-2.

[22] S. Salehi, S. Rasoul-Amini, N. Adib, M. Shekarchi, Synthesis of molecular imprinted polymers for selective extraction of domperidone from human serum using high performance liquid chromatography with fluorescence detection, J. Chromatogr. B Anal. Technol. Biomed. Life Sci. 1027 (2016) 165–173. doi:10.1016/j.jchromb.2016.05.035.

[23] G. Van Biesen, J.M. Wiseman, J. Li, C.S. Bottaro, Desorption electrospray ionization-mass spectrometry for the detection of analytes extracted by thin-film molecularly imprinted polymers, Analyst. 135 (2010) 2237. doi:10.1039/c0an00331j.

[24] I. Pereira, M.F. Rodrigues, A.R. Chaves, B.G. Vaz, Molecularly imprinted polymer (MIP) membrane assisted direct spray ionization mass spectrometry for agrochemicals screening in foodstuffs, Talanta. 178 (2018) 507–514. doi:10.1016/j.talanta.2017.09.080.

[25] S. Ansari, M. Karimi, Novel developments and trends of analytical methods for drug analysis in biological and environmental samples by molecularly imprinted polymers, TrAC Trends Anal. Chem. 89 (2017) 146–162. doi:10.1016/J.TRAC.2017.02.002.

[26] F. Soleimany, S. Jinap, F. Abas, Determination of mycotoxins in cereals by liquid chromatography tandem mass spectrometry, Food Chem. 130 (2012) 1055–1060. doi:10.1016/J.FOODCHEM.2011.07.131.

[27] X. Zhao, C. Jiang, Determination of ethyl carbamate in fermented liquids by ultra high performance liquid chromatography coupled with a Q Exactive hybrid quadrupole-orbitrap mass spectrometer, Food Chem. 177 (2015) 66–71. doi:10.1016/J.FOODCHEM.2015.01.025.

[28] G.L. Long, J.D. Winefordner, Limit of detection. A closer look at the IUPAC definition, Anal. Chem. 55 (1983) 712A-724A. doi:10.1021/ac00258a001.

[29] T. Tüken, Polypyrrole films on stainless steel, Surf. Coatings Technol. 200 (2006) 4713–4719. doi:10.1016/J.SURFCOAT.2005.04.011.

[30] M. Zhou, J. Heinze, Electropolymerization of pyrrole and electrochemical study of polypyrrole: 1. Evidence for structural diversity of polypyrrole, Electrochim. Acta. 44 (1999) 1733–1748. doi:10.1016/S0013-4686(98)00293-X.

[31] P. Olszowy, M. Szultka, T. Ligor, J. Nowaczyk, B. Buszewski, Fibers with polypyrrole and polythiophene phases for isolation and determination of adrenolytic drugs from human plasma by SPME-HPLC, J. Chromatogr. B. 878 (2010) 2226–2234. doi:10.1016/J.JCHROMB.2010.06.033.

[32] P.A.. Cormack, A.Z. Elorza, Molecularly imprinted polymers: synthesis and characterisation, J. Chromatogr. B. 804 (2004) 173–182. doi:10.1016/J.JCHROMB.2004.02.013.

[33] X. Li, C. Li, J. Chen, C. Li, C. Sun, Polythiophene as a novel fiber coating for solid-phase microextraction, J. Chromatogr. A. 1198–1199 (2008) 7–13. doi:10.1016/J.CHROMA.2008.05.051.

[34] M. Baldini, C. Ferfuia, R. Bortolomeazzi, G. Verardo, J. Pascali, E. Piasentier, L. Franceschi, Determination of phorbol esters in seeds and leaves of Jatropha curcas and in animal tissue by high-performance liquid chromatography tandem mass spectrometry, Ind. Crops Prod. 59 (2014) 268–276. https://www.sciencedirect.com/science/article/pii/S0926669014003136 (accessed January 27, 2019).

[35] G. Goel, H.P.S. Makkar, G. Francis, K. Becker, Phorbol Esters: Structure, Biological Activity, and Toxicity in Animals, Int. J. Toxicol. 26 (2007) 279–288. doi:10.1080/10915810701464641.

[36] T.C. Carvalho, I.F. Oliveira, L. V. Tose, G. Vanini, J.B. Kill, A.C. Neto, L.F. Machado, J.C.L. Ambrosio, V. Lacerda, B.G. Vaz, W. Romão, Qualitative analysis of designer drugs by paper spray ionisation mass spectrometry (PSI-MS), Anal. Methods. 8 (2016) 614–620. doi:10.1039/C5AY01265A.

[37] X.Z. Niu, S.L. Peng, L.Y. Liu, W.J. Wen, P. Sheng, Characterizing and Patterning of PDMS-Based Conducting Composites, Adv. Mater. 19 (2007) 2682–2686. doi:10.1002/adma.200602515.

[38] A. Sorribes-Soriano, F.A. Esteve-Turrillas, S. Armenta, A. Montoya, J.M. Herrero-Martínez, M. de la Guardia, Magnetic molecularly imprinted polymers for the selective determination of cocaine by ion mobility spectrometry, J. Chromatogr. A. 1545 (2018) 22–31. doi:10.1016/j.chroma.2018.02.055.

[39] M.K. Woźniak, M. Wiergowski, J. Aszyk, P. Kubica, J. Namieśnik, M. Biziuk, Application of gas chromatography–tandem mass spectrometry for the determination of amphetamine-type stimulants in blood and urine, J. Pharm. Biomed. Anal. 148 (2018) 58–64. doi:10.1016/j.jpba.2017.09.020.

[40] R.K. Devappa, J.-P. Bingham, S.K. Khanal, High performance liquid chromatography method for rapid quantification of phorbol esters in Jatropha curcas seed, Ind. Crops Prod. 49 (2013) 211–219. doi:10.1016/J.INDCROP.2013.04.044.

[41] G.A. Gómez-Ríos, J. Pawliszyn, Development of Coated Blade Spray Ionization Mass Spectrometry for the Quantitation of Target Analytes Present in Complex Matrices, Angew. Chemie Int. Ed. 53 (2014) 14503–14507. doi:10.1002/anie.201407057.

[42] E. Cudjoe, B. Bojko, P. Togunde, J. Pawliszyn, In vivo solid-phase microextraction for tissue bioanalysis, Bioanalysis. 4 (2012) 2605–2619. doi:10.4155/bio.12.250.